Wissenschaftszentrum Weihenstephan
für Ernährung, Landnutzung und Umwelt
Lehrstuhl für Ökologische Chemie und Umweltanalytik
der Technischen Universität München

Application of Modern On-line and Off-line Analytical Methods for Tobacco and Cigarette Mainstream and Sidestream Smoke Characterisation

Stefan Manfred Mitschke

Vollständiger Abdruck der von der Fakultät Wissenschaftszentrum Weihenstephan für Ernährung, Landnutzung und Umwelt der Technischen Universität München zur Erlangung des akademischen Grades eines

Doktors der Naturwissenschaften (Dr. rer. nat.)

genehmigten Dissertation.

Vorsitzender: Univ.-Prof. Dr. Ing. Roland Meyer-Pittroff
Prüfer der Dissertation:
1. Univ.-Prof. Dr. rer. nat., Dr. h.c. (RO) Antonius Kettrup, em.
2. Univ.-Prof. Dr. rer. nat., Dr. agr. habil., Dr. h.c. (Zonguldak University/Türkei) Harun Parlar
3. Univ.-Prof. Dr. rer. nat. Ralf Zimmermann (Universität Augsburg)

Die Dissertation wurde am 11.01.2007 bei der Technischen Universität München eingereicht und durch die Fakultät Wissenschaftszentrum Weihenstephan für Ernährung, Landnutzung und Umwelt am 13.03.2007 angenommen.

I'll always remember
The chill of November
The news of the fall
The sounds in the hall
The clock on the wall
Ticking away
"Seize the day"
I heard him say
Life will not always be this way
Look around
Hear the sounds
Cherish your life
While you're still around

Mike Portnoy

Contents

Contents

Contents

1 Introduction

1.1 Historical aspects of tobacco

1.1.1 Origins of tobacco and tobacco consumption

Tobacco belongs to the family of the nightshades and originated in North and South America. It is believed that tobacco consumption is as old as 6,000 B. C. when the natives of North and South America used the chewed or smoked plant as a natural stimulant or hallucinogen. It is known that in the first century A. D. tobacco consumption was a common habit in both Americas and tobacco plants were even used as currency. The first illustrations showing tobacco use are as old as the 11th century, inscribed and painted on vessels and artwork of the Maya in the Yucatan region of Mexico.

At the discovery of the Americas by western civilisation by Christopher Columbus in 1492, he was given various presents, including dried tobacco, which was believed to have no value because it was of no use to nutrition. In the early 16th century the habit of smoking cigarettes by the Aztecs was discovered by the Spanish conquistador Hernando Cortez in South America and brought back to Spain, while Jaques Cartier observed the smoking of dried leaves on the Island of Montreal. The Aztecs made smoking articles from crushed tobacco leaves which were wrapped in corn husk, a common way until the early 17th century, when the corn husk was replaced by paper, and also used the tobacco in pipes, for chewing, as enema, or to embalm.

Tobacco was first cultivated in Europe in the middle of the 16th century by Jean Nicot, who presented smoking as a treatment for migraine headaches to the royal court in Paris. Soon the plant was grown all over Europe and by 1570 tobacco was granted the scientific name "Herba Nicotina" by Jean Libault in honour of Jean Nicot. As early as in the 17th century English settlers in America started growing tobacco to export it to Europe and tobacco quickly became the greatest export goods of the American colonies, a fact that prolonged for approximately two centuries. In the following years smoking spread through Portugal, Italy, Greece, Turkey to southern Russia. By the 1830's cigarettes were being made in Spain and crossed

the Pyrenees and reached France. At that time tobacco was already imported from Ohio, Maryland, and Kentucky into Russia and blended with local tobacco. Around 1850 Turkish leaf was introduced in Russian cigarettes, which further increased the popularity of smoking.

After the Crimean War (1853–1856) British troops brought the habit of smoking cigarettes back to England where PHILIP MORRIS, a tobacconist from London, went into cigarette production. By then cigarettes were hand-rolled, mainly by workers from Russia and Poland, who managed to roll up to 40 cigarettes per minute. In the United States the production of a few million cigarettes per year started in 1864 in New York City. The first working cigarette machines were invented around 1879. James Bonsack applied for a patent in 1880. The machine, though sold in the United States and Europe, had several major disadvantages and was improved by JAMES BUCHANAN DUKE and WILLIAM T. O'BRIAN in 1886. The success of the machine allowed them to absorb the four leading U.S. tobacco companies of that time, Allen and Ginter, Goodwin, Kimball and Kinney and form the American Tobacco Company.

1.1.2 Tobacco in health research prior to the 20th century

The controversial discussion of tobacco started as early as 1586, when tobacco was labelled a "violent herb" in the book "De plantis epitome utilisma" that contained some first cautions to its use. In 1604 King James I of England wrote about the harmful effects of tobacco in "A counterblaste to tobacco" and in 1610 Sir Francis Bacon described how hard it was for him to quit smoking. In 1665 Samuel Pepys reported the death of a cat, after being fed with a drop of tobacco distillate. A first tobacco related clinical study was undertaken in 1761 by John Hill, who concluded that snuff users were more vulnerable to nasal cancer, followed by Percival Scott, who linked lip-cancer to tobacco snuff in 1787. In 1795 Sammuel Thomas von Soemmering recognised a higher affinity to lip-cancer for pipe-smokers. Despite this, the reputation of tobacco as a medical plant still remained intact.

The evolution of chemical and medical knowledge and the search for single health active ingredients lead to the isolation of nicotine by Wilhelm Heinrich Posselt and Ludwig Reimann at the University of Heidelberg in 1828. However, the chemical structure of nicotine (3-(1-Methyl-2-pyrrolidinyl)pyridine) was unknown until its discovery by Adolf Pinner in 1895. In 1849 Joel Shew associated 87 diseases to tobacco and by the end of the 19th century many cancers of face organs were referred to as "smoker's cancers".

1.2 Chemical composition of tobacco leaf

The chemical composition of the plant and the dried tobacco is mainly influenced by the tobacco type and the curing process, which immediately follows the harvesting and varies in duration from several days to several weeks, depending on the tobacco type and desired quality. The characteristic agronomic data of three of the most important tobacco types is presented in Table 1.1.

Burley tobacco is cultivated mainly in the USA. Usually it is grown on fertile, heavier-textured grounds and fertilised with nitrogen using ammonium nitrate and urea. It is air-cured. During the relatively long curing-phase of several weeks the leaves hang without additional heating and plant-carbohydrates are depleted to a major extent. In the final stage of the curing the leaves die leaving the brown leaf with a relatively low sugar content. This results in high contents of nitrogen-containing-compounds such as proteins, alkaloids, amino acids and nitrates [1, 2].

In contrast Virginia tobacco is usually cultivated throughout the world on sandy soils with low organic matter and nitrogen content. It is the major component of branded cigarettes sold in Great Britain, Australia and Canada. It is flue-cured, whereby curing of the leaves is done in a barn by applying circulating air at various temperatures, ranging from 35 to 75 °C over several days, leaving the chlorophyll destroyed. At this so called yellowing stage the curing is stopped by applying drier and hotter air [2–4].

Oriental tobacco is grown mainly on rocky soils, which are usually low in nutrients, in the eastern Mediterranean and Balkan regions. The small and compact leaves are highly aromatic. During growing the top leaves of the crop are not removed, irrigation and fertilisation is not as important as for other tobacco types. It is sun-cured, whereby the harvested leaves are cured by hanging them directly in the sun for twelve to seventeen days. The tobacco inhibits lower amounts of nitrogen-containing compounds, and sugars and sugar esters, which are believed to be important factors of the unique aroma [5].

Table 1.2 illustrates an overview of the chemical compositions of the most common tobacco types. It reflects the effects of the different curing processes and growing conditions discussed earlier. Burley tobacco exhibits relatively high contents in all nitrogen-containing substance classes, an absence of reducing sugars, as well as most of the acids, pectin and the crude fibre, while Virginia stands out with a high amount of reducing sugars. Oriental is characterised by a high content of alcohol soluble compounds, as well as certain acids and a medium content of reducing sugars.

Several publications deal with the specific chemical composition of tobacco leaf in

	Virginia tobacco	**Burley tobacco**	**Oriental tobacco**
Growing region	no preference	mainly USA	Eastern Mediterranean and Balkan regions
Soil type	sandy, infertile	heavier-textured, more fertile	poor and rocky
Fertilisation	little	medium to strong	none
Curing process	flue-cured	air-cured	sun-cured
Curing duration	5 to 9 days	5 to 7 weeks	12 to 17 days

Table 1.1: Growing and processing the tobacco types Virginia, Burley and Oriental [6].

	Virginia [%]	**Burley [%]**	**Maryland [%]**	**Oriental [%]**
Total volatile bases as ammonia	0.282	0.621	0.366	0.289
Nicotine	1.93	2.91	1.27	1.05
Ammonia	0.019	0.159	0.130	0.105
Glutamine as ammonia	0.033	0.035	0.041	0.020
Asparagine as ammonia	0.025	0.111	0.016	0.058
α-Amino nitrogen as ammonia	0.065	0.203	0.075	0.117
Protein nitrogen as ammonia	0.91	1.77	1.61	1.19
Nitrate nitrogen as NO_3^-	Trace	1.70	0.087	Trace
Total nitrogen as ammonia	1.97	3.96	2.8	2.65
Total volatile acids as acetic acid	0.153	0.103	0.090	0.194
Formic acid	0.059	0.027	0.022	0.079
Malic acid	2.83	6.75	2.43	3.87
Citric acid	0.78	8.22	2.98	1.03
Oxalic acid	0.81	3.04	2.79	3.16
Volatile oils	0.148	0.141	0.140	0.248
Alcohol-soluble resins	9.08	9.27	8.94	11.28
Reducing sugars as dextrose	22.09	0.21	0.21	12.39
Pectin as calcium pectate	6.19	9.91	12.14	6.77
Crude fibre	7.88	9.29	21.79	6.63
Ash	10.81	24.53	21.98	14.78
Calcium as CaO	2.22	8.01	4.79	4.22
Potassium as K_2O	2.47	5.22	4.40	2.33
Magnesium as MgO	0.36	1.29	1.03	0.69
Chlorine as Cl^-	0.84	0.71	0.26	0.69
Phosphorus as P_2O_5	0.51	0.57	0.53	0.47
Sulphur as SO_4^{2-}	1.23	1.98	3.34	1.40

Table 1.2: Analysis of different tobacco types (Leaf web after aging, moisture-free basis) [7].

general (e.g. [8]) or essential oils and flavour compounds extracted from Burley [9–11], flue-cured [12] and its acids [13] and Greek (e. g. [14–17] as well as Turkish [18, 19] and Latakia [20, 21] tobacco have been published. Latakia tobacco is nowadays mainly produced in Cyprus, originally coming from Syria. It is cured over a stone pine or oak wood fire and is an essential part of many pipe tobacco mixtures.

In some countries, e.g. the USA and Germany, commercial cigarettes are a mixture of different tobacco types and are known as US blended cigarettes. Small amounts of flavours and casing materials are often added to these cigarettes. In other countries, e.g. Britain, Canada, Australia and India, only one main type of tobacco is used in most commercial cigarettes (Virginia) and flavours and casing materials are not added.

1.3 Composition of cigarette smoke

During the smoking of a cigarette several streams of smoke are formed. The smoke inhaled by the smoker during a puff, the so called mainstream smoke, is probably the most important to look at, if one is considering the health effects on the smoker. In addition to mainstream smoke the sidestream smoke of a cigarette is formed from several processes, namely the combustion at the glowing tip during smoulder between puffs, and the diffusion of gases through the paper between puffs. Furthermore, combustion at the tip and effusion at the rod also happens during a puff. As illustrated in Fig. 1.1 every stream emerging from the cigarette rod is referred to as sidestream smoke. Exhaled mainstream smoke and sidestream smoke diffuse into the atmosphere where they form the complex mixture of environmental tobacco smoke (ETS).

1.3.1 Mainstream smoke

The analysis and characterisation of mainstream smoke started in the 1950's mainly focusing on design parameters and health effects. KOSAK [22] listed less than 100 compounds present in mainstream smoke in 1954. By 1982 about 4000 different compounds had been identified in mainstream smoke [23]. The latest estimate is that there are about 4800 known constituents in tobacco smoke [24]. It has been speculated that there could be as many as 100,000 constituents, the remainder being at minute levels. Figure 1.2 gives an overview of the chemical composition of whole mainstream smoke from an unfiltered US blended cigarette which yields 500 mg of whole smoke. The major part of the 500 mg consists of background gases, such as
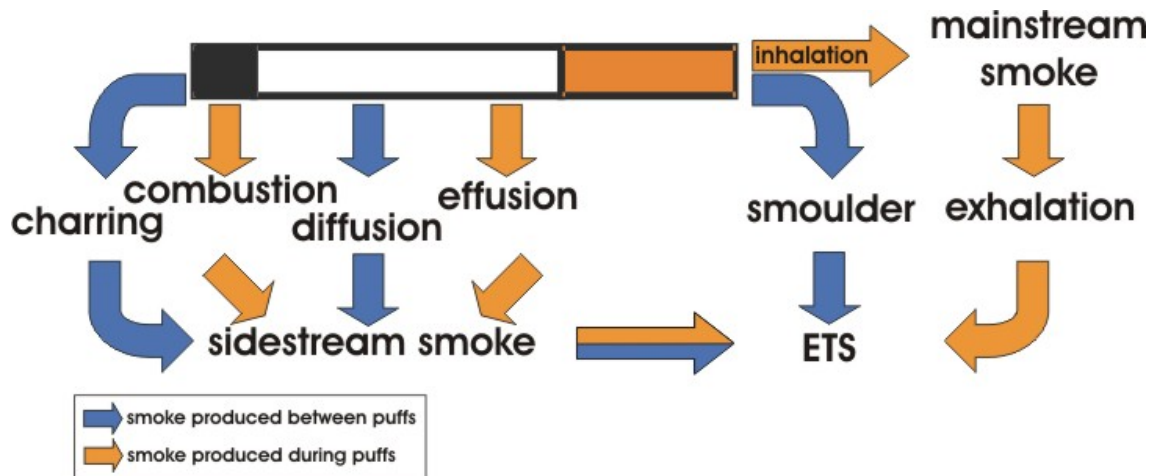
Figure 1.1: Streams from a burning cigarette

nitrogen and oxygen ($\approx$ 75 %), about 18 % of the total weight are total particulate matter (TPM) ($\approx$ 4.5 %) and vapour phase ($\approx$ 13.5 %), of which only about 10 % differ from carbon dioxide and water. In this thesis two different modern methods of analysis are utilised to investigate mainstream cigarette smoke, namely comprehensive GCxGC and photoionisation mass spectrometry. The latter is perfectly suited for the analysis of complex gaseous mixtures, while GCxGC inhibits some major advantages for the analysis of complex particulate matter samples.

Table 1.3 shows the number of compounds in certain compound classes in mainstream smoke. Dube and Green [23] listed 3875 identified substances, a number that is considerably lower than the 4720 mentioned compound classes. This results from compounds inhibiting more than one functional group. About 500 can be found in the vapour phase and about 300 can be classed as semi-volatiles [25]. The authors also estimated the numbers of substances present in tobacco to be 2550, of which 1135 are transferred unchanged into the smoke and 1414 are unique to tobacco, in fact are not volatile enough to be transferred into smoke and therefore decompose during burning.

1.3.2 Sidestream smoke

In general, the composition of sidestream smoke is very similar to mainstream smoke. The quantities of each substance may vary, though. There is a considerable large amount of data available on the various sidestream/mainstream ratios of many smoke constituents for different cigarette types [26–39], which has been collected by Baker [40] and can be found in the appendix (Table A.1). Most of the substances are present in larger amounts in sidestream smoke. However, the organic

22.5 mg TPM

500 mg whole smoke

67.5 mg vapour phase

6.75 mg

unidentified compounds 16.5 %

smoke pigment 4 %
misc. compounds 5 %
alkanes 5 %
terpenoid hydrocarbon 5 %
phenols 3.5 %
esters 3.5 %
other alkaloid der. 3.5 %
nicotine 6 %
alcohols 8 %
aldehydes & ketones 11 %
carboxylic acids 13 %
water ~16 %

4.5 %
13.5 %
N_2 ~ 62 %
O_2 ~ 13 %
CO 4 %
$CH_4 + CO_2$
$H_2 + A$

others ~ 10 %
H_2O ~ 10 %
CO_2 ~ 80 %

esters (1 %)
acids (1.5 %)
methanol (2 %)
heterocyclic compounds (2 %)
nitriles 9.5 %
misc. compounds 7.5 %
ketones 12 %
aldehydes 20 %
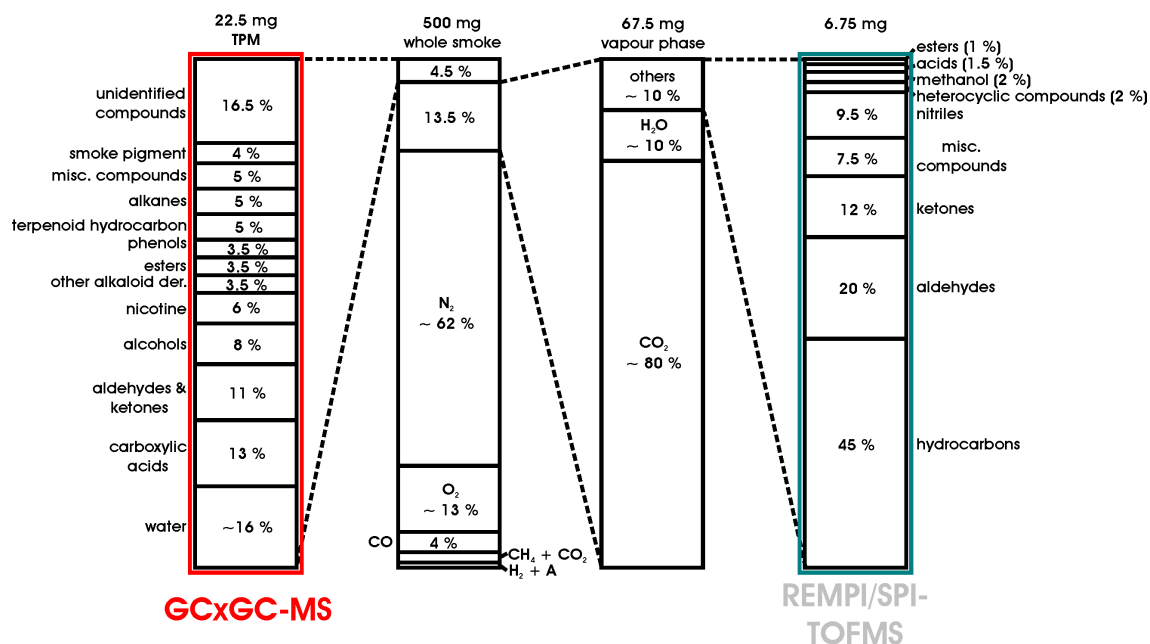hydrocarbons 45 %

GCxGC-MS

REMPI/SPI-TOFMS

Figure 1.2: *Composition of mainstream cigarette smoke* [23].

acids containing more carbon atoms than acetic acid, as well as the inorganic compounds carbonyl sulphide and hydrogen cyanide show higher amounts in mainstream smoke. Especially large amounts of most PAH can be observed in sidestream smoke, as well as a huge number of nitrogen containing compounds and a selection of unsaturated hydrocarbons. The problem of associating possible health effects directly to sidestream smoke was addressed by REASOR in the late 1980s [41]. People are not directly exposed to pure sidestream smoke, but rather a mixture of sidestream smoke and exhaled mainstream smoke which has undergone significant effects of aging.

1.3.3 Environmental tobacco smoke

ETS consists mainly of sidestream smoke, only 15 to 43 % of the particulate matter of ETS and 13 % of the vapour phase constituents can be traced back to exhaled mainstream smoke [42]. After diffusion into the atmosphere from the cigarette both mainstream and sidestream smoke become greatly diluted, resulting in a great variety of physical and chemical changes. Levels of ETS components in a room are dependant on air circulation, room ventilation and deposition onto surfaces. The effects of air exchange rates on the level of selected components was recently investigated by KOTZIAS et al. [43]. Currently, ETS is under much investigation, especially concerning its possible health risks for non-smokers. However, because ETS is a con-

Class	Number
Amides, imides, lactames	237
Carboxylic acids	227
Lactones	150
Esters	474
Aldehydes	108
Ketones	521
Alcohols	379
Phenols	282
Amines	196
N-Heterocyclics	921
Hydrocarbons	755
Nitriles	106
Anhydrides	11
Carbohydrates	42
Ethers	311
Total	4720

Table 1.3: Approximate number of compounds identified in some major compound classes of mainstream smoke. Additionally about 100 metallic and inorganic ions and compounds can be found in tobacco mainstream smoke [23].

stantly changing mixture, strongly dependant on the surrounding environment, this thesis will not deal with ETS itself, but with sidestream and mainstream smoke as sources in particular. A detailed discussion about ETS can be found in [39].

1.4 Motivation

Tobacco, tobacco products and tobacco burning products are one of the most controversially discussed health topics of the last few years. The large number of compounds found in mainstream smoke not only reflects its complexity but moreover the huge research effort that has been spent over the last 60 years. However, routine analysis of cigarette smoke is still limited to a small set of compounds with conventional off-line methods, such as liquid chromatography (LC) e. g. [24, 44–47] and gas chromatography (GC) e. g. [24, 48–55], where compositions can be altered due to sampling, analytical processing such as separation, trapping and derivatisation [56–58]. Furthermore, these conventional methods deal almost exclusively with whole or even several cigarettes and can not provide information about ongoing pro-

cesses in a burning cigarette. REMPI/SPI-TOFMS can provide useful information on a quasi real time basis for a large number of different gas phase smoke compounds.

In addition, the application of new high resolution multidimensional techniques, such as comprehensive GCxGC, can be utilised for the identification of more trace compounds or for the classification of tobacco or tobacco products by certain sum parameters. However, as first results show [59], the amount of data available from this high-resolving method is enormous and the identification of single peaks is hardly possible. Therefore, new methodologies for the classification of sum parameters will be presented.

1 Introduction

2 Methods and Instrumentation

2.1 Principles of photo ionisation processes

2.1.1 Single photon ionisation (SPI)

The absorption of photons by molecules or atoms leads to excited states of the species. If vacuum ultraviolet (VUV) light ($E_{ph} > 6.9$ eV, $\lambda < 180$ nm) is used this interaction leads to excited electronic states. These undergo different mechanisms to undo the excitation, namely ionisation or dissociation into neutral or charged subparts. The probability of each process is thereby dependant on the molecule itself and the energy of the photon.

2.1.2 Resonant multi photon ionisation

In resonant multi photon ionisation, atoms or molecules are ionised by absorption of two or more photons [60–62]. The energy of a single photon is smaller than the ionisation potential of the atom or molecule, therefore it is necessary to absorb more than one photon. Multi photon processes can be divided into several groups. If the photon energy is in resonance to an excited state of the molecule or atom the process is called resonance enhanced multi photon ionisation otherwise non resonant multi photon ionisation.

Furthermore, multi photon processes are subdivided into two-, three-, or multi photon ionisation as well as by the number of involved "colours" (different laser wavelengths) into one-, two-, and three-colour multi photon ionisation. The theory of multi photon processes is well described throughout the literature [63, 64].
In the analysis of organic substances, mainly one colour two-photon REMPI processes are used. Additionally one colour processes are useful to minimise the instrumental requirements.

Molecules are typically irradiated with intense laser pulses ($\approx 10^6$ W cm^{-2}, 10 ns pulse duration). High efficiencies can only be achieved if:

- the laser wavelength is in resonance with the excitation energy of a UV-spectroscopic active state of the target molecule. The resonance enhancement increases sensitivity by several orders of magnitude and is the basis of the high selectivity of the method.

- the sum of the energy of two photons is higher than the corresponding ionisation potential, that means ionisation is energetically possible and

- the life time of the excited state is not much shorter than the pulse duration (typically $\approx$ 10 ns)

Different molecules hold different ionisation potentials and UV-bands. Therefore only certain compounds can be analysed in a specific wavelength. The wavelength dependent selectivity enables the detection of selected trace compounds within very complex samples. Furthermore, for many compound classes a better detection limit is reached compared to electron impact ionisation (EI).

The magnitude of the selectivity is strongly dependent of the temperature of the analytes and the method of injection. With cooled molecules, e. g. created in supersonic-beam or jet-inlet systems, a very high selectivity is achieved [65]. Effusive injection of the sample gas into the ion source results in sample molecules at the temperature of the inlet system. UV spectroscopic transitions of organic molecules in the gas phase at room temperature or higher are heavily energy broadened by excitations of internal degrees of freedom (rotation, vibration). In complex mixtures this may lead to overlaps. Nevertheless, a high optical selectivity can sill be achieved, which gives access to the ionisation of similar compounds with a specific wavelength (class-selective ionisation). The sensitivity and the degree of fragmentation in a REMPI process is also influenced by the focus of the laser beam. High focus leads to high energy densities and therefore to fragmentation, as ions have a high probability of being hit by an additional photon.

2.2 Time-of-flight mass spectrometry

Time-of-Flight Mass Spectrometry has become an established method over the last years as a useful tool for the observation of fast processes because of its high time-resolution. In principle a full mass spectrum can be recorded in the region of a few microseconds. The basic principles are well documented in the literature [66–68], therefore only a brief introduction will be given.

In the so called ion source, which consists of two electrodes with opposite polarity, namely a positively charged repeller and the negatively charged extraction electrode,

ions are generated via a broad range of methods (e. g. EI). Ions with the corresponding charge z and mass m are accelerated by the potential V to the velocity v:

$$v = \sqrt{\frac{2zV}{m}} \tag{2.1}$$

The ions are accelerated through a hole in the extractor into the drift tube of length L. After a certain time t the ions reach a detector located at the end of the drift tube. Therefore, the time needed to pass the drift tube can be expressed as:

$$t = \frac{L}{v} = L\sqrt{\frac{m}{2qV}} \tag{2.2}$$

$$t \approx \sqrt{\frac{m}{q}} \tag{2.3}$$

This shows that the time-of-flight is proportional to the square root of the ratio of the molecular weight and the charge of the ion.

Since the location of the ionisation is not uniform but exhibits a finite diameter, not all ions are generated at the same position. This results in different starting conditions of single ions and leads to a broadening in the time-dimension of ions with the same mass. Ions generated closer to the extractor are accelerated less but need to pass a smaller distance. At the so-called spatial focal point both effects are minimised. On one-step extraction instruments, as introduced earlier, this spatial focal point is too close to the ion source to achieve satisfactory mass separation. Therefore a more sophisticated two-step approach was introduced by WILEY and MCLAREN [67], where ions are not accelerated immediately with the full acceleration voltage but are pre-accelerated by a lower potential out of the ion source and later post-accelerated in a second step. The shifting of the spacial focus point to a detector, which is located further away, leads to a longer flight distance and therefore to a higher resolution of the mass spectrometer.

Additionally, higher mass resolutions can be achieved by the reflectron introduced by MAMYRIN *et al.* [69], where the kinetic energy of isobaric ions is corrected by an ion mirror. This mirror is two-staged, like the Wiley-McLaren ion source. The first, the so called bremsfeld, is used to delay ions at the entry point of the mirror or accelerate them at the exit. The reflection itself is achieved in a second stage, the so called reflector field. Ions with larger kinetic energy can intrude further into the ion mirror and therefore have a longer delay within it. This leads to a focus of slower and faster isobaric ions. The spacial focus of the Wiley-McLaren ion extraction is put somewhere before the ion mirror. Ions are later focussed on the detector by the energy-corrected ion mirror. By this energy compensation step and the prolonged flight distance the mass resolution can be significantly increased compared to a linear system of comparable size. However, the overall sensitivity of reflectrons is lower, as a smaller part of the ions reach the detector, due to losses in the reflection step.
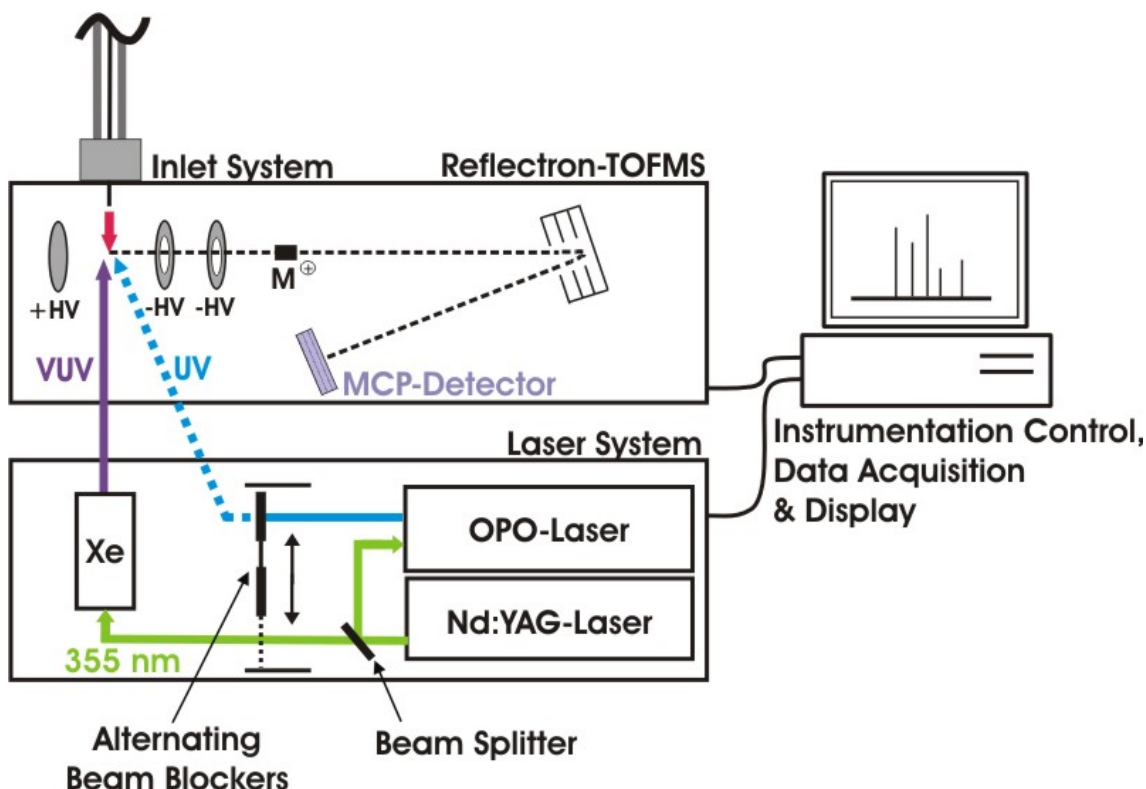
Figure 2.1: Schematic overview of the REMPI/SPI-TOFMS instrument.

2.3 General instrumental setup

The instrument mainly used for the experiments of this thesis was built, described, and thoroughly characterised in a previous PhD thesis by MÜHLBERGER [70] and is published elsewhere [71]. Therefore only a brief description will be included here.

The instrument can quasi-simultaneously operate with three different ionisation modes, namely electron impact ionisation (EI), single-photon-ionisation (SPI) and resonance-enhanced-multi-photon-ionisation (REMPI). A Nd:YAG laser (Surelite-III, Continuum, Santa Clara, USA) with a fundamental wavelength of 1064 nm, a pulse duration of 3–5 ns, and a repetition rate of max. 10 Hz is frequency-tripled by a third-harmonic-generator (THG). The resulting laser beam of 355 nm is divided into two parts: a major one of 89 % ($\approx$ 205 mJ) is used to pump an optical-parameter-oscillator (OPO) (GWU Lasertechnik, Erftstadt, Germany) equipped with a second harmonic generation (SHG) unit used for frequency doubling. The resulting laser beams used for REMPI exhibit a range from 219 to 345 nm with a linewidth of 5–7 cm^{-1}. The minor part of 11 % ($\approx$ 225 mJ) is used for VUV-generation in a THG-rare gas cell filled with xenon (Xe 4.0; p = 12 mbar). A MgF$_2$-lens is used to separate the 355 nm pump beam from the resulting 118 nm VUV-beam by hitting it off-centre,

taking advantage of the different refraction indices.

The mass spectrometer (Kaesdorf, Munich, Germany) can be operated in linear or reflectron mode, the latter one is the only one used in this thesis. In reflectron mode the field-free drift region is 801 mm long. Mass resolution $R_{50\%}$ was calculated by means of the full width at half maximum (FWHM) method to be 1800, calculated at $m/z = 92$. This means that at $m/z = 1800$ the baseline between two adjacent peaks is not higher than 50 % of the signal intensity of the two peaks, and subsequently, the peaks can be clearly resolved.

Two turbomolecular pumps (TMU 521, TMU 261, Pfeiffer Vacuum, Aslar, Germany) with 520 L/s (N_2) and 210 L/s (N_2) are used to differentially pump the flight tube and the ionisation chamber. Without sample flow into the ion source the vacuum achieved in the ion source is $\approx 10^{-6}$ mbar and in the flight tube ca. 10^{-8} mbar. With a typical sample flow of 8 mL/min the vacuum decreases by approximately two orders of magnitude in each section. A two-stage multichannel plate detector (MCP) in chevron assembly with 40 mm active diameter is used for ion detection. The TOF mass spectra are recorded via a transient recorder card (Aqciris, Switzerland, 250 MHz, 1 GS, signal resolution 8 bits (256 points)). During the work an additional card of the same type has been build into the system. This second card continuously monitors the low-voltage region of the spectrum (typically below 50 mV) with a resolution of 8 bit. The combination with the data of the first card yields a greater dynamic range. Data processing is done by a LabView (National Instruments, USA) based on purpose-written software.

The recorded time-of-flight spectra are processed for data reduction. As can be seen in Fig. 2.2 the mass peaks are integrated with a precision of $m/z = 0.5$. The picture shows the raw (top) and integrated (bottom) extraction of a mass spectra of the 10 ppm gas standards of benzene, toluene, *p*-xylene, and n-octane. For further clarification an enlarged view of the benzene-peak is also plotted. Furthermore, every datapoint is marked in the raw spectrum. The comparison shows, that no information is lost in the mass axis.

Further analytical devices are connected to the REMPI/SPI-TOFMS instrument by a heated transfer line (1.5 m, 250 °C), which contains a deactivated silica capillary of 0.32-mm i. d. Reactions inside the capillary have not been observed; the retention time is less than 1 s.

Different SPI detection limits of common tobacco smoke compounds are listed in Table 2.1. The detection limits of the instrument were determined according to WILLIAMS *et al.* [72] by using the equation.
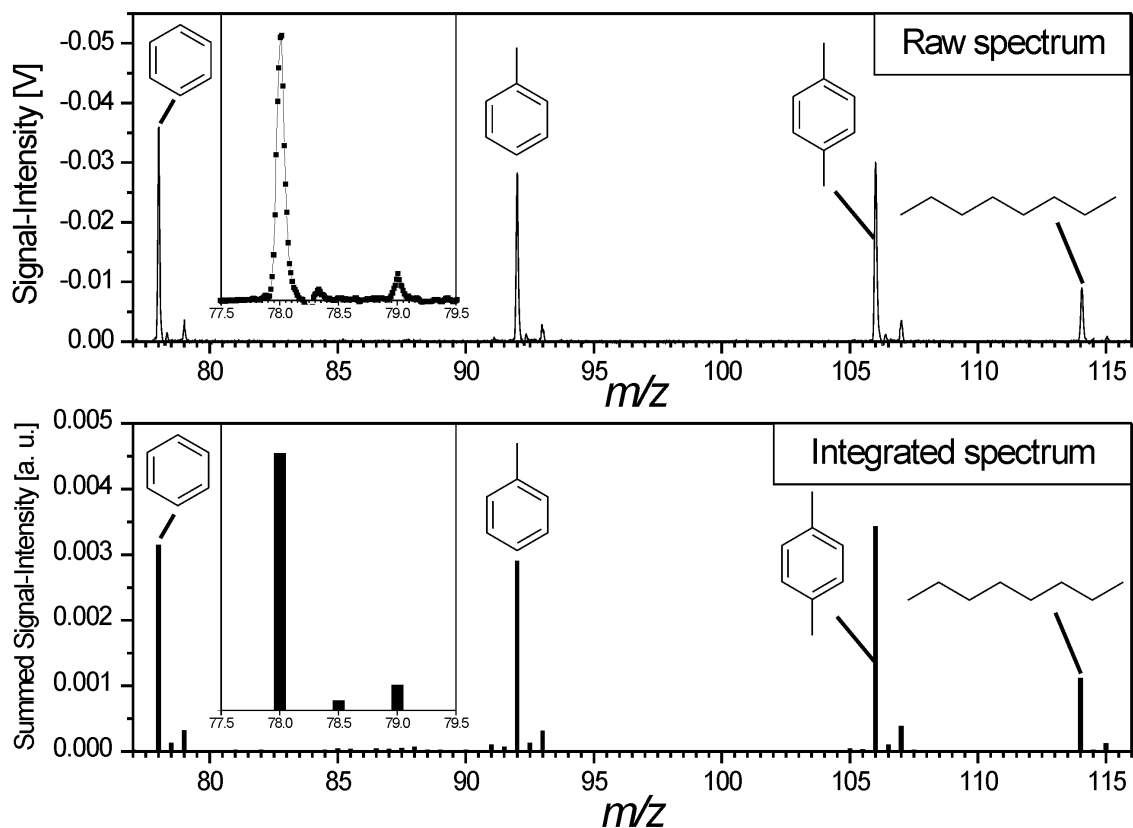
$$d = \frac{rcs}{p - m} \tag{2.4}$$

Figure 2.2: Example for data reduction by integration of peaks of the time-of-flight spectrum of standard gas mixtures (10 ppm in N_2) of benzene, toluene and p-xylene.

The detection limit d is calculated by the product of the concentration of the standard gas c and the standard deviation of the noise levels s multiplied by a factor of the signal-to-noise ratio r and divided by the difference of the signal peak height of standard gas p and the mean value of the noise level (baseline) m. In this study detection limit calculations refer to a signal-to-noise ratio (S/N) r of greater than two. The corresponding REMPI data are strongly dependent on the applied wavelength; therefore, only a short overview is given in Table 2.2. Additional information can be found in refs [71, 73]. The detection limit for chlorobenzene (34 ppb, average 100, S/N > 2) is similar to the value achieved by TONOKURA *et al.* [74]. To prove the linearity of the instrument for SPI, different concentrations of benzene (1000, 500, 250, 10 ppm) were measured. The corresponding ^{13}C and $2 \cdot {}^{13}C$ peaks were used to extend the limits to three orders of magnitude. The results are given in Fig. 2.3. Linearity in the range of four orders of magnitude with a comparable SPI-TOFMS instrument set-up is reported by TONOKURA *et al.* [74]. For the REMPI-TOFMS method, OSER *et al.* demonstrated the linearity for the detection of benzene to be in the range of six [75] and of naphthalene in the range of five [76] orders of magnitude.

Compound	cal. gas [ppm]	Spectra averaged					
		1 [ppb]	2 [ppb]	3 [ppb]	5 [ppb]	10 [ppb]	100 [ppb]
Alkanes							
Pentane	10.2	670	408	393	324	273	105
Hexane	10.5	228	197	170	126	96	38
Heptane	10.2	156	132	110	82	61	23
Alkenes							
Propene	10.8	87	71	45	42	30	10
Butene	10.2	39	30	28	21	15	6
Pentene	9.47	52	42	39	32	22	8
Butadiene	9.2	64	54	37	34	20	8
Isoprene	9.1	93	85	59	45	29	11
Alkynes							
Propyne	9.97	36	26	18	17	12	4
Butyne	9.01	47	36	25	23	16	5
Aromatics							
Benzene	10.0	56	45	46	36	28	16
Toluene	9.3	92	72	66	55	44	25
m-Xylene	9.1	109	89	82	68	53	30
Styrene	9.2	82	71	47	44	27	10
Carbonylic compounds							
Acetaldehyde	11.4	82	92	74	75	43	14
Acetone	10.6	82	92	78	74	39	14
Acroleine	10.5	62	50	38	33	25	8
Other compounds							
Nitric oxide	5110	26322	18330	15443	11920	8878	3094
Nitric dioxide	487	2044	1048	1497	1011	751	282

Table 2.1: SPI limits of detection

2.4 Smoking device

A BORGWALDT single port smoking machine was initially used to generate smoke. Customisation became necessary because of the lack of on-line capabilities of the conventional smoking machine, where the smoke is first aspirated into a glass tube and then blown out by a piston. During initial measurements with the commercial system, significant memory effects from volatile and semivolatile smoke compounds were observed (Fig. 2.5, top). The contamination during the first cleaning puff may

	224 nm	266 nm	272.5 nm
benzene	2.3 ppm	670 ppb	-[a]
aniline	-[a]	7.2 ppb	5.5 ppb
indole	-[a]	2.9 ppb	4.8 ppb
naphthalene	40 ppb	8.4 ppb	22 ppb

Table 2.2: REMPI limits of detection [73].

[a]Compound is not detectable at selected wavelength.

be explained by smoke still present in the dead volume of the cigarette holder. The further presence of compounds strongly indicates condensation and adsorption effects inside the machine. Mixing of the smoke in the glass tube also results in the complete loss of the subpuff time resolution. Therefore, the original Borgwaldt valve was connected directly to a modified and heated Swagelok branch connection, where the sampling capillary could be inserted directly into the sample flow (Fig. 2.4). A membrane sampling pump (KNF-Neuberger, Germany) was installed and adjusted to a continuous flow rate. To protect the pump section from contamination with unfiltered smoke two different particle filter systems can be implemented. The commercially available high performance particle filter and a conventional Cambridge filter pad were used, the latter representing an effective and cheaper way of filtering. The continuous ambient air flow between the cigarette puffs is used to clean the sampling branch connection; however, it is possible to connect any other gas for that purpose. For further cleaning of the sampling system, two additional blank puffs were taken between the smoking puffs. For that purpose the cigarette was removed carefully from its holder. If any contamination was observed during the cleaning puffs, the signal was added to the puff it succeeded. Both smoking machines were compared by their ratio of total ion signal of a single whole smoke puff to the summed ion signals of the succeeding cleaning puffs. For the original Borgwaldt single-port machine, the average contamination is 88.7 % of the original puff area while it is 30.8 % for the custom-built machine (Figure 2.5).

2.5 Cigarette and tobacco samples

The chemical composition of off-gases of a burning cigarette is heavily influenced by the tobacco blend and additives used, as well as physical parameters of the paper and filter. The tobacco itself, especially its chemical composition, is mainly influenced by factors such as soil type and the curing process as illustrated in chapter 1.2. The physical parameters, e. g. pressure drop, filter type and filter ventilation of each brand is designed to match the needs of the smokers. The usage of addi-
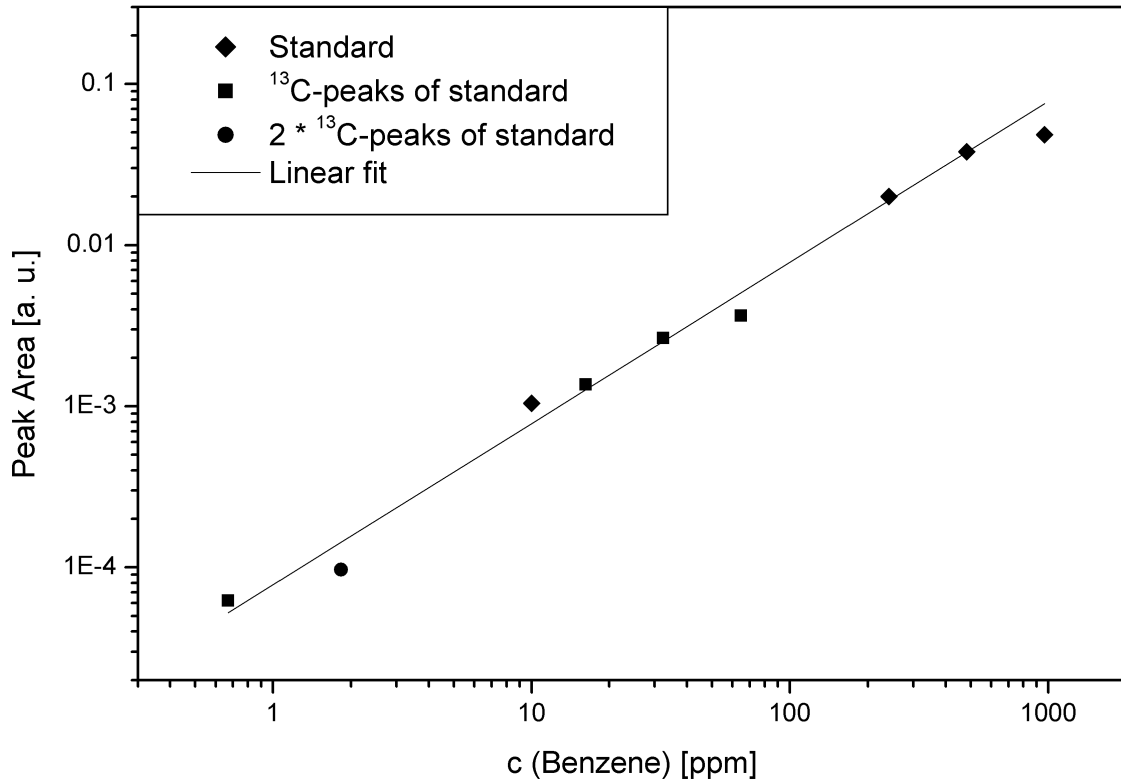
Figure 2.3: Proof of linearity for the TOFMS instrument with SPI [77].

tives as well as varied physical properties makes it difficult to compare different types of commercial cigarettes as one single brand may inhibit different compositions in distinct regions of the world or may evolve within a short period. Therefore a standard cigarette type, the 2R4F Kentucky Research Cigarette is used throughout the experiments, which is blended from four tobacco types, namely Virginia, Burley, Maryland, and Oriental, by the University of Kentucky, Kentucky Tobacco Research & Development Center (KTRDC). The composition is illustrated in Fig. 2.3. In addition to the four tobacco types a relatively large amount of reconstituted tobacco is included. Reconstituted tobacco consists of material which can not be used as filler materials due to its size range and was originally introduced to lower productions costs [78] but can also be used to control taste, burn rate, and smoke composition [78, 79]. Glycerol is commonly used as a humectant at a percentage of 1–3 % to simplify industrial tobacco processing and to improve taste [80, 81]. Invert sugar is a hydrophilic mixture of glucose and fructose which is used to keep the tobacco moist [80]. Filter material, pressure drop and filter ventilation as well as the chemical composition of the 2R4F research cigarette and its predecessor, the 1R4F are thoroughly examined and published in the literature [82].
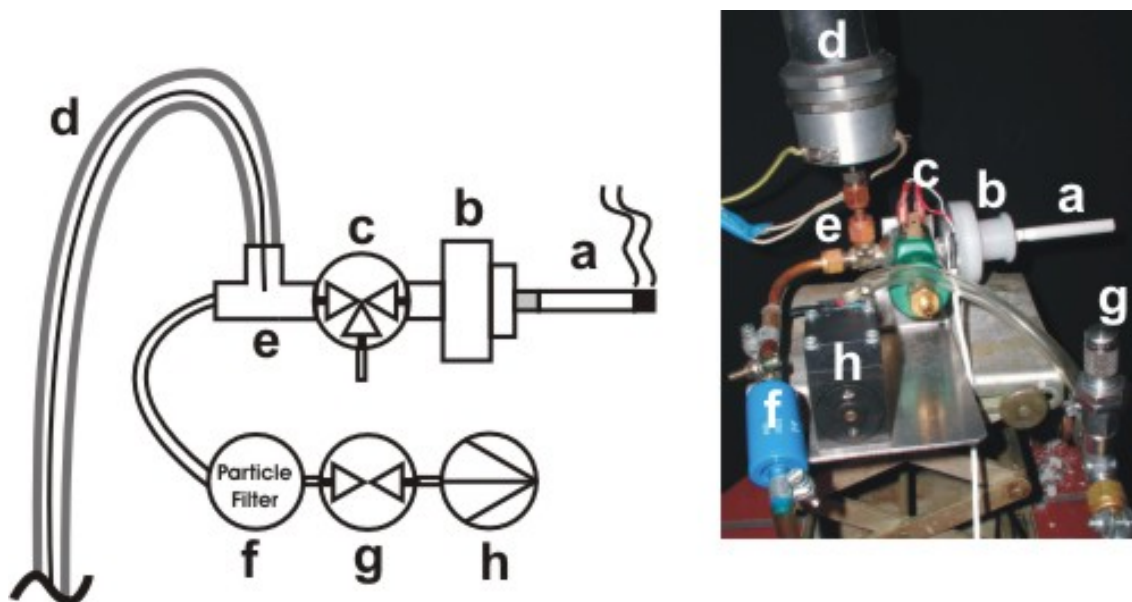
Figure 2.4: Set-up of the newly designed cigarette sampling system: (a) cigarette sample, (b) Cambridge filter holder, (c) original Borgwaldt valve, (d) heated transfer line, (e) heated branch connection, (f) particle filter, (g) flow control, valve, and (h) membrane sampling pump.

Furthermore, a set of pure tobacco cigarettes (Burley, Virginia, and Oriental) with standardised physical parameters was obtained from British American Tobacco (BAT) R&D Centre Southampton, where chemical differences could be observed eliminating the influences of e.g. pressure drop and filter permeability. The mainstream chemical composition was evaluated by ADAM [6, 83]

Constituent	%
Virginia tobacco	32.5
Burley tobacco	20.0
Maryland tobacco	1.06
Oriental tobacco	11.1
Reconstituted tobacco	27.2
Glycerol	2.80
Invert sugar	5.30

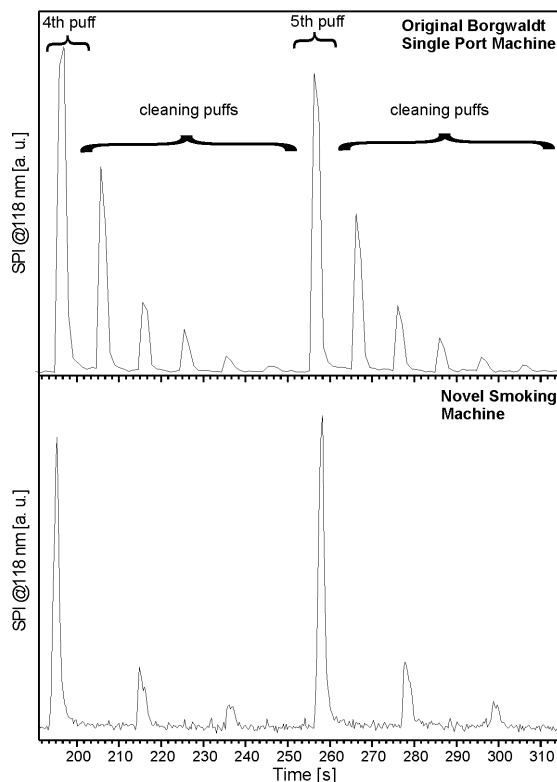*Table 2.3: Percentage composition of the University of Kentucky 2R4F research cigarette [82].*

Figure 2.5: Comparison of the smoking profiles of the original Borgwaldt single-port smoking machine and the novel sampling system, shown for the fourth and fifth puffs of 44 m/z (acetaldehyde) of a 2R4F research cigarette. The cigarette was removed after the main peaks and five cleaning puffs were taken with the old machine, while two were taken with the newly designed system [77].

2.6 Data evaluation

2.6.1 Fragmentation

In principle excited molecules can undergo different pathways to compensate the additional energy. After the absorption of a single photon with energy higher than the ionisation potential, two types of relaxations are known, namely direct ionisation and superionisation. In direct ionisation the molecule decays in an ion and an electron, while in superionisation there are three different possibilities, in fact autoionisation, dissociation and other pathways, the latter contributing only a minor part. The energy extending the ionisation potential is thereby transferred to the molecule, which can lead to fragmentation. The positive charge is usually held by the fragment with the smallest ionisation potential. In Fig. 2.6 the fragmentation behaviour of toluene is presented. Below 11.8 eV no fragmentation of the mother
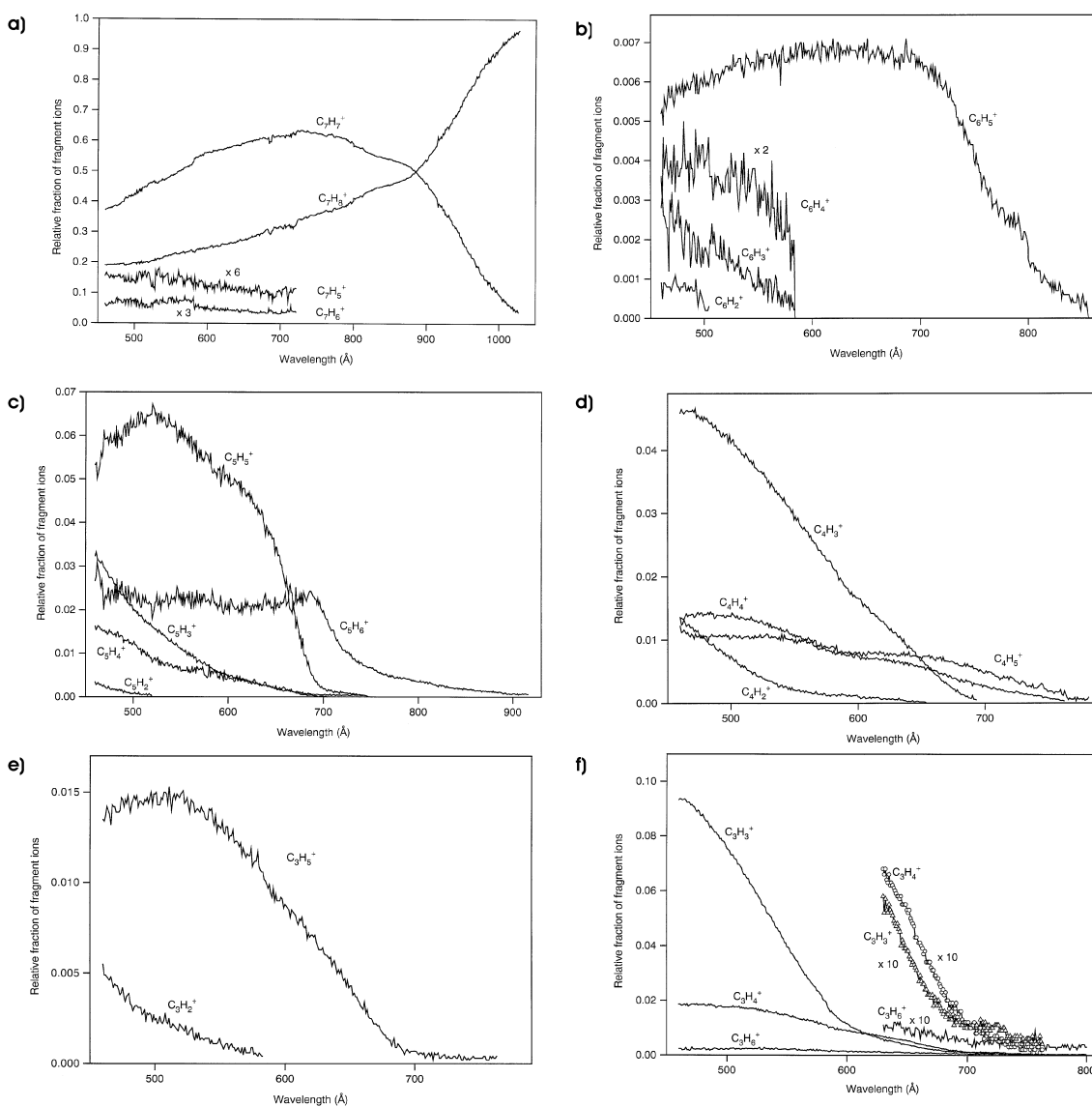
Figure 2.6: VUV-fragmentation pattern of toluene: relative abundance of a) mother ion and C_7-, b) C_6-, c) C_5-, d) C_4-, and e) & f) C_3-fragments [84].

ion can be observed. As shown in Fig. 2.6 a hydrogen atom is split off with higher energies, followed by several other dissociations.The emission of a CH_3-molecule is observed at about 72 nm. Short wavelengths of 50 nm lead to total decomposition of the toluene molecule down to C_3 fragments.

Cooling of internal degrees of freedom of molecules is mainly used in REMPI spectroscopy to achieve more spectroscopic information because of unpopulated higher vibrational states. Therefore the molecules are cooled by means of supersonic beams, which is technically done by jet expansion into the ionisation vacuum. In SPI the loss of thermal energy results in less fragmentation. Fig. 2.8 shows spectra of nonane measured with EI ionisation (a), as well as SPI ionisation with effusive (b) and jet inlet (c). The characterisation of the jet with different buffer gases is shown in Fig. 2.7. The cooling efficiency of supersonic jets is strongly dependant on buffer gas mixture, with increasing efficiency in the order of helium, nitrogen, and argon. In EI only a minor amount of the mother ion $m/z = 128$ can be detected, while the major fragment peaks include $m/z = 41$, 43, 57, 71, and 85. In comparison both SPI spectra show significantly less fragmentation. The heated effusive inlet (T_{rot} ≈ 500 K) shows small fragment peaks on masses $m/z = 56$, 57, 84, 85, and 102, though the highest fragmentation peak at $m/z = 56$ is still only about three times as high as the corresponding ^{13}C-peak of the mother ion at $m/z = 129$. However, the use of a capillary jet inlet system (buffer gas helium, $T_{rot} \approx 200$ K) causes an additional decrease in fragmentation, best seen at the ratio of about 1 : 2 to the corresponding ^{13}C-peak of the mother ion. The application of jet systems to tobacco smoke analysis is rather suited for application with multidimensional techniques such as GCxGCxMS [85] than in the analysis of high-concentrated, complex gas mixtures including semi-volatiles and even low-volatiles such as in tobacco smoke, which would lead to contamination and loss of jet-performance within a short time.

2.6.2 Mass assignment in tobacco samples

The mass spectra recorded by the transient recorder cards were digitally processed in order to obtain data reduction. When two cards are used to increase the dynamic range the two single spectra are merged. The precision of the overlap of both cards is about 1–3 ns. To further reduce the data points in the mass-axis, peaks are integrated to a precision of 0.5 m/z.

Mass assignment can be done by investigation of conventional off-line methods including spectroscopic considerations such as ionisation potential or UV-absorption spectra. Further investigations have been carried out by ADAM [6] to assign more
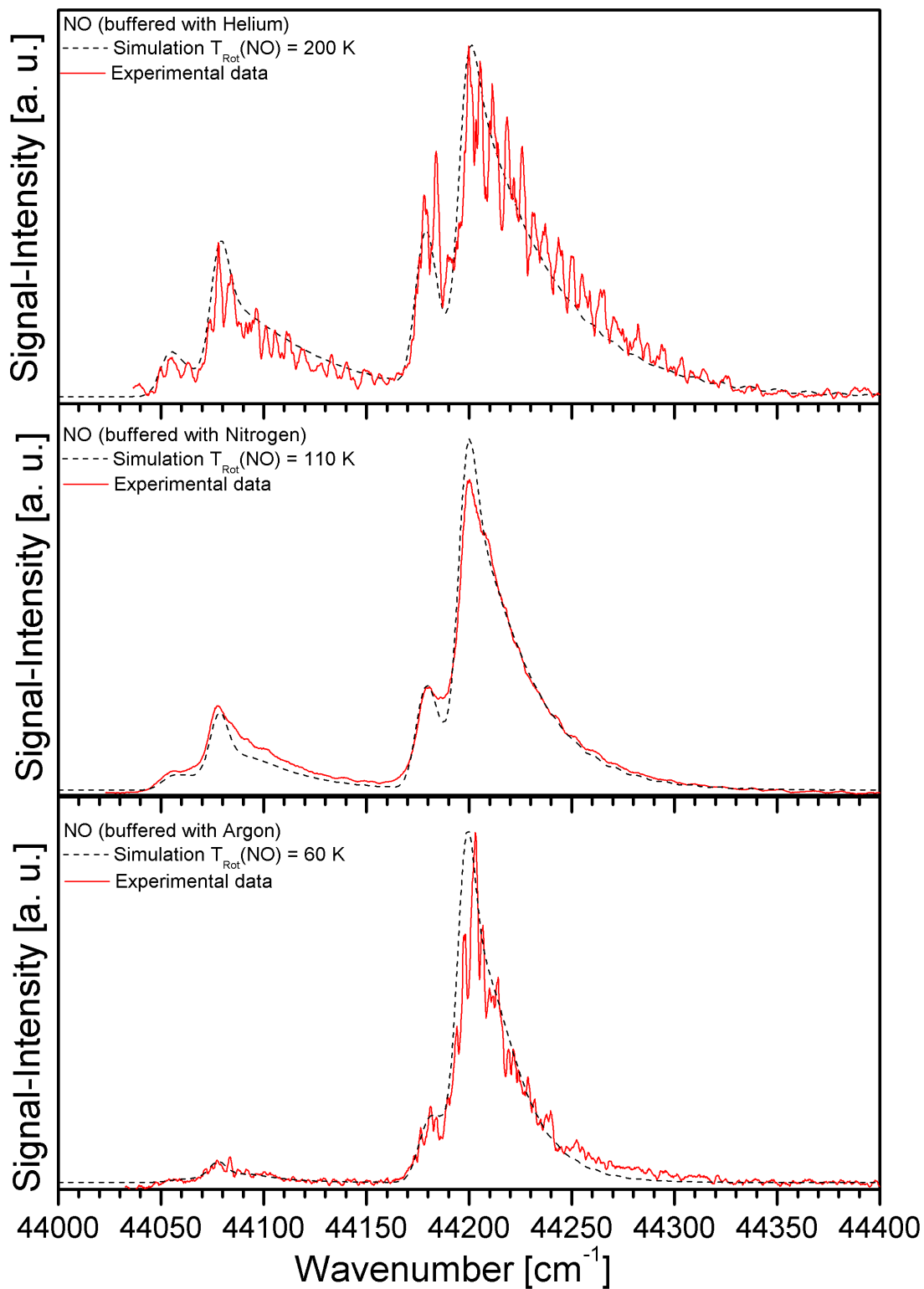
Figure 2.7: Different cooling efficiencies with a capillary cw-jet system in three different buffer gases measured on NO [85].
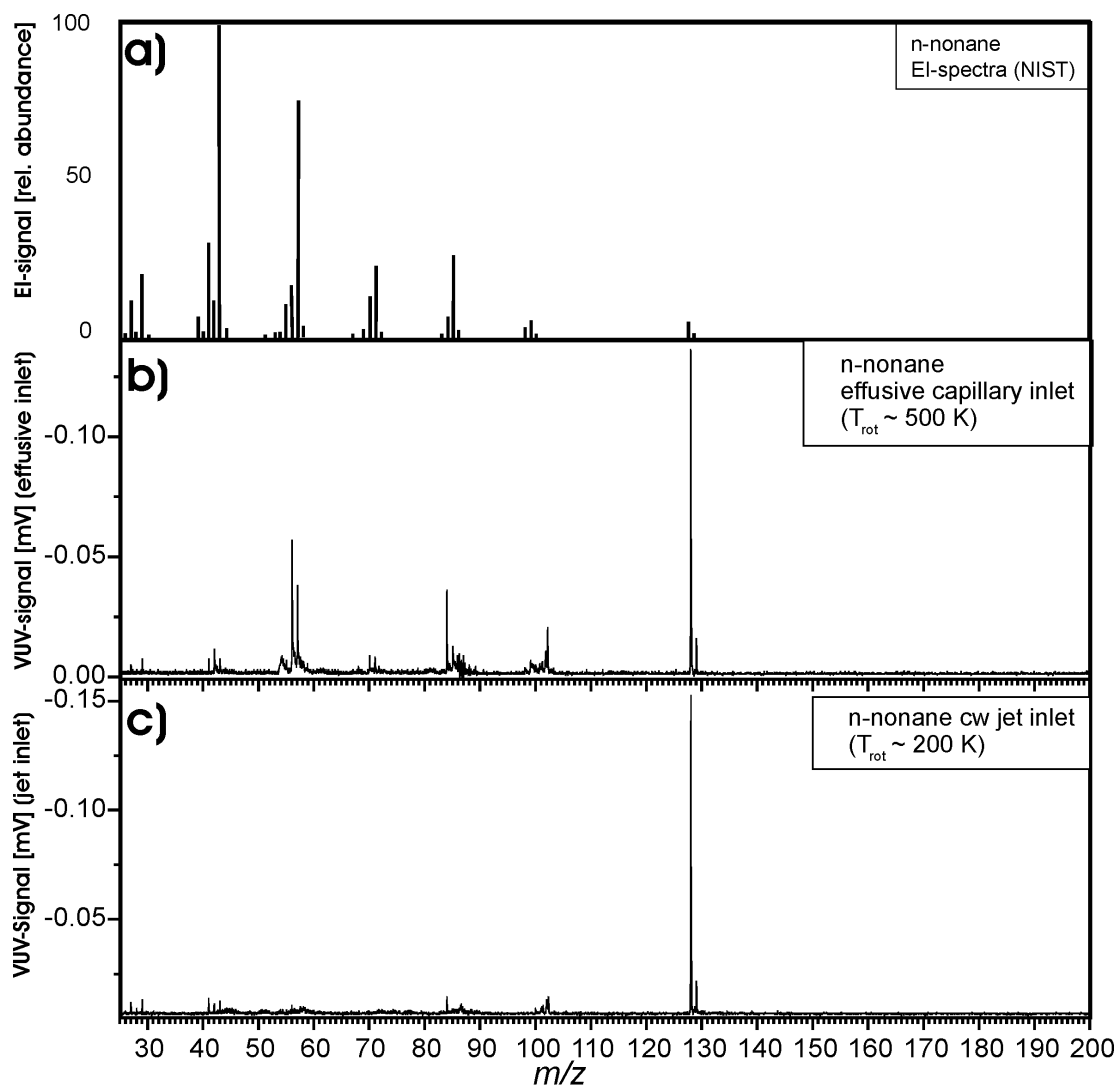
Figure 2.8: Spectra of nonane with a) EI ionisation effusive inlet and SPI ionisation with b) effusive and c) jet inlet [85].

concrete compounds. The very common mass $m/z = 68$ consists of several compounds (furan, isoprene, 1,3-pentadiene, and cyclopentene), of which isoprene and furan have been identified in cigarette main and sidestream smoke [8, 86] and isoprene exceeds furan by a factor of five to ten [40, 78]. The corresponding mass peak $m/z = 68$ can therefore be interpreted as isoprene. Additional information on ionisation potential also proved useful, shown recently for the analysis of gasoline flame studies [87]. In tobacco smoke e. g. in case of the assignment of mass $m/z = 30$, which can in principle be assigned to nitric oxide and formaldehyde, the latter inhibiting an ionisation potential of 10.9 eV and thus is not detectable at a wavelength of 118 nm ($\approx$ 10.5 eV).
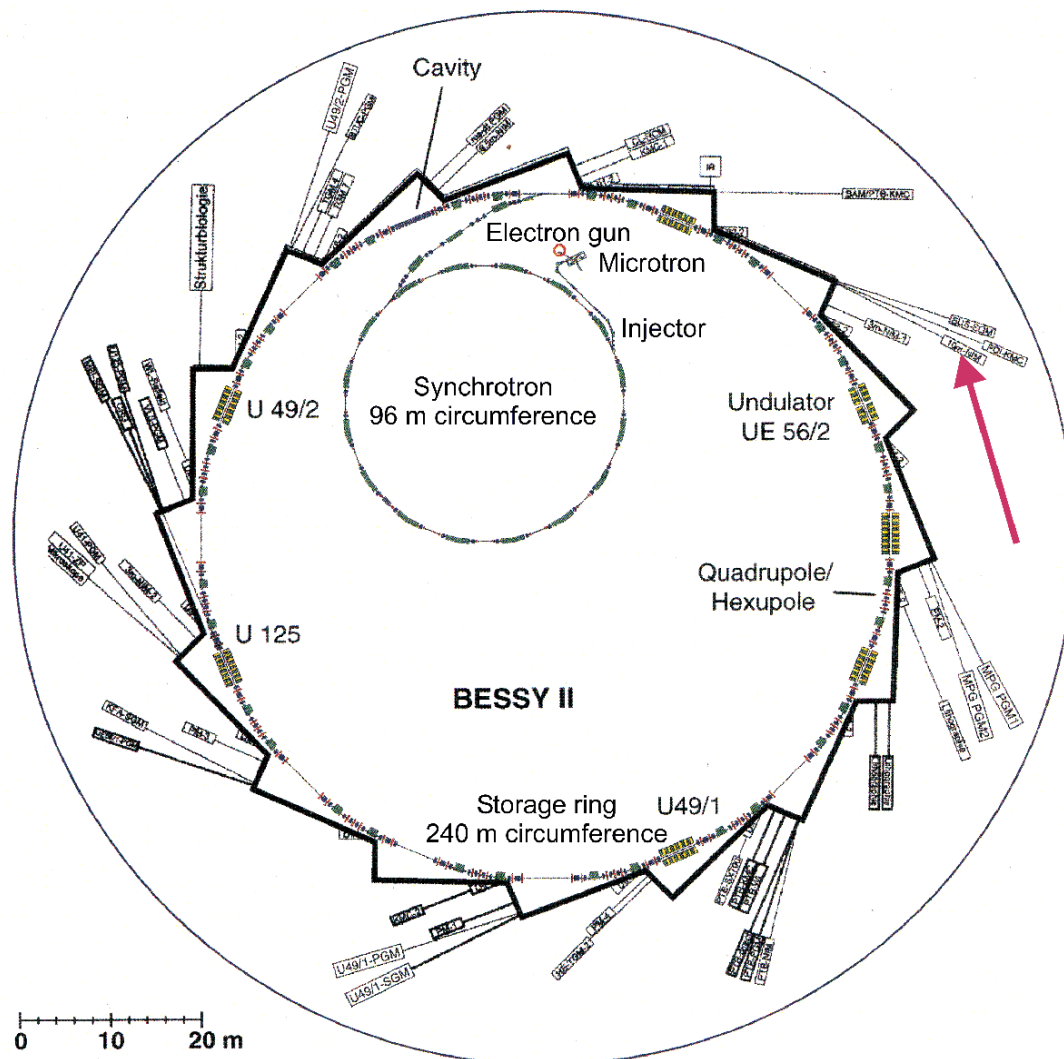
Figure 2.9: Overview of the BESSY II and its beamlines.

Additionally, some measurements on tobacco smoke with tunable synchrotron VUV-radiation have been carried out at the BESSY (Berliner Elektronenspeicherring-Gesellschaft für Synchrotronstrahlung). A schematic overview of the facility and the attached beamlines can be seen in Fig. 2.9. Electrons, which are generated in an ion gun are accelerated in a microtron with a final energy of 50 MeV before being transferred to a synchrotron ring of 96 m circumference with a diameter of $4 \cdot 8$ cm where they are further accelerated to a final energy of 1.7 GeV. The electrons are finally transferred to a storage ring of 240 m circumference. The experiments were carried out at the 10 m-normal incidence (NIM) monochromator beamline [88] at the quasi-periodic undulator stage U125-2 [89] at BESSY-II (marked in Fig. 2.9). This light source can provide tunable radiation in the range from 7–40 eV.
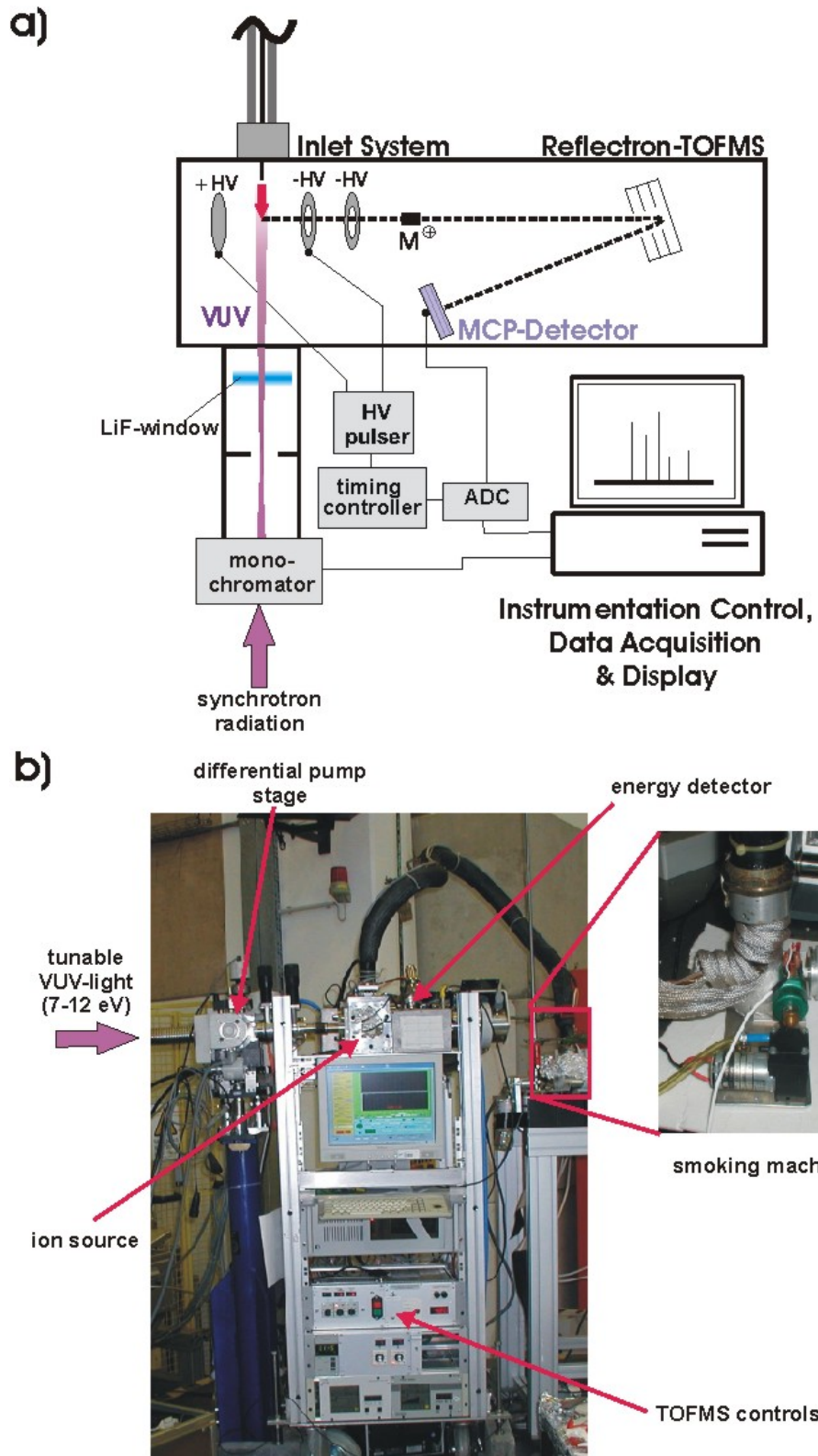
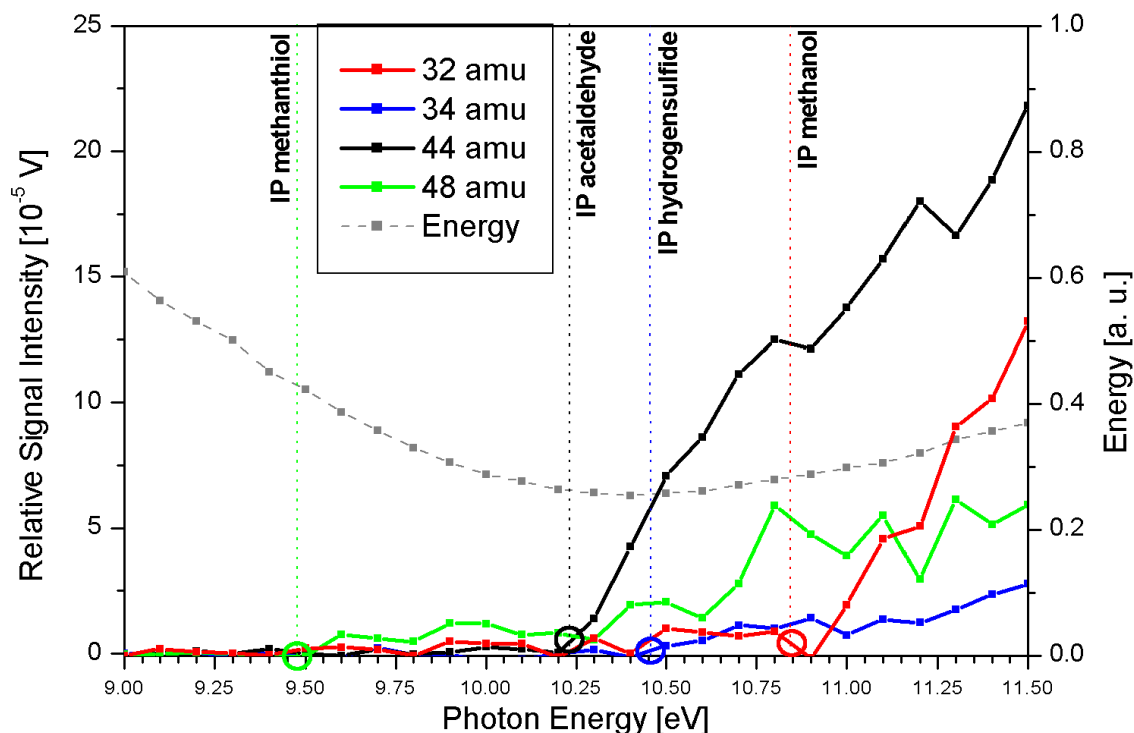*Figure 2.10: Instrumental setup at BESSY II.*

Figure 2.11: Wavelength scan from 9–11.5 eV of masses $m/z = 32$, 34, 44, and 48 in cigarette smoke.

During the experiments cigarette smoke was created from a 2R4F research cigarette by applying constant suction with a flow rate of ≈ 4.5 mL/s on the modified smoking machine, illustrated in section 2.4. The instrumental setup is illustrated in Fig. 2.10. The ionisation chamber of a small mobile TOFMS system, which had been previously used for the analysis of human breath and cigarette smoke [90], was adapted for the application of SPI by synchrotron-generated VUV-radiation. A LiF filter was inserted into the beam path to filter higher harmonic wavelengths, therefore the scan range of the system can be adjusted from 7–12 eV.

To demonstrate the advantages of tunable VUV-radiation for the identification of compounds in complex mixtures Fig. 2.11 shows a selection of four mass traces ($m/z = 32$, 34, 44, and 48). Mass $m/z = 32$ can in principle be assigned to hydrazine (IP = 8.1 eV), methanol (IP = 10.84 eV) and oxygen (IP $\approx$ 12.07 eV). Only hydrazine is detectable with the regular instrumental setup of the smoking experiments, oxygen representing a bulk compound, which is unwanted to be detected during the analysis. At $m/z = 34$, 44 and 48 only single compounds are known to appear in tobacco smoke, namely hydrogen sulphide (IP = 10.457 eV), acetaldehyde (IP = 10.229 eV) and methanthiole (IP = 9.439 eV). Fig. 2.11 illustrates that the detection of these compounds starts at the corresponding ionisation
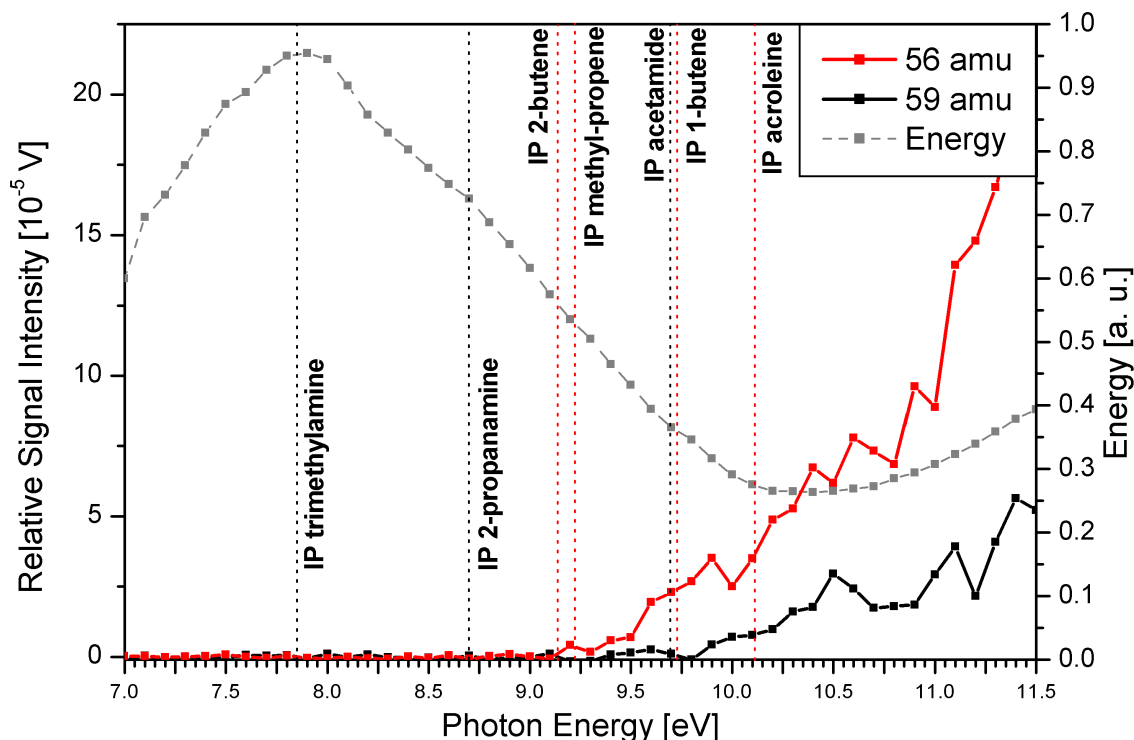
Figure 2.12: Wavelength scan of $m/z = 56$ and 59 in mainstream tobacco smoke.

potentials. Based on this sufficient identification these compounds can be assigned to the corresponding m/z.

As an additional example for identification of compounds in tobacco smoke Fig. 2.12 represents the wavelength scan in the range of 7–11.5 eV for $m/z = 59$ which can in principle be assigned to trimethylamine (IP = 7.85 eV), 2-propanamine (IP = 8.7 eV) and acetamide (IP = 9.96 eV). Under normal burning conditions acetamide gives relatively high yields of $\approx$ 70–100 μg, while both other substances are present in much lower amounts. This is also demonstrated quite well by the graph in Fig. 2.12, which shows a considerable ion-signal only after crossing the IP of acetamide. On $m/z = 56$ acroleine, butene and methyl-propene can be detected. Though acroleine is present in the highest amounts of all three in tobacco smoke ($\approx$ 60–100 μg) the signal increase after crossing the corresponding IP can not be differentiated from the signal increase due to concentration effects. Instead, detection of $m/z = 56$ begins at $\approx$ 9.2 eV, which corresponds very well to the IP of 2-butene (IP = 9.13 eV) and methyl-propene (IP = 9.22 eV). Therefore, with a ionisation energy of 10.5 eV as used in the conventional laboratory setup in this thesis, a sufficient discrimination of acroleine and the other compounds can not be achieved. However, for quantification of acroleine it will be possible to chose a wavelength between acroleine and the other three substances in the future with novel light sources, such as excimer lamp
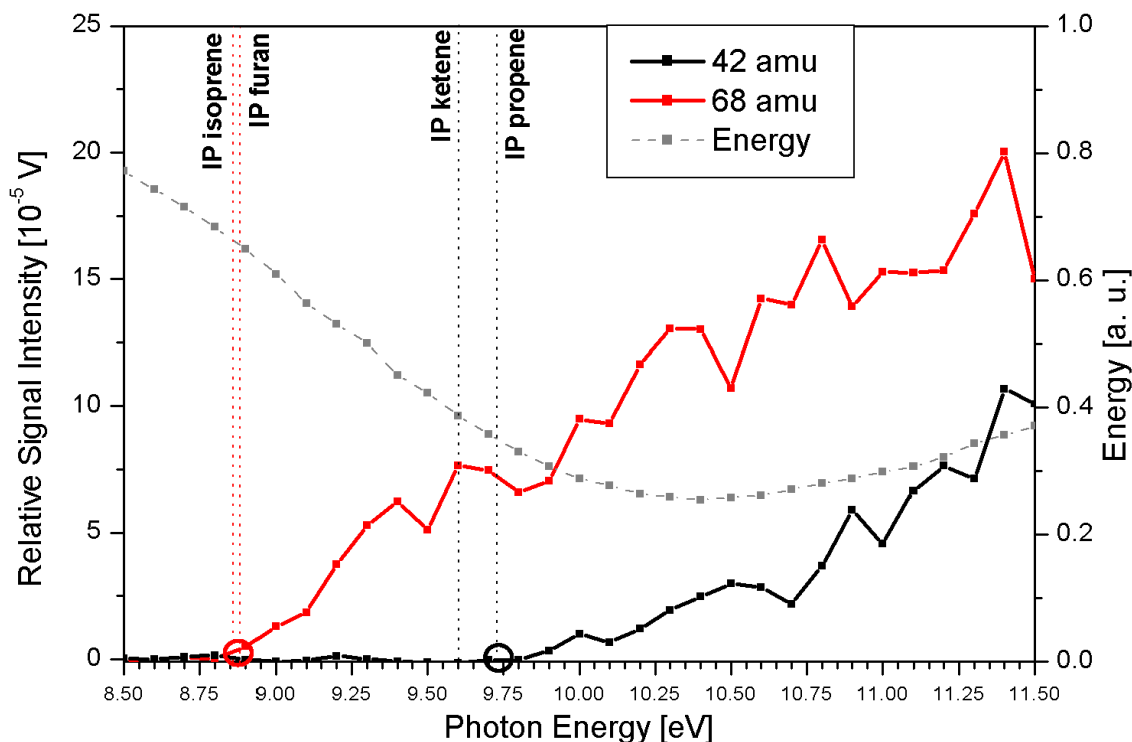
Figure 2.13: Wavelength scan of $m/z = 42$ and 68 in mainstream tobacco smoke.

systems, as the difference between the IPs is big enough and thus determine the part of the signal corresponding to acroleine.

As additional example of the possibilities and limits of mass assignment in Fig. 2.13 the mass traces of $m/z = 42$ and $m/z = 68$ are shown, the first one being occupied by ketene (IP $= 9.61$ eV) and propene (IP $= 9.73$ eV). No significant signal increase can be found after reaching the IP of ketene, the mass trace therefore can be assigned to propene. As already mentioned in this chapter, two substances can be detected for $m/z = 68$, namely isoprene (IP $= 8.86$ eV) and furan (IP $= 8.88$ eV). The difference between these two IPs is too small to achieve a sufficient separation of both compounds in this instrumental setup. Therefore, in this case no valuable information can be obtained throughout the VUV-wavelength scans. In conclusion, the combined knowledge of concentration ranges from off-line experiments, physical parameters, such as IP, and chemical functional groups leads to a efficient method of assigning single compounds to specific m/z.

To clarify the significance of VUV-wavelength scans on future routine analysis and instrument development a list of selected accessible wavelengths and the corresponding sources is presented in Table 2.4. Representatives of the three basic principles for the generation of VUV light (laser-generated, excimer lamps, arc lamps) were cho-

Excimer VUV-Lamps				
gas medium	source of light	centre wavelength [nm]	photon energy at centre wavelength [eV]	bandwidth [nm]
Kr	Kr_2^*	150	8.3	11
Ar	Ar_2^*	126	9.8	9
Ne + H_2	H^*	121.6	10.18	< 0.1
Arc-lamps				
gas medium	source of light	centre wavelength [nm]	photon energy at centre wavelength [eV]	bandwidth [nm]
D_2	D^*	121.6	10.18	< 0.1
	D_2^*	n.a.	n.a.	160–400
Laser generated				
gas medium	source of light	centre wavelength [nm]	photon energy at centre wavelength [eV]	bandwidth [nm]
Xe	THG	118	10.49	n. a.

Table 2.4: Selection of possible wavelengths generated by different light sources.

sen. The laser-generated VUV light, which is commonly used throughout this thesis, has the highest energy of the listed methods. The spectral bandwidth depends on the physical properties of the pump-laser system. The necessity of a laser also represents significant technological effort compared to the other methods. Lamp based sources offer a broad range of different wavelengths, adjustable by the used gas or gas-mixture, while the spectral bandwidth depends on the type of transition which is used for the creation. This results in values reaching from < 0.1 nm (Lyman-α line of hydrogen) to several nanometres. However, the generation of the very narrow Lyman-α line in arc lamps, e. g. deuterium lamps, is accompanied by a spectral continuum from 160–400 nm, which is originating from molecular transitions within the D_2 molecule. Further optical equipment is needed to eliminate this continuum. Furthermore, arc lamps suffer from other disadvantages, such as flickering and burnout of the electrodes, which may lead to additional spectral lines. Therefore, novel excimer lamp systems, which lack these continuums and side-effects, can be used to increase selectivity of the method by carefully selecting the wavelength.

Possible applications to tobacco smoke can be illustrated with Fig. 2.14, where VUV-spectra of tobacco smoke are presented at six different wavelengths from 9.0–11.5 eV. A relatively small amount of substances posesses a IP lower than 9.0 eV. However, it is already possible to select compounds with several m/z, e. g. $m/z = 68$ (isoprene, furan), 92 (toluene), 94 (phenol), 96 (dimethylfurans), and 106 (xylenes, ethyl-benzene). At this wavelength the dimethylfurans are not superimposed by furfural (IP = 9.22 eV) and $m/z = 106$ lacks the presence of benzaldehyde, which
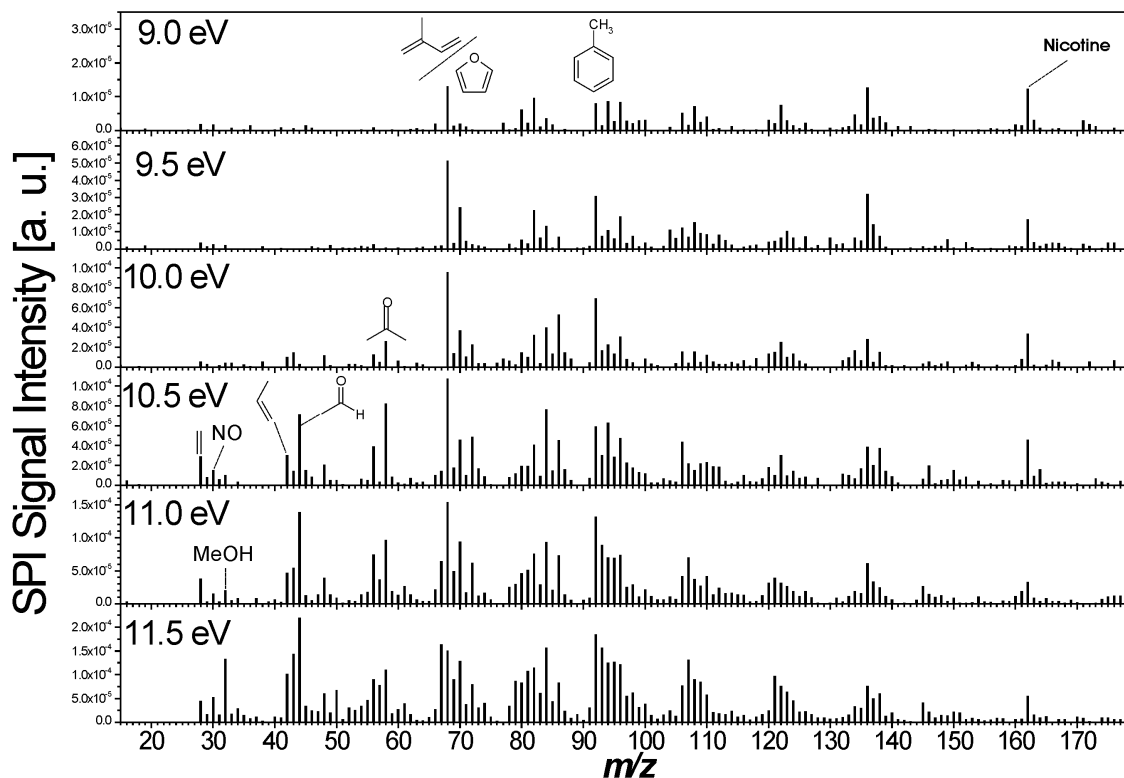
Figure 2.14: Overview of accessible compounds of cigarette smoke at selected wavelengths, exemplarily shown on a 2R4F research cigarette.

can not be detected until an energy of 9.5 eV. Nicotine and anabasine can be detected everywhere in the presented energy range. Though the spectra were normalised to energy the overall concentration increase during the burning of the cigarette, as previously explained by ADAM [6], could not be taken into consideration with this setup. Therefore, changes in signal height can not be associated directly to the detection of an additional compound.

A similar experiment was taken out on cigarette smoke with REMPI, using the OPO system described earlier (chapter 2.3). In REMPI the intermediate excited state of the target molecule can provide additional information about the molecule. In the usable wavelength region of the instrument of 219–375 nm, the wavelength region where aromatic ring systems in general show high ionisation efficiencies is included. The instrumental setup is outlined in Fig. 2.15. A glass chamber of 22.5 L volume was filled with several 35 ml puffs of a 2R4F research cigarette within 10–20 s. Though the smoke is continuously drawn out of the chamber at about 8 mL/min the total volume is sufficient to avoid a significant decrease in concentration during the measurement. To observe effects of aging and deposition all scans were repeated from higher to lower energies and vice versa. The spectra were recorded in two
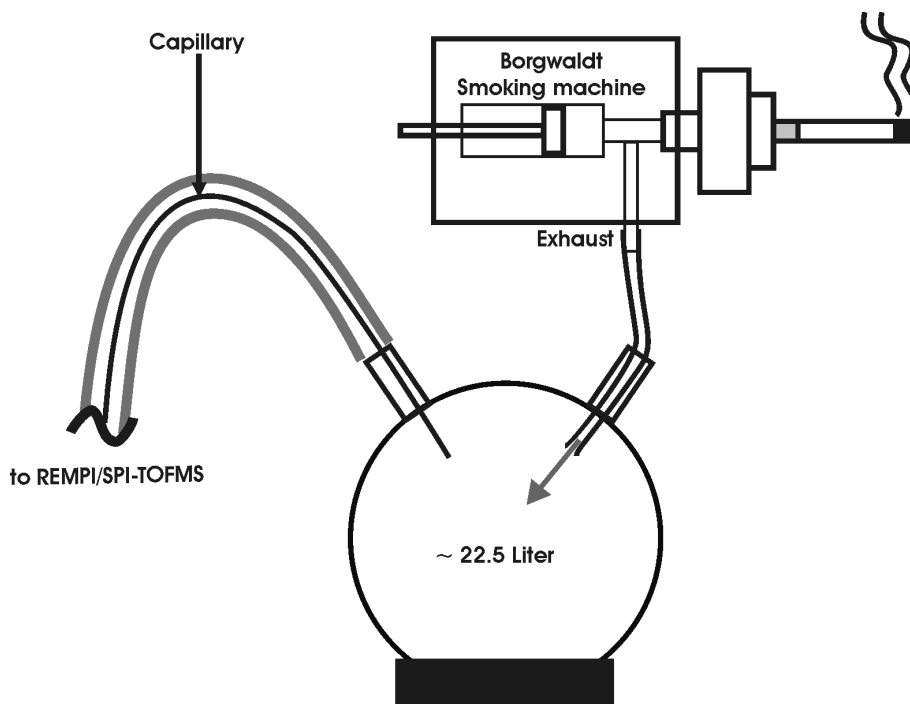
Figure 2.15: Experimental setup for the REMPI wavelength scans on tobacco smoke.

steps, ranging from 220–257 nm and 257–320 nm at a rate of 2 nm/min. The energy of each laser pulse was recorded, the resulting raw spectra are normalised with a polynominal fit of the recorded energy to eliminate energy-related signal fluctuations. Several measurement points at 266 nm were erased, since an exceptional high energy peak at this wavelength could not be fitted sufficiently.

An overview of the whole REMPI wavelength scan from 225–320 nm of mainstream smoke is shown in Fig. 2.16. Because of the high intensities of $m/z = 30$, 78, 92, and 106 the corresponding mass traces are divided by factors of 20, 5, 10, and 10, respectively.

As a first example of visual spectrum comparison to identify possible ingredients in complex matrices the combined spectra of mass traces $m/z = 78$, 92, 106, and 120 in tobacco smoke (a) and three reference spectra of benzene (a), toluene (b) and xylene (c) [73] are presented in Fig. 2.17. $m/z = 78$, 92 and 106 correspond very well to the effusive spectra of benzene, toluene and xylene at $T_{Rot} \approx 300$ K. However, several effects have to be taken into consideration when visually comparing REMPI spectra. The reference spectra are recorded with a smaller laser bandwidth (half-width of the energy distribution ≈ 0.1 cm^{-1} compared to 5 cm^{-1} of the OPO system). As a conclusion, the energy of a laser system with small bandwidth is concentrated on a smaller range than with a broader one. At an equally high energy the maximum of the energy distribution of the narrow laser system is 50 times higher. This has severe
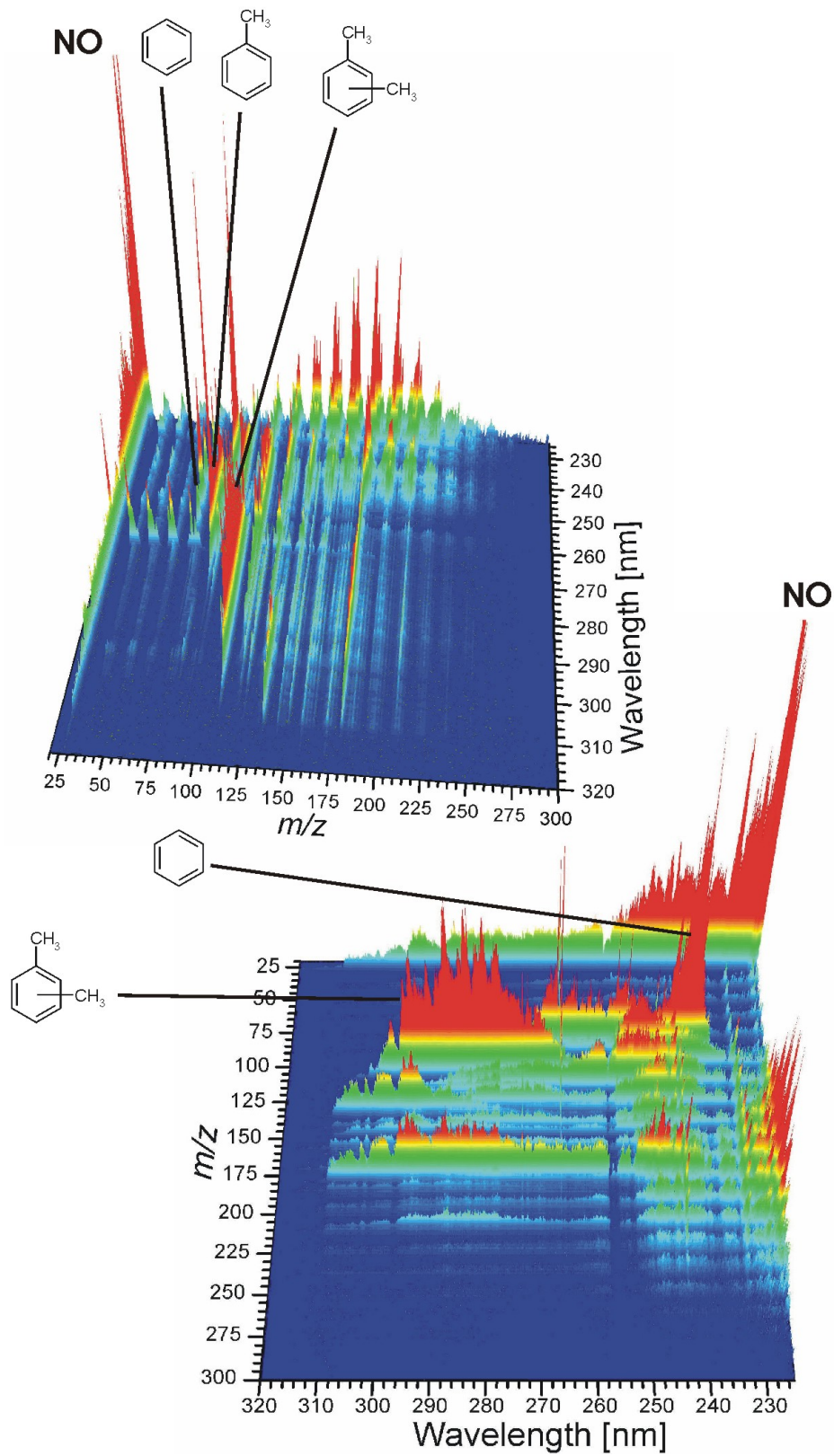
Figure 2.16: 3D plot of REMPI scan from 225–320 nm of mainstream smoke.

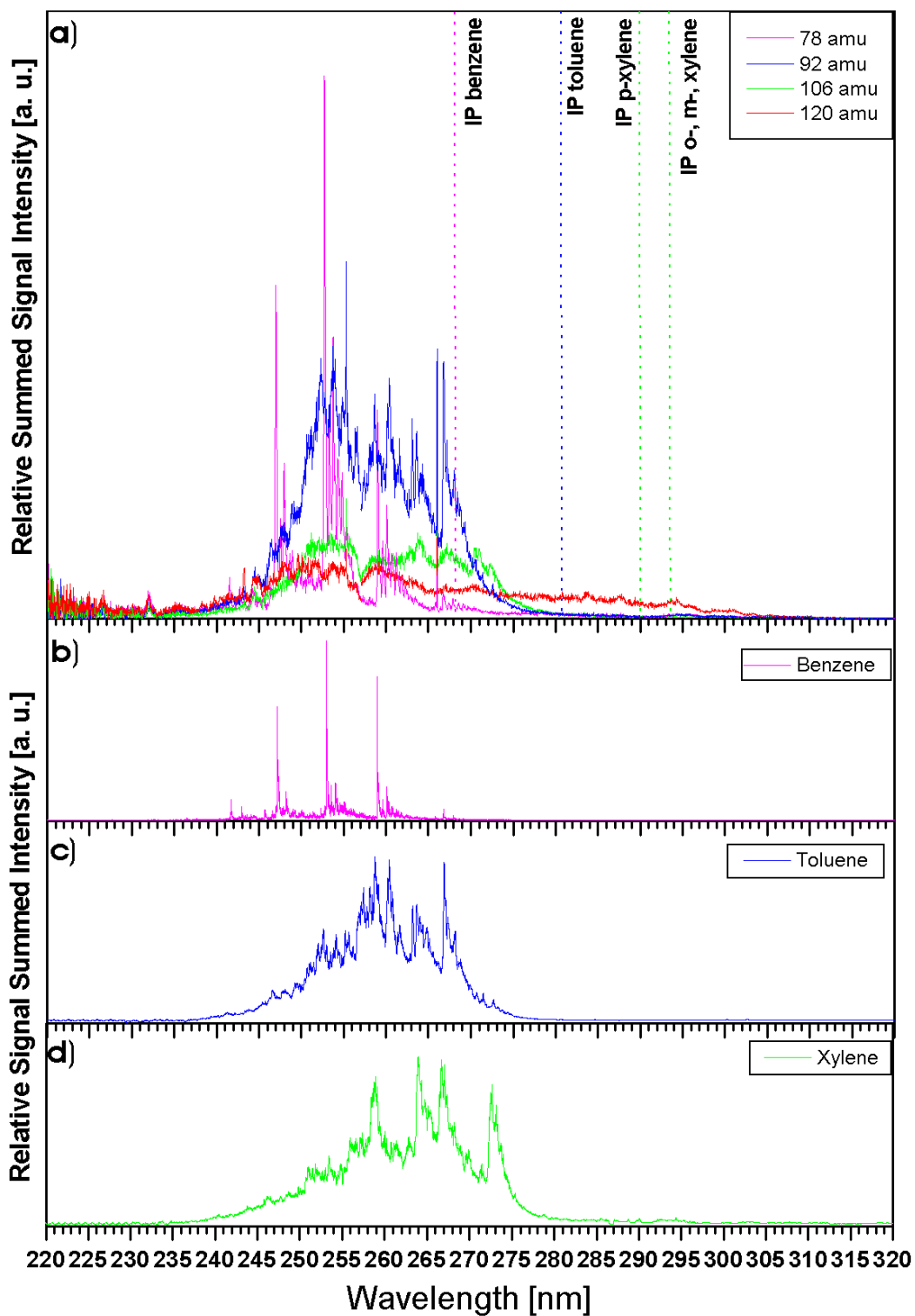*Figure 2.17: REMPI scans of m/z=78 (benzene), 92 (toluene) and 106 (xylenes). Spectra a) are measured in tobacco smoke, b), c) and d) show reference spectra of benzene, toluene and xylene.*

effects on molecule spectra with sharp bands, as the sharp bands are superimposed by the spectral width of the broader OPO system and only a small portion of the total energy is used for the excitation. Therefore, sharp bands are not as intense in the used instrumental setup compared to the reference spectra. Additionally, the reference spectrum of *p*-xylene represents one isomer, while the spectrum in tobacco smoke describes the chemical composition of the three xylenes and possible superimposition with ethyl-benzene. The spectra of $m/z = 92$ (toluene) and $m/z = 106$ (isomeric xylenes) clarify the character of resonant ionisation methods: although the ionisation potential, IP = 8.828 eV (for toluene) and IP = 8.45–8.56 eV (for the xylenes) are not reached, the ionisation efficiencies drop by several orders of magnitude after leaving the region, where sufficient intermediate molecule states are present ($\lambda > 270$ nm for toluene and $\lambda > 275$ nm for xylenes). However, methylated aromatics, such as toluene and the isomeric xylenes, usually feature a broader, more complex spectrum due to free rotation of the methyl groups.

The combination with jet inlet systems can lead to extremely narrow excitation bands and enable a detection and separation of single isomeric compounds with extraordinary limits of detection, as shown in the application to polychlorinated dibenzo-p-dioxins, biphenyls and benzenes [91].

As an additional example for visual interpretation of REMPI spectra of tobacco smoke the spectra of $m/z = 30$ and 180 (a), $m/z = 117$ (b), as well as a reference spectrum for indole [73] (c) is presented in Fig. 2.18. The enlarged view of the sharp peak of $m/z = 30$ at ≈ 226 nm shows very good compliance with NO, which has been presented at several T_{Rot} earlier in this chapter (Fig. 2.7). Both spectra b) and c) show good agreement as well. $m/z = 180$ can be still ionised at red shifted wavelengths. The spectrum of $m/z = 136$ (not shown) shows almost identical behaviour ranging from 285–290 nm, which could result from fragmentation of $m/z = 180$ to 136.

As a final example of possibilities and limits of visual interpretation of REMPI spectra for the assignment of single compounds to specific m/z the wavelength scans of $m/z = 110$ and 124 are presented in Fig. 2.19. On $m/z = 110$ several compounds are known, dominated by hydroquinone and catechole and including methyl-furfural. No full reference spectrum of the three uncooled isomeric dihydroxy-benzenes hydroquinone, resorcinol and catechol could be obtained from the literature in the range from 222–320 nm. However, the high resolution multi photon spectra of these substances were published by DUNN *et al.* In the jet-cooled spectrum hydroquinone exhibits two main excited states at 298.51 nm and 298.21 nm, resorcinol three at 278.17 nm, 276.50 and 276.3 nm and catechol three at 280.52 nm, 279.64 nm and 278.55 nm. Though an interpretation of the mixture of these isomers and the lack of jet-cooling makes it difficult to assign certain values to this m/z strong REMPI-
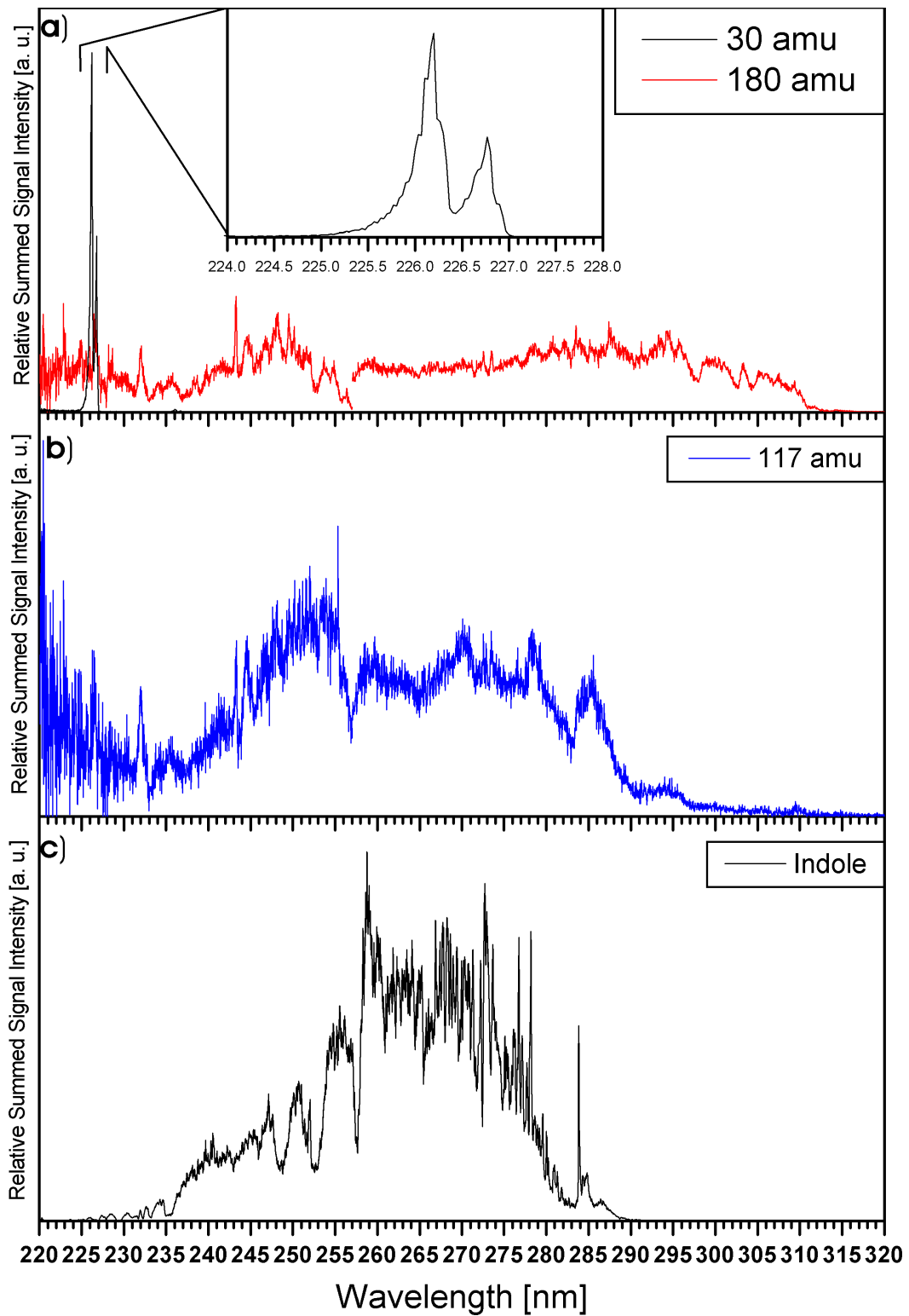
Figure 2.18: Wavelength scan of $m/z = 30$ and 180 (a) and $m/z = 117$ (b) in tobacco smoke and reference spectrum of indole (c).
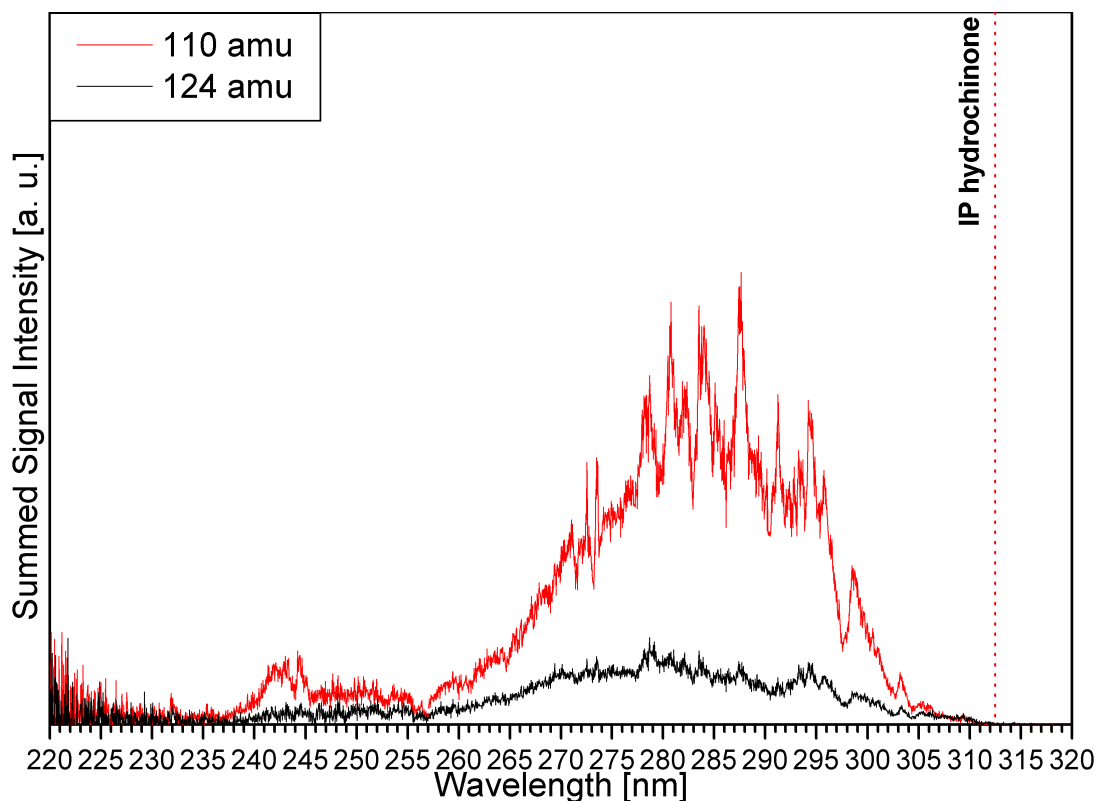
Figure 2.19: REMPI-wavelength scan of $m/z = 110$ and 124 in tobacco smoke.

signals can be obtained at ≈ 280.5 nm, 278–279 nm and 298.5 nm indicating the presence of all of the isomers. However, none of the molecules show strong absorption at 287.5 nm and quantification is not possible without the knowledge of relative cross-sections, as the spectrum rather reflects the spectroscopic properties of the isomers. Methyl-hydroquinone, methyl-catecholes, guaiacol, 2-acetyl-5-methylfuran are found on $m/z = 124$. Although there is no spectroscopy available on these substances the spectrum shows great similarity from 255 to 305 nm indicating structural similarities of the compounds.

A list of observed masses and possible compound assignments can be found in the appendix (Table B.1). The list combines information about occurrence in tobacco and tobacco leaf, and of course, due to the enormous amount of information available, only represents a small part of the total published information. However, the table combines information of a detailed review about tobacco smoke and leaf in general by STEDMAN [8] and several later publications about the leaf composition of single tobacco types [11, 12, 14–17], as well as numerous articles on tobacco smoke and pyrolysis off-gas composition. Additionally, available information on IP and structure have been collected, which may be utilised to select appropriate wavelengths for SPI, e. g. with future applications of excimer gas lamps filled with different gases or gas

Substance	Relative Cross-Sections		
	this work (relative signal height)	this work (35 ml puff)	*Adam* [6] (relative signal height)
Acetaldehyde	0.21	0.22	0.20
Acetone	0.33	0.35	0.31
Acroleine	0.26	0.27	0.22
Ammonia	0.01	< LOD	n. a.
Benzene	1.00	1.00	1.00
Butadiene	0.56	0.61	0.60
Butene	0.36	0.33	0.37
Butyne	0.88	0.81	0.91
Isoprene	0.55	0.58	0.59
n-Heptane	0.19	0.16	0.16
n-Hexane	0.11	0.10	0.11
Pentene	0.31	0.28	0.34
Propene	0.36	0.35	0.39
Propyne	0.84	0.80	0.86
Styrene	1.03	0.53	1.13
Toluene	0.96	0.81	0.87
Xylene	1.03	0.68	0.91

Table 2.5: Relative cross-sections of selected tobacco smoke ingredients.

mixtures. Moreover, the detectability with REMPI is indicated by the presence of aromatic systems. However, some masses are occupied by a large number of compounds. Therefore, in the context of this thesis only the compounds which are considered to be most likely are presented within the text, as complete information can be extracted from the appendix.

2.7 Quantification

The method of quantification for puff-resolved measurements is based on the method developed by *Adam* [6] using standard puffs with calibration gases. For the quantification of selected tobacco compounds a predefined concentration of a standard mixture in nitrogen is put into a gas container from which puffs are drawn with the smoking machine (e. g. 35 ml, 2 seconds duration under ISO conditions). The peak integral of the corresponding mass then equals the amount of substance present in 35 ml. However, due to the nature of photo ionisation the ratios of the integrals of different compounds remains constant. This concept of relative cross-sections was also described by *Adam* [6] and is used for the quantification of the data in this

work.

The relative cross-sections are determined for different puff volumes by a set of calibration gases ($\approx$ 10 ppm in nitrogen) and standardised to the benzene value. The results are exhibited in Table 2.5. It can be seen that during the measurements of the integral with a standard 35 ml puff and a puff duration of 2 s significant loss of aromatic compounds occurs. This phenomenon originates from a high affinity of the aromatic compounds to the teflon coating of the bags used.

For the quantification of sidestream smoke puff-resolved measurements are not necessary. Therefore standard gas mixtures can be directly measured. The amount m_x of a substance x with the known concentration of c_x in the volume element flowing beneath the tip of the capillary and analysed by a laser shot can be calculated with the corresponding molar Mass M_x, the measurement frequency f, the molar volume V_m and the flow rate of the analysed gas $\dot{V}_{tip}$. The flow rate into the instrument $\dot{V}_{instr}$ can be cancelled down as follows:

$$m_x = \frac{\dot{V}_{tip}}{\dot{V}_{instr}} \cdot \dot{V}_{instr} \cdot V_m \cdot \frac{1}{f} \cdot c_x \cdot M_x \qquad (2.5)$$

The measured signal intensity of the corresponding peak of the mass spectrum is then used as reference value. For measurements with constant flow rates during the whole experiment, e. g. sidestream smoke analysis, the summed ion count can be used to calculate the amount, whereas in experiments with frequently changing flow conditions, such as the analysis of human smoking behaviour, it is necessary to calculate the amount stepwise for every different flow rate.

2.8 Statistical methods

2.8.1 Fisher values

Differences between single data sets often can not be seen with the human eye only. Therefore it is necessary to apply statistical methods. A common, simple, mathematically reliable, and effective way to get information about single data points which can be used to differentiate between whole data sets are Fisher-Ratios (also called Fisher values (FV). FISHER suggested a criterion for selection of features in terms of their discriminative power in the case of a two-way classification problem [92]. Accordingly, the pair wise Fisher-Ratio between any two classes is defined as the ratio of between-class scatter and within-class scatter. The best features in descending order of the Fisher-Ratios can then be selected for the classification task [93–96]. In

addition, the Fisher criterion can be extended to multi-class problems enabling the simultaneous distinction between several groups [97, 98].

For the calculation of the Fisher-Ratios the mass spectra were normalised to total ion signal to eliminate influences on absolute mass signal values due to slightly changing experimental conditions (e.g. air flows, laser power etc.) (equation 2.6). The new variables obtained were calculated according to

$$y_k = \frac{x_k}{\sum x_k} \tag{2.6}$$

where x_k is the observed integrated ion signal in the average spectrum for compound k. From a set of measurements, the corresponding mean value μ_k and standard deviation σ_k for a compound k is calculated from the individual measurements values y_k. Fisher-Ratios were calculated for two classes according to [98] as

$$F_{ijk} = \frac{(\mu_{ik} - \mu_{jk})}{\sigma_{ik}^2 + \sigma_{jk}^2} \tag{2.7}$$

Here μ_{ik} and μ_{jk} denote the means for the kth compound in classes i and j, σ_{ik}^2 and σ_{jk}^2 are the corresponding variances, respectively. It can be seen that the Fisher-Ratio becomes largest when inter-class separation is high and intra-class variability is minimised.

The extension to three classes was calculated with

$$F_k = \frac{1}{J(J-1)} \frac{\sum_{i=1}^{J} \sum_{j=1}^{J} P_i P_j F_{ijk}}{\sum_{i=1}^{J} \sum_{j=1}^{J} P_i P_j} \; ; \; i \neq j \tag{2.8}$$

according to KRISHNAN *et al.* [98], where P_i and P_j are the a priori probabilities of the classes i and j, respectively, and J describes the total number of classes. Usually the test set was regarded as a fair representation and thus the probabilities as proportional to the number of performed measurements.

2.8.2 Principal component analysis

In general, modern analysis techniques enable powerful and sophisticated investigations of all sorts of samples. At the same time the immense amount of data obtained often requires reduced datasets in order to focus on the most relevant features. In this way, chemometrics, the application of mathematical or statistical methods to scientific data, has gained great influence in modern analytical chemistry [99], which is expressed in the great number of publications and textbooks dealing with this topic, e.g. [100–106]. In this context Principal Component Analysis (PCA) is

only one common method of choice. It basically seeks to reduce the dimensionality of a dataset consisting of a large number of interrelated variables, while retaining as much of the present variation as possible. This is achieved by transformation to a new set of variables, the Principal Components (PCs), which are uncorrelated and ordered so that the first few components contain most of the variation of the entire original data set. The PCA is based on the covariance matrix of the entire data set. The eigenvectors of the covariance matrix are the so-called loading vectors (which projects the original data to the new space spanned by the Principal Components) and the respective eigenvalues represent the fraction of the variance explained by the Principal Component. Often a projection of the original data spanned by the first two PCs is sufficient. The outcome of PCA is mostly depicted by two two-dimensional plots, the loading-plot and the score-plot. The loading-plot visualises the influence of the original variables on the respective Principal Components, the scores are the projected data in the lower dimensional subspace defined by the PCs [107–109]. In respect of agricultural goods it is widely applied for classification or characterisation, such as beverages e.g. [110–122], tobacco e.g. [86, 123–125], and foods e.g. [126–131]. The first step of processing the dataset was performed by normalisation to total ion signal and autoscaling. Autoscaling is often useful when variables span different ranges in order to make the variables of equal importance. It is carried out by mean centering the data, i.e. subtracting the mean and subsequent variance scaling, i.e. division by the standard deviation to make the data independent of scaling [105, 107, 108, 132]. Pre-selection of relevant masses was done by calculating the Fisher-Ratios as described in the previous section.

3 Thermal Desorption of Tobacco

3.1 Basics of thermal analysis

Pyrolysis as well as thermal analysis in combination with mass spectrometry or gas chromatography (Py-MS or Py-GC/MS as well as TGA-MS and TGA-GC/MS) are well established and reliable methods for the analytical investigation of polymers, see e.g. [133–139] providing classic approaches for degradation of large molecules and subsequent analysis of the pyrolytic or thermally evolved products. In recent years, several other analytical techniques have also been utilised for the investigation of pyrolysis products, e.g. Fourier transform ion cyclotron resonance mass spectrometry (FT-ICR-MS) [140], infrared spectroscopy (IR) [141], and comprehensive two-dimensional gas chromatography (GCxGC). However, thermal desorption and pyrolysis also allow the quality control of various food products e. g. Italian vinegar [131,142], milk [130], saffron [143] and olive oils [144]. In this context, tobacco is a very challenging biomatrix because of the large number of substances present in the feedstock as well as in the generated thermal degradation products. Most of these species are present at trace levels, indicating the necessity of highly sensitive analytical techniques for sufficient monitoring of such products. In the past, a wide range of pyrolysis and TGA studies on tobacco, e.g. [4,145–154] has been carried out, mainly by application of conventional analytical methods such as gas chromatography/mass spectrometry and Fourier transformed infrared spectroscopy (FT-IR). However, in recent years, application of soft ionisation methods, e.g. molecular beam mass spectrometry [86] and field ionisation mass spectrometry [123,151] coupled to pyrolysis devices has been of growing interest. Soft ionisation in mass spectrometry offers the advantage that, despite the complexity of the matrix tobacco, a fast and comprehensive characterisation of the evolved gas is possible in contrast to techniques such as EI that cause fragmentation and thus further complicate the interpretation of the resulting mass spectra.
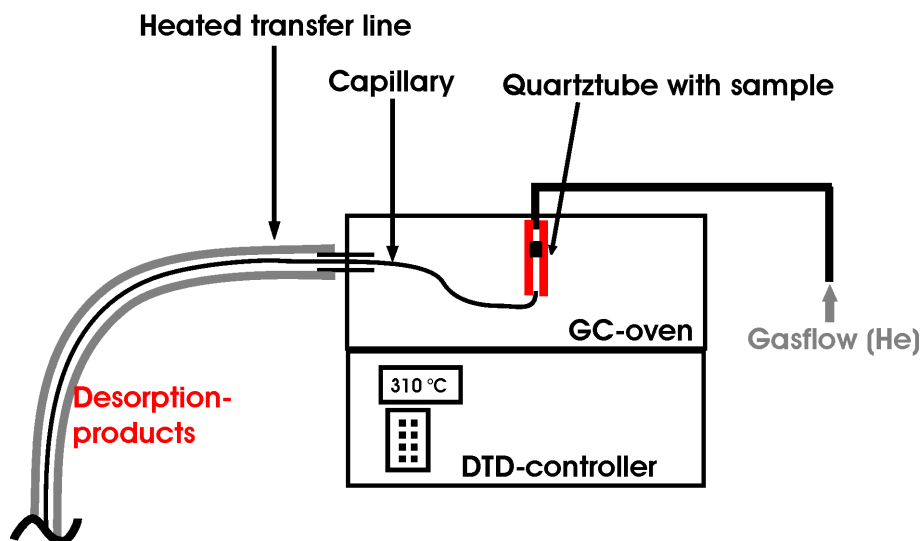
Figure 3.1: *Schematic overview of the desorption experiments.*

3.2 Experimental setup of the thermodesorption/pyrolysis experiments

Three different single tobacco samples have been investigated in this study, viz. Burley, Virginia and Oriental. Prior to thermal treatment, 5 mg of tobacco was ground. Overall, six replicates with both REMPI-TOFMS and SPI-TOFMS have been measured for every tobacco sample. A schematic overview of the instrumental setup is shown in Figure 3.1. The ground tobacco samples were put in a quartz glass liner, which is inserted into a GC injector heatable up to 350 °C. A temperature program including three steps (190 °C, 250 °C, 310 °C) was used. These values were based on observations by Fenner [155, 156]. Temperature steps were adjusted by means of maximum possible heating rate (approx. 80 K/s). It took about one to two seconds to move to the next temperature. Evolved compounds were detected until no SPI- or REMPI-TOFMS signal could be observed anymore, thus ensuring that all desorbed species have been detected before moving on to the next temperature step. All single mass spectra at every temperature step were added up subsequently.

3.3 Results of the thermodesorption/pyrolysis experiments

Fig. 3.2 shows the total ion profiles of both REMPI@275 nm and SPI@118 nm as functions of the measurement time. In the graph at the top, the respective desorp-
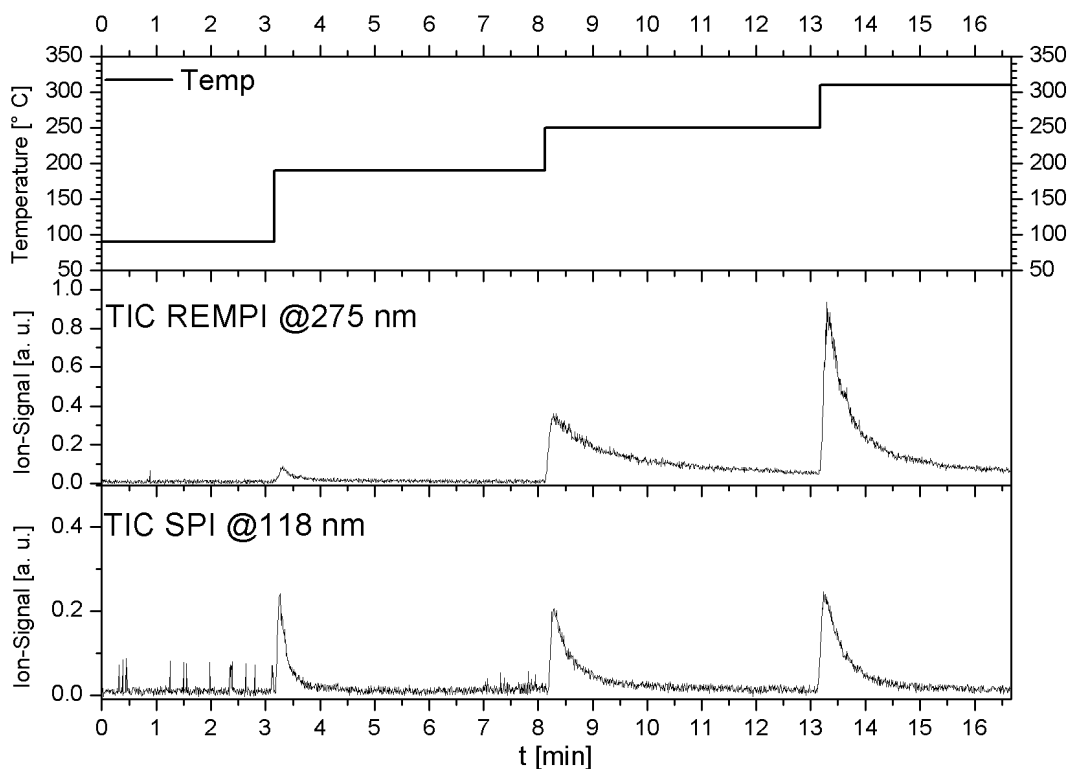
Figure 3.2: SPI and REMPI Total Ion Profiles of tobacco samples.

tion temperature is depicted. Since REMPI is a selective ionisation technique for (poly)aromatic compounds, the peaks in the REMPI spectrum could be interpreted as sum value of the respective aromatic content. In the same vein, the corresponding peaks in the SPI spectrum could serve as sum parameters for the total organic content, if the ionisation potential threshold selectivity is taken into account. At 190 °C the total REMPI signal is comparably low. This reflects the selective nature of REMPI, since most small volatile compounds are not ionised and the semi-volatile PAH and other aromatic compounds are not desorbed on a large scale at this temperature. In contrast, many small aliphatic hydrocarbons and inorganic compounds such as ammonia would desorb and are accessible with SPI, thus contributing to the respective total ion current. However, at the applied wavelength of 118 nm some substances, such as formaldehyde, can not be ionised due to their IP exceeding 10.49 eV and do not contribute to the observed total ion profile. When moving on to 250 °C, there is now a much larger REMPI signal detectable. At this temperature, a huge variety of PAH and other aromatic substances is desorbed from the tobacco. Finally, at 310 °C, a comparable high signal can be observed for total ion profile of REMPI, partially arising from still desorbing species, however, another part of the signal may be derived from beginning pyrolytic degradation of larger molecules.
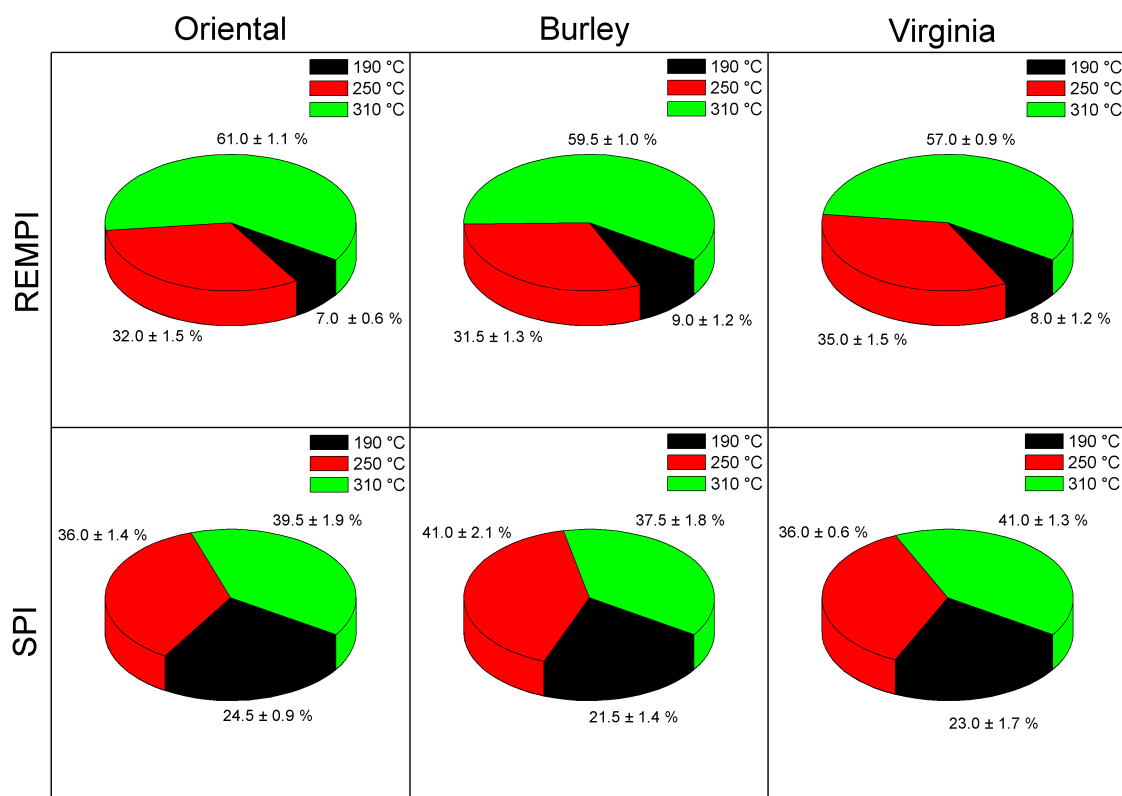
Figure 3.3: Distribution of total ion signal between the temperature steps at different tobacco types and measurement techniques.

The SPI signal at the elevated temperatures is larger compared to that at 190 °C, albeit not changing significantly between the two temperatures.

As indicated in Fig. 3.2 there are differences in the amount of substances analysed in each temperature step, indicated by the total ion stream, at both ionisation methods. In application of TD to urban aerosol samples, these are often characterised by sum parameters, e. g. total carbon content (TC), elemental carbon content (EC) and the sum of organic compounds (OC). These parameters can provide useful information of the chemical composition of aerosols and possible related health effects. To clarify the influence of tobacco type and temperature on sum parameter of TD coupled to PI-MS, the total ion yield (Fig. 3.3) shows a comparison of the six measurements of the three tobacco types with both ionisation methods. In general, the distribution within the temperature steps shows significant differences between REMPI and SPI. In fact, with REMPI at a wavelength of 275 nm less ions are detected at 190 °C and more on 310 °C. At this temperature it is to be expected, that a large fraction of the detected molecules originate from thermal degradation of plant material, which can be very effectively detected with this method. The changes in the fraction at 190 °C represent the nature of both ionisation methods very well. SPI allows efficient

detection of small chemical substances, which usually inhibit lower boiling points, while REMPI at this wavelength is especially sensitive for various aromatic, higher boiling, species. However, the fraction of 250 °C remains almost constant in Virginia tobacco, while Oriental and especially Burley show higher proportions with SPI.

As a conclusion, discrimination of tobacco types according to the different total ion values of each temperature step is hardly possible, neither with REMPI nor SPI. Only small changes are visible in REMPI, just above the standard error. However, as already mentioned earlier, in SPI the temperature step of Burley at 250 °C seems to be more dominant than in the other tobacco types. Though major chemical differences are known to exist between the tobacco types a sufficient characterisation by this sum parameter is not possible without further knowledge about the chemical composition of the off-gas at each temperature step.

To evaluate the possibilities and detectable compound classes of both PI-MS methods, Fig. 3.4 depicts the respective mass spectra for Oriental tobacco at 310 °C. To achieve sufficient comparability the spectra are normalised due to their ion stream. The SPI-TOFMS spectrum shows intensive peaks of $m/z = 44$ (acetaldehyde), $m/z = 58$ (acetone, propanal), $m/z = 68$ (isoprene, furan), $m/z = 94$ (phenol, methylpyrazine), and $m/z = 110$ (catechol, acetylfuran, methylfurfural). In addition, homologue rows of unsaturated hydrocarbons and aldehydes are visible (indicated by the asterisk). The signal at $m/z = 136$ can be assigned to a series of substituted pyrazines, phenols and various other compounds, the signal at $m/z = 256$ can be assigned to palmitic acid. The corresponding REMPI spectrum shows on the one hand the same abundant oxygenated species such as $m/z = 94$ (phenol, methylpyrazine), the $m/z = 108$ (anisole, dimethylpyrazines, isomeric cresols, benzylalcohol), $m/z = 110$ (catechol, acetylfuran, methylfurfural), $m/z = 124$ (guaiacol, dihydroxymethylbenzenes), and $m/z = 150$ (vinylguiacol, p-allylcatechol, o-acetyl-p-cresol). The occurrence of the phenolic compounds is a typical indication for biomass feedstock, produced by thermal decomposition of lignin. In contrast to the SPI spectrum, a much larger peak of $m/z = 117$ (indole) can be observed in the REMPI spectrum. This is due to the fact that the utilised REMPI wavelength of 275 nm is favourable for the ionisation of indole, because this molecule exhibits appropriate electronic transitions in this wavelength region leading to a higher - resonance enhanced - ion yield. Furthermore, in the mass region above $m/z = 180$ many relatively small peaks appear which are pointed out in the insert. By doing this, a variety of PAH can be detected such as $m/z = 202$ (pyrene), $m/z = 228$ (chrysene), and $m/z = 252$ (perylene) along with their alkylated derivatives.

The development of the product pattern with increasing desorption temperature as detected by SPI-TOFMS is shown in Fig. 3.5 for Virginia tobacco. The mass spectra,
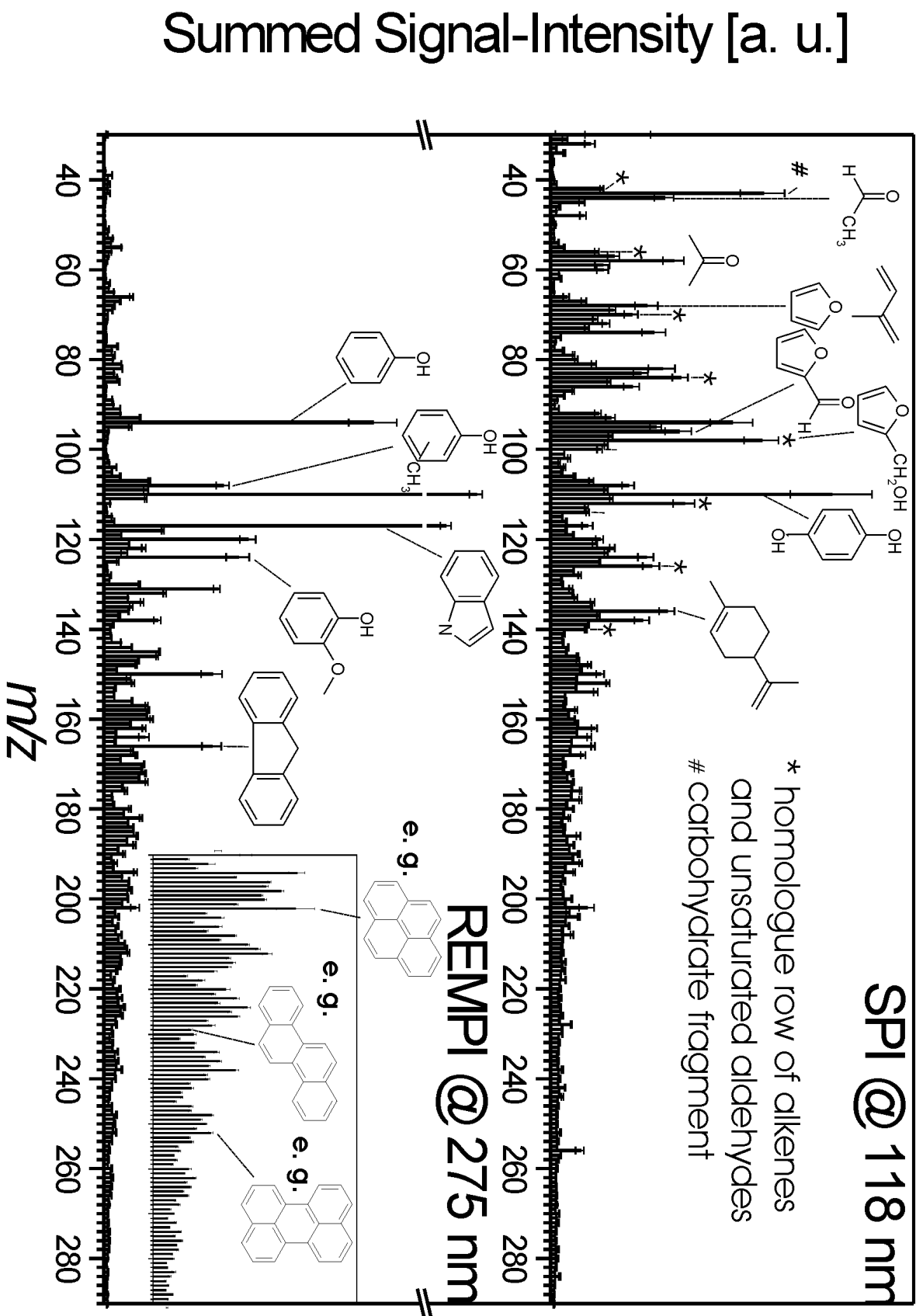
Summed Signal-Intensity [a. u.]

Figure 3.4: Thermodesorption mass spectra of Oriental tobacco with REMPI and SPI at a desorption temperature of 310 °C.
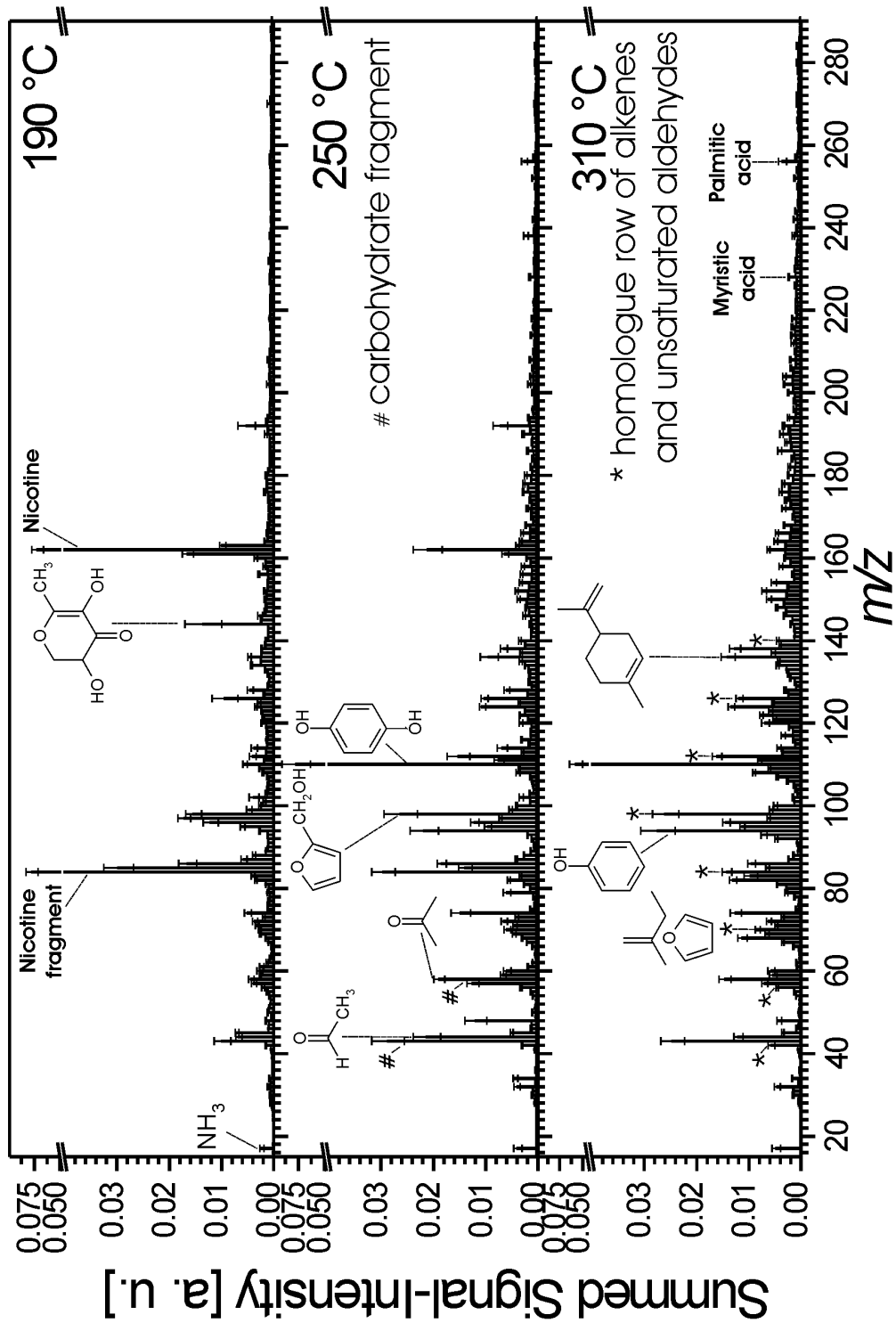
Figure 3.5: Comparison of the SPI mass spectra at the three temperature steps of Virginia tobacco.

which are normalised to their total ion stream for comparability, reflect the respective average of the six different measurements along with the standard deviations. The latter show a feasible reproducibility of the measurement technique. The spectrum at 190 °C is dominated by $m/z = 162$ (nicotine) and the signal at $m/z = 84$, which is a well known thermal fragment of nicotine [8], consisting out of the methylpyrrolidine ring of the nicotine molecule. At 250 °C, nicotine and its fragment are still present, but other masses become predominant. The base peak is at $m/z = 110$, which can be assigned to catechol, acetylfuran, and methylfurfural, well known abundant components of tobacco thermal treatment. Besides that, other oxygen containing compounds such as $m/z = 44$ (acetaldehyde), $m/z = 58$ (acetone), and $m/z = 94$ (phenol) are visible. The peak at mass $m/z = 74$ can be assigned to water eliminated glycerol [146, 157]. Furthermore, typical decomposition products from the thermal degradation of carbohydrates such as cellulose, lignin and sugars (e.g. $m/z = 43, 44, 56, 58, 72, 82, 86, 96,$ and 98) are present [8,86,123,146,149,157–159]. Moving to even higher masses, two signals at $m/z = 228$ and $m/z = 256$ emerge at 250 °C, which can be assigned to fatty acids, namely myristic and palmitic acid, respectively. Both are known constituents of Virginia tobacco [160] and have also been detected with SPI in urban aerosol [161]. Finally, in the lower mass range $m/z = 17$ (ammonia) is observable. The overall picture does not change very much when moving on to 310 °C. The nicotine peak has almost vanished, which is due to the fact that the nicotine present in the tobacco has nearly been completely desorbed. The appearance of many small volatile molecules, e.g. a homologue row of alkenes and unsaturated hydrocarbons ($m/z = 56, 70, 84$ (superimposed by the nicotine fragment), 98 (superimposed by furfuryl alcohol), 112, 126, and 140) and some odd masses (thermal fragments) at this relatively high temperature argues for the occurrence of pyrolytic reactions decomposing larger molecules.

Fig. 3.6 shows the corresponding normalised REMPI-TOFMS spectra for thermal desorption of Virginia tobacco. As already seen in Fig. 3.2, at 190 °C there are only a few compounds detectable such as $m/z = 110$ (catechol, acetylfuran, methyl-furfural), $m/z = 117$ (indole), $m/z = 120$ (mesitylene), $m/z = 124$ (guiacol), $m/z = 150$ (vinylguiacol), and $m/z = 180$ (methylfluorene). The general pattern does not change very much at the higher temperatures - exceptions are the much larger peaks of $m/z = 94$ (phenol) and $m/z = 166$ (fluorene) at 250 °C and the increase in indole peak intensity at 310 °C. Moreover, at the highest temperature there are more signals visible in the higher mass range representing a large variety of PAHs.

To investigate the chemical differences between the tobaccos in the lower boiling point region up to 190 °C, Fig. 3.7 illustrates a comparison of the ion stream nor-malised thermodesorption spectra of the three tobacco types measured with SPI at
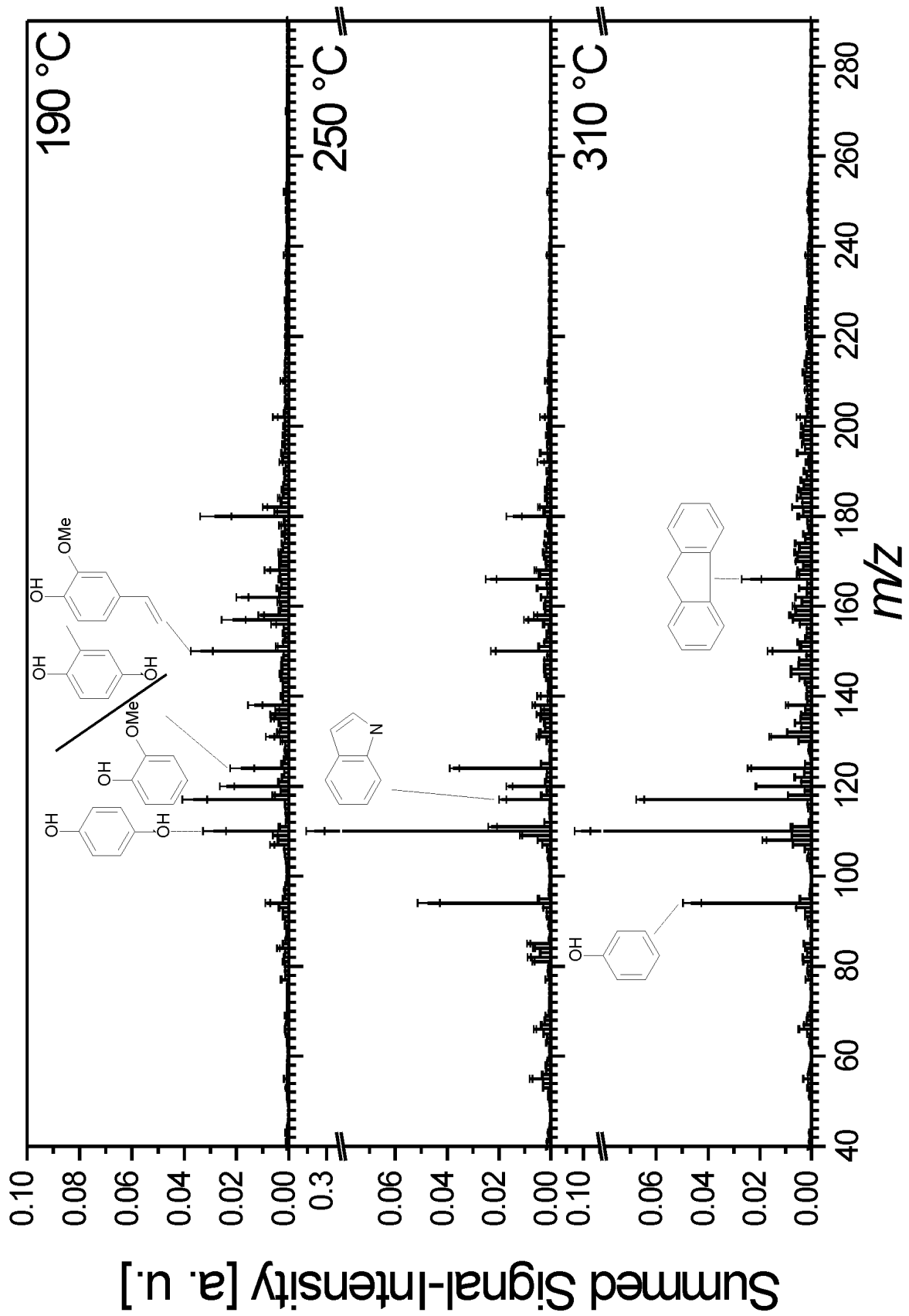
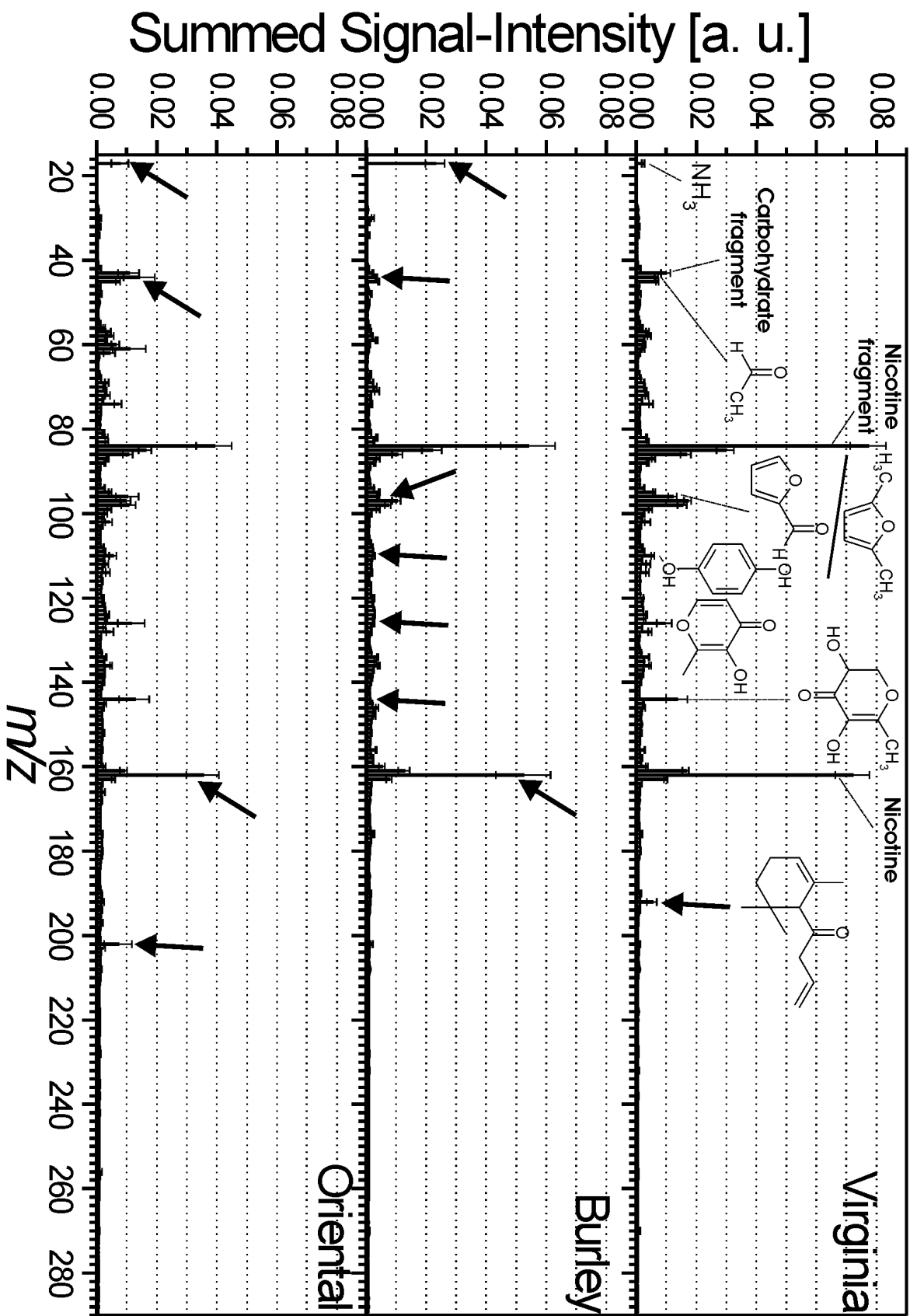Figure 3.6: Comparison of the REMPI mass spectra at the three temperature steps of Virginia tobacco.

Figure 3.7: Comparison of the three thermodesorption SPI mass spectra of the three tobacco types Virginia, Burley and Oriental at 190 °C.
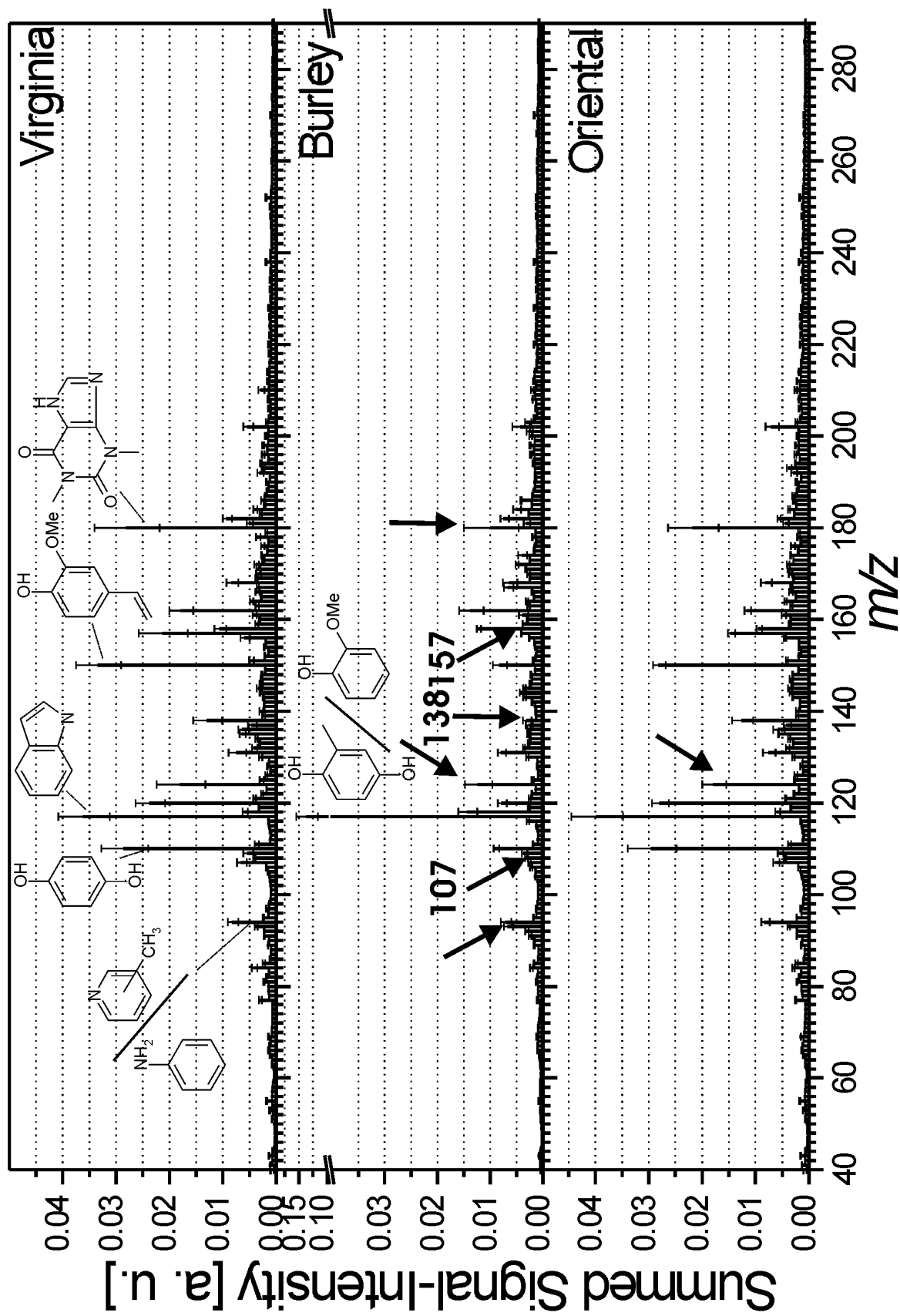
Figure 3.8: Comparison of the three thermodesorption REMPI mass spectra of the three tobacco types Virginia, Burley and Oriental at 190 °C.

190 °C. The relatively high presence of $m/z = 17$ (ammonia) in Burley tobacco could be expected from the agricultural profile mentioned earlier. Oriental and Virginia exhibit much lower signals, the lowest one in virginia. The lack of ammonia in a thermodesorption step at 190 °C in flue-cured tobaccos compared to air-cured ones has already been observed earlier by FENNER [155, 156]. The ratio of nicotine is decreasing from Virginia, Burley to Oriental. Burley tobacco also shows lower intensities of some oxygen containing species, $m/z = 44$ (acetaldehyde), 96 (furfural, dimethylfuran), 98 (furfuryl alcohol), 110 (hydroquinone, catechol), 126 (dimethylmaleic anhydride, formyl-methyl-thiophenes, acetyl-thiophenes, maltol), 144 (cyclotene), as well as the typical carbohydrate fragment $m/z = 43$. In addition to that, two unique masses can be found in either Burley and Oriental, namely $m/z = 192$ (scopoletin) and $m/z = 202$ (pyrene, fluoranthene). Scopoletin (7-hydroxy-6-methoxy-coumarin) is a known component of tobacco [8] and has been identified in chloroform-extract of Burley [11]. In the REMPI spectrum of the corresponding temperature step (Fig. 3.8) the most significant difference occurs in $m/z = 117$ (indole), which dominates the spectrum of Burley with significantly lower ratios in both other tobacco types. Again, a lack of oxygen containing compounds in Burley is visible, e. g. $m/z = 124$ (guaiacol, methylhydroquinone, methylcatechol) and the higher homologue $m/z = 138$, as well as $m/z = 150$ (vinylguaiacol) and $m/z = 180$ (caffeic acid). The odd mass peak $m/z = 157$ (dimethylquinolines) can be found in Oriental and Virginia tobacco.

For further investigation of medium boiling compounds of the tobacco types Fig. 3.9 and 3.10 provide a comparison between the three tobacco types for thermal desorption at 250 °C. At a first glance, there are not many differences between the SPI (Fig. 3.9) and REMPI (Fig. 3.10) mass spectra, respectively. For example, signal intensities of some abundant species such as nicotine, acetaldehyde, and acetone are on the same level for all three tobaccos. However, slight distinctions can be ascertained by taking a closer look. With Burley tobacco, a higher signal for $m/z = 17$ (ammonia) and $m/z = 117$ (indole) is observed, whereas Virginia tobacco exhibits higher levels for $m/z = 110$ (hydroquinone, catechol) and $m/z = 94$ (phenol) as well as some unsaturated hydrocarbons such as $m/z = 136$ (limonene). The signal intensity of oxygen-containing compounds in Oriental tobacco are situated somewhat between the respective intensities of Virginia and Burley tobacco, although the differences are not large. This reflects the chemical characteristics of the leaves, as discussed in chapter 1.2.

Fig. 3.11 and 3.12 show the normalised spectra of the desorption step at 310 °C for SPI and REMPI, respectively. In SPI (Fig. 3.11) Burley shows unique behaviour in some low mass compounds, namely $m/z = 43$ (carbohydrate fragment), 44 (acetaldehyde), 58 (acetone), and 98 (furfuryl alcohol). In contrast Virginia tobacco shows elevated peaks of $m/z = 94$ (phenol) and 110 (hydroquinone, catechol) with

Figure 3.9: Comparison of the three thermodesorption SPI mass spectra of the three tobacco types Virginia, Burley and Oriental at 250 °C.

Figure 3.10: Comparison of the three thermodesorption REMPI mass spectra of the three tobacco types Virginia, Burley and Oriental at 250 °C.

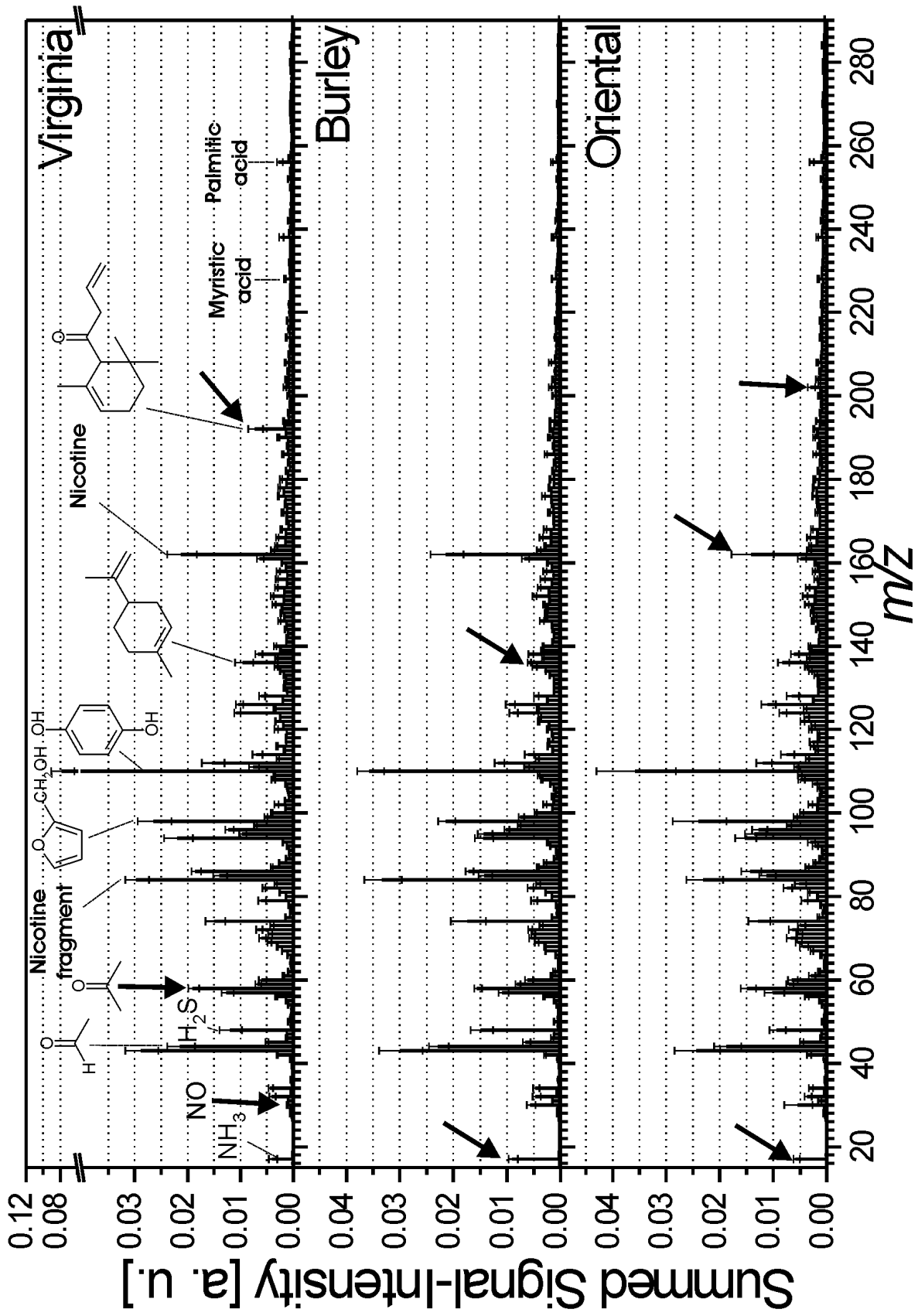*Figure 3.11: Comparison of the three thermodesorption SPI mass spectra of the three tobacco types Virginia, Burley and Oriental at 310 °C.*
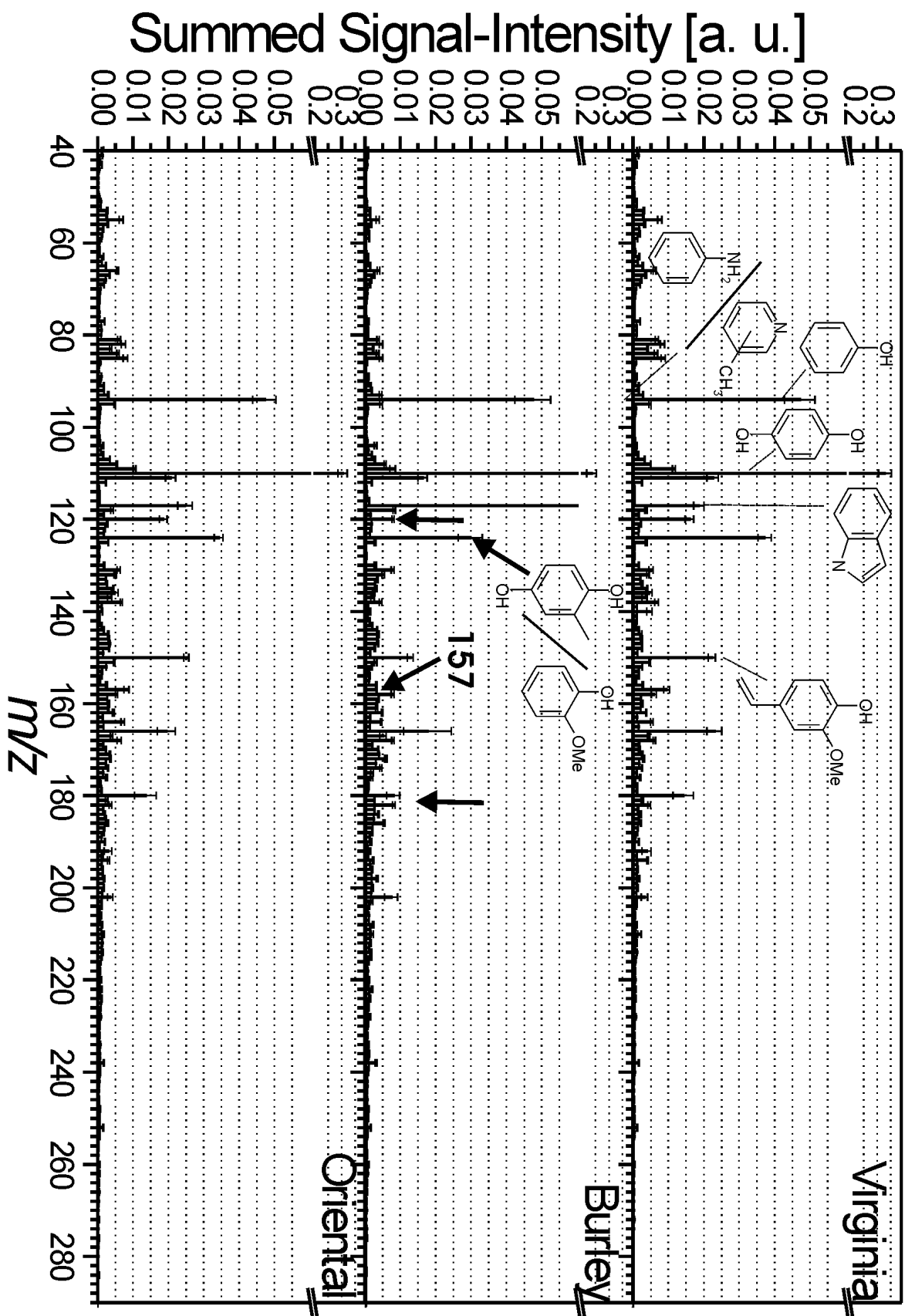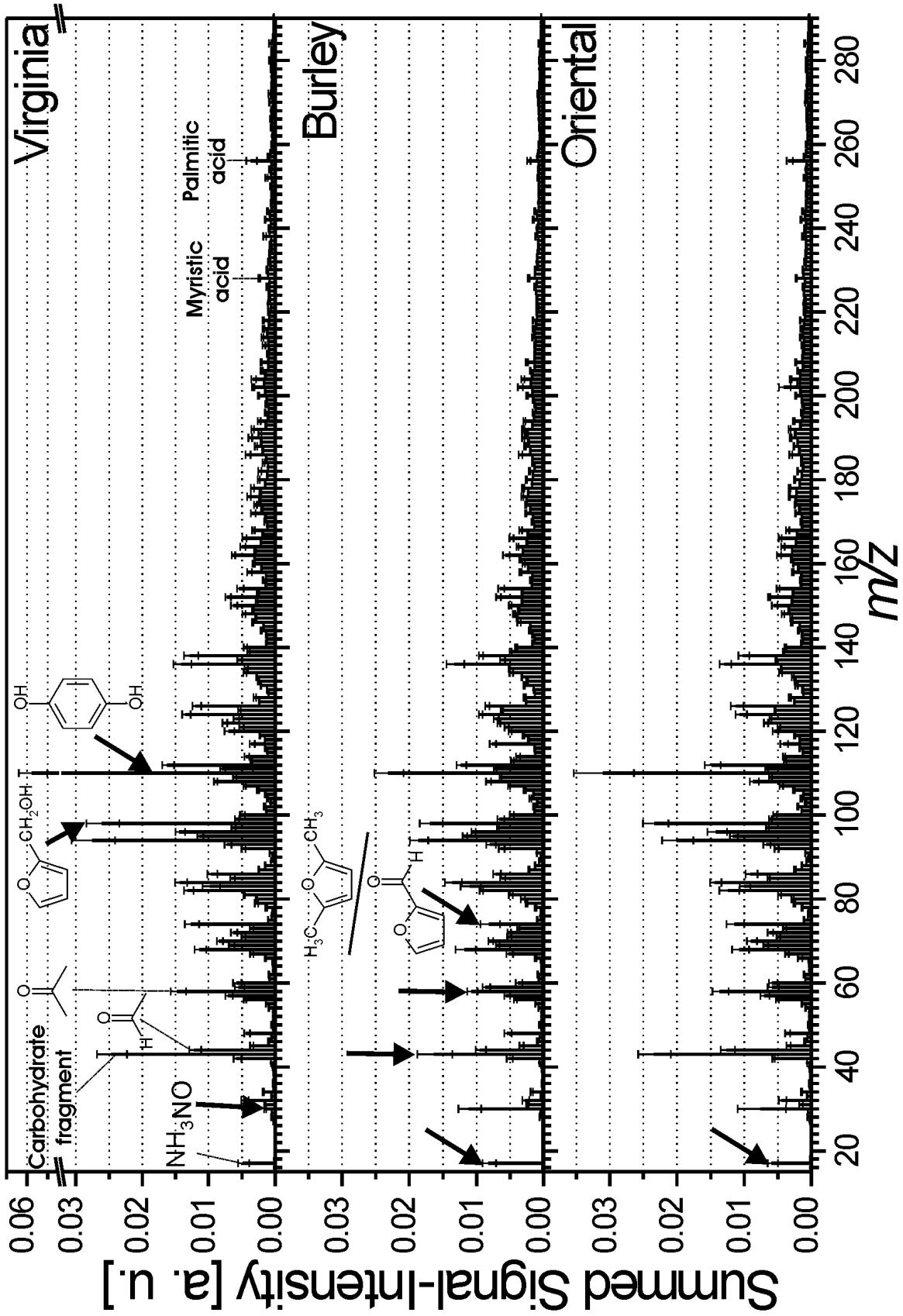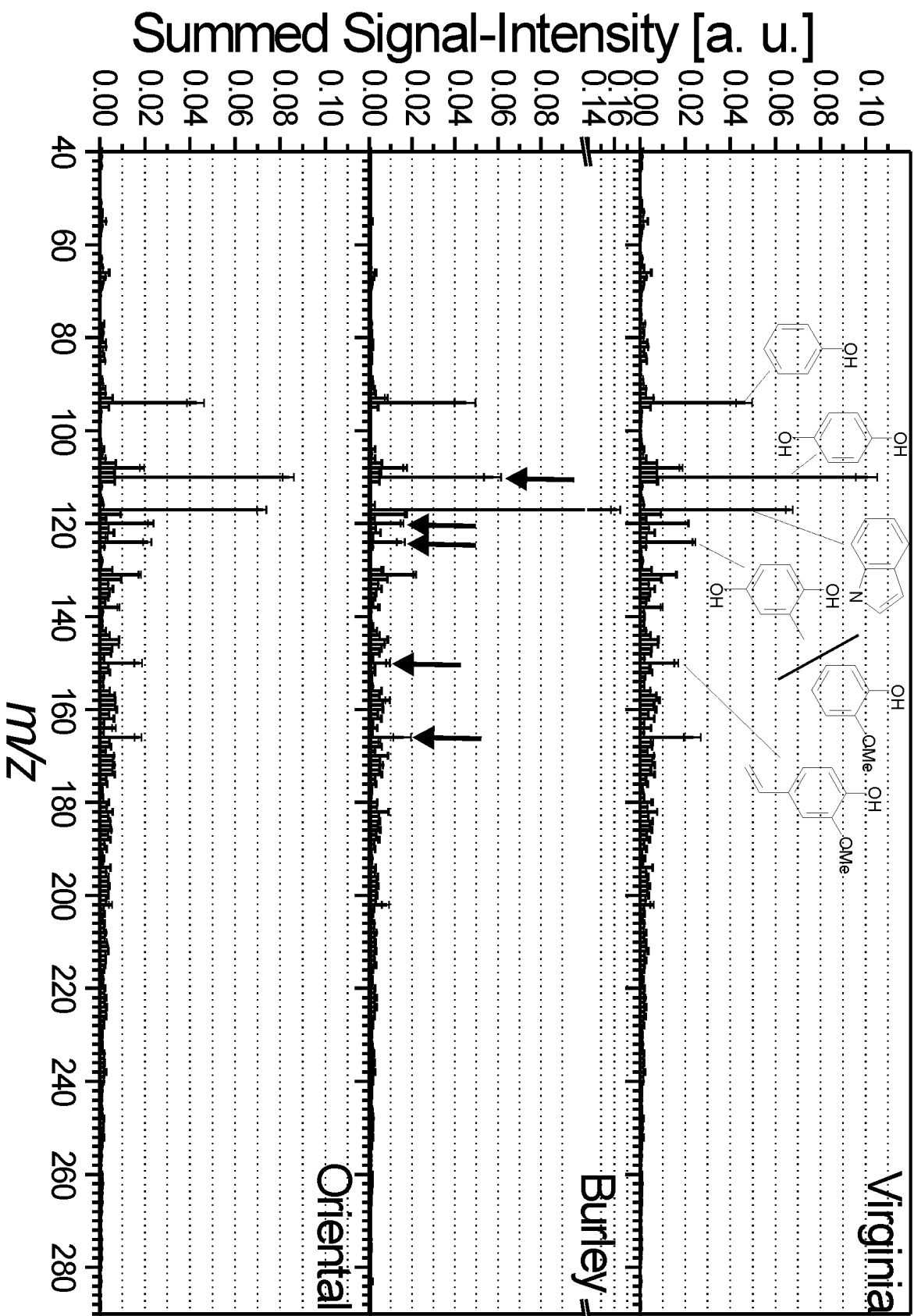
Figure 3.12: Comparison of the three thermodesorption REMPI mass spectra of the three tobacco types Virginia, Burley and Oriental at 310 °C.

the higher homologues at $m/z = 124$ and 138. Again Virginia is unique with a low content of $m/z = 17$, accompanied by a low percentage of $m/z = 30$ (nitric oxide) at this temperature. The lower peaks of oxygen-containing species in Burley is shown in the comparison of the REMPI spectra at 310 °C as well (Fig. 3.12), in fact $m/z = 110$ (catechol, acetylfuran, methylfurfural), 120 (phenylacetaldehyde, acetophenone), 124 (guaiacol, methylated hydroquinone/catechol), 138 (5-acetyl-2-furaldehyde, salicyclic acid, isophorone), 150 (vinylguiaicol), and 166. Furthermore, Burley again shows unique behaviour with the dominance of $m/z = 117$ (indole) in the spectrum.

The spectra at all three temperatures prove, that is comparatively easy to separate one tobacco type from the other two, usually Burley is differentiated by the high nitrogen and lower oxygen contents. However, it becomes increasingly difficult to distinguish between the other two tobacco types. Therefore statistical methods, as described in chapter 2.8, were applied to the ion stream normalised datasets. Without a normalisation, concentration effects would superimpose the chemical differences. Therefore, it was necessary to remove any effects of concentration differences by normalisation to the total ion stream of the corresponding measurement. To reduce the dataset efficiently for PCA analysis a set of Fisher-values was calculated for each temperature step and PI-method. Fisher-values have previously proven to be useful in various investigations involving statistical analysis of tobacco samples [6, 162].

As an example for statistical analysis of mainly aliphatic low-boiling compounds Fig. 3.13 shows the score (a) and corresponding loading (b) plot of a PCA of the ten highest FV from the SPI data at 190 °C. All three tobacco types can be distinguished quite well, the first PC divides the dataset with Burley on the one side and Oriental and Virginia on the other, with about 50 %, while the second PC allows differentiation between these two with about 27 %. The masses of the nitrogen-containing species $m/z = 17$ (ammonia), 31 (methylamine), and 156 (bipyridyl, dimethylpyridine) contribute towards Burley tobacco, while masses $m/z = 33$, 45 (ethylamine), 46 (ethylaclohol), and 76 (glycolic acid, propylenglycol) point towards Oriental and Virginia, all of them well known components of tobacco leaf, except $m/z = 33$ for which no assignment could be made so far. The only compound known to NIST with $m/z = 33$ is hydroxylamine. There are two masses responsible for the separation of Oriental and Virginia, namely $m/z = 52$ (3-Buten-1-yne) and $m/z = 53$ (propennitrile or eventually the ^{13}C peak of $m/z = 52$.

The corresponding analysis for the aromatic content is shown in Fig. 3.14 where the same statistical plot is shown for the REMPI data of the ten highest FV at 190 °C. The first PC explains the data set by more than 90 %, while the second one only contributes about 4 %. However, the separation of the three sample types is sufficient,
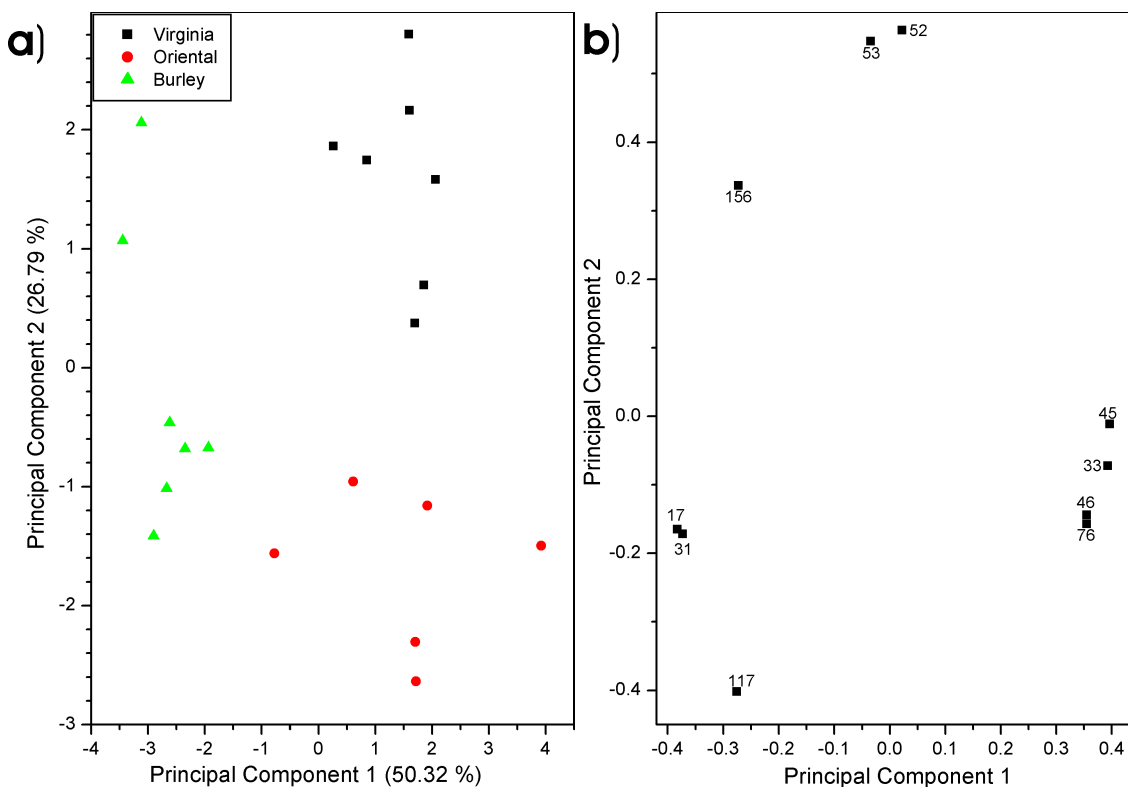
Figure 3.13: Score (a) and loading (b) of a PCA of the thermodesorption data measured at 190 °C with SPI.

with most masses, $m/z = 77$ (probably associated with benzene), 128 (naphthalene), 135 (alkylated pyridines, benzothiazole), 150 (vinyl-guaiacol, p-allyl-catechol, o-acetyl-p-cresol), 151 (probably ^{13}C of 150), 152 (vanillin, methylsalicylate, o-anisic-acid), 157 (dimethylchinoline), and 165 pointing to Virginia and Oriental. Vanillin and the other isobaric compounds on $m/z = 150$ have previously been reported as a flavour compound in Burley tobacco extract [11], 5-isopropyl-2-methylpyridine has been identified in essential oil from flue-cured tobacco [12], dimethylchinoline is previously known to occur in tobacco smoke [163] but no references to leaf have been found so far. However, $m/z = 120$ (acetophenone, phenylacetaldehyde, p-vinylphenol) plays an important role by separating the Burley from the other two tobacco types, as well as contributing a great part to the second PC, dividing the remaining two.

The PCA score (a) and loading (b) plot of the thermodesorption/pyrolysis step at 250 °C measured with SPI is exhibited in Fig. 3.15. The first PC splits the plot into the three tobacco types with a corresponding relevance of about 66 %, while the second PC allows further separation of Oriental (12 %). $m/z = 192$ is the only mass directly pointing to Virginia . Eight of the remaining masses, in fact
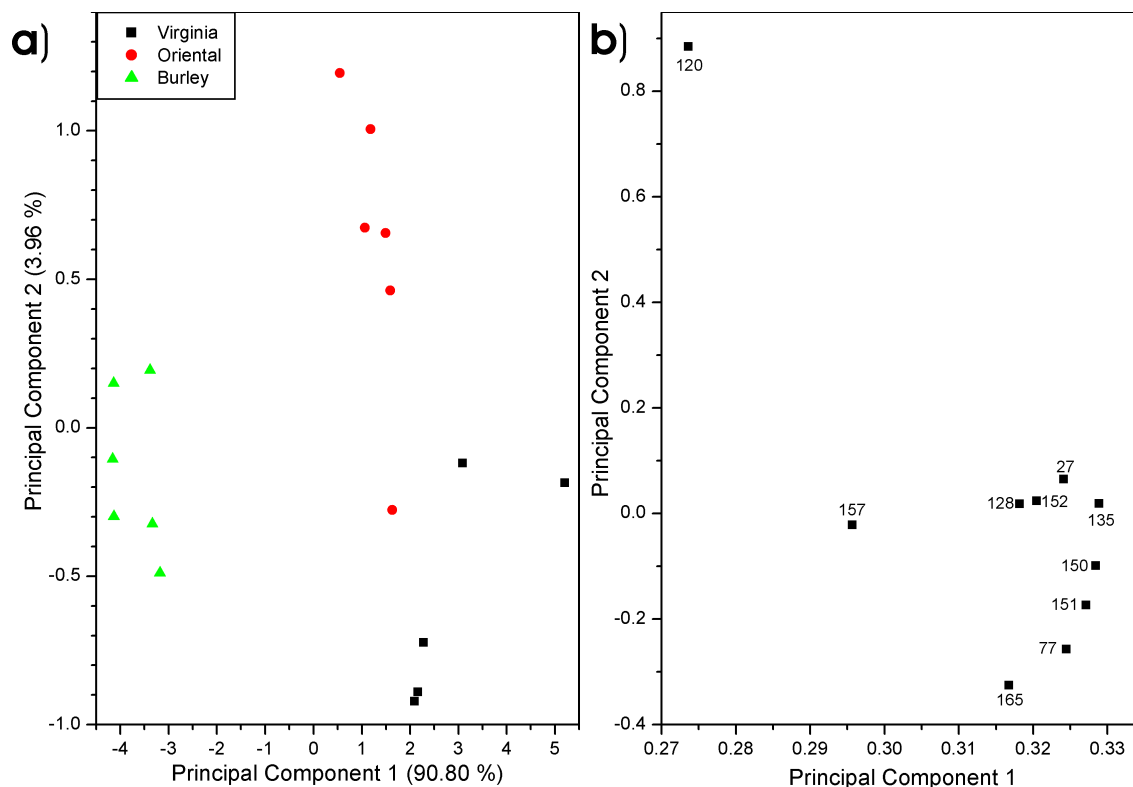
Figure 3.14: Score (a) and loading (b) of a PCA of the thermodesorption data measured at 190 °C with REMPI.

$m/z = 30$ (nitric oxide), 92 (toluene), 104 (styrene), 117 (indole) and the nitrogen compounds $m/z = 123$ (acetyl-methyl-pyrroles), 139 (methylethylmaleimide, 2-propyl-maleimide, 2-ethylidene-3-methyl-succinimide), 155 (phenylpyridine, histidine), and 169 (cysteic acid) are pointing towards Oriental and Burley, while $m/z = 129$ (quinoline, pipecolic acid, pyrrolidin-2-acetic acid, N-(3-Methylbutyl)-acetamide) can be used to separate Oriental from Burley. Acetyl-methyl-pyrrole, methylethylmaleimide and phenylpyridine have been identified in tobacco leaf extracts [9] as well as in tobacco smoke [163].

The aromatic counterpart of the medium boiling fractions of the single tobacco types is depicted in Fig. 3.16 a, where the score plot of the PCA of the thermodesorption/pyrolysis data at 250 °C of the three tobacco types measured with REMPI-TOFMS is presented. From this, a satisfactory separation of the tobaccos could be observed. The relatively high value of the first principal component of approximately 85 % confirms the good discrimination achieved by the chosen Fisher values. With the first PC, it is possible to separate Burley from the other two tobaccos, and with the second principal component, Virginia and Oriental can be distinguished. The corresponding loading plot (Fig. 3.16 b) reveals the components, which point to Bur-
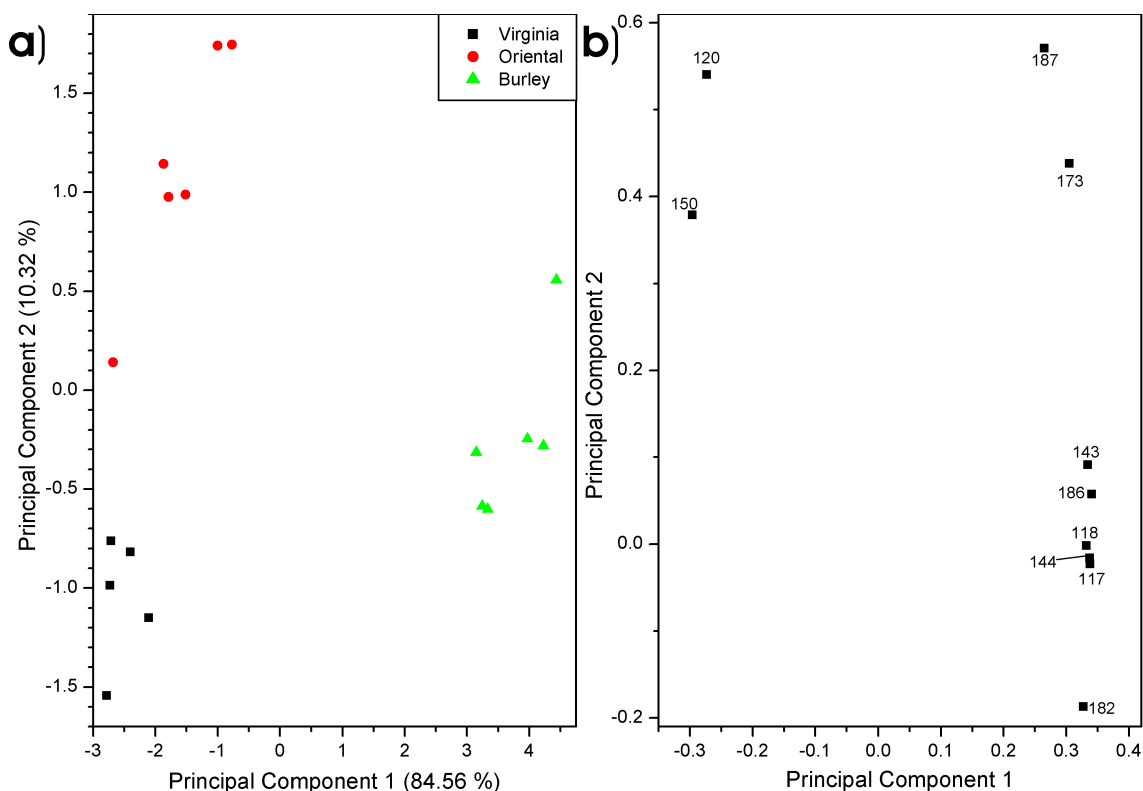
Figure 3.15: Score (a) and loading (b) of a PCA of the thermodesorption data measured at 250 °C with SPI.

ley to be either members of the homologue row of indole (117, 173, 187 m/z) or the methylated quinolines (143 m/z). This reflects the above mentioned predomination of nitrogen containing species in Burley. On the other hand, there are two compounds indicative of Oriental and, to a lesser extent, Virginia, namely $m/z = 150$ (vinylguiacol), a typical degradation product of oxygenated structures, accentuating the influence of carbohydrate pyrolysis products for the identification of the two non-Burley tobaccos, as well as the aromatic species $m/z = 120$ (acetophenone, phenylacetaldehyde, p-vinylphenol).

To complete the chemical investigation of the tobacco types with the high boiling, mainly aliphatic, compounds the statistical analysis of the thermodesorption/pyrolysis experiment at 310 °C measured with SPI is presented in Fig. 3.17. As with the temperature step at 250 °C the first PC contributes about 70 % to a separation of all three tobacco types. Further separation can be achieved with the second PC, which further divides the Oriental from the remaining two with about 12 %. Masses directly pointing to Virginia tobacco are $m/z = 54$ (butadiene) and $m/z = 124$ (guaiacol, methylated hydroquinone or catechol). Burley tobacco is classified by masses $m/z = 104$ (styrene), 117 (indole), 118 (probably ^{13}C of 117) and the
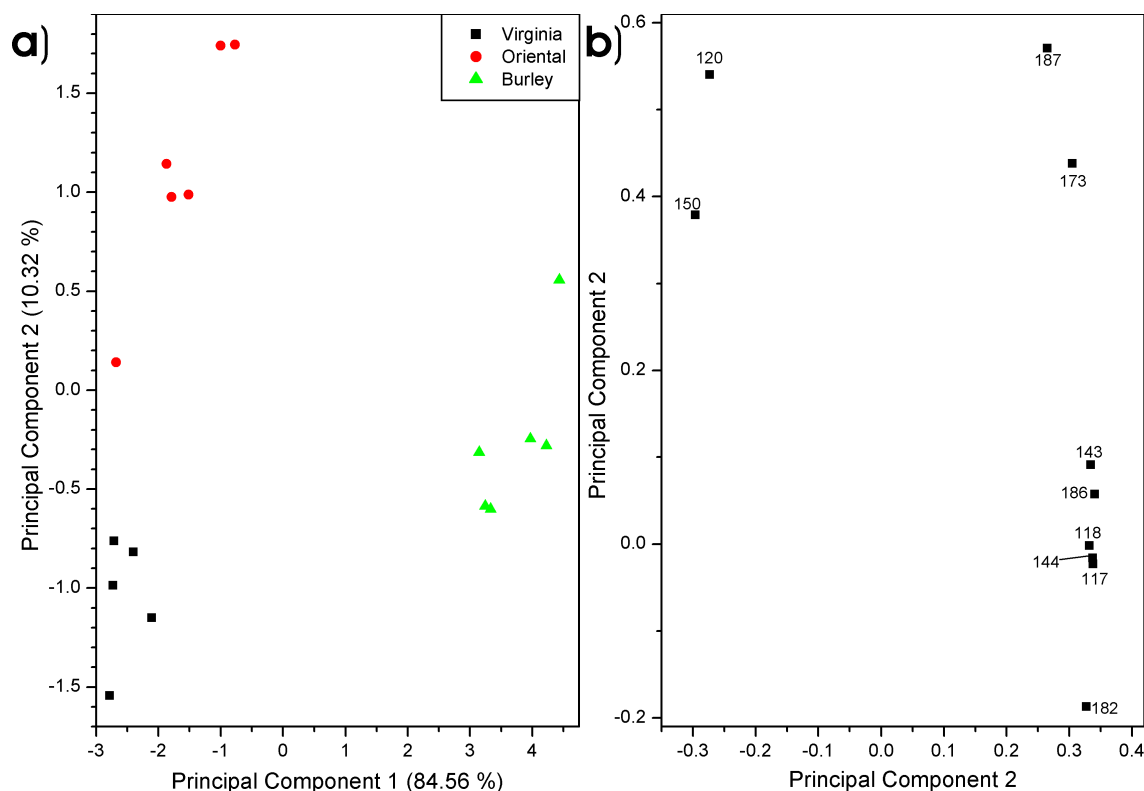
Figure 3.16: Score (a) and loading (b) of a PCA of the thermodesorption data measured at 250 °C with REMPI.

nitrogen containing compounds $m/z = 119$ (3-propenylpyridine, homoserine), 147 (glutamic acid) and 161 (aminoadipic acid), however an exact assignment to Burley or Oriental is not possible. Masses $m/z = 129$ (quinoline, pipecolic acid, pyrrolidine-2-acetic acid, N-(3-methylbutyl)-acetamide) and $m/z = 169$ (cysteic acid) point towards Oriental.

In Fig. 3.18 an excellent separation of the three tobacco types was achieved with the first PC clarifying about 80 % and the second one about 15 %. Masses $m/z = 117$ (indole) and $m/z = 118$ (probably ^{13}C of 117, methylstyrenes, benzofuran) directly point to Burley, while masses $m/z = 55$ (probably mathematical artefact, as no substance can be found in the database, which could be detected with REMPI at this wavelength), 82 (methylfuran), 84, 85, 152 (vanillin) point to Oriental. $m/z = 142$ (methylnaphthalenes) contributes to both Burley and Virginia, mass $m/z = 141$ (probably related to 142) points to Oriental and Virginia and has previously been identified in essence and essential oil of flue-cured tobacco [12]. The occurrence of these masses is irregular, as no aromatic substances can be assigned to the corresponding mass to charge ratios.
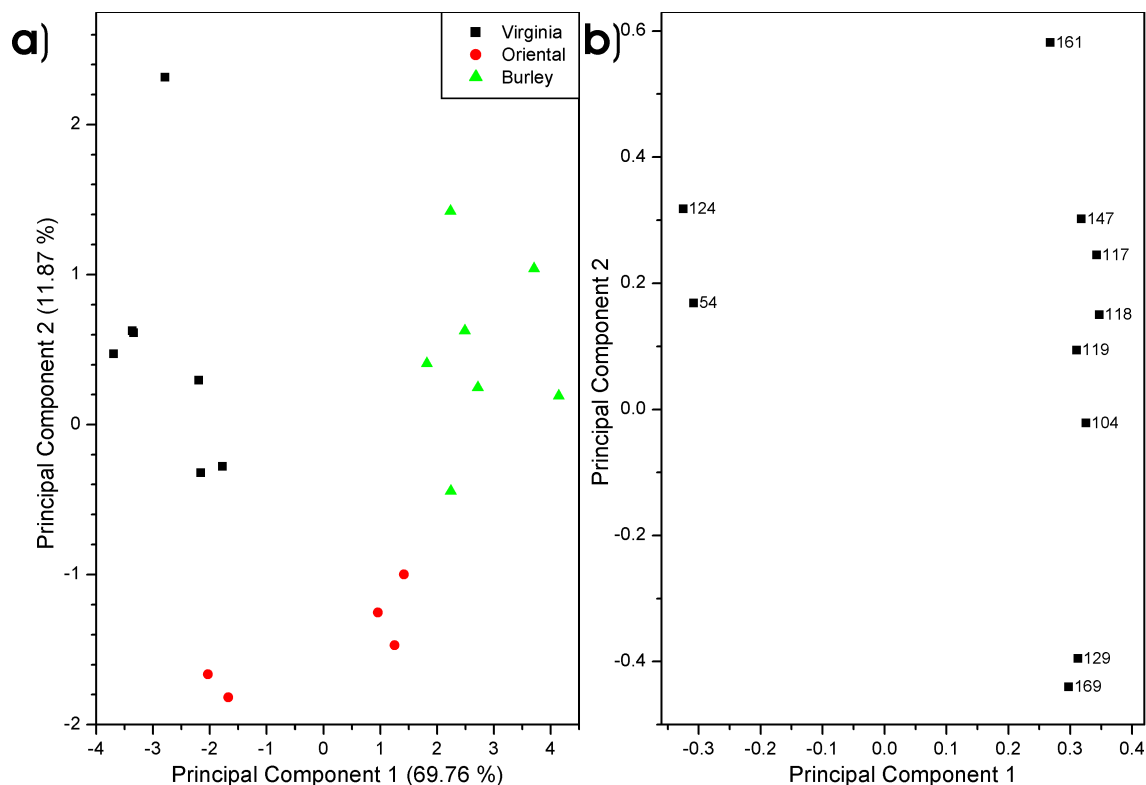
Figure 3.17: Score (a) and loading (b) of a PCA of the thermodesorption data measured at 310 °C with SPI.

3.4 Conclusion of the thermodesorption/pyrolysis experiments

The use of photoionisation methods with advanced statistical methods provides a powerful tool for the analysis of different tobacco types. It was demonstrated that SPI and REMPI complement another when looking at the chemical composition of thermodesorbed/pyrolysed plant material. While, unlike with urban aerosols, characterisation of different single tobacco types is hardly possible with sum parameters such as total ion streams of the temperature steps, it could be shown that changes in the chemical matrix are accessible by both methods. Some differences can already be seen in the mass spectra, while a sufficient separation can be achieved with PCA using only the ten highest FV. In every fraction of the analysed tobacco samples the changes within the analysed matter reflect the chemical properties of the different tobacco types, illustrated in chapter 1.2, very well. However, as REMPI does not necessarily represent the actual concentrations present in the analyte, but rather reflects the spectroscopical properties, absolute mass assignment can only be done if the spectroscopic data of specific target compounds or compound classes is known,

Figure 3.18: Score (a) and loading (b) of a PCA of the thermodesorption data measured at 310 °C with REMPI.

accompanied by detailed knowledge about the composition of the trace compounds present in tobacco leaf. Therefore, SPI methods are perfectly suited for the monitoring of the whole spectrum, especially with modern, easy-to-use VUV-lamp systems while REMPI in combination with jet inlet systems can provide an effective highly sensitive monitoring device for single compounds or compound classes.

4 Mainstream Smoke Analysis

4.1 Machine smoking

4.1.1 Development of standardised machine smoking methodologies

Automatic smoke generation was first reported in the early 1900s when the first machines applying continuous suction to cigarettes were introduced. Soon after that improvements included manual interruptions to adapt to human smoking behaviour. Completely automatic machines have been used since the 1930s, soon after the development of automatic timing devices. In 1933 PFYL *et al.* [164] examined the different smoking procedures of seven human smokers and constructed a machine based on their observations. They also emphasised the need to standardise "the artificial smoking of tobacco products". In 1936 BRADFORD *et al.* [165] postulated that a successful smoking experiment "should be reproducible" and "the smoking procedure, the cigarettes smoked and the environment while smoking should be definitely characterised". Furthermore "it should sufficiently approximate the conditions of human smoking for conclusions from experiments *in vitro* to admit of interpretation *in vivo*".

Starting from these early developments and protocols many different types of devices and procedures were developed until the late 1960s. By that time different national standardisation authorities had already developed or at least started to develop their own smoking methods. WYNDER and HOFFMANN [157] pointed out the need for a completely standardised smoking-machine methodology in 1967.
Starting in 1966 the Federal Trade Commission (FTC) started working on a smoking methodology. It included the puff-volume of 35 ml and puff-duration of 2.0 s once every minute as used by BRADFORD in 1936 and was finally published in 1969 [166]. The smoke should be trapped on a Cambridge filter pad introduced by WARTMAN *et al.* [167] which was evaluated by OGG [168] in 1964.
In Europe the Centre de Coopération pour les Recherches Scientifiques Relatives au Tabac (CORESTA), which was founded in 1956, started working on a recommended

method for machine smoking in the late 1960s. The method was published in 1969 [169] as well. By 1977 the CORESTA method was accepted without further changes as the world wide ISO standard and was published in its original version [170]. By 1991 some minor changes were included. Table 4.1 gives a short overview on different standard methods.

4.1.2 Problems and limits of standardised machine smoking

As a matter of fact no machine can completely simulate the behaviour of every single human smoker at all times, nor is this the target of using standardised methods. This was already recognised by the FTC in 1967. There's a huge variety of human smoking behaviour, which has been studied on various occasions since the 1930s [164, 172, 173]. However, according to BAKER [171] "The specified smoking parameters, i.e. puff volume, duration, interval, etc., are well within the established ranges of human smoking [...]". Nevertheless different authorities are already starting to develop new "intense" smoking conditions to better match the parameters of human smoking, namely the federal government of Canada, the provincial government of British Columbia and the Commonwealth of Massachusetts. The individual parameters are summarised in Table 4.2. The implementation of these new protocols is a result of an ongoing discussion about the compensation behaviour of human smokers when confronted with different products. DJORDJEVIC *et al.* [174] investigated the smoking behaviour of 133 smokers of low-yield cigarettes and found increased puff volumes of 48.6 mL/puff with puff intervals of 21.3 s for cigarettes with less than 0.8 mg nicotine/cigarette and 44.1 mL/puff and intervals of 18.5 s for cigarettes with 0.9–1.2 mg nicotine/cigarette. A decreased puff duration of 1.5 s could be observed in both cases. The more intense smoking conditions compared to the regular machine smoking lead to increased amounts of nicotine, carbon monoxide, tar, benzo[a]pyrene, and 4-(methylnitrosamino)-1-(3-pyridyl)-1-butanone [174]. A huge discussion has been ongoing in the media for the last few years about the role of low-tar products and the compensational behaviour of smokers, who adapt the low machine-smoked tar results to higher tar and nicotine yields by changing the puff parameters or, conscious or unconscious, blocking of filter ventilation holes. This discussion finally led to the ban of the use of "light" in cigarette brand names and advertising in the European Union (EU).

Parameter	Standard method					
	FTC	**UK**[a]	**DIN**[a]	**Canada**[ab]	**Original CORESTA/ISO**[c]	**Revised CORESTA/ISO**[d]
Puff volume [mL]	35 ± 0.5	35 ± 0.5	35	35	35 ± 0.3	35 ± 0.25
Puff duration [s]	2.0 ± 0.2	2	2	2	$(1.8\text{–}2.2) \pm 0.03$	2 ± 0.05
Puff frequency [puff/min]	1	1	1	1	1^e	1^f
Butt length - plain cigarette [mm]	23	20	23	30	23	23
Butt length - filter cigarette [mm]	$T + 3^g$	$T + 3^h$ / $T + 5^k$	$T + 3^i$ / $F + 8^i$	30^j / $T + 3^j$	$T + 3^i$ / $F + 8^i$	$T + 3^i$ / $F + 8^i$
TPM trapping system	C	C	E	C	C or E	C
Water analysis	GC	KF or GC	KF or GC	KF or GC	KF or GC	KF or GC
Nicotine analysis	GS or GC	GC	GC	GC	GC	GC
Ambient temp [°C]	23.9	22	22	22	22	22
Ambient RH [%]	60	60	60	60	60	60

Table 4.1: Different standard machine smoking protocols (BAKER [171]).

[a]Superseded by the revised ISO method.
[b]also Australia, New Zealand and Japan
[c]Prior to 1991.
[d]After 1991. Air flow conditions around the cigarette are also specified, including their distribution and how they should be measured.
[e]One puff every 60 ± 1 s.
[f]One puff every 60 ± 0.5 s.
[g]23 mm or (T + 3) mm, whichever is longer.
[h]For cigarettes ≤75 mm, 20 mm or (T + 3) mm, whichever is longer.
[i]23 mm or (T + 3) mm, or (F + 8) mm, whichever is longer.
[j]30 mm or (T + 3) mm, whichever is longer.
[k]For cigarettes ≥75 mm, 20 mm or (T + 5) mm, whichever is longer.

Agency	Puff parameter			% of filter ventilation blocked
	Volume [mL]	Duration [s]	Frequency [s]	
FTC/ISO/CORESTA	35	2	60	0
Canada-intense	55	2	30	100
Massachusetts-intense	45	2	30	50
FTC-intense	55	2	30	0

Table 4.2: Intense smoking regimes

4.2 Summary of previous work on mainstream smoke

REMPI/SPI-TOFMS has been used for the investigation of mainstream smoke and pyrolysis products of tobacco by ADAM [6]. A short overview of the results concerning mainstream tobacco smoke is given here.

In Fig. 4.1 a three dimensional overview of the mass spectrometrical data of whole smoke of a 2R4F research cigarette smoked under ISO conditions gathered with SPI-TOFMS is presented. In Fig. 4.1 a) the different puffs can clearly be distinguished, dominated in each puff by $m/z = 44$ (acetaldehyde), 58 (acetone, propanal), and 68 (isoprene, furan). The enlarged view of the third and fourth puff is exhibited in (Fig. 4.1 b) showing additional peaks of $m/z = 78$ (benzene), 92 (toluene, glycerol), and 106 (xylenes, ethylbenzene, benzaldehyde, diethylenglycol). Between the two puffs the cleaning puffs of the smoking device, as illustrated in chapter 2.4, are visible.

Fig. 4.2 shows a comparison of REMPI and SPI spectra measured with and without a Cambridge filter pad, respectively. While SPI, in general, is more suitable for monitoring aliphatic and carbonyl-containing substances, REMPI gives a good overview on polyaromatic substances. Peak alignment was done using known information such as total yields from previous publications together with consideration of the selectivity criteria of the different photoionisation methods resulting from the different spectroscopic properties of the substances. The assignments are presented in Table B.1. The SPI spectra with and without filtering the smoke using a Cambridge filter pad (Fig. 4.2 a, b) look very similar. Differences can be seen in the higher mass region (> 100 m/z), where most compounds are located in the particulate phase and therefore are adsorbed on the filter. The REMPI spectrum at a wavelength of 260 nm with the filter pad (Fig. 4.2c) illustrates that larger aromatic species and most other detectable substances except benzene, toluene, and xylene (BTX) are also adsorbed on the filter pad. The REMPI spectra presented in Fig. 4.2 c, d only represent a small part of the available data, as the use of different, selected wavelengths can provide further information.
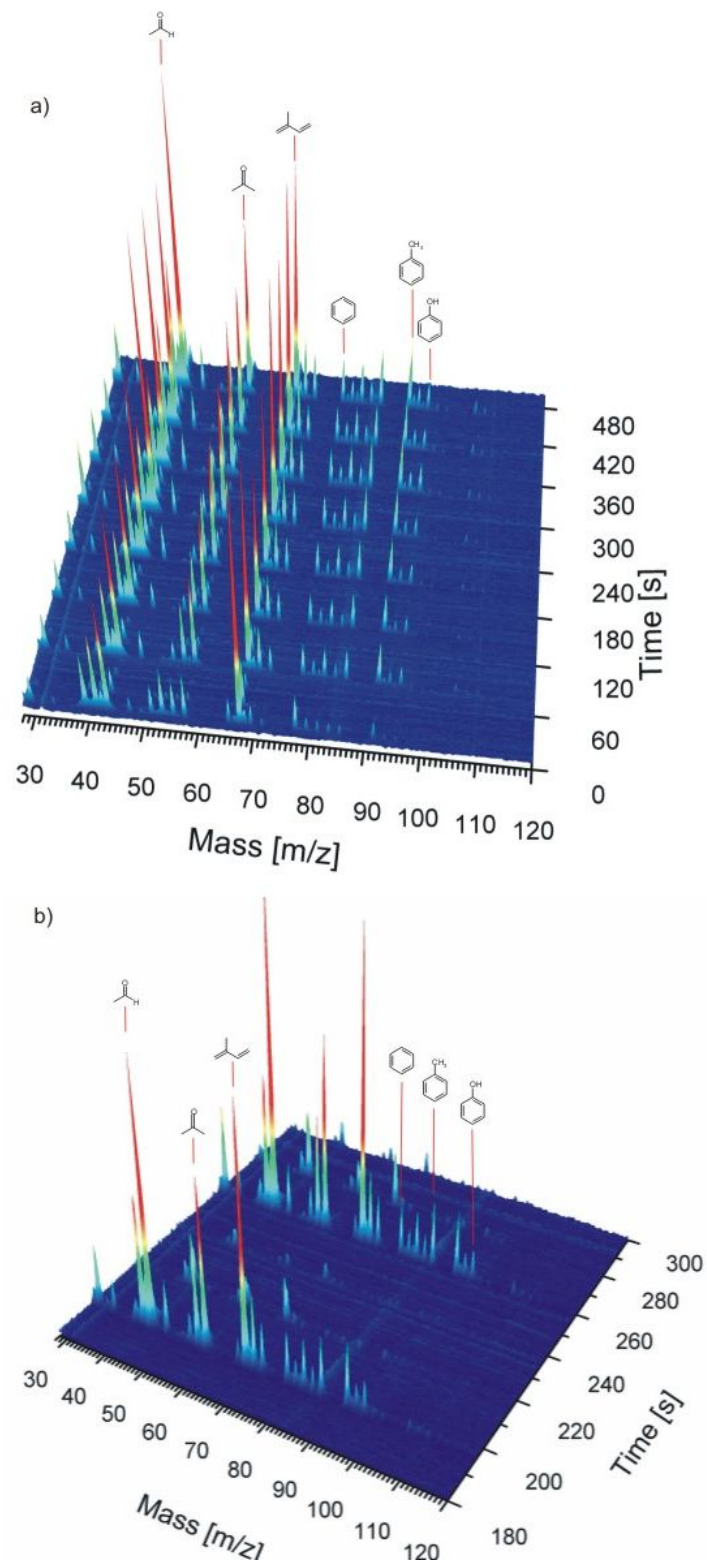
Figure 4.1: (a) 3D plot of measured SPI mass spectra during the smoking cycle of a Kentucky 2R4F research cigarette. (b) Enlarged third and fourth puffs showing the reduced memory effects of the novel smoking machine.
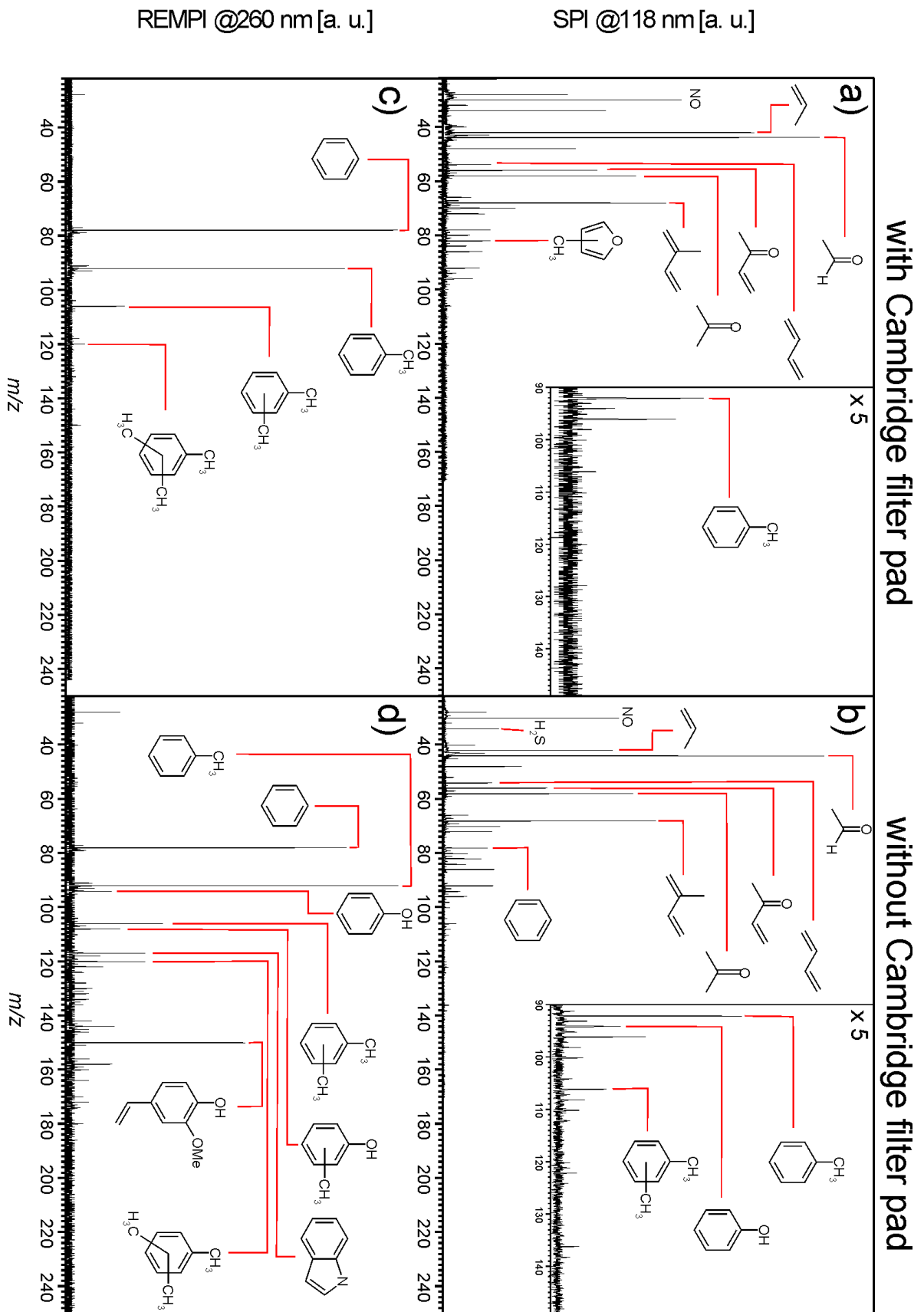
Figure 4.2: Comparison of REMPI and SPI raw mass spectra with and without cambridge filter pad [77].
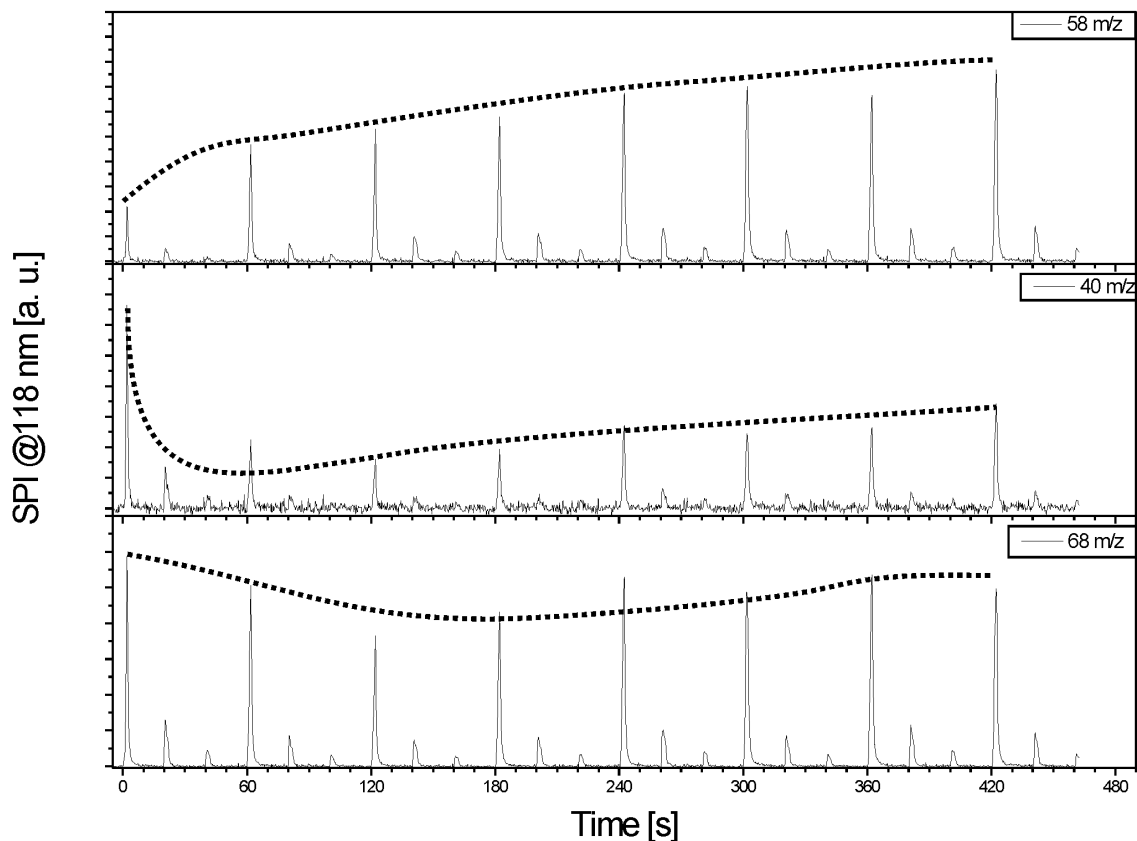
Figure 4.3: SPI time profiles of 40 (propyne), 58 (acetone), and 68 m/z (isoprene) recorded during the smoking cycle of a Kentucky 2R4F research cigarette [77].

Fig. 4.3 depicts an exemplary overview of the three different puff by puff profiles observed and thoroughly characterised for different cigarette blends and single tobacco type cigarettes by ADAM [6]. For most of the compounds e.g. $m/z = 58$ (acetone, propanal) higher yields can be observed with increasing puff number. However, some unsaturated species, e. g. $m/z = 40$ (propyne), 52 (1-buten-3-yne), and 54 (butadiene, butyne) have higher yields especially during the first puff, while a third group exhibits no clear preference and influence of puff-number. In addition to the qualitative overview about different profiles several toxic compounds were quantified by ADAM *et al.* [6,175]. As an example for these results a selection of various compounds is presented in 4.4, namely nitric oxide, acetaldehyde, butadiene, acetone, isoprene, benzene, toluene, and xylene/ethylbenzene. The puff behaviour observable in the time profiles can also be observed in the quantified data, including the exceptionally high amounts in the first puff of some unsaturated components, such as butadiene.
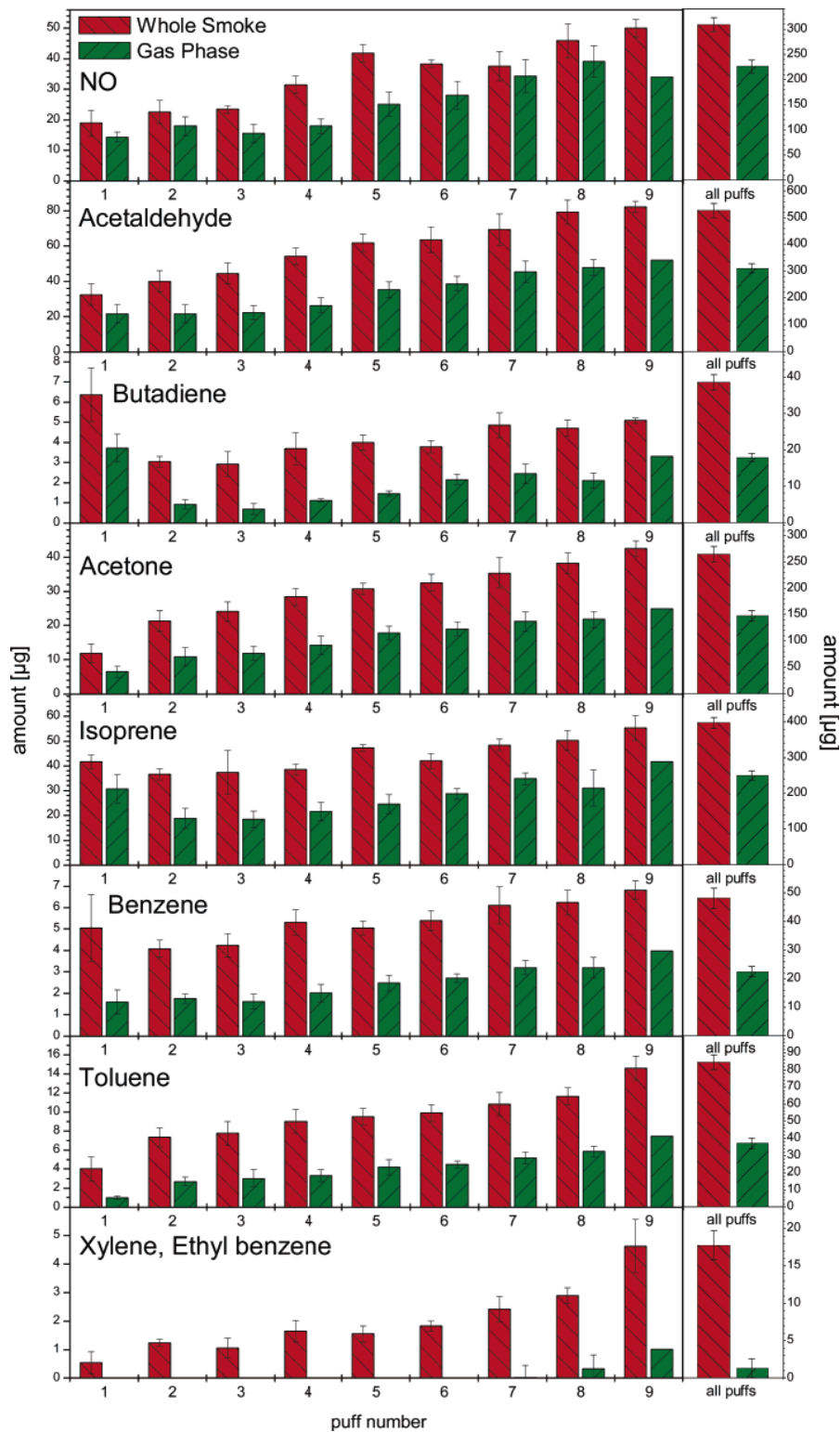
Figure 4.4: Quantification and puff behaviour of selected toxic compounds of a 2R4F research cigarette whole smoke (i. e., no Cambridge filter pad present) and "gas phase" (i. e., Cambridge filter pad present) [175].
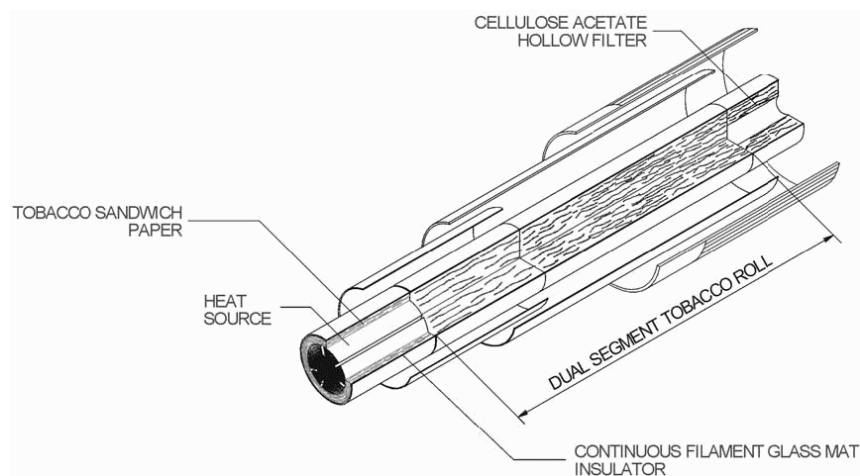
Figure 4.5: Design of a novel cigarette "Eclipse" which heats not burns tobacco [176]. The tip consists of a piece of coal, which serves as the heat source.

4.3 Comparison of a novel cigarette and a conventional 2R4F research cigarette

Various methods have been introduced in the last few years to achieve a reduction of harmful substances in cigarette smoke. This includes new developments in filters, e. g. the addition of charcoal and other additives to the filter material. However, there are also trends towards a new generation of cigarettes, where tobacco is not burned but flavour active ingredients are thermodesorbed off the tobacco, or where the product does not include any tobacco at all, from a set of flavour components and nicotine. The generation of hot air can be achieved by either electric heating, in the last year a charcoal heated product hit the markets across the world ("Eclipse"). A schematic drawing of the cigarette is shown in Fig. 4.5. The heatsource, a piece of charcoal with defined ventilation tubes, is implemented into the tip of the cigarette and provides hot air, which is drawn through the dual segment tobacco roll. A conventional acetate filter is installed at the mouth-end of the cigarette. However, since the major part of the tobacco does not undergo pyrolytic processes, unlike in conventional cigarettes, a filtration of the smoke is not needed. Therefore, the hollow filter just stabilises the end of the cigarette and provides an unfiltered air flow of the desorbed tobacco products. A range of several publications on the toxicity [176–184], free-radical chemistry [185] and chemical constitution [176,179,183,186–190] of these products have been made available to the public. In general, the tar, nicotine, and Hoffmann-analytes yields are lower than with conventional cigarettes. However, no information on the dynamics of this product is known.
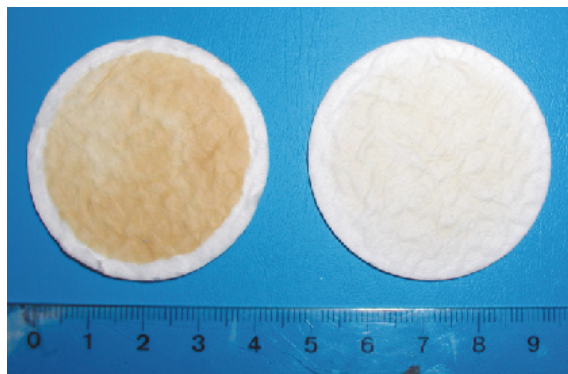
Figure 4.6: Cambridge filter pads, showing the collected particulate matter of a 2R4F research cigarette (left) and the novel cigarette (right) under ISO conditions.

4.3.1 Experimental setup for the comparison of a a cigarette that primarily heats, not burns, tobacco and a conventional 2R4F research cigarette

Two cigarettes were smoked for the comparison under ISO conditions with the machine described earlier, one novel cigarette which heats tobacco and a conventional 2R4F research cigarette. Again, two blank puffs were taken between two succeeding puffs for cleaning purposes. The charcoal at the tip of the novel product was preheated with a Borgwaldt electric lighter for 60 s. Due to the fact that the novel product has no specific end marker unlike burning cigarettes, the measurements were stopped when no significant signal could be observed any more. For the REMPI experiment a wavelength of 263 nm was carefully chosen, because it is located between the classically available laser wavelengths of 248 nm and 266 nm, respectively. Therefore, a reasonable aromatic fingerprinting is possible at this wavelength.

4.3.2 Results of the comparison of a cigarette that primarily heats not burns tobacco and a conventional 2R4F research cigarette

Fig. 4.6 exhibits the filter pads after the smoking of one 2R4F research cigarette (left) and the novel cigarette design (right) under ISO conditions. While there is significant contamination visible on the regular cigarette, it is hardly visible on the right filter pad. This is a result of the different mechanisms of smoke generation. While tobacco is burned in the 2R4F research cigarette, it is thermodesorbed in the new cigarette. Thus, only low and medium volatile compounds are extracted with the hot air.
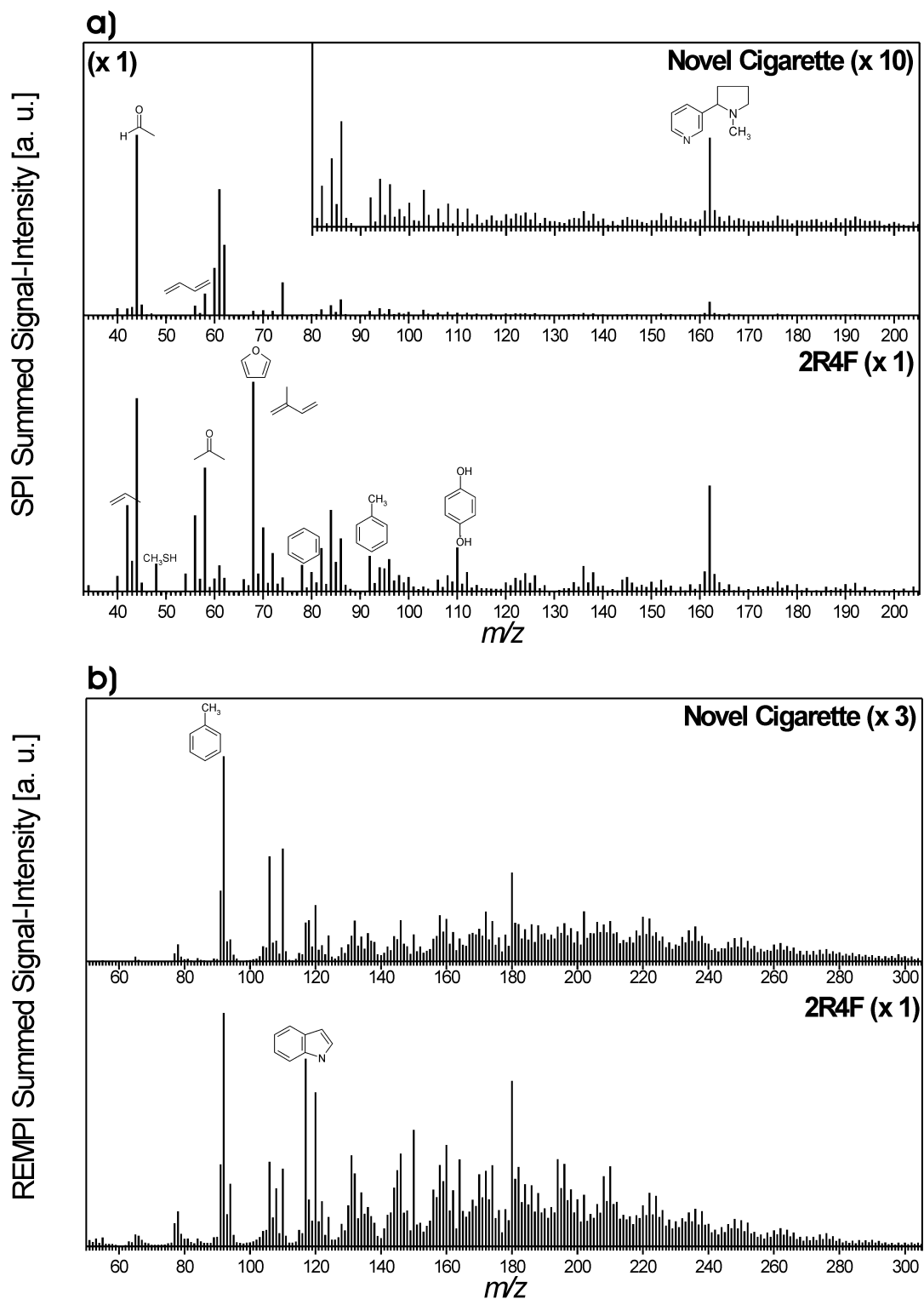
Figure 4.7: Comparison of summed SPI (118 nm) (a) and REMPI (263 nm) (b) mass spectra of a novel cigarette which heats and not burns tobacco (top) and a 2R4F research cigarette (bottom) smoked under ISO conditions.

In Fig. 4.7 the summed SPI (a) and REMPI (b) mass spectra are compared for the novel cigarette (top) and a conventional 2R4F research cigarette (bottom) smoked under ISO conditions. It can be clearly seen in the SPI spectrum (Fig. 4.7 a), that for most compounds the yield for the new product is significantly lower than with the 2R4F cigarette. Additionally, besides $m/z = 162$ (nicotine), which is reduced by a factor of 5–10, little ion yield can be observed in the mass region $m/z > 112$. However, there are certain similarities, in fact the similar amount of $m/z = 44$ (acetaldehyde) present in both cigarettes. Besides that, the chemical fingerprint of both cigarettes is significantly different. While typical combustion products of tobacco, like the sulphur containing compounds H_2S and methanthiole, unsaturated hydrocarbons, carbohydrate fragments, low boiling aldehydes, volatile aromatic compounds, and phenols are clearly visible in the burned cigarette, they are lacking in the new product.

The aromatic fingerprint presented in the comparison of the REMPI mass spectra in Fig. 4.7 b) shows, that there is a significantly lower amount present in the novel product. Therefore, only a comparison of the overall chemical composition can be done. While $m/z = 117$ (indole) is one of the dominating peaks in the 2R4F smoke it is less dominant in that from the novel product. Though there is considerably less difference in the profile, it is remarkable that there is a lack of $m/z = 108$ (anisole, dimethylpyrazine, benzylalcohol) in the thermal desorption cigarette.

To further differentiate between both cigarette types, selected components and their dynamic puff bevhaviour are presented in Fig. 4.8 and 4.9. In Fig. 4.8 the time profiles of $m/z = 44$ (acetaldehyde) (a), $m/z = 68$ (isoprene) (b), $m/z = 78$ (benzene) (c), and $m/z = 162$ (nicotine) (d) under ISO conditions measured with SPI are shown, each exhibiting the thermal desorption product on top and the 2R4F research cigarette at the bottom. The smoking dynamics show significant differences, visualising the basic principles of both cigarette types. As Fig. 4.8 a) and d) clarify for $m/z = 44$ (acetaldehyde) and $m/z = 162$ (nicotine), the first puff of the novel product is lower than the following ones, for the semi-volatile $m/z = 162$ (nicotine) even resulting in almost total absence. This could result from the need of pre-heating of the tobacco in the first puff to achieve efficient thermodesorption of the substances in later puffs. However, the low boiling benzene exhibits the highest concentration in the first puff, with a decrease in the following puffs, as shown in 4.8 c). In regular cigarettes, due to the shortening of the tobacco rod as the cigarette is smoked, the concentration of the substances generally increase. Some exceptions have already been discussed in an earlier chapter of this thesis, one of these $m/z = 68$ (isoprene, furane), presented in Fig. 4.8 b). In the alternative cigarette $m/z = 68$ (isoprene, furane) also yields high concentrations in the first puff, however, in succeeding puffs the level drops but does not show significant decrease before vanishing.
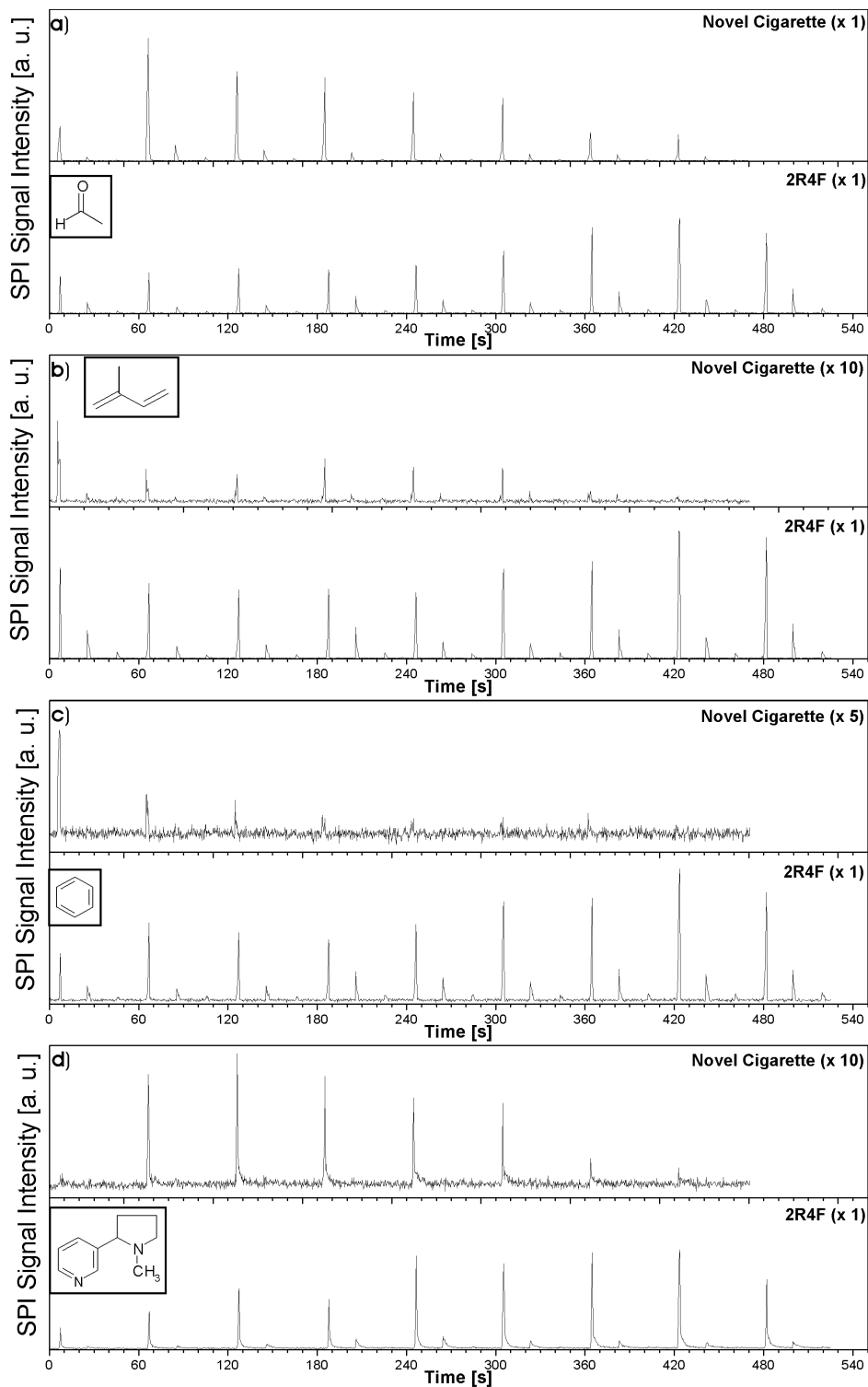
Figure 4.8: Comparison of the time profiles of acetaldehyde (a), isoprene (b), benzene (b), and nicotine (d) of a cigarette that heats not burns tobacco (top) and a 2R4F research cigarette (bottom) smoked under ISO conditions by SPI-TOFMS at 118 nm.
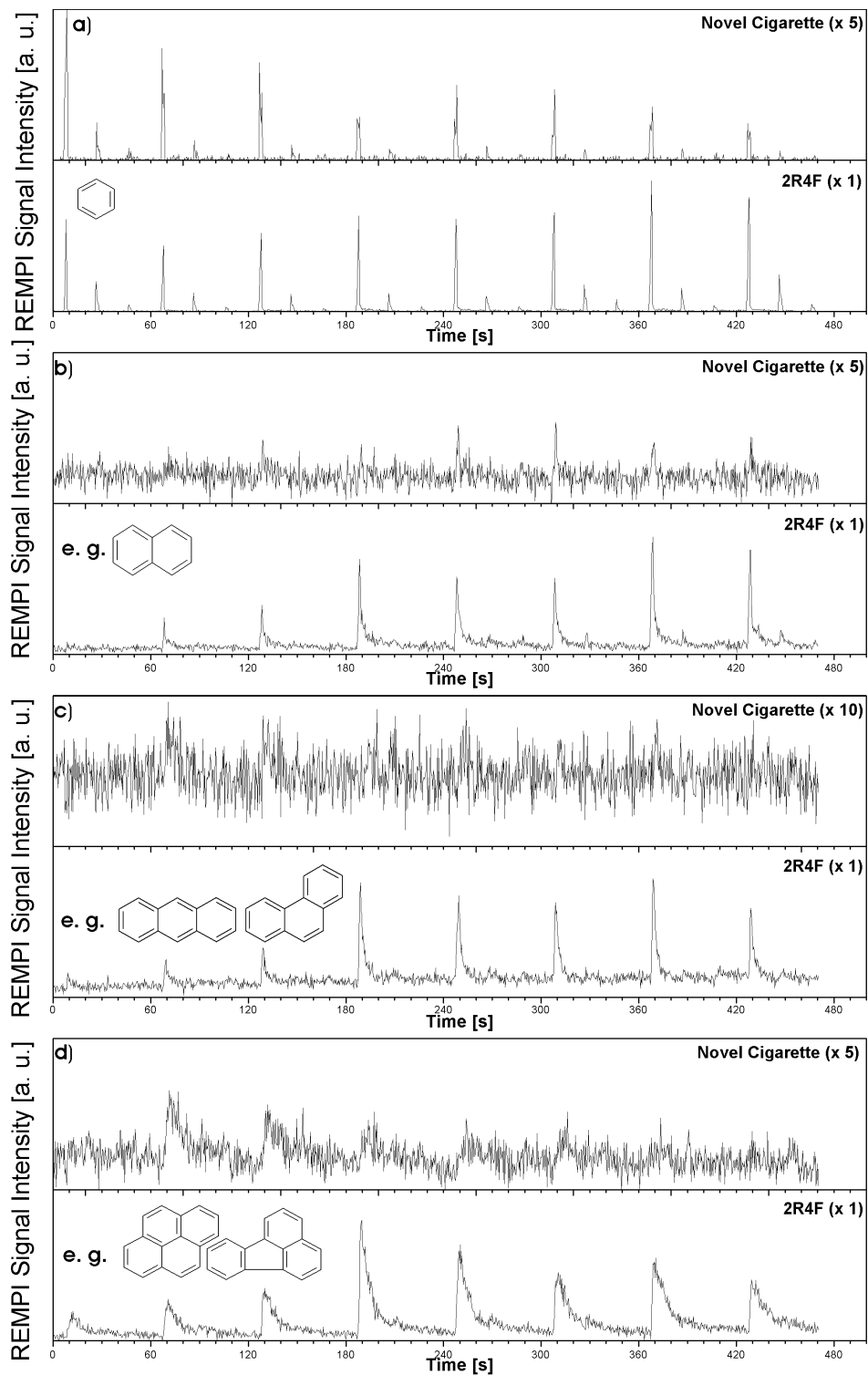
Figure 4.9: Comparison of the time profiles of benzene (a), naphthalene (b), anthracene/phenanthrene (c), and chrysene/fluoranthene (d) of a cigarette that heats not burns tobacco (top) and a 2R4F research cigarette (bottom) smoked under ISO conditions by REMPI-TOFMS at 263 nm.

In Fig. 4.9 the comparison of the time profiles of $m/z = 78$ (benzene) (a), $m/z = 128$ (naphthalene) (b), $m/z = 178$ (anthracene, phenanthrene) (c), and $m/z = 202$ (chrysene, fluoranthene) (d) under ISO conditions measured with REMPI are shown, each exhibiting the thermal desorption product on top and the 2R4F research cigarette at the bottom. Only single aromatic compounds are known to occur on $m/z = 78$ and 128. Therefore, the assignment for the 2R4F cigarette smoke can be done with uttermost certainty. However, the signals on $m/z = 178$ (anthracene, phenanthrene) and 202 (fluoranthene, pyrene) represent mixtures of the isobaric PAH. Additionally, $m/z = 178$ may be superimposed by small amounts of esculetin. The used mass assignment list (Table B.1) reflects both, the ingredients of tobacco leaf and smoke. While there is little overlap of multiple compounds on the PAH masses (except esculetin on $m/z = 178$) for "classical" cigarette smoke the composition of the mainstream smoke of the novel product may vary due to the different mechanisms of the smoke generation. Therefore, in contrast to other applications (e. g. waste-incineration) where no other organic compounds are detectable at the PAH masses and to the well known composition of "conventional" cigarette smoke there may other substances (e. g. leaf components which are usually not found in MSS) superimposing the PAH masses which may be transferred to the Eclipse MSS due to these different mechanisms. The applied wavelength of 263 nm clearly enables the monitoring of aromatic hydrocarbons in the smoke. The high sensitivity of the method is especially shown in 4.9 a) where, in comparison to the SPI mass spectrum in 4.8 c), a much better signal to noise ration can be observed, despite the fact that the sensitivity for the detection of benzene can still be improved by several orders of magnitude by further shifting the wavelength towards the main excited states at 259 nm. In the remaining puff profiles 4.9 b)–d) it is clearly visible that the higher PAH, typical pyrolysis and combustion products, are not present in the cigarette based on thermal desorption while they show up in reasonable amounts in the conventional 2R4F cigarette.

4.4 Experimental setup of the smoking regime experiments

2R4F research cigarettes were smoked five times with the customised smoking device described earlier (chapter 2.4) with different machine-smoking conditions and analysed using SPI-TOFMS. In addition to the ISO conditions (60 s puff interval, 35 ml puff volume, 2 sec puff duration, 0 % filter ventilation holes blocked) three different intense smoking parameters, namely Canadian Intense (post 2001) (30 s puff interval, 55 ml puff volume, 2 s puff duration, 100 % filter ventilation holes

Filter ventilation	20 s	30 s			60 s	
blocked	55 mL	35 mL	45 mL	55 mL	35 mL	55 mL
0 %	16.2	14.2	13.0	11.8	8.4	8.0
50 %	13.2	13.2	12.6	11.2	8.2	7.4
100 %	14.4	13.8	12.0	10.6	8.2	7.6

Table 4.3: Average puff numbers.

blocked), Canadian Intense (prior 2001) (20 s puff interval, 56 ml puff volume, 2 s puff duration, 100 % filter ventilation holes blocked) and the Massachusetts Intense conditions (30 s puff interval, 45 ml puff volume, 2 s puff duration, 50 % filter ventilation holes blocked) were programmed on the Borgwaldt smoking machine. For further investigation of the influence of filter ventilation on the chemical composition of MSS, these regimes were also smoked with the remaining filter ventilations to get a set of 100 %, 50 % and 0 % ventilation hole blocking for each. Two additional data parameter sets (60 s puff interval, 55 ml puff volume, 2 s puff duration and 30 s puff interval, 35 ml puff volume, 2 s puff duration) have been programmed to investigate the influence of puff volume and puff duration on the chemical composition of MSS. Ventilation hole blocking was performed with sellotape. The tape was mounted to the end of the cigarette, covering half of the length of the filter paper to simulate the lips of a smoker.

4.5 Results of the smoking regime experiments

Table 4.3 shows the 18 different machine smoking regimes applied and their respective influence on the puff number. In general, an unblocked filter results in the highest puff number. However, in half of the applied conditions (20 s puff interval/55 ml puff volume, 30 s puff interval/35 ml puff volume, and 60 s puff interval/55 ml puff volume) an increase from half blocked to totally blocked ventilation holes results in higher puff number, while the number decreases in two conditions (30 s puff interval/45 ml puff volume and 30 s puff interval, 55 ml puff volume) and remains constant in one (30 s puff interval, 35 ml puff volume). The blocking of ventilation holes results in higher air-flow through the cigarette tip which would be expected to increase the tobacco consumption and therefore reduce the puff number. However, in a study of different brands DARRALL [191] found similar behaviour for some cigarette brands.

	ISO conditions									
	this work		ADAM [6]		CHEN *et al.* [82]		WAGNER *et. al* [192]		COUNTS *et al.* [193]	
	μg	se	μg	sd	μg	sd	μg	sd	μg	sd
Benzene	27.1	1.9	48.2	3.6	43.39		51.8		40.5	2.6
									37.3	3.1
Isoprene	256.1	20.7	397.2	15.3	297.68		391		397	19
									342	27
Butadiene	33.6	2.7	38.5	2.2	29.94		37.1		42.8	3.3
									39	2.3
Toluene	52.0	3.2	84.5	4.3	64.91		88		65.2	5
									61.2	5.4
Acetaldehyde	622.4	44.8	527.1	26.7	560.84		562		574	57
							583.74	13.18	518	43
Acetone	245.5	17	265.1	15.1	264.74		248		312	22
							261.62	7.35	282	21

Table 4.4: *Total yields of selected smoke compounds of a 2R4F research cigarette smoked under ISO conditions.*

4.5.1 Comparison of ISO, Canadian and Massachusetts Intense smoking conditions

Quantification is done by a procedure previously introduced by ADAM [6] and described in detail in chapter 2.7. Table 4.4 shows a comparison of previous yields of 2R4F cigarette smoke components using ISO conditions documented in the literature. The values obtained show reasonable agreement with the previous investigations, especially with the novel calibration method based on relative cross sections. The relatively low yields of benzene and toluene may be explained by an affinity of these substances to the used teflon-coated gas containers.

In table 4.5 a comparison of a previous quantitative investigation on intense smoking regimes with research cigarettes by COUNTS *et al.* [194] is presented. Unfortunately the publication deals with the predecessor of the research cigarette used in this study, the 1R4F. Nevertheless, a comparison should still be possible. While the quantities of benzene, isoprene, and butadiene are a good match in the Massachusetts parameter set, acetone yields remarkably higher amounts and acetaldehyde and toluene show almost double the amount present in the previous study. Additionally, these trends are comparable in the Canadian regime, though there is a better agreement for toluene. However, the reason for the relatively high deviation in the amount of acetaldehyde is unclear as it can not solely be explained by the different cigarette types used.

	Massachusetts Intense Conditions				Canadian Intense Conditions			
	this work		COUNTS *et al.* [194]		this work		COUNTS *et. al* [194]	
	μg	se	μg	sd	μg	se	μg	sd
Benzene	88.3	5.6	64.9	7.9	118.7	7.5	83.3	8.2
			67.2	7.4			76.1	9.1
Isoprene	765.5	65.3	630	106	954.9	70.9	952	73
			726	89			929	68
Butadiene	108.9	8.8	78.6	11	147.1	10.7	105	6.9
			79.1	9.1			93.9	9.2
Toluene	229.4	10.6	130.5	19.9	297.9	16.6	176.2	15.7
			132.9	19			156.3	21.8
Acetaldehyde	1950.8	132.5	1007	56	2796.2	191.3	1448	43
			1101	81			1359	105
Acetone	740.8	44.9	567	24	1005.8	59.9	755	27
			585	34			687	45

Table 4.5: Total yields of selected smoke compounds of a 2R4F research cigarette smoked under Massachusetts and Canadian Intense conditions.

The puff resolved quantifications are presented for a 2R4F research cigarette smoked under ISO (Fig. 4.10), Massachusetts Intense (Fig. 4.11) and Canadian Intense (Fig. 4.12) smoking conditions, respectively. A number of selected compounds, namely propyne, propene, butadiene, acetaldehyde, acetone, isoprene, benzene, toluene, and xylene are presented. In Fig. 4.10 the typical first puff behaviour (explained earlier in chapter 4.2) can be observed for the unsaturated compounds and to a smaller extent acetaldehyde, as well as an increase in the later puffs, as already reported in [6,77] The standard deviations are relatively low, except for the ninth puff, which can be explained by the fact that instead of ten it took less than nine puffs to smoke the cigarette, and, therefore, fewer data for this puff is available. In Fig. 4.11 the puff yields with Massachusetts Intense conditions are shown. The same first puff behaviour can be seen as with the ISO conditions. However, the increase in the later puffs is more divergent, indicated by the broader error margins, and in total less than with the ISO conditions. The increase can also only be monitored up to the ninth puff, followed by an increase and a steady level, unfortunately accompanied by larger error margins resulting from the great variety in puff numbers. In Fig. 4.12 the quantitative data for Canadian Intense Conditions is depicted showing the same first puff results as in the previous two parameter sets in the unsaturated species and acetaldehyde, followed by an increase up to the ninth puff, after which a smaller amount is observed.
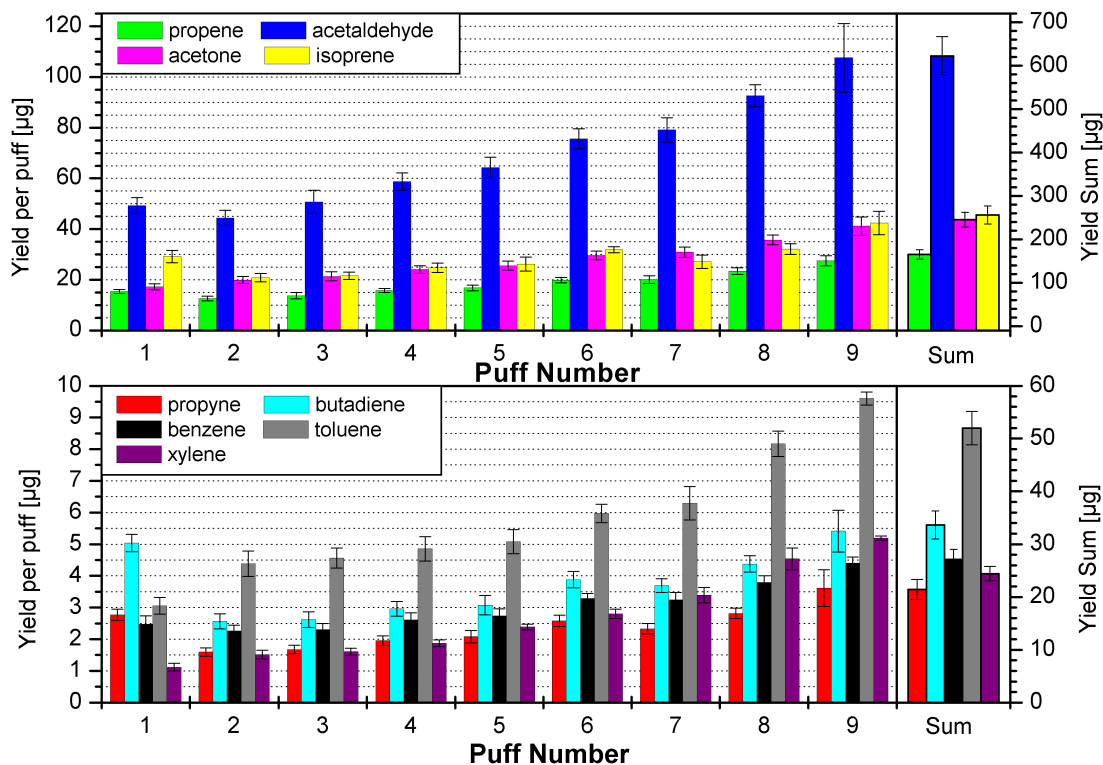
Figure 4.10: Puff resolved quantification of selected compounds of a 2R4F research cigarette smoked under ISO smoking conditions.

For a first comparison of the three different smoking conditions the three SPI mass spectra are presented in Fig. 4.13. The spectra are normalised to the corresponding total ion stream. A selection of typical MSS components is given within the picture. In general, the amount of observable differences is limited. However, the amount of $m/z = 17$ (ammonia), 30 (nitric oxide), 42 (propene), and 68 (isoprene, furan) generated under ISO conditions is higher than under Massachusetts or Canadian Intense conditions. These compounds, with the exception of $m/z = 17$ (ammonia), have been previously reported to have unique behaviour in the first puff (chapter 4.2) resulting from different burning temperatures during the first puff. It can be assumed that a change of the puff parameters influences the temperature profiles within the cigarette tip during and between the puffs probably influencing these compounds, as well. However, for a more detailed comparison statistical methods have to be applied.

Fig. 4.14 illustrates the increase in yields of the 100 highest peaks of a 2R4F research cigarette smoke under ISO conditions compared to Massachusetts (Fig. 4.14 a) and Canadian (Fig. 4.14 b) Intense conditions. To get a better overview of the effects on the single mass traces, each is divided by the corresponding ion signal of
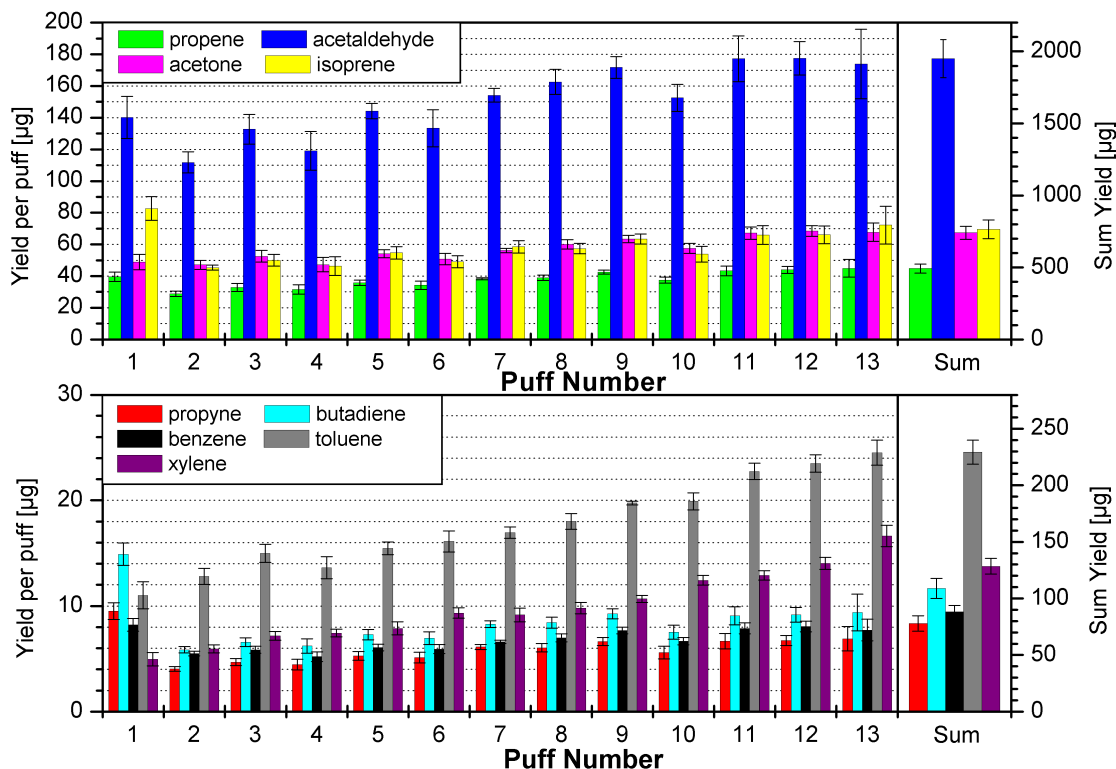
Figure 4.11: Puff resolved quantification of selected compounds of a 2R4F research cigarette smoked under Massachusetts Intense smoking conditions.

the ISO-yield. Therefore the graphs exhibit the factorial increase of each compound in the two intense regimes compared to the ISO conditions. The red lines indicate an optically chosen average value for each of the measurements, the green line in Fig. 4.14 b) shows the corresponding factor of the Massachusetts conditions in the Canadian graph, to further investigate the behaviour of the chemical species. In the Massachusetts Intense conditions most of the compounds have yields about 2.4–2.8 times higher compared to ISO-conditions, while in the Canadian Intense conditions only a smaller number of substances can be assigned to a constant factor. However, if possible, a line can be drawn at a factor of approximately 3.6–4.0 compared to the ISO conditions. In both parts of the picture homologue rows starting at $m/z = 51$ and ending at $m/z = 121$ (Fig. 4.14 a) and $m/z = 107$ (Fig. 4.14 b), respectively, as well as starting at $m/z = 92$, ending at $m/z = 134$ are emphasised, which yield higher ratios compared to most of the other substances. No compounds have previously been reported at $m/z = 51$ and $m/z = 65$ and the NIST database search only results in the carbonitrile compound cyanoacetylene and nitrogenchloride oxide. No literature could be obtained marking these compounds as tobacco or tobacco smoke ingredients. However, starting at $m/z = 79$ the homologue row of pyridine, joined by
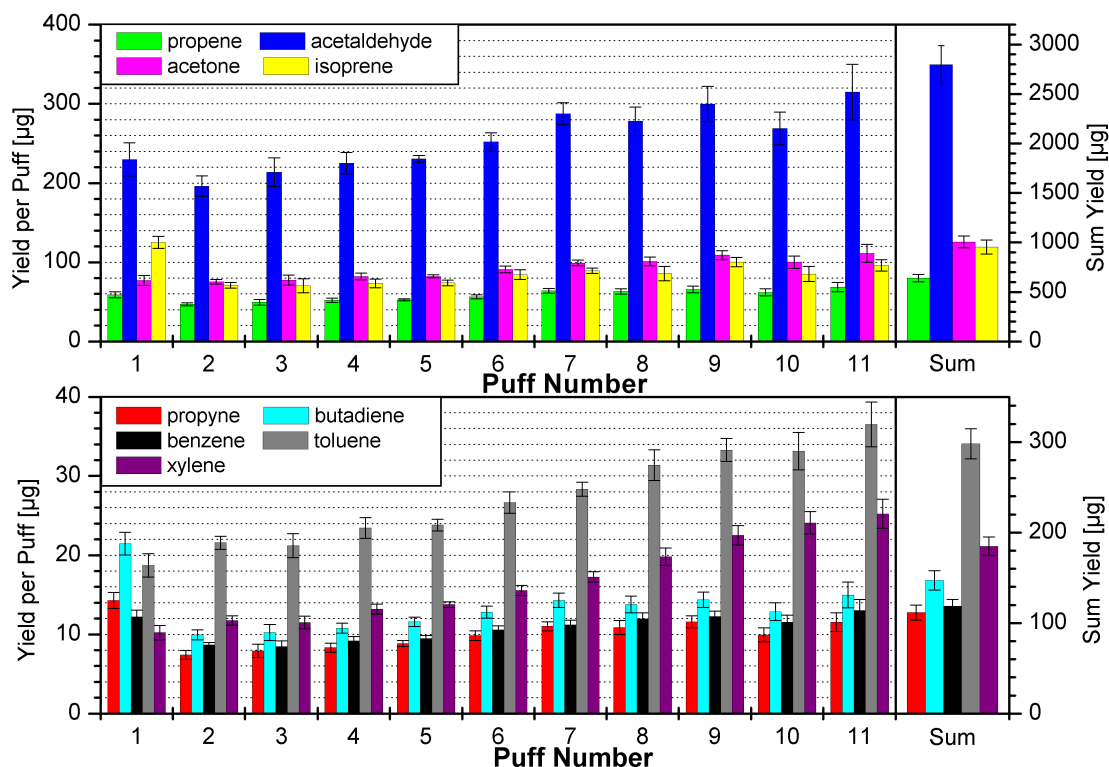
Figure 4.12: Puff resolved quantification of selected compounds of a 2R4F research cigarette smoked under Massachusetts Intense smoking conditions.

aromatic amines at $m/z = 93$ is visible. Furthermore the homologue row $m/z = 92$ (toluene, glycerole), 106 (xylenes, ethylbenzene, benzaldehyde), 120 (trimethylbenzenes, methyl-ethyl-benzenes, p-vinyl-phenol), and 134 (isopropyltoluene) is marked. The changes in smoking conditions have higher influence on these substances, than on most of the others. Additionally, exceptionally high factors can be observed at $m/z = 52$ (1-buten-3-yne), 53, 67 (pyrrole), 81 (methyl-pyrrole), 91, 103 (benzonitrile, amino-butyric acids), 104 (styrene, pyridine-carbonitrile), 117 (indole), 122 (benzoic acid, ethylphenols, hydroxybenzaldehydes, trimethylpyrazines, methyl-ethyl-pyrazines, phenethylalcohol), and 145 (2-(4-pyridyl)furan, 2,3-dimethyl-1H-indole, 3-ethylindole) in the comparison of the Massachusetts to the ISO conditions while exceptionally low ones can be seen at $m/z = 17$ (ammonia), 30 (nitric oxide), and 114 (2-hydroxy-3-methyl-2-cyclcopenten-2H-pyran-2-one). In the Canadian Intense regime only $m/z = 91$ and $m/z = 117$ (indole, valine) attract attention in this matter. It is noteworthy that the masses $m/z = 34$ (hydrogen sulphide), 42 (propene), 48 (methanthiole), 56 (2-propenal, butene, methylpropene), 68 (isoprene, furan), and 70 (2-butenal, methyl-vinyl-ketone, methylbutene, pentene, 2-methyl-2-propenal, butenone) show little to no increase in yield going from the Massachusetts
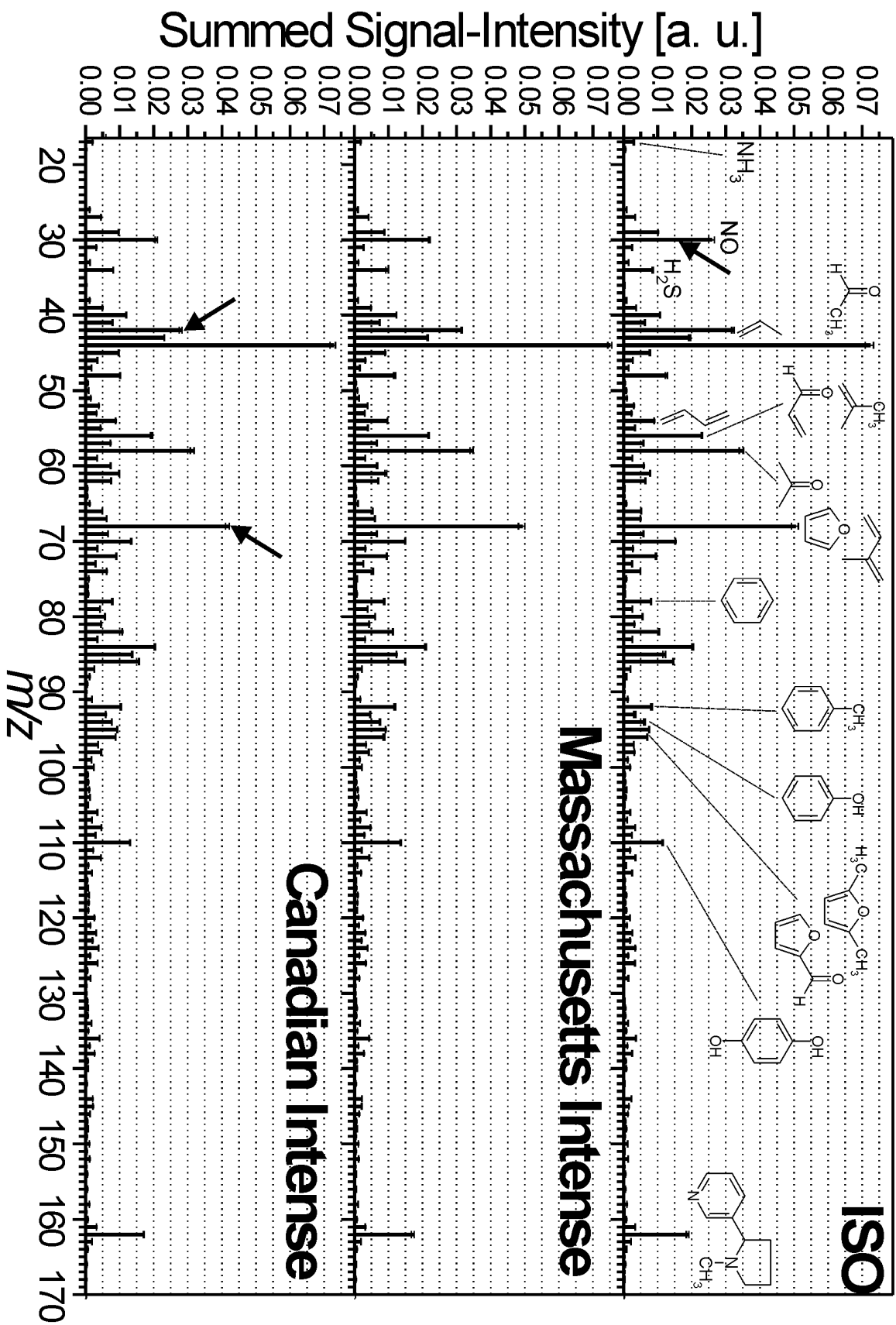
Figure 4.13: Comparison of the SPI mass spectra of a 2R4F research cigarette smoked with ISO, Massachusetts Intense and Canadian Intense smoking conditions.
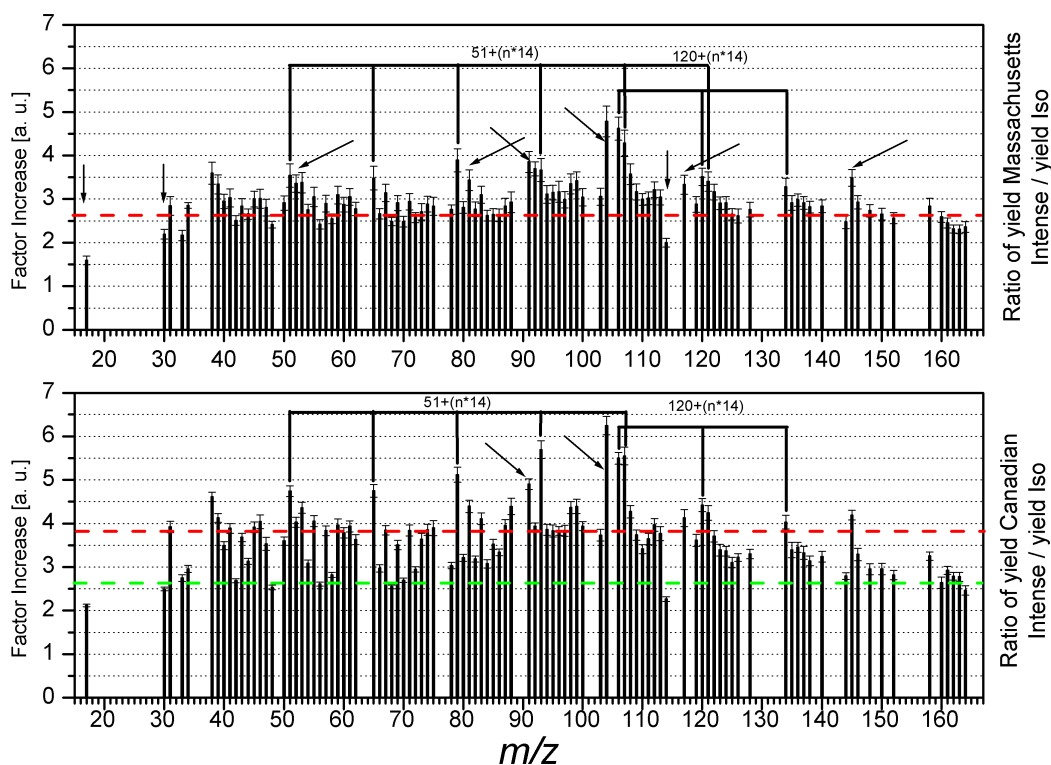
Figure 4.14: Comparison of the 100 highest mass peaks of a 2R4F research cigarette smoked under ISO conditions and Massachusetts Intense (a) and Canadian Intense (b) parameters.

to the Canadian Intense conditions, as well as most substances with $m/z > 140$.

In Fig. 4.15 the score (4.15 a) and loading (4.15 b) plot of a PCA of the 50 highest FV discriminating the three smoking regimes is presented. The datasets are standardised to the corresponding total ion count of the spectrum, thus only changes in the chemical fingerprint are visible. The predominance of the first and second PC with 84 % and 6 % is high, therefore the dataset should be interpretable. However, though there is a displacement of the three regimes, the chemical profiles of both intense smoking conditions do not differ significantly. As discovered earlier, $m/z = 145$ (2-(4-pyridyl)furan, 2,3-dimethyl-1H-indole, 3-ethylindole) plays an important role in separating the ISO conditions, as well as $m/z = 87$ (isoamylamine), while the majority of the compounds do not contribute significantly to a further separation of the Massachusetts and Canadian Intense conditions in the first PC. Nevertheless, the second PC provides information in this matter, in fact $m/z = 40$ (propyne) and $m/z = 96$ (furfural, dimethylfuran) points to the Massachusetts parameter set, while $m/z = 56$ (2-propenal, butene, 2-methylpropene), 57 (carbohydrate fragment, 2-propen-1-amine), 60 (propylalcohol), 74 (propionic
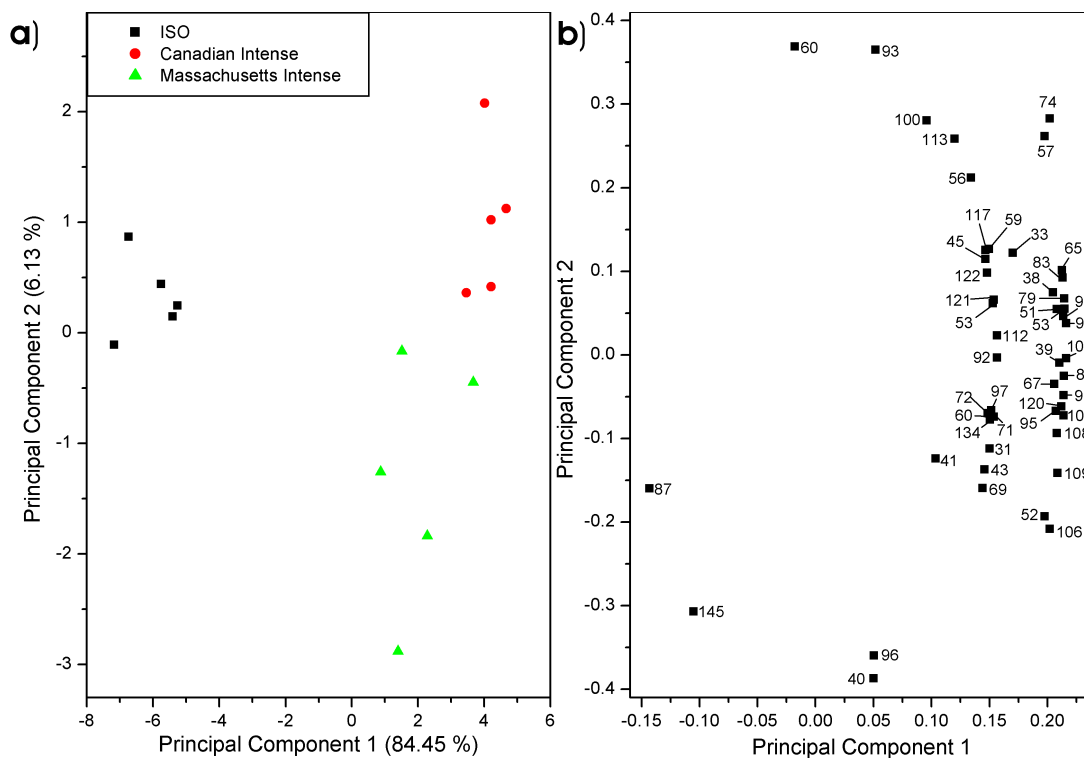
Figure 4.15: Score (a) and loading (b) plot of a PCA of the 50 highest FV discriminating ISO, Massachusetts Intense and Canadian Intense smoking conditions.

acid, butylalcohol, isobutylalcohol), 93 (aniline, methylpyridines), 100 (tiglic acid, 3-hexen-1-ol), and 113 (methylsuccinimides) point to the Canadian Intense regime. However, tiglic acid and 3-hexen-1-ol have previously only been reported in tobacco leaf, no references of appearance in mainstream smoke could be found.

The three puff regimes used have been thoroughly investigated by the Scientific Committee on Tobacco and Health (SCOTH) in 2000, dealing with nicotine free dry particulate matter (NFDPM), nicotine and CO [195], PAH [196], and nitric oxide yields [197]. This large study included a huge variety of commercially availably cigarette brands. Unfortunately, no account has been taken of research cigarettes, except in nitric oxide yields, where the 1R4F was characterised. The puff numbers have been reported to be 8.27 (ISO), 13.34 (Massachusetts Intense), and 11.41 (Canadian Intense), respectively. The puff numbers observed in this study (Table 4.3) are in good agreement, since a different type of research cigarette (2R4F) is used. The nitric oxide yields observed in the study are 0.312 mg/cig (ISO), 0.548 mg/cig (Massachusetts Intense), and 0.714 mg/cig (Canadian Intense). Normalised to the ISO-yield this results in a factorial increase of 1.75 and 2.29, which is in good agreement with the values observed in this study. The measurements indicate that the use of intense smoking conditions does not affect all substances the same way.

However, the influence seems to be greater for nitrogen-containing compounds and (alkyl-)benzenes and lower for small, unsaturated alkenes and carbonyl compounds, as well as the majority of of compounds with $m/z > 120$. Additionally, the chemical fingerprint seems to change little, as seen in the statistical data evaluation. Again nitrogen containing compounds seem to have higher influence, as well as some small alcohols.

4.5.2 Effect of filter ventilation on the chemical composition of mainstream smoke

Fig. 4.16 and Fig. 4.17 show the effect of blocking filter ventilation holes on different machine smoking regimes. To get a better overview of the effects on the single mass traces each one is divided by the total ion signal of the yield with no ventilation holes blocked. As a result the factor of increase relative to the unblocked measurement is visible. In Fig. 4.16 a) and b) the effect on the regimes with 60 s puff interval and 35 ml and 55 ml puff volume, respectively, are presented. It can be clearly seen that the ion-yields of all the masses only varies little around a factor of 1.5, while the difference between the yields at half and fully blocked ventilation holes is significantly lower than between fully open and half blocked ventilation holes. However, some additional effects can be observed on the set including the ISO conditions, in fact, a decreasing effect of filter ventilation with higher masses, starting at 2.0 on mass $m/z = 30$ and ending with a factor of 1.5 at $m/z = 162$. While these effects can be observed for most of the 100 highest peaks of the spectra there are certain exceptions. Higher yields are visible for $m/z = 38$ and 39 and $m/z = 65$, $m/z = 79$ (pyridine), $m/z = 91$ and 92 (toluene), and $m/z = 106$ (xylenes, ethylbenzenes, benzaldehyde) as well as $m/z = 145$ (2-(4-pyridyl)furan, 2,3-dimethyl-1H-indole, 3-ethylindol). With increased puff volume of 55 ml there is no difference in the effect on high or low masses. However some masses still show unique behaviour, in fact $m/z = 17$ (ammonia), 30 (nitric oxide), 34 (hydrogen sulphide), 145 (2-(4-pyridyl)furan, 2,3-dimethyl-1H-indole, 3-ethylindole), and 158 (nicotyrine, nonanoic acid) yield lower ratios at half blockage, while only $m/z = 17$ (ammonia), 30 (nitric oxide), and 34 (hydrogen sulphide) show different behaviour at full blockage. Fig. 4.16 c) presents the effect of filter ventilation on the yields at 20 s puff interval and 55 ml puff volume. While there is a significant increase of a factor of about 2.0 from 0 % blocked ventilation holes to 50 % at $m/z = 30$, then linear decreasing to 1.5 at $m/z = 162$, there is no further increase in yield for higher masses at full blockage. For lower masses there is even a decrease to a factor of about 1.5. However, there is one significant exception at the 50 % to 0 % blockage factor, $m/z = 145$ (2-(4-pyridyl)furan, 2,3-dimethyl-1H-indole, 3-ethylindole) which also shows a higher
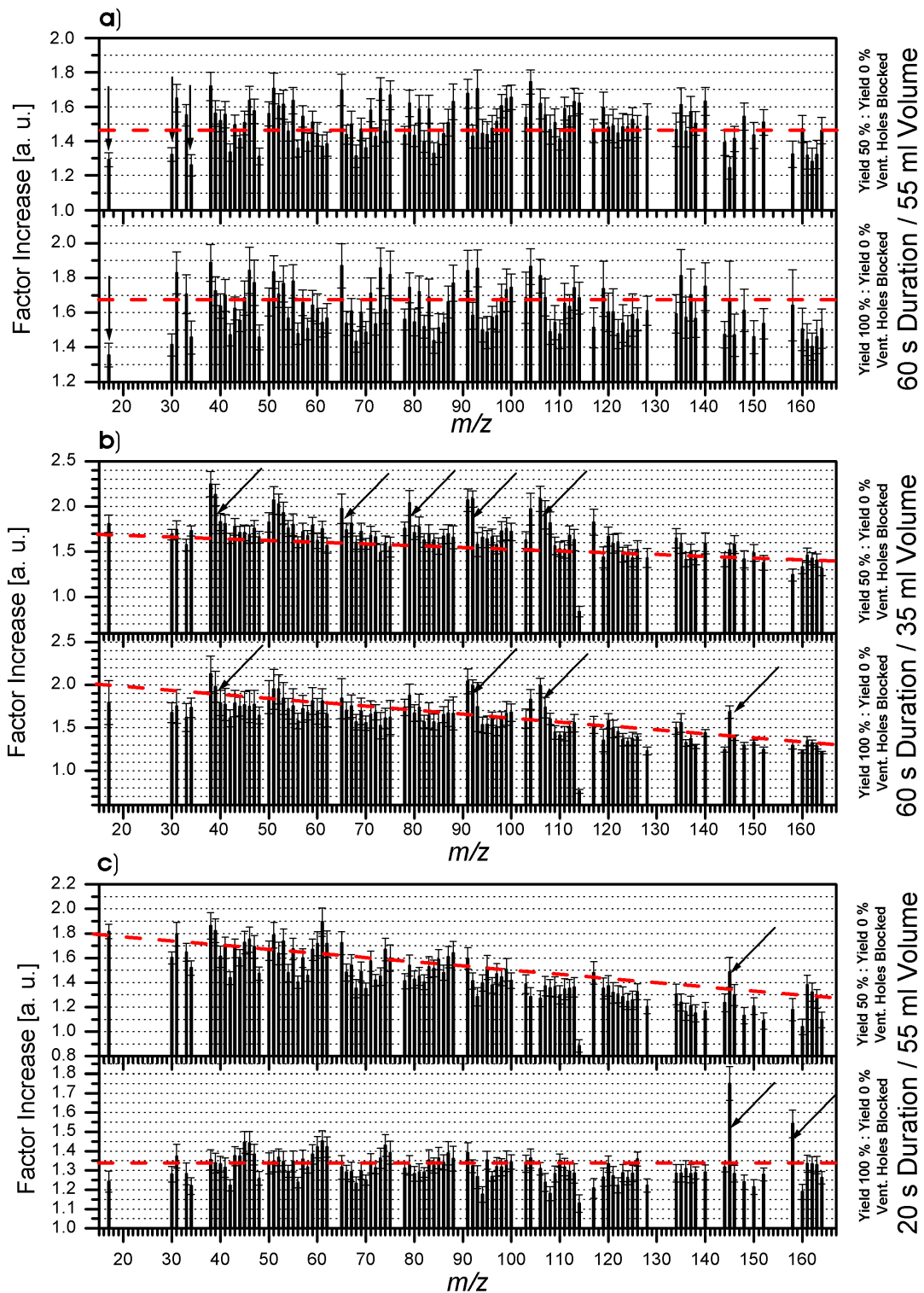
Figure 4.16: Influence of ventilation hole blocking on the 100 highest mass peaks of a 2R4F research cigarette smoked under ISO conditions on smoking regimes 60 s / 55 ml (a), 60 s / 35 ml (b), and 20 s / 55 ml (c).

ratio when 100 % is compared to 0 %.

Fig. 4.17 exhibits the influence of the filter ventilation on puff regimes with 30 s at 35 ml (Fig. 4.17 a), 45 ml (Fig. 4.17 b), and 55 ml (Fig. 4.17 c), respectively. Again, the yields are standardised to the ion signal of the mass at 0 % of the filter ventilation holes blocked.

As with the regime of 60 s puff interval and 35 ml puff volume presented in Fig. 4.16 a) no consistent factor can be observed in Fig. 4.17 a). Moreover, no linear decrease can be assigned starting from the low masses, instead a stepwise drop at $\approx m/z = 90$–100 can be found, beginning at a factor of 1.6–1.8 at low masses and 1.2–1.4 at higher masses. A significantly higher yield at 50 % ventilation is seen on $m/z = 93$ (methylpyridines, aniline), no exceptionally low values can be identified. A comparison of the fully blocked ventilation holes with the unblocked one results in similar observations. Though the position of the step again is in the mass range of $m/z = 90$–100 and the factor for the low masses is similar (1.4–1.6), the yields of higher masses ($m/z > 100$) are even lower than in the 50 % blocking case. Only minor exceptions can be assigned on $m/z = 93$ (aniline, methyl-pyridines) and $m/z = 106$ (xylenes, ethylbenzene, benzaldehyde, diethylenglycol). The same plot for 30 s puff interval and 45 ml puff volume is presented in Fig. 4.17 b). An almost constant increase of a factor of 1.5 can be seen for all of the 100 substances after blocking half of the ventilation holes, while only four compounds show exceptional behaviour, namely $m/z = 17$ (ammonia) and $m/z = 117$ (indole, valine) with reduced yields, and $m/z = 145$ (2-(4-pyridyl)furan, 2,3-dimethyl-1H-indole, 3-ethylindole) and $m/z = 158$ (nicotyrine, nonanoic acid) exhibit slightly increased amounts. It is remarkable that the amount of ammonia even stays constant. Full blockage of the ventilation results in a complete change of behaviour, as no universal factor can be assigned to the spectrum anymore, but a more or less linear decrease starting from 2.0 at $m/z = 30$ declining to 1.4 at $m/z = 164$ with many exceptions probably describes the regime best. This means that most of the substances with $m/z > 100$ show little or no increase when going from 50 % to 100 % blocking. The most prominent exceptions include higher yields of $m/z = 88$ (butyric acid, pyruvic acid), 93 (aniline, methyl-pyridines), 145 (2-(4-pyridyl)furan, 2,3-dimethyl-1H-indole 3-ethylindole), and 158 (nicotyrine, nonanoic acid) and lower yields at $m/z = 17$ (ammonia), 30 (nitric oxide), 34 (hydrogen sulphide), 42 (propene), and 48 (methanthiole), which show almost no increase compared to the measurements with half blocked ventilation holes. Fig. 4.17 c) evinces the last observed smoking regime with 30 s puff interval and 55 ml puff volume. Both factor-plots show a slight decrease in yields starting from 1.75 at $m/z = 30$ and ending at 1.25 at $m/z = 162$. All of the substances show almost identical yields with either half or fully blocked ventilation holes. Again, some masses deviate from the postulated linear decrease,
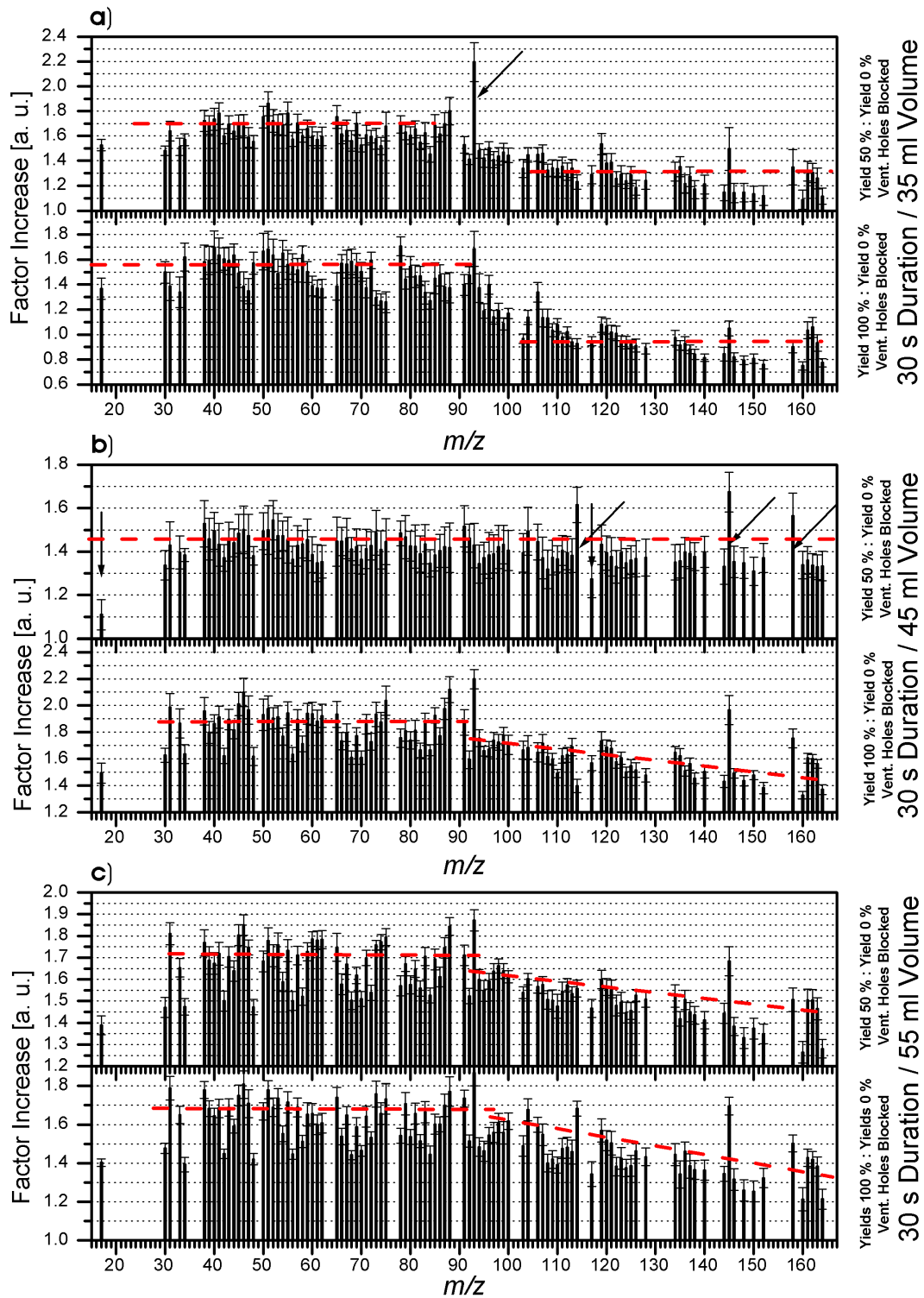
Figure 4.17: Influence of ventilation hole blocking on the 100 highest mass peaks of a 2R4F research cigarette smoked under ISO conditions on smoking regimes with 30 s puff interval and 35 ml (a), 45 ml (b), and 55 ml (c) puff volume.

Flow-rate [mL/s]	Total ventilation [%] at vent. hole blocking			
	0 %	50 % (1)	50 % (2)	100 %
17.5	53	14	24	11
22.5	46	13	33	12
27.5	43	12	22	11

Table 4.6: Effect of blocking ventilation holes of a 2R4F research cigarette no total ventilation. 50 % (1) represents blocking of the whole circumference on half of the filter, 50 % (2) blocking of half the circumference on the whole length of the filter.

$m/z = 17$ (ammonia), 30 (nitric oxide), 34 (hydrogen sulphide), 42 (propene), and 48 (methanthiole) and $m/z = 93$ (methylpyridines, aniline) and $m/z = 145$ (2-(4-pyridyl)furan, 2,3-dimethyl-1H-indole 3-ethylindole).

In conclusion, no universal behaviour was found which is valid for all parameter sets, instead each puff duration and puff-volume set seems to have unique reactions on filter ventilation hole blocking, the effect seems to be cross-related to other effects. The filter ventilation of a 2R4F research cigarette was determined to 28 % [82]. This is a relatively low value compared to the majority of the commercial low-tar cigarettes. As a result, the effects of ventilation hole blocking on total yields and the chemical composition is expected to be much higher in these cases. The blocking of filter ventilation holes simulating the lips of a smoker may provide important data for the estimation of the effect of filter ventilation hole blocking. However, there are different ways of blocking the filter ventilation holes, the covering of 50 % of the filter area from the mouth end to the middle of the filter and from the mouth end to the end of the filter, covering half of the circumference. Table 4.6 shows a comparison of the measured total ventilation of the used 2R4F research cigarettes. It can be seen, that there are major differences in total ventilation values with both methods. This may result in an uneven distribution of the primary ventilation holes on the filter. Therefore, for a more thoroughly investigation of the effect of filter ventilation, it would be useful to use sets of special cigarettes, with known values of filter ventilation, e. g. 30, 60 and 90 %. With this enlarged dataset the effects on medium and high ventilated cigarettes could be investigated more efficiently. Additionally, the total ventilation of the cigarette shows a strong dependance on the flow rate through the cigarette, at higher flow rates an even greater part of the total airflow is drawn through the tip of the cigarette. Nevertheless, it is remarkable that quite a few regimes show constant factors for all the examined masses, and others at least show similar effects in well defined groups of substances, classified by the mass to charge ratio. It is also noteworthy, that the mass traces with unique behaviour keep recurring throughout the different regimes. Additionally, a basic

set of information, which may help to fully understand the behaviour of different compounds and compound classes is presented. However, the complexity of the data gathered with different machine smoking parameters can only be a basis for the even more complex spectrum of human smoking behaviour.

4.5.3 Effect of puff interval and puff volume on the composition of mainstream smoke

In Fig. 4.18 an overview of the effect of puff volume on the chemical composition of mainstream smoke is given. All measurements are done at a constant puff interval of 30 s and include puff volumes of 35 ml, 45 ml, and 55 ml. As described earlier, the increase is presented as a factor, calculated by dividing the signal of the higher puff volume by the lowest one. The graphic shows the results for the three investigated filter ventilation blockings 0 % (Fig. 4.18 a), 50 % (Fig. 4.18 b), and 100 % (Fig. 4.18 c). The comparison of the 45 ml puff volume with the 35 ml measurement at 100 % filter ventilation clarifies an increase of a factor of about 1.4–1.6 for all 100 presented substances. However, minor exceptions can be observed at $m/z = 79$ (pyridine), 93 (aniline, methylpyridines), 104 (styrene, pyridinecarbonitrile), and 114 (4-hydroxy-5,6,dihydro-2H-pyran-2-one) which yield slightly higher factors, while $m/z = 17$ (ammonia) and the majority of the peaks $m/z > 130$ inhibit slightly lower yields. In principle, the same observations can be made while comparing the 55 ml puff volume to the 35 ml at 0 % filter ventilation blocked. Most of the signals increase by a factor of 1.9–2.2 compared to the lower volume. Exceptional behaviour can be assigned to the same compounds, $m/z = 79$ (pyridine), 93 (aniline, methylpyridines), 104 (styrene, pyridinecarbonitrile), and 114 (4-hydroxy-5,6,dihydro-2H-pyran-2-one) which seem to be more influenced, while a few more masses are influenced less by the volume change, namely $m/z = 30$ (nitric oxide), 34 (hydrogen sulphide), 42 (propene), and 48 (methanthiole) in addition to the previously reported $m/z = 17$ (ammonia) and the mass range of $m/z > 130$.

Fig. 4.18 b) visualises the factorial increase of the compounds at 45 ml to 35 ml and 55 ml to 35 ml at a filter ventilation blocking of 50 %. Again a factor of 1.3–1.5 can be assigned to the comparison of 45 ml to 35 ml puff volume. However, the mass range of $m/z > 120$ seems to show a slightly higher increase, in contrast to 100 % ventilation. Masses $m/z = 79$ (pyridine), 92 (toluene, glycerol), 104 (styrene, 3-pyridinecarbonitrile), and 114 (4-hydroxy-5,6,dihydro-2H-pyran-2-one) show increased presence, $m/z = 17$ (ammonia), 85 (methylpyrrolidine, piperidine, 2-pyrrolidone), and 88 (butyric acid, pyruvic acid) slightly decreased one. A further increase to a puff volume of 55 ml shows significant differences. While most of the sub-
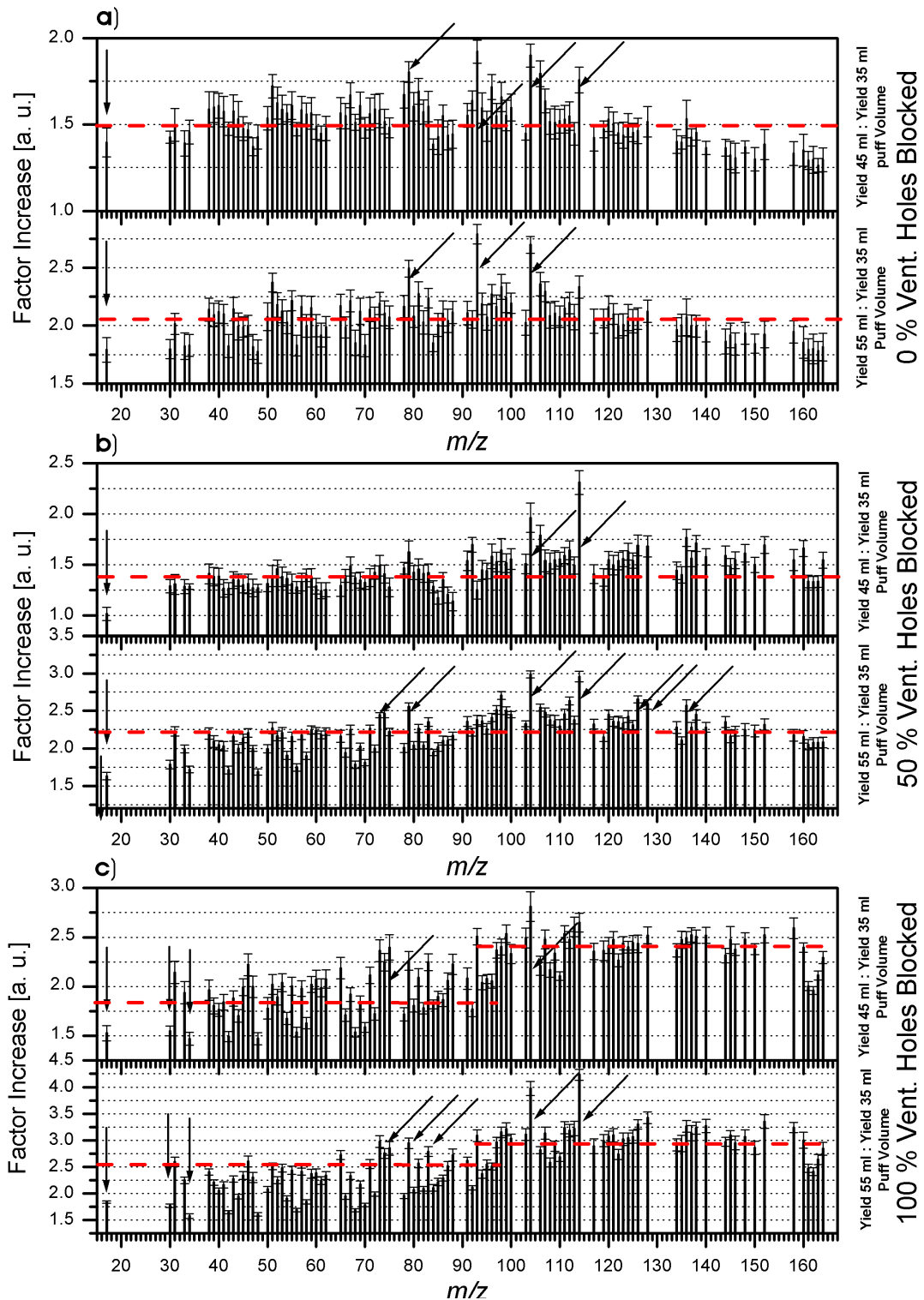
Figure 4.18: Influence of puff volume on the 100 highest mass peaks of a 2R4F research cigarette smoked under ISO conditions at smoking regimes with 30 s puff interval and 0 % (a), 50 % (b), and 100 % (c) ventilation hole blocking.

stances increase by a factor of 2.0–2.2, the region from $m/z = 91$–128 and $m/z = 73$ (isobutylamine, butylamine), 74 (propionic acid, butylalcohol, isobutylalcohol) and 79 (pyridine) are more influenced. The usual compounds exhibiting lower influence ($m/z = 17$ (ammonia), 30 (nitric oxide), 34 (hydrogen sulphide), 42 (propene), and 48 (methanthiole)) are accompanied by $m/z = 56$ (2-propenal, butene, methyl-propene), 58 (acetone, propanal), 68 (isoprene), 70 (butenal, methylvinylketone, methylbutene, pentene, methylpropenal, butenone), most of them reported earlier to play an important role in distinguishing between the intense smoking regimes.

In Fig. 4.18 c) effects of increase of puff volume at fully blocked filter ventilation holes are visualised. In the plot comparing 45 ml and 35 ml puff volume the substances can, in principle, be divided in two major subclasses, divided by $m/z = 90$. Prior to this mass most substances yield an increase of a factor of about 2.0, while higher masses increase by a factor of approximately 2.5. Again ($m/z = 17$ (ammonia), 30 (nitric oxide), 34 (hydrogen sulphide), 42 (propene), and 48 (methanthiole)) are accompanied by $m/z = 54$ (butadiene, butyne), 56 (2-propenal, butene, methylpropene), 58 (acetone, propanal), 68 (isoprene), 70 (butenal, methylvinylketone, methylbutene, pentene, methylpropenal, butenone) seem to be less influenced, while $m/z = 73$ (isobutylamine), 74 (propionic acid, butylalcohol, isobutylalcohol), 75 (glycine), and 104 (styrene, 3-pyridinecarbonitrile) seem to increase.
The last comparison of 55 ml to 35 ml at fully blocked ventilation holes shows more variances than previous plots. However, certain tendencies are again visible. The spectrum may be divided into two subparts, borderlined by $\approx m/z = 90$, where a step from a factor of 2.3–2.5 to a factor of 3.0–3.2 occurs. Unfortunately, the list of exceptions is quite long, including the higher peaks, $m/z = 31$, 65, 73 (isobutylamine), 74 (propionic acid, butylalcohol, isobutylalcohol), 75 (glycine), 79 (pyridine), 81 (methyl-pyrrole), 83, 104 (styrene, 3-pyridinecarbonitrile), and 114 (4-hydroxy-5,6,dihydro-2H-pyran-2-one).

As a conclusion it can be said that the effect of a change of puff volume is as complex equally as the change of filter ventilation described earlier. However, as seen previously, the large differences can be reduced to a small range of substances. Again, organic nitrogen containing hydrocarbons, especially $m/z = 79$ (pyridine), seem to be highly influenced to yield higher amounts when the puff volume is increased. In contrast, small inorganic compounds like $m/z = 17$ (ammonia) and $m/z = 30$ (nitric oxide) and unsaturated and oxygenated compounds $m/z = 42$ (propene), 56 (2-propenal, butene, methylpropene), 58 (acetone, propanal) as well as the two known main sulphur containing substances $m/z = 34$ (hydrogen sulphide) and $m/z = 48$ (methanthiole) usually exhibit less increase with puff volume than other compounds. However, this study is limited to an experimental set of only one constant puff interval value and therefore only can serve as a first indication on what is happening

in the chemical fingerprints of tobacco smoke during modified machine smoking conditions.

In Fig. 4.19 the effect of puff duration on the composition of mainstream cigarette smoke of the 100 highest peaks of a 2R4F research cigarette smoked under ISO conditions at a constant puff volume of 55 ml and puff intervals of 20 s, 30 s, and 60 s at 100 % (a), 50 % (b), and 0 % (c) filter ventilation holes blocked is presented. As seen in Fig. 4.19 it is in general more difficult to assign one or two single factors to the whole spectrum. However, the first part up to $m/z = 90$–100 circles around a value of 2.0, the higher masses approximately around a value of 3.0, though a large number of masses differ significantly from this value. In the first part this is especially valid for even masses, e. g. $m/z = 30$ (nitric oxide), 34 (hydrogen sulphide), 48 (methanthiole), 54 (butadiene, butyne), 56 (2-propenal, butene, methylpropene), 58 (acetone, propanal), 66 (cyclopentadiene), 68, 70, and 72 and $m/z = 17$ (ammonia), which show lower ratios. In contrast the uneven masses $m/z = 65$, 73 (isobutylamine, butylamine), 75 (glycine), 79 (pyridine), 81 (methylpyrrole), 83, 135 (trimethylaniline),137 (p-tyramine), and $m/z = 88$ (butyric acid, pyruvic acid), 140 (ethylmethylmaleic anhydride), 148 (p-isopropylbenzaldehyde, cinnamic acid, phthalic anhydride) exhibit higher increase with decreasing puff interval. However, $m/z = 137$, 140, and 148 have previously not been reported in tobacco smoke, but only in tobacco leaf. It is also remarkable, that the amount of ammonia emitted stays nearly constant. Even more drastic differences can be found comparing the 20 s puff interval with the 60 s one. The low mass region up to $m/z = 90$–100 still varies around a factor of 2.0–2.5. However, most of the odd masses are more influenced than even masses, with the usual exception of $m/z = 17$ (ammonia), again at almost the same amount than in the 60 s puff interval measurement. In the second half of the spectrum an average factor of approximately 3.8 can be seen. However, the number of exceptions exceeds all previous observations. $m/z = 104$ (styrene, pyrdidinecarbonitrile, 114 (4-Hydroxy-5,6-dihydro-2H-pyranon-2-one), 128 (naphthalene), 135 (trimethylaniline), 137 (p-tyramine), 140 (ethylmethylmaleic acid), 148 (p-isopropylbenzaldehyde, cinnamic acid, phthalic anhydride) exceed the factor of 3.8, while $m/z = 110$ (hydroquinone, methylfurfural), 126 (5-hydroxymethylfurfural), 144 (pyranone, octanoic acid), 145 (2-(4-pyridyl)furan, 2,3-dimethyl-1H-indole, 3-ethylindole), 146 (myosmine, glutamine), 161 (aminoadipic acid), and 162 (nicotine, anabasine) have lower ratios than 3.8. Substances on masses $m/z = 137$, 140, 148, and 161 have previously only been reported in tobacco leaf.

In Fig. 4.19 b) the results for 50 % filter ventilation holes blocked are presented. As with the previous comparison at 0 % holes blocked the spectrum can be divided into two parts with a border-area of $m/z = 90$–100, the lower mass part exhibiting a factor of about 2.2–2.4, and the higher masses a factor of about 2.8. Additionally,
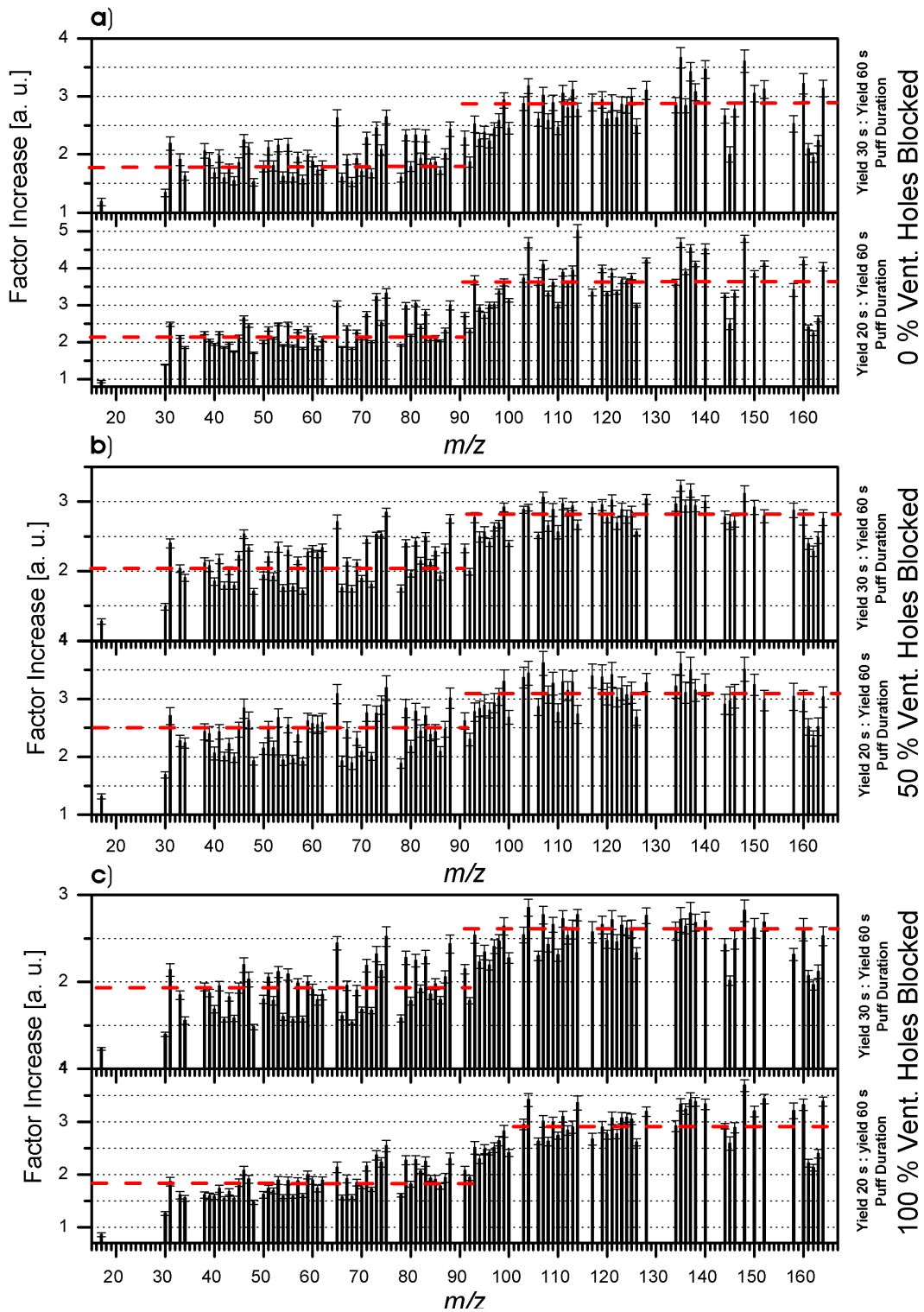
Figure 4.19: Influence of puff interval on the 100 highest mass peaks of a 2R4F research cigarette smoked under ISO conditions at smoking regimes with 55 ml puff volume and 0 % (a), 50 % (b), and 100 % (c) ventilation hole blocking.

great variance between most of the odd and even masses are visible. The substances with lower factors can be narrowed down to $m/z = 17$ (ammonia), 30 (nitric oxide), 42 (propene), 44 (acetaldehyde), 48 (methylsulphide), 54 (butadiene, butyne), 56 (2-propenal, butene, methylpropene), 58 (acetone, propanal), 66 (cyclopentadiene), 68 (isoprene, furan), 70 (methylbutene, pentene, methyl-propenal, butenone), 72 (methylpropanal, butanone, butanal, tetrahydrofuran), 78 (benzene), 106 (xylenes, ethylbenzene, benzaldehyde), 110 (catechole, hydroquinone, methylfurfural), 126 (5-hydroxymethylfurfural), 161 (aminoadipic acid), and 162 (nicotine, anabasine), while higher factors can be observed at $m/z = 65$, 75 (glycine), 88 (butyric acid, pyruvic acid), 93 (aniline, methylpyridines), and 99 (succinimide). A comparison of the 20 s puff interval with the results at 60 s puff interval exhibit an identical behaviour in the region up to $m/z = 90$ despite a slightly higher average factor of about 2.6. In the higher mass region the factor of 3.4 can be observed, though the error margins are significantly higher than in previous measurements. The same masses as in the comparison of 30 s to 60 s show exceptional behaviour, accompanied by a lower value of $m/z = 114$ (4-hydroxy-5,6-dihydro-2H-pyran-2-one).

In Fig. 4.19 c) the factors of yield increase are visualised when comparing 30 s to 60 s puff interval and 20 s to 60 s puff interval at 100 % of the holes blocked. As with most of the previous comparisons the spectrum again is divided at $m/z = 90$–100. The average factors are 2.0 and 2.75. Again, major differences can be observed between most of the even and odd masses. Lower ratios of amount can be observed for $m/z = 17$ (ammonia), 30 (nitric oxide), 40 (propyne), 42 (propene), 44 (acetaldehyde), 48 (methylsulphide), 52 (1-butene-3-yne), 54 (butadiene, butyne), 56 (2-propenal, butene, methylpropene), 58 (acetone, propanal), 66 (cyclopentadiene), 68 (isoprene, furan), 70 (methylbutene, pentene, methyl-propenal, butenone), 72 (methylpropanal, butanone, butanal, tetrahydrofuran), 78 (benzene), 92 (toluene, glycerol), 100 (tiglic acid, 3-hexen-1-ol), 106 (xylenes, ethylbenzene, benzaldehyde), 110 (catechole, hydroquinone, methylfurfural), 126 (5-hydroxymethylfurfural), 145 (2-(4-pyridyl)furan, 2,3-dimethyl-1H-indole, 3-ethylindole), 146 (myosmine, glutamine), 161 (aminoadipic acid), and 162 (nicotine, anabasine). Slightly higher yields can be found at $m/z = 31$ (methylamine), 46 (ethylalcohol, nitrogen dioxide), 65, 71 (pyrrolidine), 73 (isobutylamine, butylamine), 74 (propionic acid, butylalcohol, isobutylalcohol), 75 (glycine), 79 (pyridine), 81 (methylpyrrole), 83, and 88 (butyric acid, pyruvic acid). Going to even lower puff intervals does not change the chemical profile in the mass region $m/z < 90$ including the average ratio. Some minor changes can be observed in the region $m/z > 90$ where a slightly increased average factor of about 2.9–3.2 can be spotted. In this area $m/z = 104$ (styrene, pyridinecarbonitrile), 114 (4-hydroxy-5,6-dihydro-2H-pyran-2-one), 135 (trimethylaniline), 136 (limonene, p-methoxybenzaldehyde, 2-ethyl-5-methylphenol, dimethyl-ethyl-pyrazine, pheny-

lacetic acid, trimethylphenols), 137 (p-tyramine), 138 (5-acetyl-2-furaldehyde, salicyclic acid, isophorone), and 144 (5-quinolineamine) have higher values, while $m/z = 106$ (xylenes, ethylbenzene, benzaldehyde), 108 (anisole, dimethylpyrazines, methyl-phenols, benzylalcohol), 117 (indole, valine), 126 (5-hydroxymethylfurfural), 145 (2-(4-pyridyl)furan, 2,3-dimethyl-1H-indole, 3-ethylindole), 161 (aminoadipic acid), and 162 (nicotine, anabasine) have slightly lower ones.

For further analysis of the influences of puff volume and puff interval a PCA is carried out for all parameter sets on specific filter ventilation blocking 0 %, 50 %, and 100 %. The results are presented in Figures 4.20, 4.21 and 4.22. The scores of PC 1 (53.6 %) and PC 2 (21.5 %) of Fig. 4.20 a) at 0 % ventilation blockage are respectively high and describe the plot very well. It can be seen, that the PC 1 resembles the influence of time, while PC 2 visualises the influence of volume. On the right side of the plot the two measurements at 60 s puff interval with 35 ml and 55 ml puff volume show up, while on the upper right side the measurement at 20 s puff interval and 55 ml puff volume appears. The measurement at 30 s puff interval and 35 ml puff volume fits perfectly into the time-volume axis-scheme described earlier. However, measurements at 30 s / 45 ml and 30 s / 55 ml can not be separated by the first PCs but still fit acceptably into the model. The loading plot Fig. 4.20 b) reveals further information about the chemical shifts when altering the puff regimes. PC 1, describing the time influence, can be clearly divided into two parts. On the left, pointing towards larger puff intervals, are masses $m/z = 17$ (ammonia), 30 (nitric oxide), 34 (hydrogen sulphide), 42 (propene), 54 (butadiene, butyne), 56 (propenal, butene, methylpropene, 58 (acetone, propanal), 70 (butenal, methyl-vinylketone, methylbutene, pentene, methylpropenal, butenone), 72 (methylpropanal, butanone, butanal, tetrahydrofuran), and 78 (benzene), most of them reported earlier in this chapter to show exceptional behaviour. These substances show little influence on the second PC. On the right a large number of masses show up, in fact $m/z = 41$, 45 (ethylamine, dimethylamines), 57 (carbohydrate fragment, 2-propen-1-amine), 60 (propylalcohol), 62 (ethylene glycol), 71 (pyrrolidine), 74 (propionic acid, butylalcohol, isobutylalcohol), 79 (pyridine), 81 (methylpyrrole), 82 (methylfuran, methylcyclopentene, dimethylbutenes, hexene, cyclohexene, 2-cyclopenten-1-one), 85 (2-methylpyrrolidine, piperidine, 2-pyrrolidone), 93 (aniline, methylpyridine), 94 (phenol, vinylfuran, methylpyrazine), 95 (pyridinol, ethylpyrrole, dimethylpyrroles), 96 (dimethylfurans, furfural), 108 (anisole, dimethylpyrazines, methylphenols, benzylalcohol), 110 (catechole, hydroquinone, methylfurfural), 124 (methyl-catecholes, guaiacol, dihydroxymethylbenzene), 136 (limonene, p-methoxybenzaldehyde, 2-ethyl-5-methylphenol, dimethylethyl-pyrazine, tetramethylpyrazine, phenylacetic acid, trimethylphenols). These compounds show little to no influence on PC 2, which can be set equal to a low
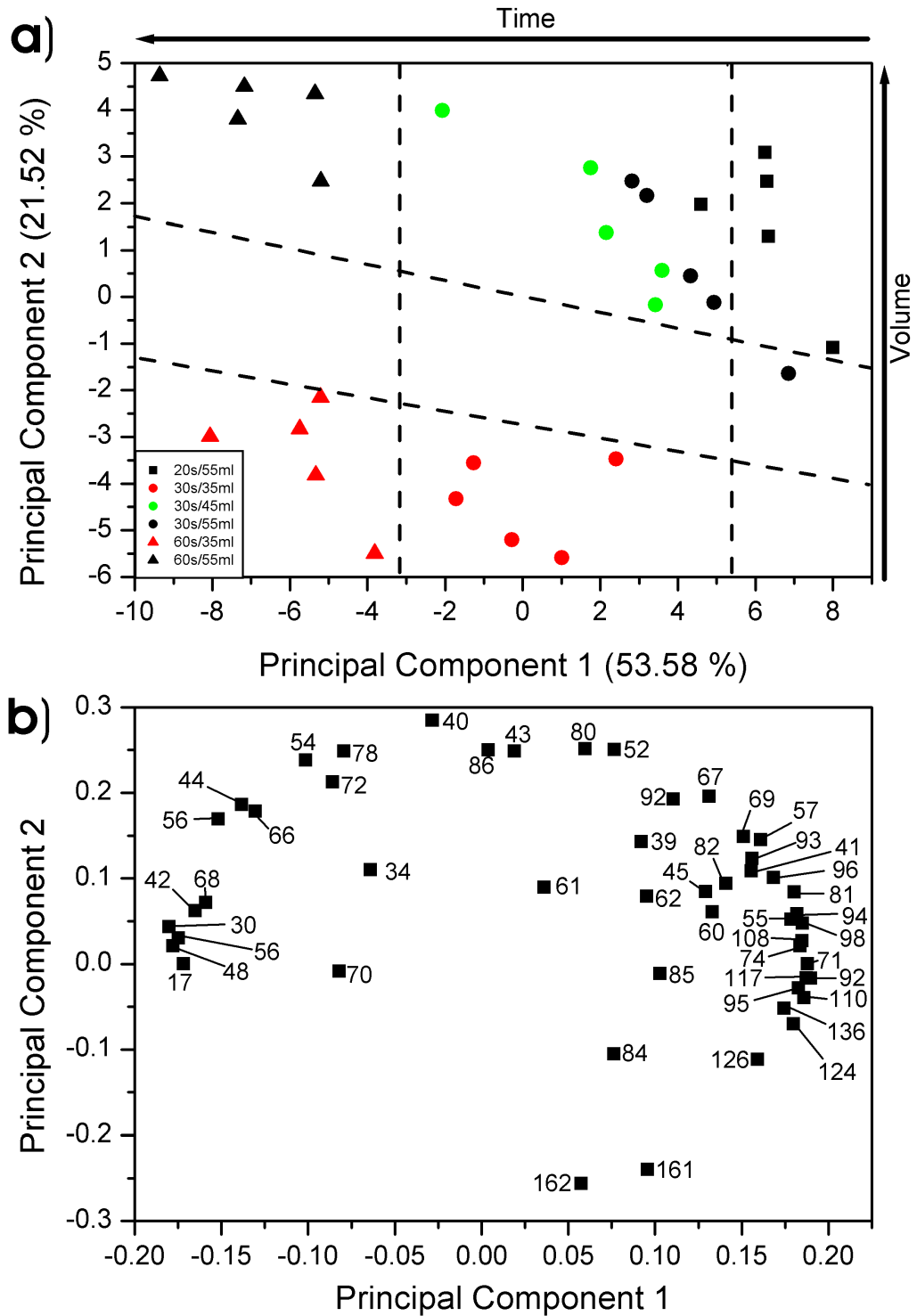
Figure 4.20: Score (a) and loading (b) plot of a PCA of a 2R4F research cigarette smoked under different machine smoking parameter sets at a constant filter ventilation hole blocking of 0 %.

or negligible influence on volume. On the upper edge of the loading plot masses highly influenced by puff volume appear, in fact $m/z = 54$, 78, and 72, which are also point towards larger puff intervals, and $m/z = 40$ (propyne), 43 (carbohydrate fragment), 52 (1-buten-3-yne), 67 (pyrrole), 80 (pyrazine), 86 (methylbutanal, 3-methyl-2-butanone, pentanones, 2,3-butanedione), and 92 (toluene, glycerol), which show high effects at increased puff volume, while $m/z = 161$ (aminoadipic acid) and $m/z = 162$ (nicotine, anabasine) point towards low volumes.

Fig. 4.21 shows the same PCA score (a) and loading (b) plot for the measurements at 50 % filter ventilation holes blocked. It is not as easy as without filter ventilation blockage to assign time and volume behaviour with the first two PCs, though these PCs cover 59.4 % and 13.3 % of the variance of the dataset. Even so, the first PC can be used to determine differences in the chemical composition with changes in puff intervals. Both regimes with 60 s puff interval are located on the left side of the score plot, while the two regimes with 30 s / 35 ml and 30 s / 45 ml can be seen in the middle of it. It is not possible to distinguish between the regimes of 20 s / 55 ml and 30 s / 55 ml, however, since both puff intervals' regimes are on the far right side of the plot, where the 20 s puff volume data should be expected according to the presumed time-axis. No clear relationship between PC 2 and puff volume can be made. Nevertheless the grid-lines indicate a slightly shifted dependance of both PCs. Despite the two overlaying parameter datasets good agreement is found. The corresponding loading plot shown in Fig. 4.21 b) confirms that the following m/z values are associated with lower volumes: $m/z = 17$ (ammonia), 30 (nitric oxide), 42 (propene), 44 (acetaldehyde), 48 (methanthiole), 54 (butadiene, butyne), 56 (propenal, butene, methyl-propene, 66 (cyclopentadiene), 68 (isoprene), 70 (butenal, methyl-vinylketone, pentene, butenone), 72 (methylpropanal, butanone, butanal), and 78 (benzene) point towards longer puff intervals, while $m/z = 41$, 55, 57 (carbohydrate fragment, 2-propen-1-amine), 61, 67 (pyrrole), 69 (pyrroline), 71 (pyrrolidine), 74 (propionic acid, butylalcohol, isobutylalcohol), 81 (methylpyrrole), 82 (methylfuran, methylcy-clopentene, 2-cyclopentene-1-one), 85 (methylpyrrolidine, piperidine, 2-pyrrolidone), 86 (methylbutanal, pentanones, 2,3-butanedione), 93 (aniline, methylpyridines), 94 (phenol, 2-vinylfuran, methylpyrazines), 95 (pyridinol, alkylated pyrroles, formylpyr-role), 96 (dimethylfurans, furfural), 97 (maleimide), 98 (furanmethanols, 2-methyl-pentenal, methyl-2($5H$)furanones), 108 (anisole, dimethylpyrazines, methylphe-nols, benzylalcohol), 110 (catechole, hydroquinone, methylfurfural), 124 (methyl-hydroquinone, methyl-catecholes, guaiacol), 126 (5-hydroxymethylfurfural), 136 (limonene, alkylated pyrazines, trimethylphenols) direct to lower ones. In PC 2 only a few masses can be used for interpretation, namely $m/z = 40$ (propyne), 42 (propene), 44 (acetaldehyde), 52 (1-buten-3-yne), and 86 (methylbutanal, 3-methyl-2-butanone, pentanones, 2,3-butanedione) indicating higher volumes, while
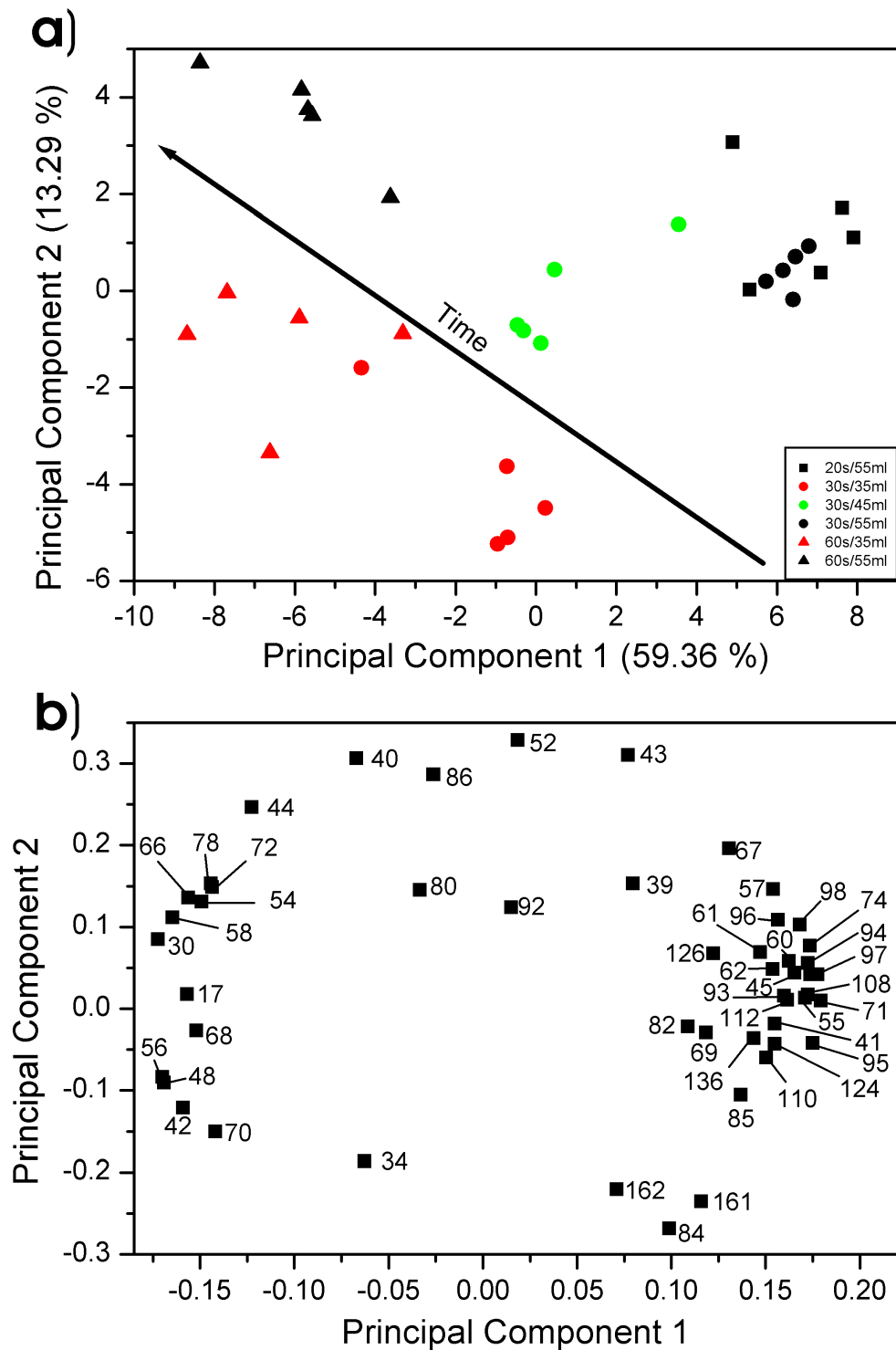
Figure 4.21: Score (a) and loading (b) plot of a PCA of a 2R4F research cigarette smoked under different machine smoking parameter sets at a constant filter ventilation of 50 % holes blocked.

$m/z = 34$ (hydrogensulphide), 84 (nicotine fragment, cyclopentanone, 3-methyl-3-buten-2-one, methylbutenal), 161 (aminoadipic acid), and 162 (nicotine, anabasine).

Fig. 4.22 exhibits the PCA score (a) and loading (b) plot for the measurements at 100 % holes blocked. In contrast to the previously investigated filter ventilations, no clear relationship between time and volume can be found within the first two PCs. Though there are high ratios of the first PCs with about 59.6 % and 18.0 % the six parameter sets can just be subdivided into two groups with no effect on either time or volume. However, the less harsh conditions of both sets, including 60 s puff interval and the 30 s / 35 ml set, form a separate group, as well as the more intense conditions of 30 s / 45 ml, 30 s / 55 ml, and 20 s / 55 ml. The discriminating factors are $m/z = 17$ (ammonia), 30 (nitric oxide), 34 (hydrogen sulphide), 40 (propyne), 42 (propene), 44 (acetaldehyde), 48 (methylsulphide), 54 (1,3-butadiene, butyne), 56 (2-propenal, butene, methylpropene), 58 (acetone, propanal), 66 (cyclopentadiene), 68 (furan, isoprene, 1,3 pentadiene, cyclopentene), 70 (2-butenal, pentene, 2-methyl-2-propenal), 72 (2-methylpropanal, 2-butanone), and 78 (benzene) on the left side and $m/z = 45$ (ethylamine, dimethylamine), 55, 57 (carbohydrate fragment, 2-propen-1-amine), 60 (propylalcohol), 61, 62 (ethylenglycol), 67 (pyrrole), 69 (pyrroline), 71 (pyrrolidine), 74 (propionic acid, butylalcohol, isobutylalcohol), 81 (1-methylpyrrole), 82 (2-methylfuran, 2-cyclopenten-1-one), 84 (nicotine fragment, 3-methyl-3-buten-2-one), 85 (piperidine, 2-pyrrolidone), 93 (aniline, methylpyridines), 94 (phenol, 2-vinylfuran, methylpyrazine), 95 (pyridinol, ethylpyrrole, dimethylpyrroles, formylpyrrole), 96 (dimethylfurans, furfural), 97 (maleimide), 108 (anisole, dimethylpyrazines, methylphenols, benzylalcohol), 110 (catechol, hydroquinone, methylfurfural), 112 (acetylcyclopentane, 2-hydroxy-3-methyl-2-cyclopenten-1-one, furoic acid), 124 (methyl-catecholes, guaiacol, dihydroxymethylbenzene), 126 (5-hydroxymethylfurfural), 136 (limonene, alkylated pyrazines, trimethylphenols), and 162 (nicotine, anabasine) on the right. Datapoints do not separate significantly within the second PC.

In conclusion it can be stated, that no universal behaviour throughout the different filter ventilations can be observed. However, from the different factor-plots the conclusion can be drawn, that masses $m/z < 90$ are influenced less than higher ones. For both areas an average increase factor can be observed, which describes the behaviour of most of the masses. In the investigation of the puff volume at a constant puff interval of 30 s, certain masses appear throughout the different filter ventilations, namely $m/z = 17$ (ammonia), 30 (nitric oxide), 34 (hydrogen sulphide), 42 (propene), 48 (methanethiole), 79 (pyridine), 104 (styrene, 3-pyridinecarbonitrile), and 114 (4-hydroxy-3-methyl-2-cyclopenten-1-one), which differ significantly from the factors previously mentioned. The influence of the puff interval on the chemical
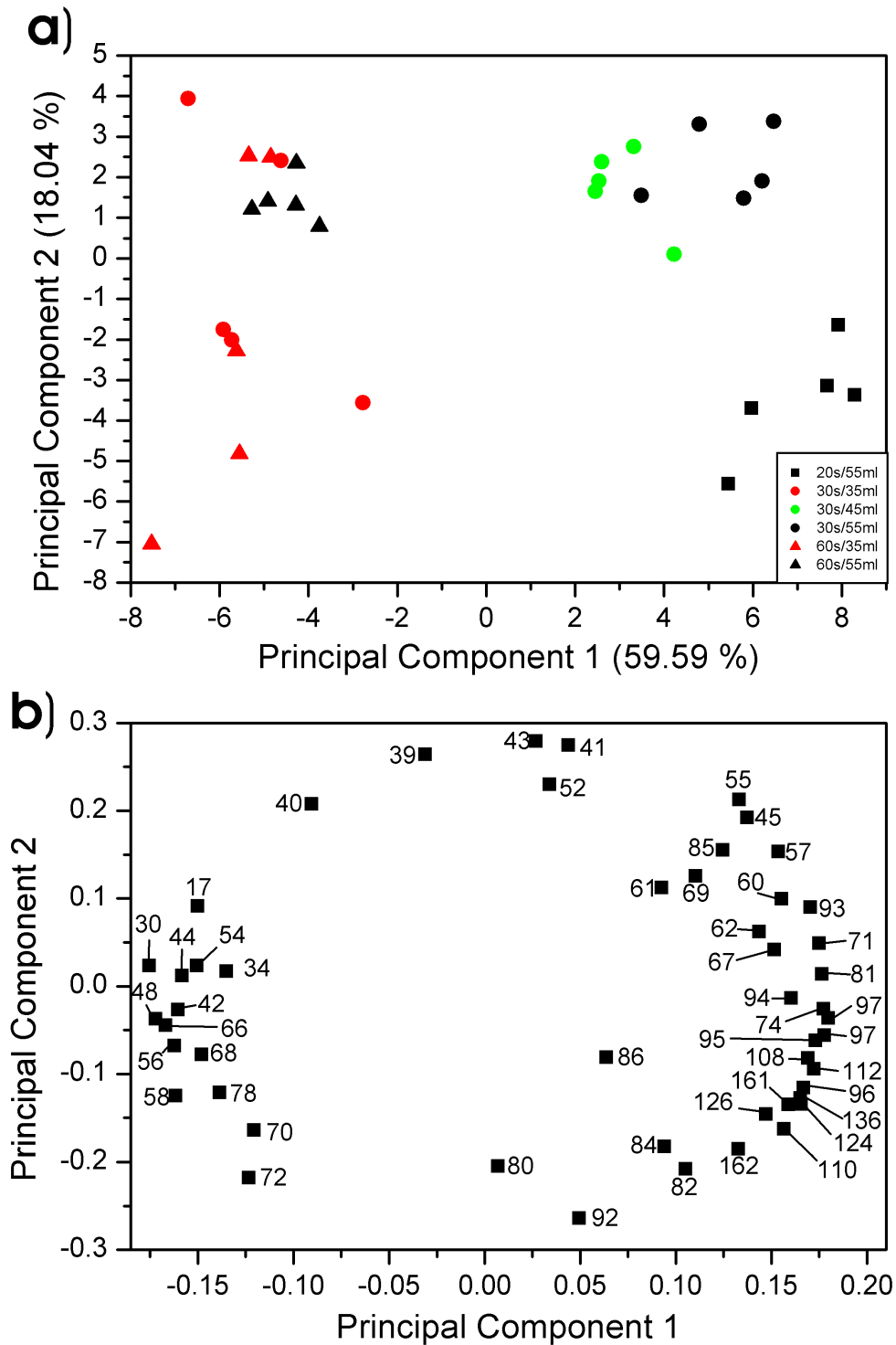
Figure 4.22: Score (a) and loading (b) plot of a PCA of a 2R4F research cigarette smoked under different machine smoking parameter sets at a constant filter ventilation (all filter holes blocked).

composition of MSS at a constant volume of 55 ml shows much larger variations, nevertheless specific factors can still be assigned to classes and mass areas. Most even masses are influenced less than odd masses, the mass range of $m/z > 90$ in general shows higher increase than the lower one.

In the PCA it can be seen that the lower the filter ventilation blockage, the more distinguished the behaviour of the different puff parameters is. In 0 % and 50 % blockage the separation in the time-axis can be achieved by a certain set of masses, mainly small, unsaturated compounds, the two known sulphur containing substances, and a few oxygenated species, partly unsaturated, pointing towards larger puff intervals and mainly aliphatic and aromatic amines pointing towards lower puff intervals. The differences in puff volume can only be assigned to a smaller number of compounds including nicotine and its typical fragment. However, although the list shows some unsaturated compounds $m/z = 40$ (propyne), 52 (1-buten-3-yne), 54 (butadiene, butyne), 66 (cylopentadiene), 78 (benzene), and 92 (toluene, glycerol) these are also accompanied by substances of other compound classes, in fact $m/z = 43$ (carbohydrate fragment), 44 (acetaldehyde), 67 (pyrrole), 72 (methylpropanal, butanone, butanal, tetrahydrofuran), 80 (pyrazine), 86 (methylbutanal, 3-methyl-2-butanone, pentanones, 2,3-butanedione). The same set of masses can be used to characterise the datasets of 50 % filter ventilation holes blocked, but not at 0 % holes blocked. Conditions can be considered more intense primarily according to their puff interval and secondarily to the puff volume, increasing from 60–20 s and 35–55 ml. As a general tendency, the more intense puffing conditions can not be differentiated the lower the filter ventilation is.

4.5.4 Possibilities of predicting smoke constituents yields

Based on the measurements previously discussed, a model to predict the increase of smoke compounds with changing smoking parameters was developed. In this way the six measurements were compared and a linear relation can be assigned to the dependance of acetaldehyde on puff volume, as well as puff interval. However, linear regression with acceptable error bands is only possible at 0 % blockage of the ventilation holes and not for conditions including lower ventilations, as the amounts differ significantly from linear behaviour. Based on the proposed linearity, a 3D-increase plot (Fig. 4.23) can be presented, which shows the relationship of different puff regimes standardised to the amounts under ISO conditions. Since the initial dataset was intended to give information about the chemical changes of smoke constituents in the different intense smoking regimes and the influence of filter ventilation blockage, the data set is capable of being used to make some preliminary evaluations of this model. However, the data set is not perfectly suited to fully evaluate the model.
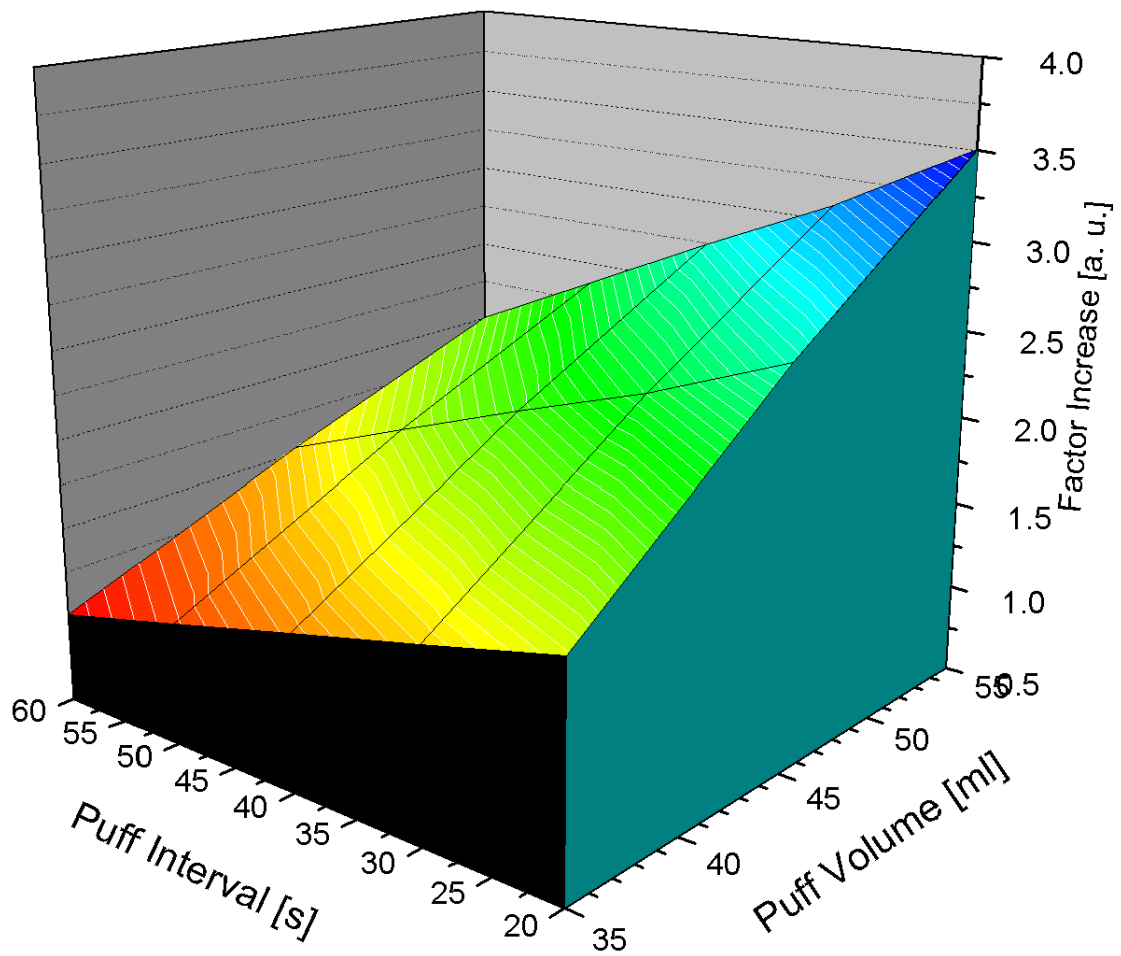
Figure 4.23: Predicted increase in amount for $m/z = 44$ (acetaldehyde) compared to ISO conditions at 100 % filter ventilation.

5 Sidestream Smoke Analysis

5.1 Sidestream smoke sampling

Various sidestream smoke trapping devices have been used in the last decades of smoke research and the variety of machines is probably even greater than with mainstream smoke generators. Only a brief resumé of the basic construction principles can be given in this thesis, complete reviews can be found in refs. [23, 30, 199, 200]. The simplest versions of collectors include inverted funnels which were used by several researchers [30, 201, 202]. CHORTYK and SCHLOTZHAUER [203] installed a large glass funnel above a rotary smoking machine. Though the possibility of smoking 30 cigarettes simultaneously overcomes variations between single cigarettes the flow rate necessary made particulate trapping impossible. Therefore, a series of liquid traps was used. A first totally enclosed chamber was constructed by NEURATH and EHMKE in 1964 [204]. One of the most important problems was the heat emerging from the burning cigarette, heating up the device and the trapping device, usually a standard Cambridge filter pad, therefore the double walled glass-housing had to be water cooled. Other problems include the possibilities of lighting the cigarette and condensation of SSS-components on the walls. However, a slightly modified version of this chamber was later utilised to determine the pH of sidestream smoke by BRUNNEMANN and HOFFMANN (Fig. 5.1). An air distributor was installed to ensure a proper uniform ventilation of the burning cigarette. Flow rates within the chambers usually vary from 1.2–1.5 l/min. Several papers evaluating the distribution of different compound classes (acids [32], bases [33], and middle and higher boiling compounds [34]) were published by SAKUMA *et al.* using a comparable instrumental setup as well. The distance between the cigarette and the filter pad was enlarged, therefore the warm smoke is likely to impact on the walls.

In contrast to the enclosed devices other researchers designed, chimney-like devices allow the smoke to rise naturally [27, 28]. The most sophisticated designs thereof were presented by HOUSEMAN and GREEN *et al.* [205, 206], the first one illustrated in Fig. 5.2. It combines the features of a chimney-like shape with the enclosed system of the previous constructions and the cooling of the walls.
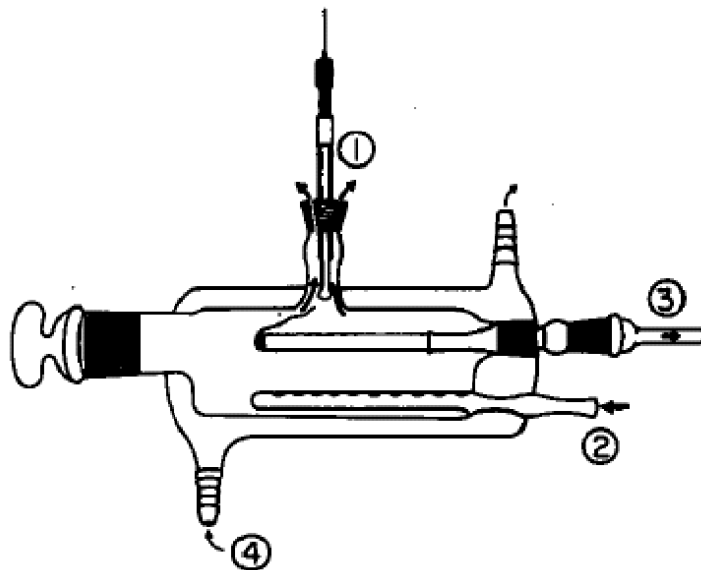
Figure 5.1: Smoke chamber for determining the pH of sidestream smoke by BRUNNEMANN *and* HOFFMANN*: (1) pH electrode; (2) air intake: (3) connection with the smoking machine; (4) cooling-water inlet [198].*

PROCTOR *et al.* [207] introduced a new sidestream sampling device in 1988, the fishtail chimney, which could be easily installed on commonly used single- and multiport smoking machines. In contrast to many of the previous developments the cigarette was not totally enclosed within the smoking chamber but a chimney is mounted on top of it. A flow-rate of 2 L/min is used, which is within the limits of ISO specifications. Effects of the sampling device on mainstream smoke were carefully investigated as well as the effect of shape and height on the collection efficiency. Deposition of sidestream smoke tar and nicotine was reduced to 20 %. Fig. 5.3 shows the dimensions of the chimney given at a CORESTA task force meeting on sidestream smoke in 1999. An ISO-standard based on the CORESTA Recommended Methods N° 53 (Determination of Nicotine and Nicotine-Free Dry Particulate Matter) and N° 54 (Determination of Carbon Monoxide in the Vapour Phase) including the fishtail chimney have been developed (ISO/DIS 20773 and ISO/DIS 20774).

5.2 Experimental setup of sidestream smoke experiments

An overview of the experimental set-up for the studies can be seen in Fig. 5.4. The cigarettes are smoked under ISO machine conditions by a Borgwaldt single port
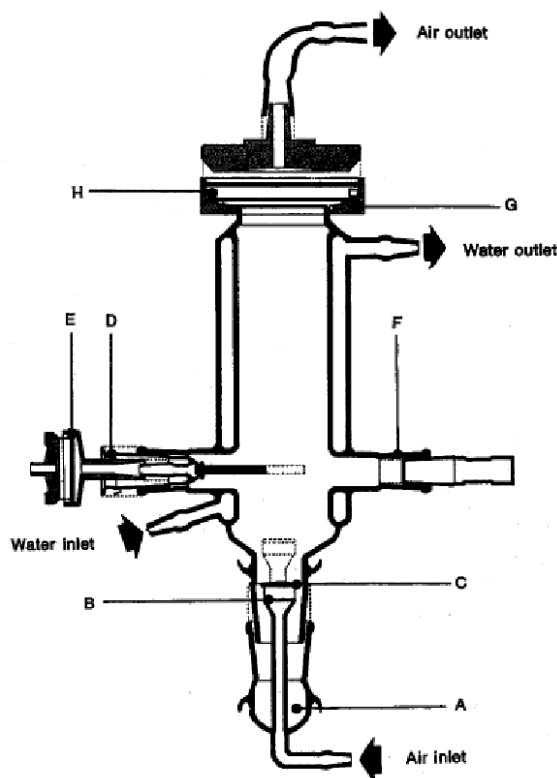
Figure 5.2: Sidestream smoking device by Houseman: *(A) Detachable ash trap; (B) Sintered-glass disc for air-diffusion; (C) Curved ash deflector; (D) Glass cigarette holder; (E) Cambridge Filter holder; (F) Stoppered port used e.g. for ignition; (G) "Nylatron-GS" sidestream filter pad holder equipped with two 115 mm Cambridge Filter discs separated by a (H) 4 mm spacing ring. [205]*

smoking machine. The sidestream smoke is collected by a fishtail smoking chimney introduced by Proctor *et al.* [207] and described in detail in chapter 5.1. The membrane vacuum pump (KNF Neuberger, Germany) adjusted to a flow rate of 2.0 L/min is used to transport the smoke through the fishtail chimney to the sampling point at the end of the chimney. A Cambridge filter is used to prevent contamination of the vacuum pump and an additional filter pad can optionally be installed right before the sampling port to allow gas phase measurements. The smoke is injected into the ionisation chamber of the SPI/REMPI-TOFMS system described in chapter 2.3 by a 0.32 mm i. d. uncoated quartz capillary tube with a length of ≈ 2.0 m. Because of adsorption of particles of the sidestream smoke onto the surface of the smoking chamber it was impossible to carry out REMPI measurements because of strong and fluctuating background contamination signals. Therefore, a satisfactory time resolution could not be achieved without further modifications (e. g. heating of the smoking chimney) which would mean a significant violation of the guidelines for sidestream sampling. However, for the clarification of the basic principles of
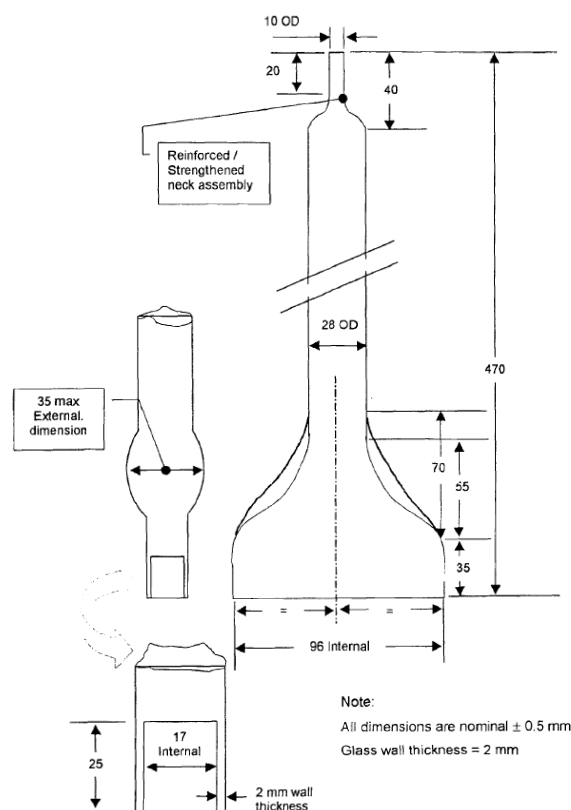
Figure 5.3: Dimension of the fishtail smoking chimney for the collection of sidestream smoke according to a 1999 CORESTA task force meeting.

time-resolved sidestream smoke analysis the use of SPI is sufficient.

A set of single tobacco filter cigarettes was used each exhibiting the same physical smoking parameters (filter drop and ventilation) and the 2R4F standard cigarette manufactured by the University of Kentucky. All cigarettes were smoked six times. The generated whole sidestream smoke (particulate & gas phase) was then analysed three. The sidestream gas phase only was also analysed three times by incorporating a Cambridge filter pad to remove the particulate phase.

5.3 Results of the sidestream smoke measurements

Fig. 5.5 a) shows a three-dimensional overview of the collected SPI mass spectra for the gas phase of sidestream smoke. A closer look at mass range $m/z = 46$–60 further clarifies the time profiles of masses m/z=48, 52, 54, 56, and 58, respectively. All substances exhibit a base concentration level between puffs, while different peaks occur immediately after a puff is drawn from the cigarette sample (Fig. 5.5 a)).
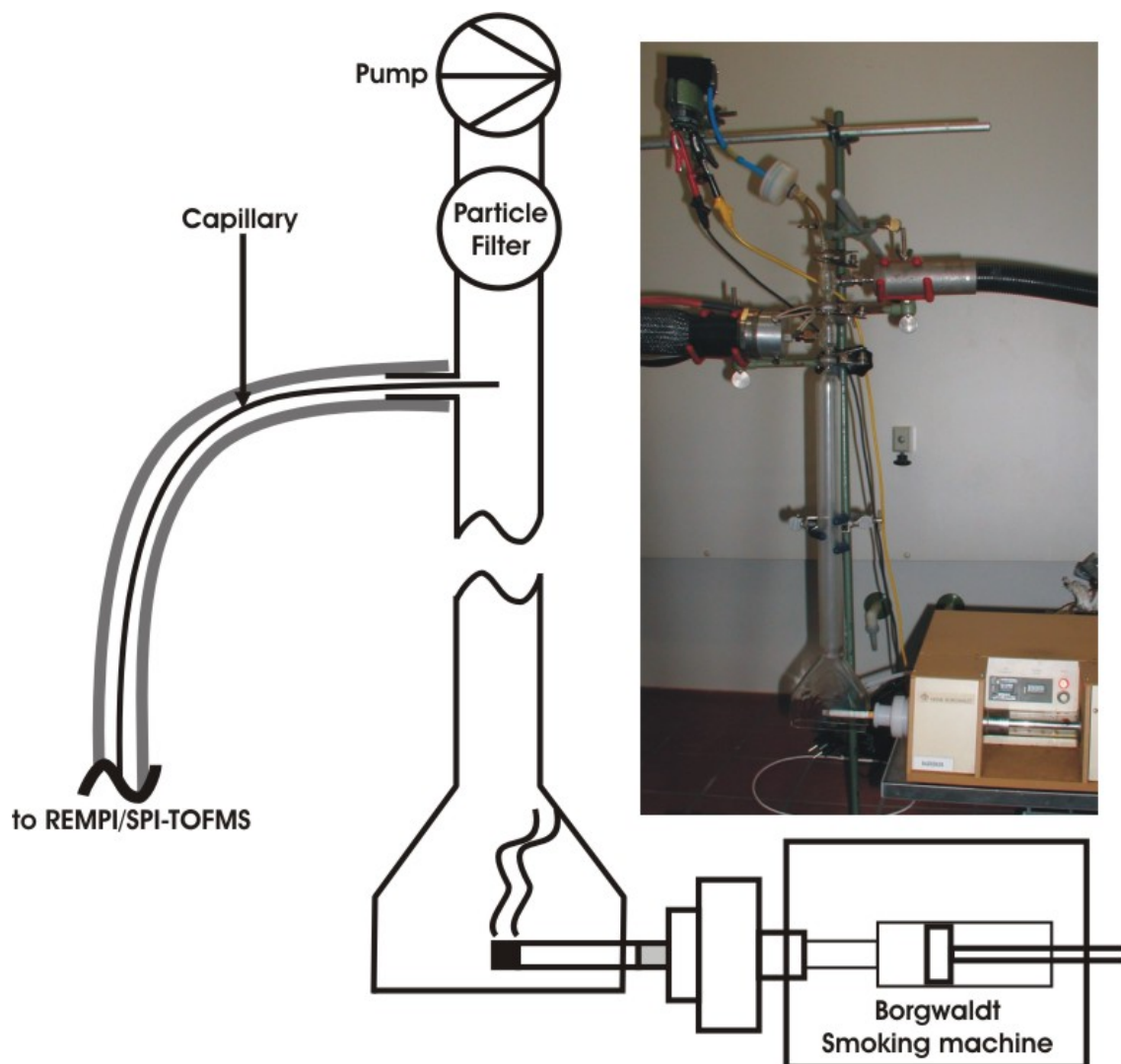
Figure 5.4: Experimental setup of the sidestream smoke experiments. A Cambridge filter pad can optionally be installed for gas phase analysis.

A quantification of selected substances (benzene, toluene and xylenes) was done for two 2R4F research cigarettes with ISO conditions. To enable a comparison to conventional analysis both were measured without a Cambridge filter pad installed.

5.3.1 Puff-resolved quantification of selected compounds in sidestream smoke

As an example of puff resolved quantification of sidestream smoke the data of the sidestream smoke of two 2R4F research cigarettes measured without a Cambridge filter pad is presented in Table 5.1. The quantification procedure is based on the

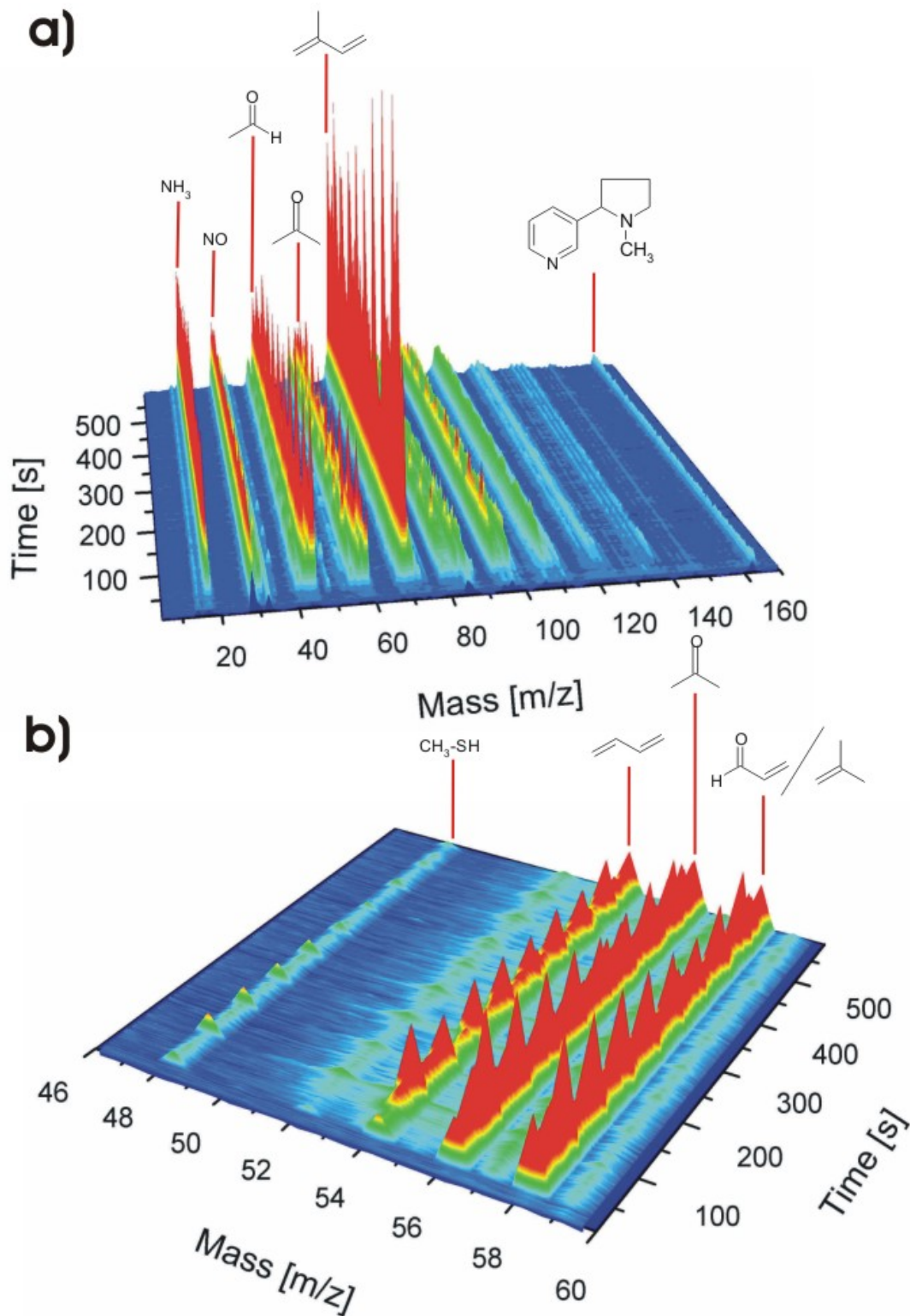Figure 5.5: *3D plot of SPI mass spectra of filtered sidestream smoke of a 2R4F research cigarette smoked under ISO conditions.*

Puff No.	Benzene		Toluene		Xylene	
	Sample 1	Sample 2	Sample 1	Sample 2	Sample 1	Sample 2
1	21.6	26.9	53.7	67.5	44.6	51.9
2	29.0	39.7	69.7	86.6	59.4	68.4
3	46.2	34.3	70.1	77.6	78.3	66.3
4	25.8	32.7	59.7	74.5	53.5	63.6
5	29.4	29.4	66.5	71.9	57.8	63.2
6	34.6	33.6	78.0	76.8	66.5	63.0
7	27.4	40.8	63.2	87.5	54.9	71.4
8	36.3	39.9	69.4	83.9	68.3	71.7
9	21.8		47.8		42.8	
Sum	272.0	277.4	578.2	626.3	526.1	519.7

Table 5.1: Quantification of benzene, toluene and xylene in unfiltered sidestream smoke of a 2R4F research cigarette.

method introduced in chapter 2.7. The summed values of benzene and toluene for a whole cigarette are well within the range of previously work (Table A.1). The total amount of xylenes is calculated based on the assumption, that the whole signal on $m/z = 106$ is originating from m-xylene. Since the different isobaric C_3-alkylated benzenes do not exhibit the same cross sections and benzaldehyde may also be contributing to the total signal, the calculated values only represent a raw estimate. The values of the different puffs show great variations without clear tendencies within any of the substances. A puff resolved analysis including benzene and toluene has previously been done by BRUNNEMANN *et al.* [208, 209]. However, these studies were published before the introduction of the Fishtail chimney or a ISO standard for sidestream smoke sampling and various cigarettes including the 1R4F research cigarette were used. The different sampling conditions and cigarette types make a comparison of absolute values impossible. As a result, the values observed in the previous study are about twice as high as the ones in this work.

5.3.2 Comparison of sidestream and mainstream smoke

In Fig. 5.6 the score (Fig. 5.6 a) and loading (Fig. 5.6 b) plots of the raw data and the score (Fig. 5.6 c) and loading (Fig. 5.6 d) plots of the averaged datapoints of a PCA of the 50 highest FV of the mainstream smoke puffs and the corresponding filtered sidestream smoke signals after the puff of a Kentucky 2R4F research cigarette are presented to evaluate differences in mainstream and sidestream smoke composition. The separation in the first (67 %) and second (22 %) PC is acceptable. In general there are three areas clearly separated, one solely describing mainstream smoke
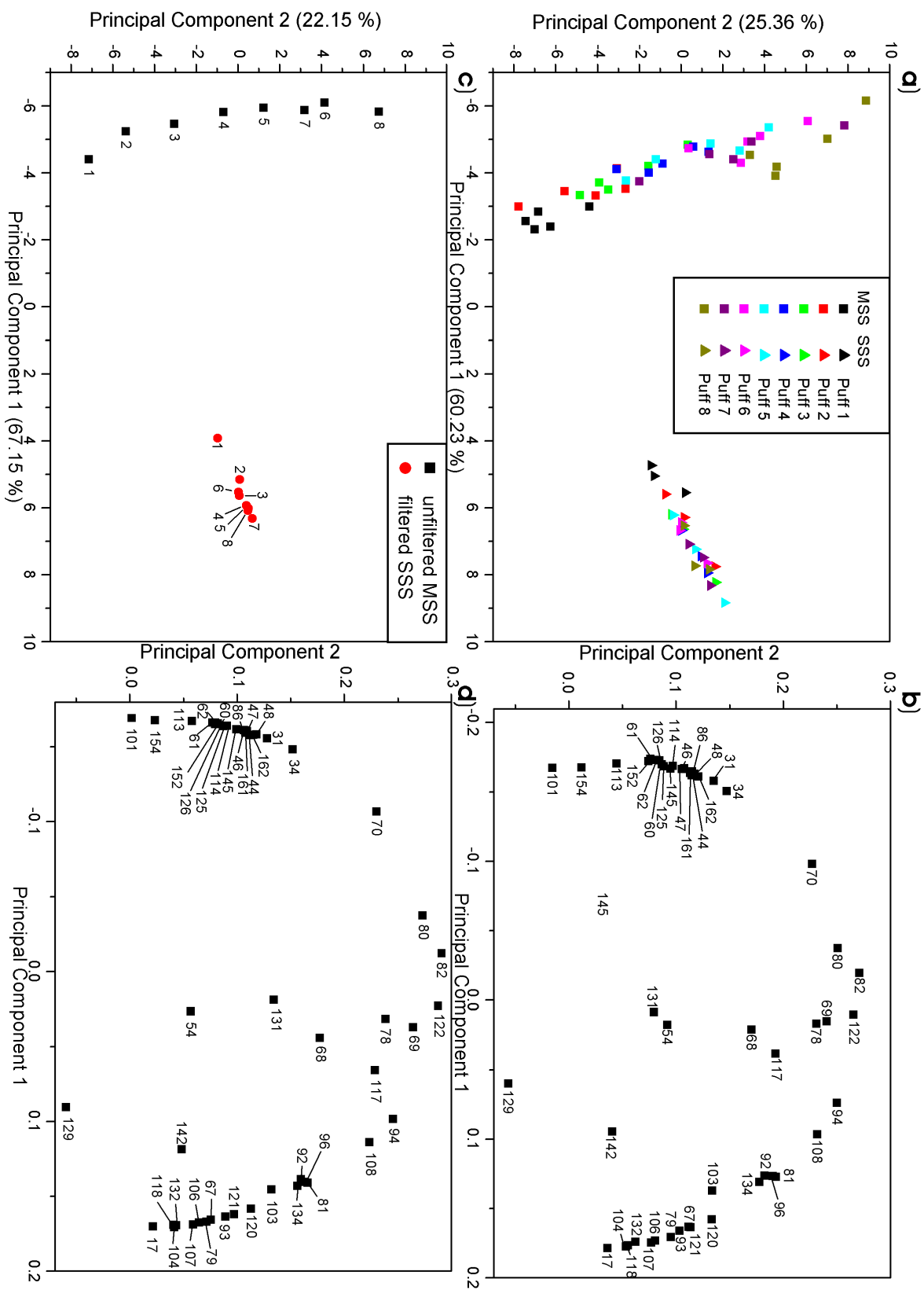
Figure 5.6: Score (a, c) and loading (b, d) plots of a PCA of a comparison of raw (a, c) and averaged (b, d) data of the sidestream and mainstream smoke of a 2R4F research cigarette (gas phase).

$m/z = 31$ (methylamine), 34 (H_2S), 44 (acetaldehyde), 48 (methanethiole, 86, 161, 162 (nicotine, anabasine), 46, 47, 114, 145, 125, 126, 60, 62, 61, 162, 113, 154, 101, 70 another sidestream smoke, namely $m/z = 17$ (ammonia), 118, 132, 107, 106, 67 (pyrrole), 79 (pyridine), 81 (methylpyrrole), 93 (aniline, methylpyridine), 121, 120, 103 (benzonitrile), 104 (styrene, 3-pyridinecarbonitrile), 92 (toluene), 94 (phenol, 2-vinylfuran, methylpyrazine), 96 (furfural, dimethylamine), 108, 134, 142 and a last one without preferences 54 (butadiene), 68 (isoprene, furan), 69 (pyrroline), 78 (benzene), 80 (pyrazine), 82 (methylfuran, methylcyclopentene, dimethylbutene, hexene, cyclohexene, 2-cyclopenten-1-one), 117 (indole), 122, 129 (quinoline), 131 (3-methyl-1H-indole). The major part of the uneven masses, containing nitrogen is pointing towards sidestream smoke comparing in both, filtered and unfiltered, sidestream smoke to mainstream smoke. This very well reflects the nature of sidestream smoke as higher nitrogen contents in sidestream smoke have been previously reported by HARDY and HOBBS [210]. They reported ≈33 times higher amounts of nitrogen in the gas phase of sidestream smoke compared to mainstream smoke, while the ratio of such substances in nicotine free dry particulate matter (NFDPM) is slightly lower.

5.3.3 Comparison of sidestream smoke emissions of single tobacco grade cigarettes (Virginia, Burley and Oriental)

To investigate the sidestream smoke behaviour of different tobacco types a set of pure tobacco type standardised cigarettes was investigated. To further clarify the consistency of the particulate and the gas phase the sidestream smoke was filtered with a Cambridge filter pad.

Fig. 5.8 shows a comparison of mass spectra of filtered sidestream smoke emissions of the single tobacco grades. The main components of the gas-phase spectra include $m/z = 17$ (ammonia), $m/z = 30$ (nitric oxide), $m/z = 42$ (propene), $m/z = 44$ (acetaldehyde), $m/z = 56$ (acroleine, 2-methylpropene, butene), $m/z = 58$ (acetone), $m/z = 68$ (isoprene, furan), $m/z = 92$ (toluene), $m/z = 94$ (phenol), $m/z = 96$ (furfural, dimethylfuran), $m/z = 105$ (vinylpyridine), and $m/z = 110$ (hydroquinone, catechole). A few minor differences can be spotted within the spectra: $m/z = 17$ (ammonia) and $m/z = 68$ (isoprene, furan) yield higher ratios with Burley tobacco, while $m/z = 30$ (nitric oxide), $m/z = 82$ (methylfuran, methylcyclopentene, dimethylbutene, hexene, cyclohexene, 2-cyclopenten-1-one), $m/z = 94$ (phenol), $m/z = 96$ (furfural, dimethylfuran), and $m/z = 110$ (hydroquinone) show lower ratios. Additionally $m/z = 79$ (pyridine) and $m/z = 92$ (toluene) exhibit lower concentrations with Oriental tobacco.

Fig. 5.9 illustrates the same set of samples without filter, i. e. for whole sidestream
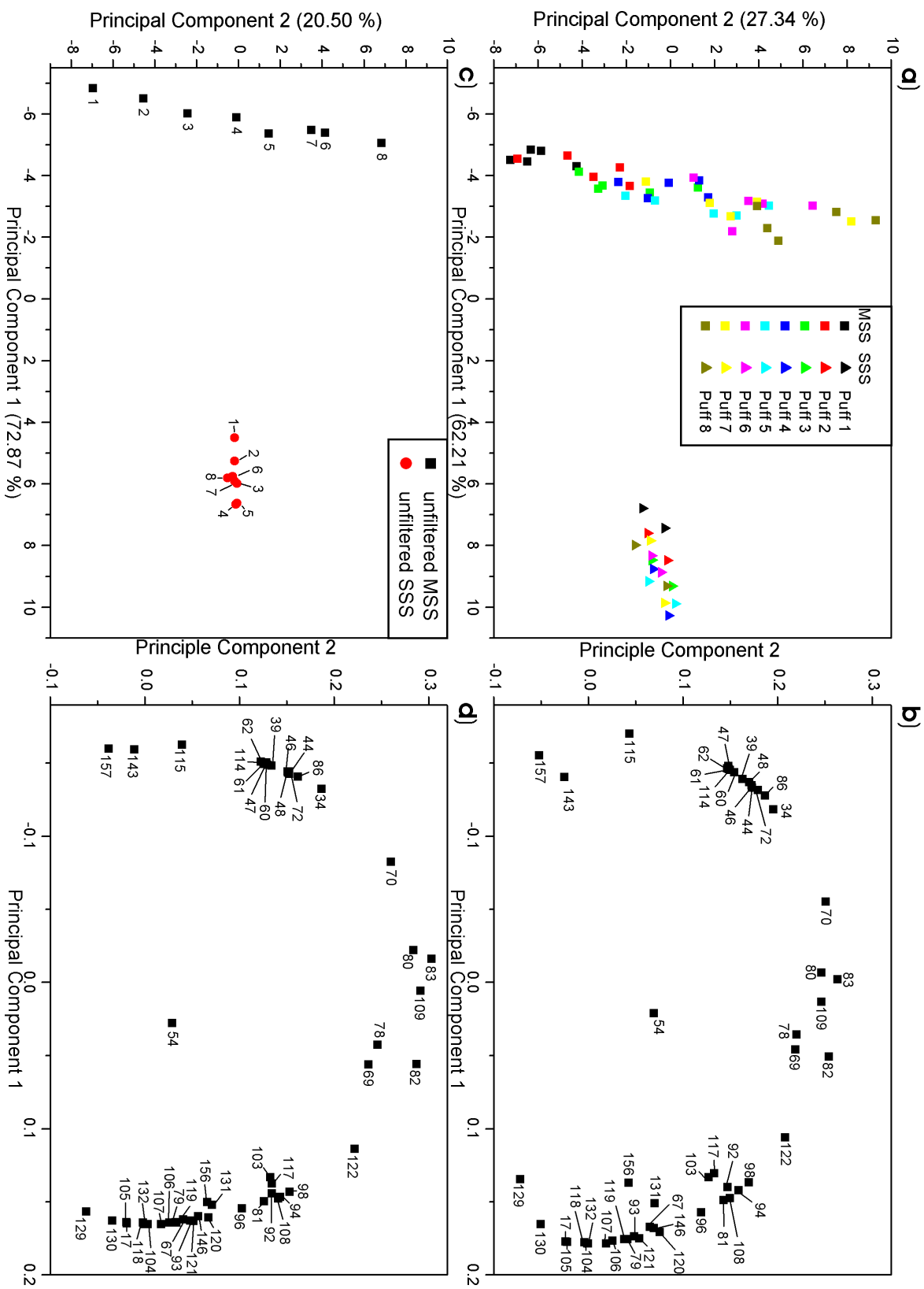
Figure 5.7: Score (a, c) and loading (b, d) plots of a PCA of a comparison of raw (a, c) and averaged (b, d) data of the sidestream and mainstream smoke of a 2R4F research cigarette (gas and particulate phase).
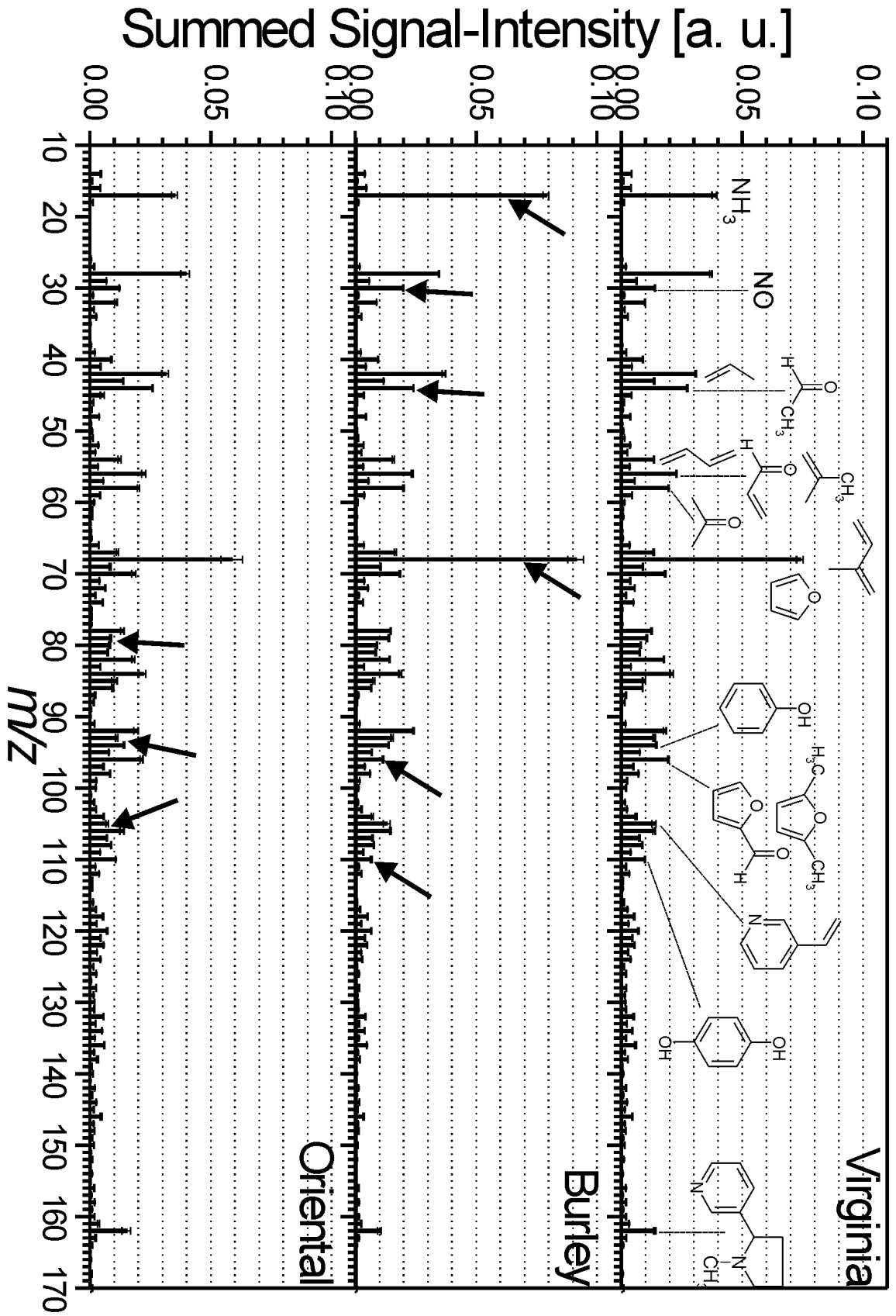
Figure 5.8: Comparison of mass spectra of sidestream emissions of single tobacco cigarettes (gas phase).

Figure 5.9: Comparison of mass spectra of sidestream emissions of pure tobacco cigarettes (gas and particulate phase).
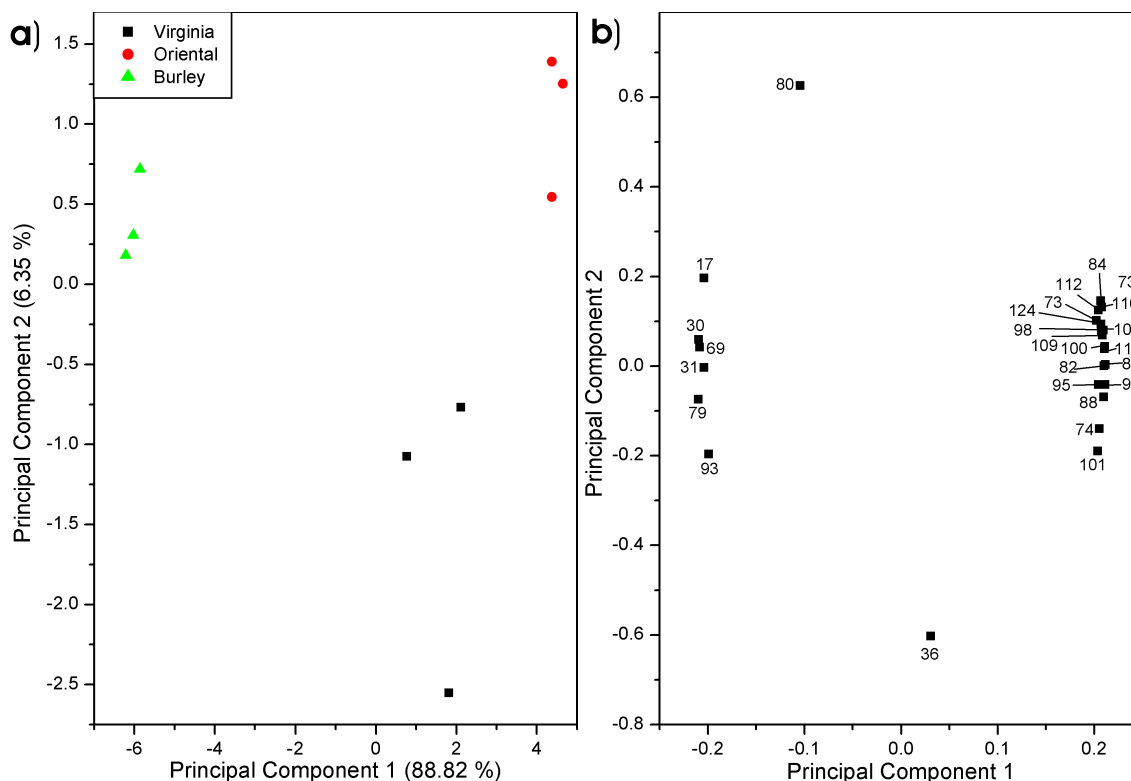
Figure 5.10: Score (a) and loading (b) plot of a PCA of single tobacco grade sidestream (gas phase).

smoke. The total composition of all sidestream smoke samples now includes a significant amount of higher masses ($m/z > 92$). However, the significant differences visible are again limited to $m/z = 17$ (ammonia) and $m/z = 68$ (isoprene, furan) with higher ratios, $m/z = 30$ (nitric oxide), $m/z = 82$ (methylfuran, methylcyclopentene, dimethylbutene, hexene, cyclohexene, 2-cyclopenten-1-one), $m/z = 94$ (phenol), $m/z = 96$ (furfural, dimethylfuran), and $m/z = 110$ (hydroquinone) with lower ratios with Burley tobacco and $m/z = 79$ (pyridine) and $m/z = 92$ (toluene) exhibiting lower concentrations with Oriental tobacco. In contrast to the gas phase data $m/z = 106$ (xylene) is lowered with Oriental tobacco.

Both the gas phase and the whole sidestream smoke spectra reflect the different compositions of the tobacco types quite well. A slight shift with Burley tobacco from oxygen to nitrogen containing compounds is evidenced by the higher peaks of $m/z = 17$ (ammonia) and lower peaks of $m/z = 94$ (phenol), $m/z = 96$ (furfural, dimethylfuran), and $m/z = 110$ (hydroquinone). The lower amounts of nitrogen present in Oriental tobacco are indicated by lower emissions of $m/z = 79$ (pyridine). Virginia tobacco has an intermediate composition.
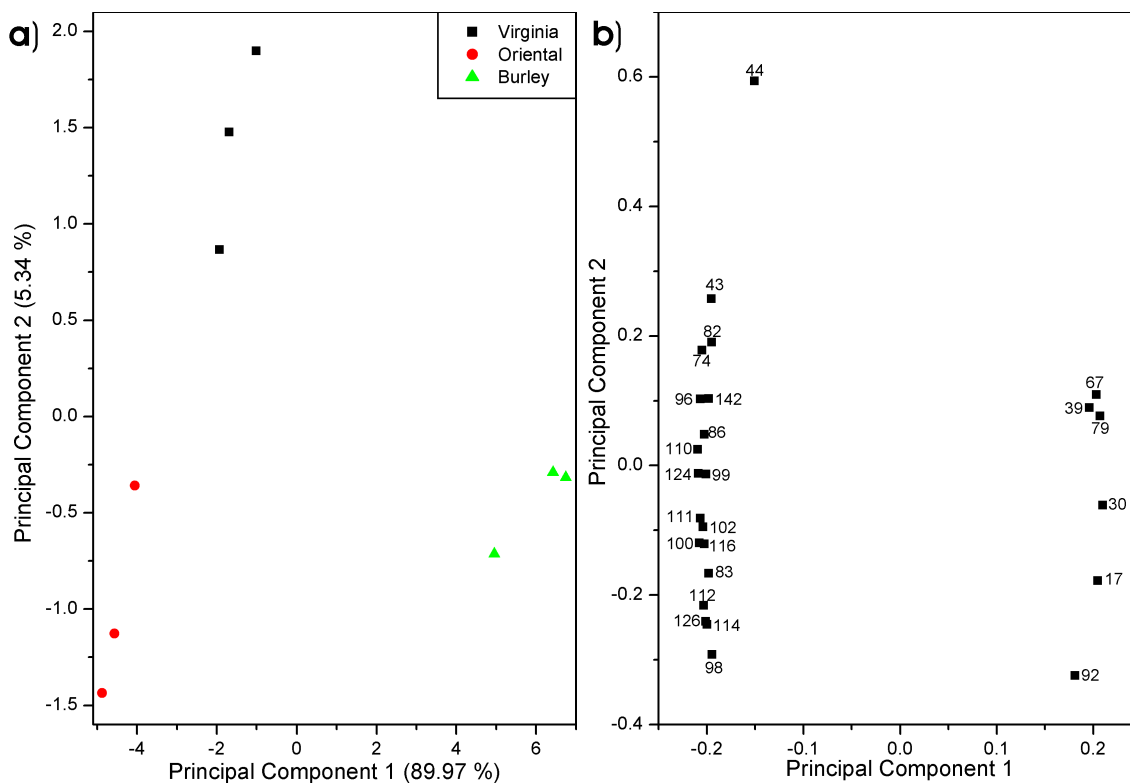
Figure 5.11: Score (a) and loading (b) plot of a PCA of single tobacco grade sidestream (gas and particulate phase).

Fig. 5.10 and Fig. 5.11 show the PCA score and loading plots of the three single tobacco samples. The data set consists of the 25 highest FV discriminating Virginia, Burley, and Oriental tobacco. A good classification with high percentage values in the first two PC can be observed in both data sets. The main separation of the gas phase data (Fig. 5.10) in the first principal component divides the Burley tobacco from the other two tobacco types by the contributing masses $m/z = 17$ (ammonia), $m/z = 30$ (nitric oxide), $m/z = 31$ (methylamine), $m/z = 79$ (pyridine), and $m/z = 93$ (aniline, methylpyridine). The other compounds point to Virginia and Oriental, without any preferences. Separation in the second level is achieved by $m/z = 36$ (yet unknown) and $m/z = 80$ (pyrazine). The corresponding data of the combined gas and particulate phase (Fig. 5.11) is divided into Burley on the one hand and Virginia and Oriental on the other hand by the first principal component. In contrast to the gas phase, different significant masses were chosen as the base of the Fisher values. Burley tobacco is separated from the other two tobacco types by means of $m/z = 17$ (ammonia), $m/z = 30$ (nitric oxide), $m/z = 67$ (pyrrole), $m/z = 92$ (pyridine), $m/z = 92$ (toluene). The major difference in the second principal component mainly results from $m/z = 44$ (acetaldehyde). The statistical
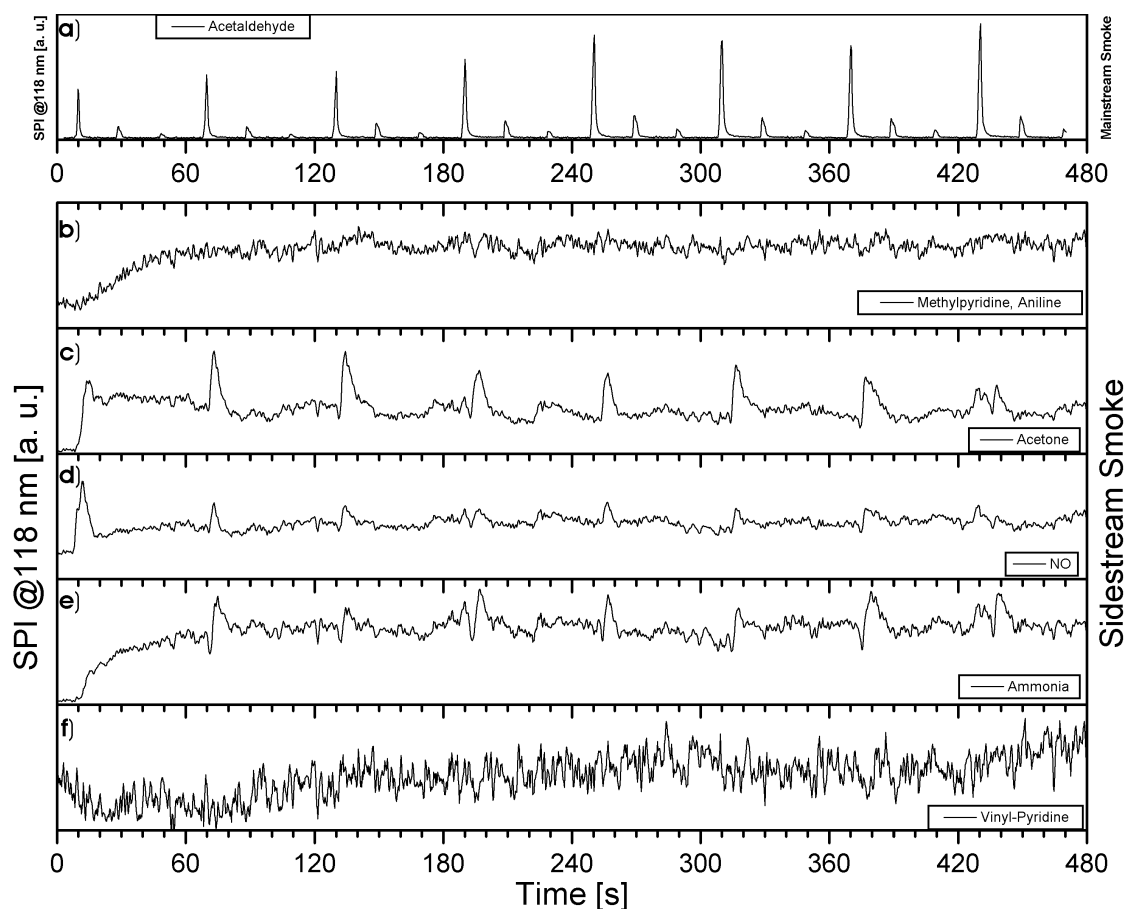
Figure 5.12: Different time profiles observed in unfiltered sidestream smoke of a 2R4F research cigarette smoked under ISO conditions.

evaluation of the data again reflects the basic chemical properties of the tobacco types, as described earlier.

5.3.4 Dynamic behaviour of sidestream smoke emissions

The different time profiles of mainstream smoke were already described earlier (Fig. 4.3) and quantified and thoroughly investigated by ADAM [6]. In contrast, sidestream smoke emissions show a larger variety of puff behaviours, as illustrated in Fig. 5.12 a–e. The time profiles of selected masses of unfiltered sidestream smoke, namely $m/z = 17$ (e), 30 (d), 58 (c), 93 (b), and 105 (f) are plotted in comparison to a typical mainstream profile, exemplarily shown at $m/z = 44$ (acetaldehyde). In general, these masses represent the five different time behaviours observed during the measurements. $m/z = 93$ (methylpyridine/aniline) (Fig. 5.12 a) shows a constant increase after ignition (1st puff) within 30–40 s. The succeeding level is constant and

125

no dependency on mainstream-puffs can be observed. Another substance exhibiting no significant puff dependance is $m/z = 30$ (NO) (Fig. 5.12 c). However, in contrast to $m/z = 93$ (methylpyridine/aniline) high concentrations within the first puff can be observed. Another compound, where relatively high emissions can be seen in the first puff is $m/z = 58$ (acetone) (Fig. 5.12 b). It increases in concentration right after ignition. In contrast to $m/z = 30$ (NO) a puff-dependency can be seen for all of the puffs, including the first. The overall peak level within the puffs seems to decrease with the puff-number. This is visible on $m/z = 17$ (ammonia) (Fig. 5.12 d) as well. However, there are no strong emissions during the first puff, instead the level increases constantly during the first 30–40 s after ignition. The concentration peaks right after a puff are not as high compared to acetone, however a much higher decrease in concentration during the puff occurs. A linear increase over the whole cigarette can be found at $m/z = 105$ (vinylpyridine) (Fig. 5.12 e), which exhibits an increase in concentrations from the ignition to the end of the cigarette without significant effects of the occurrence of the puffs.

The different time profiles can be explained by the change of conditions of the combustion processes within the cigarette. For clarification the different temperature distribution of the solid phase inside a burning tobacco tip is shown in Fig. 5.13. The comparison of the temperature profile of the end of the smoldering phase (Fig. 5.13 a) and during a puff (b) shows that the temperature during a puff is much higher than during smoldering and higher temperatures can be found in much larger areas. The temperature distribution shortly after the end of the puffing phase is presented in Fig. 5.13 and explains very well, that the zone of high temperature still consists inside the glowing tip. As previously illustrated by ADAM et al. [6, 162] in investigations of pyrolysis gases of tobacco with SPI-TOFMS, various substances are formed and decomposed at different temperatures. Therefore, they can be classified into primary (formed directly from tobacco ingredients), secondary (formed at higher temperatures from primary compounds), and tertiary products, which are formed from secondary products at very high temperatures. For sidestream smoke this explains the chemical shifts resulting from the rapid temperature increase. Additionally, as air is drawn through the tip, a constant source of fresh oxygen is provided, which lacks during the smoldering. Substances like $m/z = 93$ (methylpyridine/aniline), 30 (NO) and 105 (vinylpyridine) are not or hardly affected by the higher temperatures and oxygen content right after a mainstream puff is drawn. In contrast, due to more extreme burning conditions a large amount of acetone is formed from combustion of various carbohydrates in the hot burning zone. After the puff ends, it diffuses into sidestream smoke. The relatively constant level of emissions between all puffs suggests a state of steady burning conditions between the puffs, after re-equilibrating from the "disturbance" of a mainstream smoke puff. To describe the dynamics of
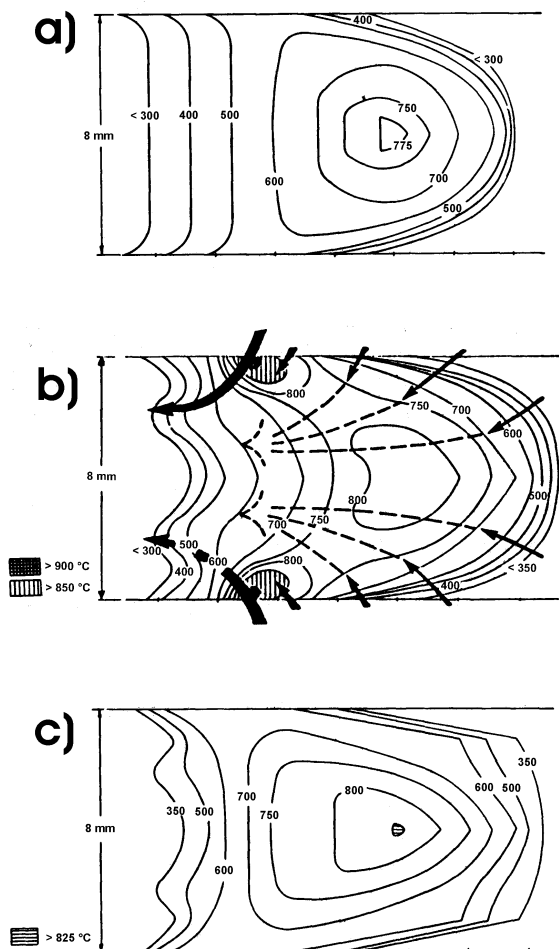
Figure 5.13: Temperature profiles of the solid phase of a cigarette tip in the end of the smoldering phase (a), during a puff (b) and shortly after the puff (c) [211].

sidestream smoke emissions more detailed, the fifth and sixth puff of the sidestream smoke emissions of $m/z = 17$ (ammonia) in unfiltered sidestream smoke are presented in Fig. 5.14. The decrease in concentration during the puff and the following increase for a period of ≈ 10 s, which is representable for all compounds with puff dependency, is in consistence with observations made by DITTMANN *et al.* [212] who performed measurements of different aerosol concentrations in sidestream smoke. This decrease in concentration occurs simultaneously with the drawing of a mainstream puff and lasts $\approx 2s$, the duration of a standard puff, and can therefore be utilised to correlate corresponding side and mainstream data. This decrease in concentration results from the air flow through the cigarette into the mainstream. Additionally, with higher oxygen content and temperature within the burning zones the chemical composition of the emissions change significantly, e. g. more NO will be formed from nitrogen-containing compounds instead of ammonia.
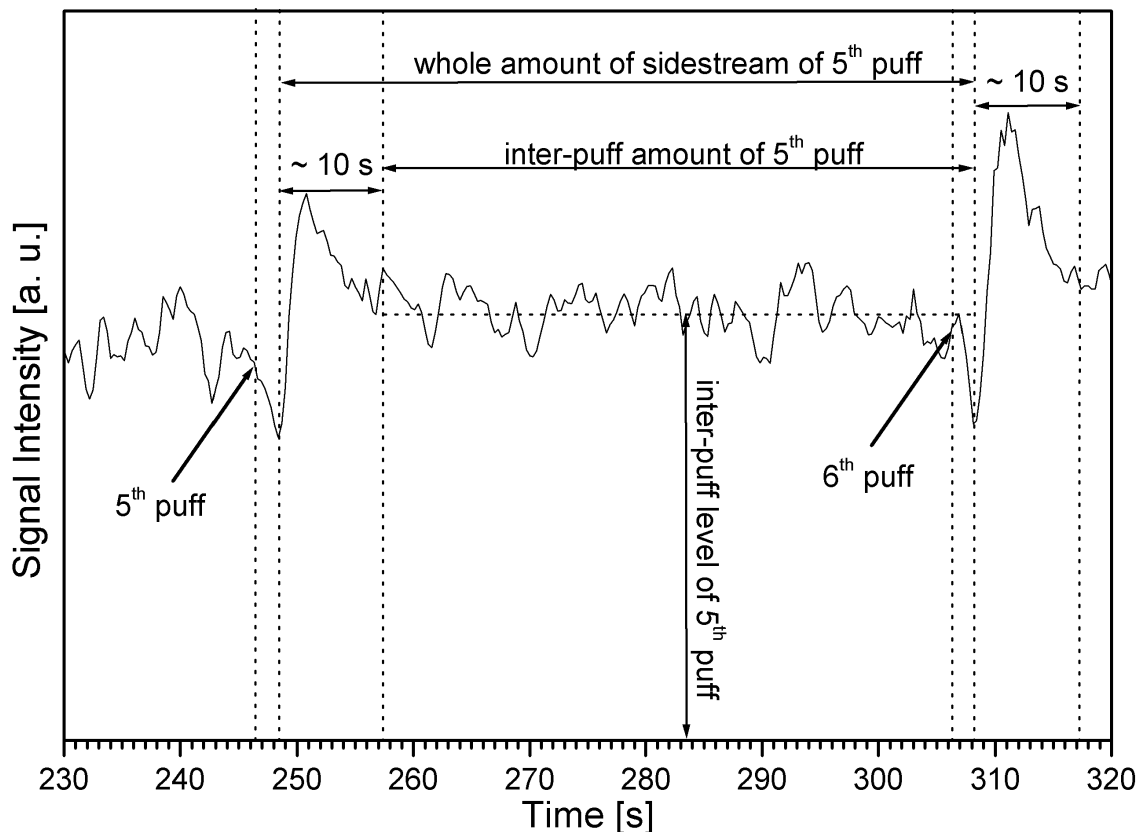
Figure 5.14: Dynamics of $m/z = 17$ of unfiltered sidestream smoke of a 2R4F research cigarette.

5.3.5 Analysis of post-mainstream- and inter-puff sidestream emissions

In contrast to mainstream smoke, sidestream smoke is constantly emitted from the burning cigarette. It was shown earlier in this chapter that significant changes in the concentrations of various compounds occur in sidestream smoke, which correspond to earlier data about particle concentrations [212]. For the comparison of the chemical characteristics the ion-stream normalised summed mass spectra of the gas phase of post-mainstream puff and the inter puff emissions of a 2R4F research cigarette smoked under ISO conditions are shown in Fig. 5.15. In principle the same compounds can be detected as in mainstream smoke, however, there are significant differences in concentrations. The peaks include $m/z = 79$ (pyridine), $m/z = 96$ (furfural, dimethylfuran), and $m/z = 105$ (vinylpyridine). The two spectra show differences in masses $m/z = 58$ (acetone) and $m/z = 68$ (isoprene, furan), both of them with higher ratios in the 10 s time period after a puff is drawn from the cigarette.
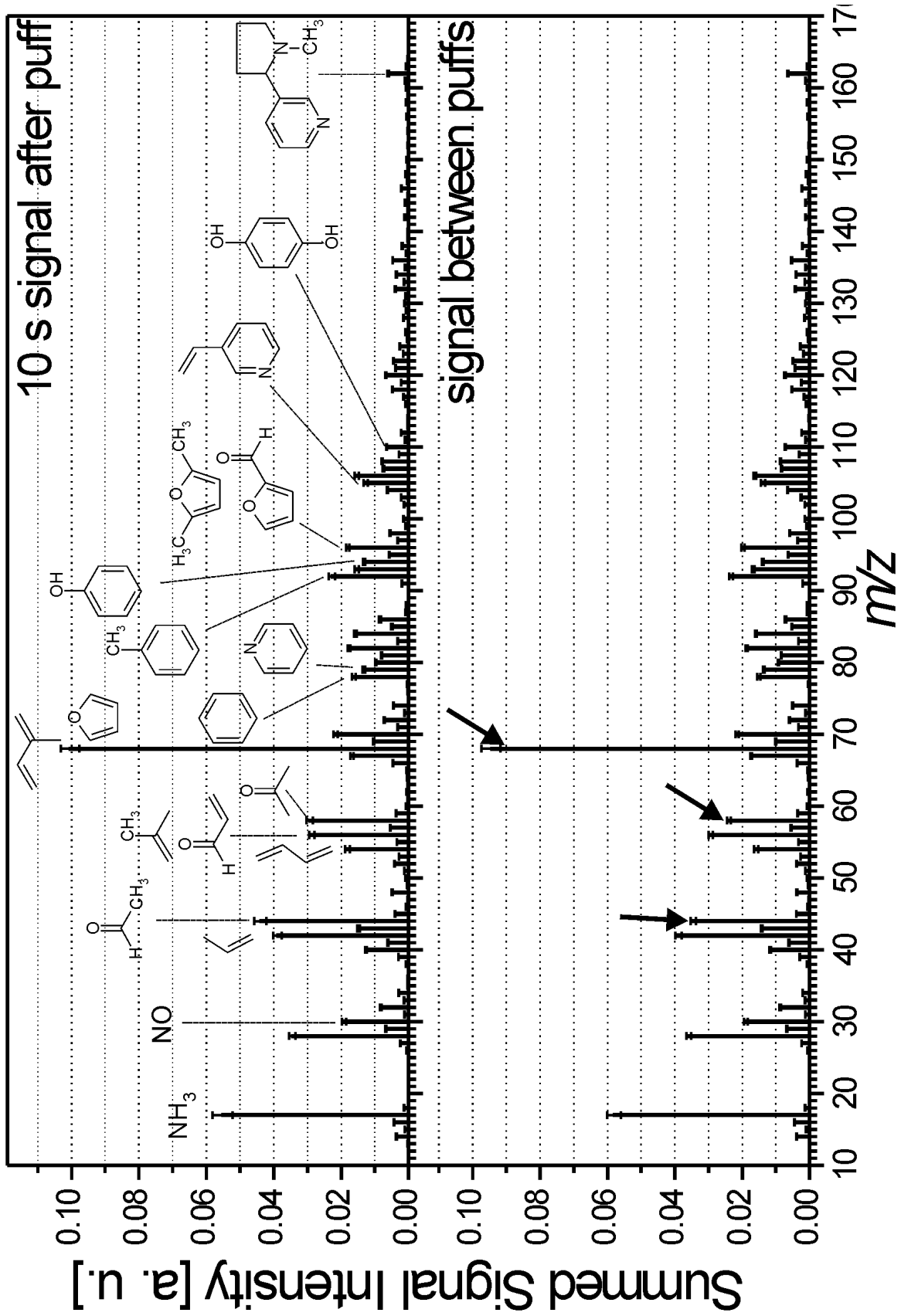
Figure 5.15: Comparison of mass spectra of post-mainstream puff and inter-puff emissions of a 2R4F research cigarette (gas phase).
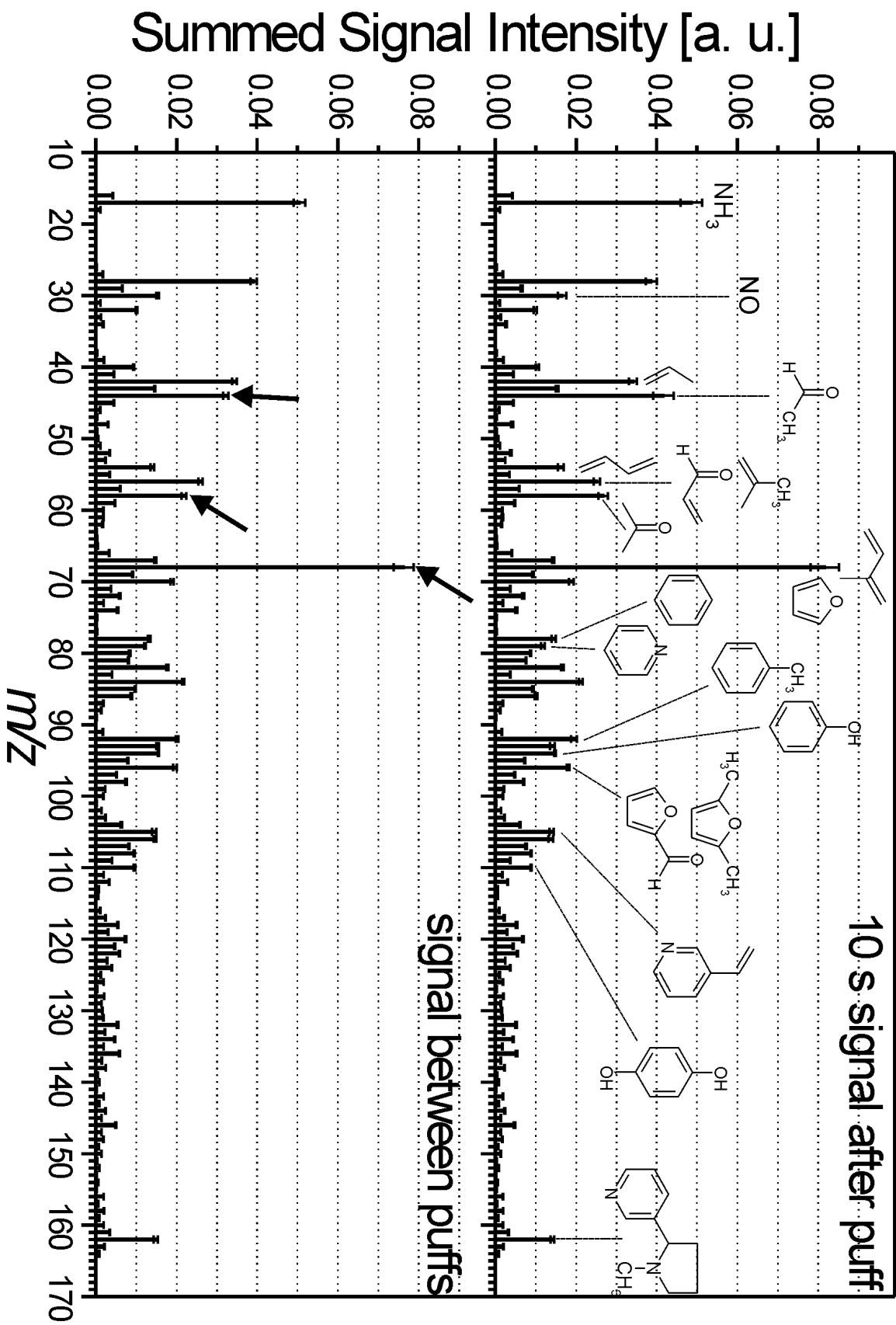
Figure 5.16: Comparison of mass spectra of post-mainstream puff and inter-puff emissions of a 2R4F research cigarette (gas and particulate phase).
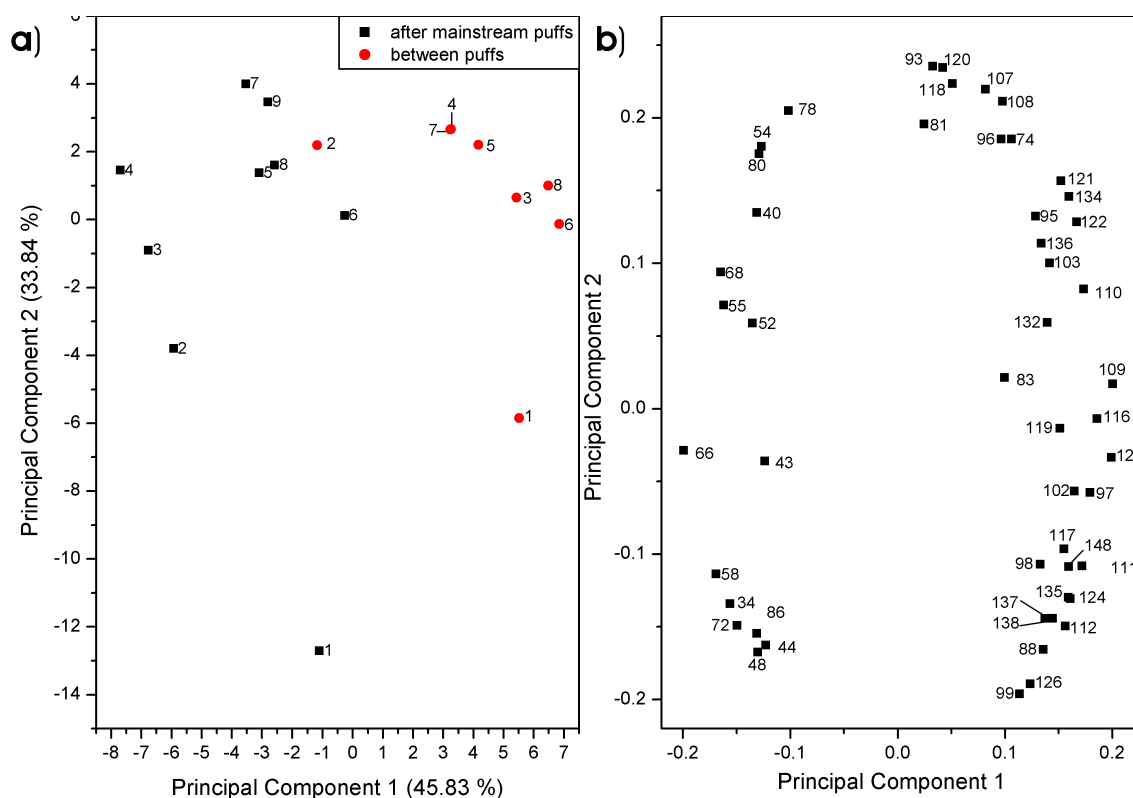
Figure 5.17: Score (a) and loading (b) plot of a PCA of post-puff and inter-puff composition (gas phase).

For a first visual comparison of both sidestream parts the normalised mass spectra are presented in Fig. 5.15 and Fig. 5.16. Fig. 5.16 illustrates the corresponding data of the combined gas and particulate phase of sidestream smoke emissions of a 2R4F research cigarette smoked under ISO conditions. In principle the same compounds as in Fig. 5.15 can be assigned. There is also a similarity in the discriminating masses, in fact $m/z = 58$ (acetone) and $m/z = 68$ (isoprene, furan) as well as a new discrimination mass $m/z = 44$ (acetaldehyde), all with higher fractions in the inter puff emissions. However, only a small number of differences can be observed in visual comparison of the normalised mass spectra. Therefore, statistical methods were applied for further data analysis.

In Fig. 5.17 a statistical comparison of gas phase post mainstream puff and inter puff data by means of PCA with the data of the highest FV is shown to anal-yse the chemical composition of post-puff and inter-puff sidestream emissions. The score plot (Fig. 5.17 a) exhibits the separation of either post mainstream puffs and inter puff within themselves with good correlations of the first (46 %) and second PC (34 %). Post mainstream puffs 1–4 show each unique behaviour com-pared to the puffs 5–9, as well as the inter puff signals after the first and second

puff, the latter one obviously quite similar in chemical composition to the late post mainstream puff signals 5–9. In principle signals of the sulphur containing components $m/z = 34$ (H_2S) and $m/z = 48$ (methanthiole), the unsaturated compounds $m/z = 40$ (propyne), 52 (1-buten-3-yne), 54 (1,3-Butadiene, butyne), 66 (cyclopentadiene), 68 (isoprene, furan), 78 (benzene), the oxygenated species $m/z = 58$ (acetone), 72 (2-butanone, 2-methylpropanal, butanal), and 86 (methylbutanal, 3-methyl-2-butanone, pentanone, 2,3-butanedione), as well as $m/z = 43$ (hydrocarbon fragment), 55, and 80 (pyrazine) strongly point to the puff-dependent signals. Furthermore, the oxygen containing compounds mentioned above seem to contribute especially to the first four signals. In contrast, the odd masses $m/z = 81$ (methylpyrrole), 83, 93 (aniline, methylpyridine), 95 (pyridinol, ethylpyrrole, dimethylpyrrole), 97, 99 (N-formylpyrrolidine, methylpyrrolidone, succinimide, piperidone), 103 (benzonitrile), 107 (acetyl-pyrrole, dimethylpyridine), 109 (methyl-formyl-pyrrole), 111, 117 (indole), 119 (3-(1-propenyl)pyridine), 121 (alkyl-pyridine, dimethyl-aniline), 123 (methyl-acetyl-pyrrole), 135 (trimethylaniline), and 137 yield higher percentages in the signal between puffs as well as 74, 88 (butyric acid), 98 (furanmethanol, methyl-2-pentenal, 5-methyl-2(*5H*)-furanone, 3-methyl-2(*5H*)-furanone), 102 (valeric acid), 108 (anisole, dimethylpyrazine, methyl-phenol), 110 (hydroquinone, catechole), 112 (acetylcylopentane, 2-hydroxy-3-methyl-2-cyclopenten-1-one, furoic acid), 116 (caproic acid), 118 (indane, methylstyrene, benzofuran, succinic acid), 120 (methylethylbenzene, trimethylbenzene), 122 (benzoic acid, ethylphenol, hydroxybenzaldehyde, trimethylpyrazine, methyl-ethyl-pyrazine), 124 (dihydroxymethylbenzene, guaiacol), 126 (5-hydroxymethylfurfural), 132 (methylbenzofuran, 1-indanone, isopropyltoluene), 134 (isopropyltoluene), 136 (limonene, methoxybenzaldehyde, 2-ethyl-5-methylphenol, dimethyl-ethyl-pyrazine, tetramethylpyrazine), 138, and 148. N-formylpyrrolidine, methylpyrrolidone, succinimide, piperidone, acetyl-pyrrole, dimethylpyridine, methyl-formyl-pyrrole, 3-(1-propenyl)pyridine, and methyl-acetyl-pyrrole have previously been reported in essential oils and extracts of various tobacco types [9, 11, 12]).

The PCA of the unfiltered sidestream smoke measurements (Fig. 5.18) illustrates substantial differences in the grouping of the puffs in the score plot (Fig. 5.18 a). While only the first and the second sidestream smoke puffs deviate from the rest, none of the inter puffs shows a unique composition. Furthermore, the later sidestream smoke puff emissions do not significantly differentiate from the chemical composition of the sidestream smoke emissions between two puffs. The loading plot (Fig. 5.18 b) clarifies that the first two after puff emissions are characterised basically by $m/z = 34$ (H_2S), 40 (propyne), 43 (carbohydrate fragment), 44 (acetaldehyde), 48 (methanethiol), 52 (1-buten-3-yne), 58 (acetone), 66 (cyclopentadiene), 72 (2-butanone, 2-methylpropanal, butanal), 86 (methylbutanal,
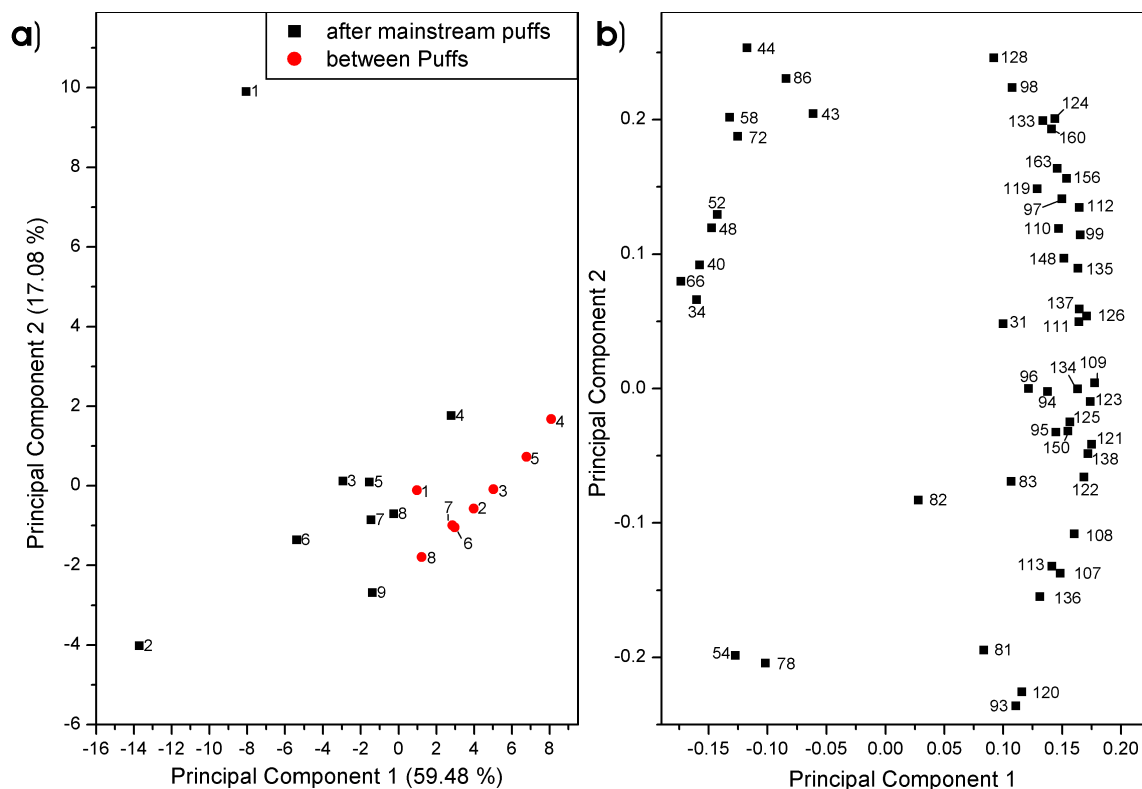
Figure 5.18: Score (a) and loading (b) plot of a PCA of post-puff and inter-puff composition (gas and particulate phase).

3-methyl-2-butanone, pentanone, 2,3-butanedione), as well as $m/z = 54$ (butadiene) and $m/z = 78$ (benzene), the latter ones separating the second one from the first. These are in general the same masses compared to the filtered sample, namely $m/z = 31$ (methylamine), 81 (methylpyrrole), 82 (methylfuran, methylcyclopentene, dimethylbutene, hexene, cyclohexene, 2-cyclopenten-1-one), 83, 93 (aniline, methylpyridine), 94 (phenol, 2-vinylfuran, methylpyrazine), 95 (pyridinol, ethylpyrrole, dimethylpyrrole), 96 (dimethylfuran, furfural), 97 (maleimide), 98 (furanmethanol, methyl-2-pentenal, 5-methyl-2($5H$)-furanone, 3-methyl-2($5H$)-furanone), 99 (N-formylpyrrolidine, methylpyrrolidone, succinimide, piperidone), 107 (acetyl-pyrrole, dimethylpyridine), 108 (anisole, dimethylpyrazine, methylphenol), 110 (hydroquinone, catechole), 111, 112 (acetylcylopentane, 2-hydroxy-3-methyl-2-cyclopenten-1-one, furoic acid), 113 (methyl-succinimide), 119 (homoserine, 3-(1-propenyl)-pyridine), 120 (methylethylbenzene, trimethylbenzene), 121 (2-phenylethylamine), 122 (benzoic acid, ethylphenol, hydroxybenzaldehyde, trimethylpyrazine, methyl-ethyl-pyrazine), 123 (methyl-acetyl-pyrrole), 124 (dihydroxymethylbenzene, guaiacol), 125 (taurine, dimethylmaleimide), 126 (dimethylmaleic anhydride, formyl-methyl-thiophenes, acetyl-thiophenes, maltol), 128 (naphthalene,
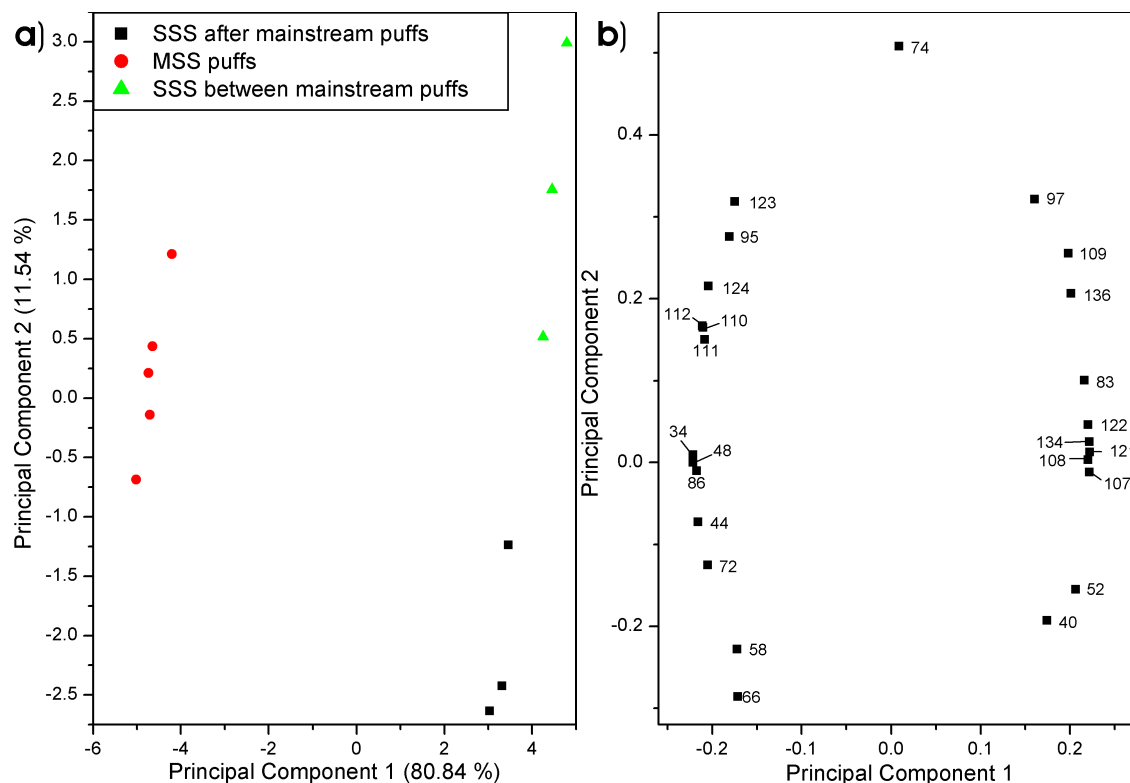
Figure 5.19: PCA plot of mainstream and filtered inter-puff and post-puff sidestream smoke of a 2R4F research cigarette.

2-heptenoic acid, 5-methylhex-2-enoic acid, 6-methyl-hept-5-en-2-ol, 1-octen-3-ol), 133 (aspartic acid), 136 (limonene, methoxybenzaldehyde, 2-ethyl-5-methylphenol, dimethyl-ethyl-pyrazine, tetramethylpyrazine), 137 (p-tyramine), 138 (5-acetyl-2-furaldehyde, salycic acid, isophorone), 148 (cinnamic acid, p-isopropylbenzaldehyde, phtalic anhydride), 150 (vinylguaiacol, thymol, p-allyl-catechol, o-acetyl-p-cresol), 156 (bipyridine, dimethylnaphthalene), 160 (2-Methyl-5-(furyl-2')-pyrazine), and 163.

As already illustrated earlier in this chapter the different combustion conditions during the smoldering and the puffing phase lead to a different chemical composition of the gases. Both PCA plots of sidestream smoke illustrated in Fig. 5.17 and Fig. 5.18 demonstrated that the composition of the smoke, which is emitted after a mainstream puff, has great similarities with mainstream smoke. This is especially valid for the sulphur containing substances, such as $m/z = 34$ (H_2S) and 48 (methanthiole) as well as major mainstream compounds, such as $m/z = 44$ (acetaldehyde), and 58 (acetone). The higher temperatures also explain an increased amount of $m/z = 43$ (carbohydrate fragment) as a result of decomposition of various sugars and plant material. Additionally, the exceptional role of the composition of the first two sig-
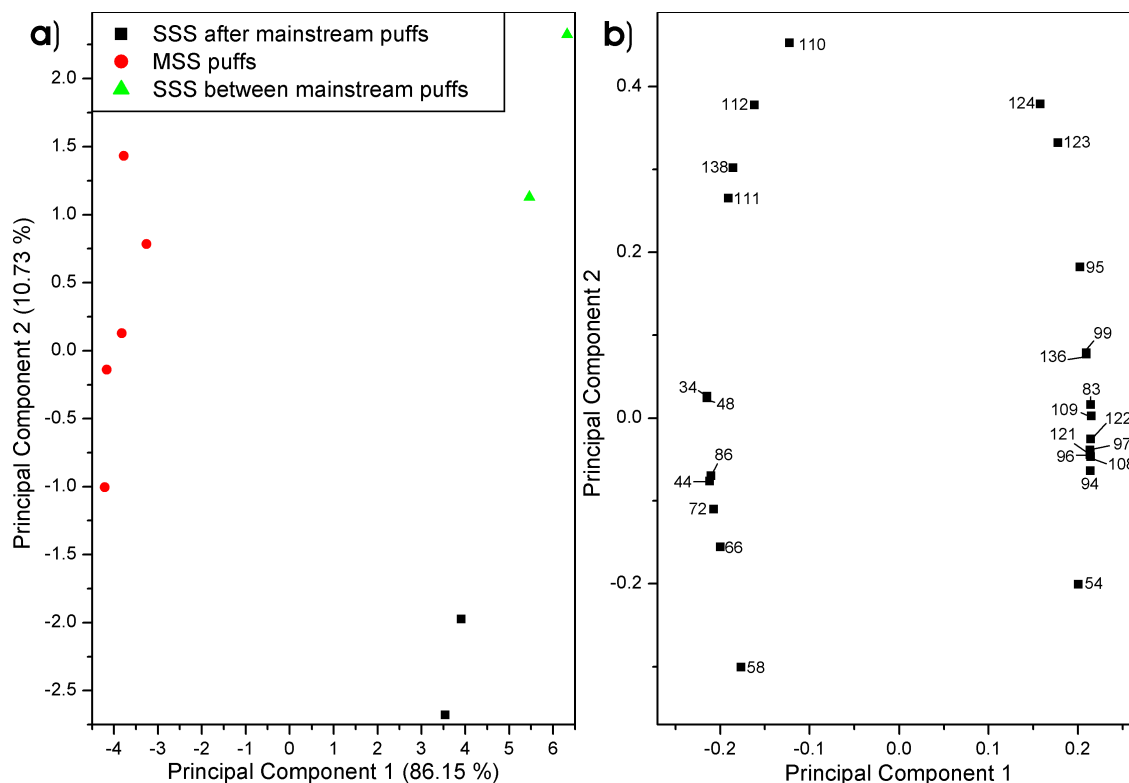
Figure 5.20: PCA plot of mainstream and filtered inter-puff and post-puff sidestream smoke of a 2R4F research cigarette.

nals after the mainstream puff are separated by masses, which can be assigned to unsaturated compounds, namely $m/z = 40$ (propyne), 54 (butadiene), 66 (cyclopentadiene), and 78 (benzene), which also play a major role in the first-puff behaviour of mainstream smoke. However, this is not the case for filtered sidestream smoke, where the exceptional position of the first four puff-related emission peaks is also caused by other important mainstream smoke components.

For further clarification of the effect of temperature on the chemical composition of tobacco smoke the PCA score (a) and loading (b) plots of mainstream smoke as well as filtered (Fig. 5.19) and unfiltered (Fig. 5.20) sidestream inter-puff and post-puff emissions is presented. The separation within the first PC is 86 % and 81 %, respectively, is more significant than the second PC (11 % in both cases) and can be interpreted as the temperature axis. The basic chemical properties of mainstream and sidestream smoke, as illustrated earlier in chapter 5.3.2, are visible in these plots, including the presence of the sulphur containing and some unsaturated compounds. Additionally, the position of the measurements of the sidestream smoke post-puff emissions are slightly shifted towards the mainstream smoke measurements. This emphasises the earlier observations of the puff-resolved analysis

of inter-puff and post-puff sidestream smoke emissions, where typical mainstream smoke masses pointed to the post-puff missions.

6 Particulate Phase Analysis by Comprehensive Two-Dimensional Gas Chromatography

6.1 Principles of multidimensional techniques

In the analysis of the particulate phase of tobacco smoke, analytical chemists are confronted with an enormous chemical complexity. Identification and quantification of individual compounds or compound classes is even more difficult if numerous closely related chemical species are present in a wide range of concentrations. A sufficient separation of trace analytes is often impossible using individual basic analytical procedures. Therefore, it is necessary to develop new analytical methods or find alternative ways of using existing techniques.

Hyphenated analytical techniques, formed by direct combination of different separation or spectrometric methods, are used to increase the analytical power in comparison to the isolated techniques and represent the current state of the art in chemical analysis. A common "hyphenation concept" is the coupling of a (chromatographic) separation technique to a spectrometric detection and identification method. By coupling spectrometry to chromatography, two-dimensional analytical techniques are generated in which retention time is used as the first-dimension variable with, for example, wavenumbers (cm^{-1}) in Fourier transform infrared spectroscopy, light wavelengths (nm) in ultraviolet-/visible light absorption (UV/vis) spectroscopy and mass-to-charge ratios (m/z) in mass spectrometry as second-dimension variables. The most common example of this is gas chromatography or liquid chromatography coupled to mass spectrometry (GC-MS, LC-MS). Hyphenated techniques, however, also include the coupling of two separation techniques, such as in "heart cut" two-dimensional gas chromatography (GC-GC) and liquid chromatography coupled to gas chromatography (LC-GC) [213]. These techniques separate compounds in a first chromatographic step (i. e., the first separation dimension), with a subsequent transfer of an eluent fraction for further analysis in an additional chromatographic separation step (i. e., second separation dimension). "Heart cut" methods increase

separation efficiency in an additive manner (m+n, where m and n are the respective peak capacities or separation efficiencies). These powerful techniques, however, are time-consuming when the entire chemical composition of a sample should be analysed. This requires a multitude of runs in which each "heart cut" covers a different section of the first-dimensional run. The current two-dimensional hyphenated techniques used in the analysis of highly complex mixtures, such as gas chromatography and mass spectrometry or "heart cut"-hyphenated chromatographic techniques, are already pushed close to their principal detection and separation limits. Therefore, only gradual further improvements can be expected, and thus, new analytical concepts need to be developed to achieve a more significant improvement.

The recently introduced comprehensively coupled separation techniques offer a very large increase in separation power. Comprehensive coupling between separation techniques means by definition that the full separation or resolution capability of the individual separation systems is retained in the combined system, and the whole comprehensive separation takes place within the time frame of the primary separation step. If the individual separation efficiencies (i.e., the peak capacities) of the primary and secondary separation technique are n and m, the theoretical separation efficiency of the comprehensively coupled system is given by the multiplication of the individual separation system efficiencies (n∗m) [214]. In this context, comprehensive two-dimensional gas chromatography (GCxGC) [215] thus can be viewed as a "heart cut" GC system with continuous cutting and second dimension analysis over the first dimension in such a way that the fractions obtained are short enough not to reduce the resolution obtained in the first separation dimension. A minimum of four cuts per first dimension peak is necessary, as described by Murphy *et al.* [216] or Marriott and Shellie [217].

Comprehensively coupled multidimensional techniques, however, have more advantages than just increasing separation efficiency. Namely, the possibility of ad hoc differentiation between various compound classes or compound groups with similar physical or chemical properties needs to be mentioned here. This is demonstrated by Giddings's theory on the concept of two-dimensional separation systems [218]. Giddings showed theoretically that the key property of a separation method, which determines whether it can show the inherent structure of a mixture being separated, is the method's dimensionality. The dimensionality of a mixture is, thus, the number of independent variables for every member of the mixture. When a mixture is then separated on the basis of these independent separation variables, each compound will separate to a unique location on a separation plane. However, because the compounds are composed of molecules with discrete but related structures, the compounds must distribute over the dimensional separation space to discrete locations, which are also related to each other.

Comprehensive two-dimensional gas chromatography (GCxGC) [215] demonstrates Giddings's theory quite well. In GCxGC, separation is achieved using two more or less orthogonal stationary phase - analyte interactions. Nonpolar stationary phase columns are most commonly used for the separation in the first dimension, resulting in the elution order of organic compounds being dominated by a temperature program. Separation is thus predominantly driven by volatility (i.e., boiling point separation). In the second dimension, which is run under quasi-isothermal conditions, the separation properties are rather focused on the chemical or physical interactions of the analyte with the stationary phase. The second-dimension separation in most applications is based on so-called polar separation using medium polar or polar columns. Note that the term "polar" separation is due to various physical-chemical interactions which, depending on the molecular interaction of the stationary phase and the analyte, can include dipole-dipole interactions, hydrogen bonding interactions or polarisability effects. The analytes of complex mixtures that have similar volatilities and polar interactions would then show up at similar locations on the two-dimensional chromatographic separation plane. This results in ordered rows or groups of compound peaks with similar chemical or physical properties [219]. These ordered chromatograms make compound identification more rational and allow for fast screening of samples.

The concept of two-dimensional gas chromatography has been applied by several research groups around the world [215, 217, 219–221] and has initiated many other similar two-dimensional separation schemes, such as comprehensive liquid chromatography gas chromatography (LCxGC) [222] or comprehensive supercritical fluid chromatography gas chromatography (SFCxGC) [223].

6.2 Pattern recognition rules

First attempts for the analysis of tobacco smoke components have been published over the last years, e. g. focussing on the acidic fraction [59]. However, as already mentioned earlier, with the capabilities of a high resolution method, such as GCxGC it is possible to differentiate between an enormous number of single chemical compounds. Therefore, new strategies of characterising complex chemical datasets by search criteria rules have been developed by WELTHAGEN *et al.* [221] and applied to urban aerosol samples [224], an equally complex mixture. The classification includes several recognition patterns based on mass spectrometrical, in fact mass fragmentation pattern, and relative ion yields, as well as two-dimensional gas chromatographic retention times. With a set of prededefined rules sum parameters of alkanes,

Compound Class/Group	Fragmentation rules
Alkanes	$m/z = 57, 71$ as rank 1 and 2
n-Alkane-2-ones	$m/z = 58, 59$ as rank 1 and 2
Alkenes and cycloalkanes	Base peak $m/z = 55$ or $m/z = 69$ with both present and at least three of $m/z = 56$, 57, 70, 83, 97 > 15 %
Terpenes & Steroids	$m/z = 69 > 15$ %, $m/z = 81 > 15$ % and $m/z = 95 > 15$ % or $m/z = 79 > 15$ %, $m/z = 91 > 15$ % and $m/z = 105 > 15$ %
n-Alkyl Acids	Base peak $m/z = 60$ and $m/z = 73$ as rank 2
n-Alkyl Acid methyl esters	Base peak $m/z = 60$ and $m/z = 102 > 40$ %
n-Alkyl Acid amides	Base peak $m/z = 59$ and $m/z = 72 > 20$ % (prim.) or $m/z = 60, 141$ as rank 1 and 2 (secondary)
PAH	Base peak $m/z = 128, 178, 202$, or 228
Alkyl-substituted PAH	Base peak $m/z = 191, 192, 206, 216, 215, 242$, or 256
Naphthalene and alkyl-substituted naphthalenes	(1) $m/z = 128 > 15$ %, $m/z = 77 > 5$ % (2) One of $m/z = 145, 155, 169 > 50$ %

Table 6.1: Used selection criteria for the characterisation of tobacco smoke particulate matter samples.

alkenes and cycloalkanes, alkane acids, alkyl-substituted benzenes, polar benzenes with or without alkyl groups, partly hydrated naphthalenes and alkanyl-substituted benzenes, naphthalene and alkyl-substituted naphthalenes can be classified to sum parameters. The use of pattern recognition rules for the characterisation of complex mixtures by sum parameters has been recently further developed by *Vogt et al.* [224]. For an application to tobacco smoke samples additional classification patterns for the typical tobacco ingredients and combustion products were introduced, namely terpenes and steroids, n-alkane methyl esters, n-alkane amides, alkane-2-ones, PAH, and alkyl substituted PAH. A summary of the selection criteria used is given in Table 6.1.

6.3 Instrumental set-up and sample preparation of the particulate phase analysis

For the puff-by-puff analysis of the particulate phase 20 cigarettes were smoked according to the ISO protocol with a Borgwaldt single port smoking machine. For each puff a different Cambridge filter pad was used and extracted for 15 minutes with 10 mL of *tert.*-Butyl-methyl-ether (TBME). For the comparison of sidestream and

6.3 Instrumental set-up and sample preparation of the particulate phase analysis

mainstream smoke the smoke of two 2R4F research cigarettes smoked under ISO conditions was collected with cryo-traps cooled by liquid nitrogen. The mainstream smoke was taken from the exhaust pipe of a Borgwaldt single port smoking machine, the sidestream smoke was collected via a fishtail chimney, introduced earlier in chapter 5.1 before being trapped in the liquid nitrogen traps. The trapped material was dissolved in 5 mL of dichlormethane.

A comprehensive two-dimensional gas chromatography time-of-flight mass spectrometer GCxGC-TOFMS was used in this study (instrumentation: Injection port: Optic III, ATAS-GL, Veldhoven, NL; GC: Agilent 6890, USA; TOFMS: Pegasus III, LECO Ltd, St. Joseph, MI, USA, GCxGC system: Pegasus 4D option, LECO Ltd, MI, USA). The two-dimensional comprehensive gas chromatographic system consists of two serially connected separation columns, a long (30 m) first-dimension column (with a non-polar stationary phase) and the much shorter (1.5 m), second-dimension column (with a polar stationary phase). A four-jet nitrogen cooled thermal modulator was used for modulation of the eluent from the first column into the second. The modulator is situated between the two columns. On the first column, a conventional high-resolution gas chromatographic separation takes place. The modulator then focuses the eluent from this first column and re-injects it as narrow injection bands into the second column, which is run under almost isothermal conditions at a temperature of typically 5 °C higher than the first column's temperature. To maintain the separation achieved by the first column, the re-injection intervals of the modulator need to be fast (e.g. 4 s) and therefore the speed of separation in the second column also needs to be fast. The faster separation in the second column is obtained by using a column with smaller inner diameter than that of the first column. Column parameters of the sets used in this study was a 30 m x 0.25 mm I.D. x 0.25 μm df BPX5 from SGE as first dimension column and a 1.5 m x 0.10 mm I.D. x 0.10 μm df BPX50 from SGE as second dimension column.

Additional instrumentation parameters were as follows: 3 μl splitless injection at 300 °C, 1.5 ml/min column flow rate, helium carrier gas, and data acquisition rate of 100 Hz. The first dimension oven was held at 60 °C for 10 min then heated to 300 °C at 1.5 °C/min while the second oven was kept at 5 °C above first oven temperature. The modulator was heated to 100°C above oven temperatures and the pulse duration of the heated pulses were set to 300 ms. The cold pulses, cooled to liquid nitrogen temperatures, were only switched off during the heating periods (warm pulses). A modulation period of 4 seconds was used.

6.4 Results of the particulate phase analysis

6.4.1 Comparison of main- and sidestream smoke particulate phase

A chemical comparison of sidestream and mainstream whole smoke by SPI-TOFMS has already been presented in chapter 5.3.2. For further investigations of the chemical differences a comparison of mainstream (a) and sidestream smoke (b) of the particulate phase of a 2R4F research cigarette smoked under ISO conditions is presented in Fig. 6.1. Both chromatograms are normalised to their corresponding TIC to enable the comparison of chemical patterns without superimposing sampling effects. A selection of compounds is assigned by automatic comparison of the acquired mass spectra with the NIST-Database, the corresponding probability count is given in 1/1000. The chemical fingerprint of both samples is significantly different. In general, the complexity of the sidestream particulate matter sample is higher as can be observed especially at first dimension retention times of $2600 < t < 4600$. Because of the nature of TIC normalisation this does not necessarily reflect the overall complexity of the sample but rather an increase in total amounts in sidestream smoke. In both spectra two rows of hydrocarbons are visible at second dimension retention times of about one second, namely high molecular weight alkanes (higher retention times in the first dimension, lower in the second) and the corresponding unsaturated ones (lower first dimension retention times, higher second dimension retention times). The intensity of the unsaturated row is significantly higher in sidestream smoke. Due to the similar character of the EI-spectra of higher n-alkanes and -alkenes and the lack of molecular peaks in the spectra, a sufficient automatic compound assignment is not possible, while assignment to compound classes is feasible by means of fragmentation patterns. However, new methodologies of combining the advantages of soft ionisation methods with gas-chromatography have been introduced [85] and recently extended to GCxGC. Both spectra are dominated by the nicotine peak accompanied by two other peaks, myosmine and bipyridine, the latter ones in higher amounts in sidestream smoke. Additionally, four areas of visible differences are marked with red circles. Vinyl-pyridine, phenol, methylated phenols, and 3-phenyl-pyridine show higher yields in sidestream smoke than in mainstream smoke. In contrast to this, pyranone exhibits much higher amounts in mainstream smoke. Additional differences can not be assigned to individual substances, as proper identification is not possible. A row of isobaric dimethylated naphthalenes, which have higher amounts in sidestream smoke, is also visualised in the spectrum of sidestream smoke. The high separation efficiency of the technique allows total separation of these compounds, which could not be distinguished by PI-TOFMS.
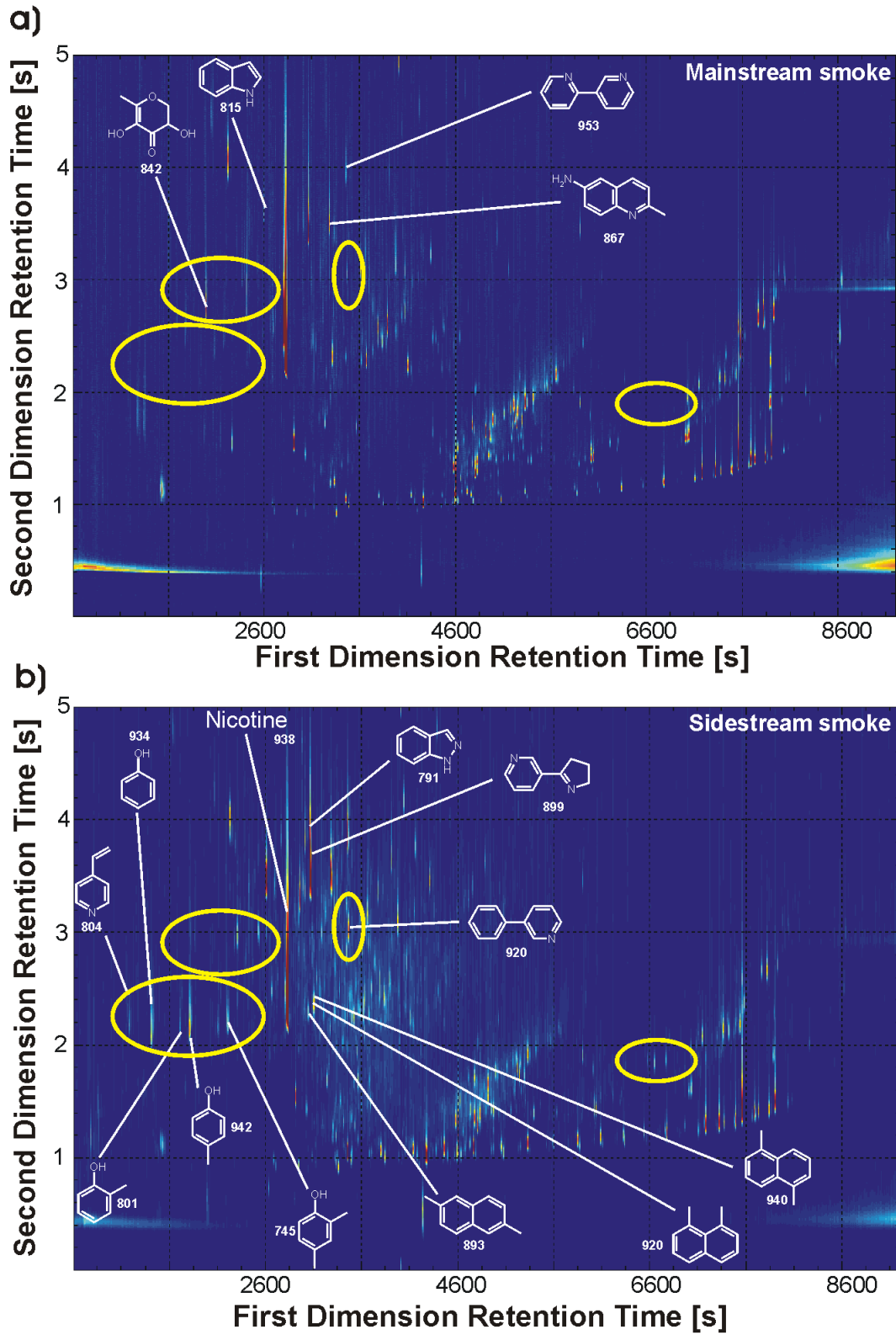
Figure 6.1: Comparison of mainstream (a) and sidestream smoke (b) of the particulate phase of a 2R4F research cigarette smoked under ISO conditions.
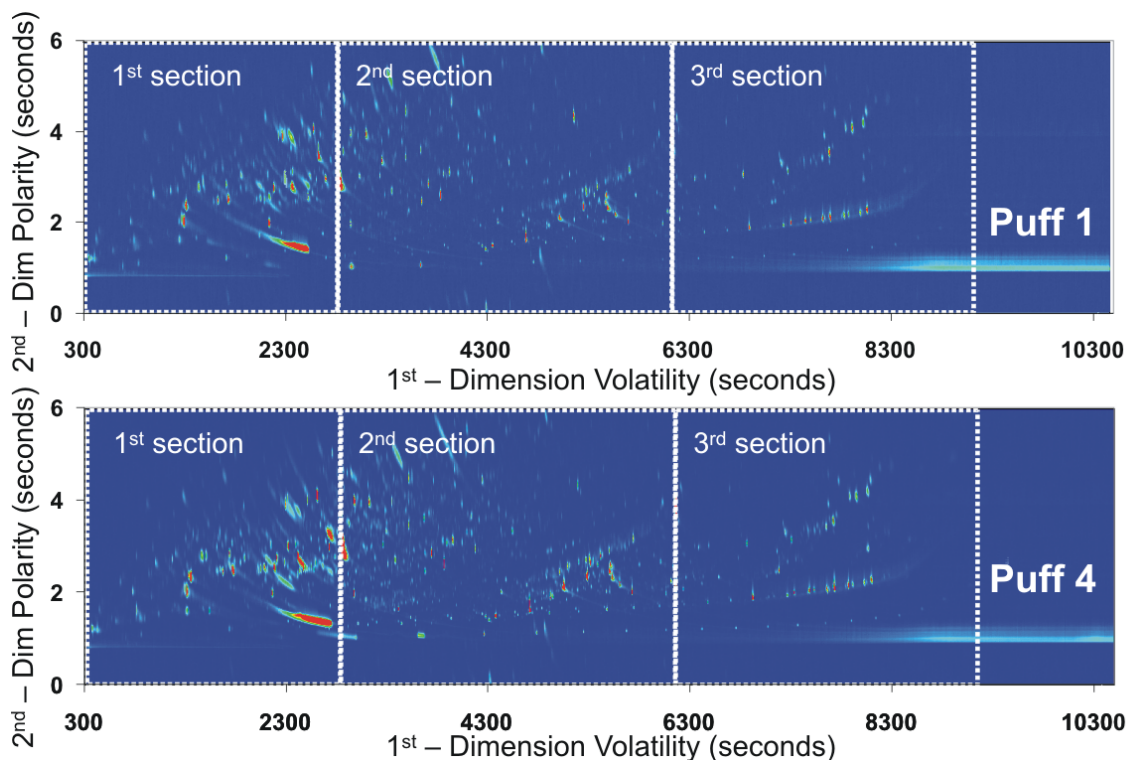
Figure 6.2: *Comparison of the whole GCxGC chromatogram of the first (a) and fourth (b) puff of the particulate phase of a 2R4F research cigarette smoked under ISO conditions.*

6.4.2 Puff resolved analysis of mainstream particulate phase

An overview of the spectra of the first (a) and fourth puff (b) of the particulate phase of a 2R4F research cigarette smoked under ISO conditions is presented in Fig. 6.2. At first sight no significant differences can be observed between the spectra. Nevertheless, the basic compound patterns are similar to the mainstream chromatogram presented earlier in this chapter. A slight increase in concentration of most compounds can be observed, especially visible in the first dimension at retention times > 2500 s. For further investigations the spectra are divided into three parts and processed separately.

Fig. 6.3 exhibits the first section of both the first (a) and the fourth puff (b) of the collected particulate phase of a 2R4F research cigarette smoked under ISO conditions including a selection of compound assignments automatically done via the measurement software. Again, the numbers represent the matching probability of a comparison with the NIST library in 1/1000. This part of the spectrum is dominated by the peak of glycerol, which of course plays an important role in tobacco and tobacco manufacturing, as well as various phenolic compounds, like hydroquinone, catechol and vinyl-guaiacole. In the area of the lower boiling compounds furfuryl
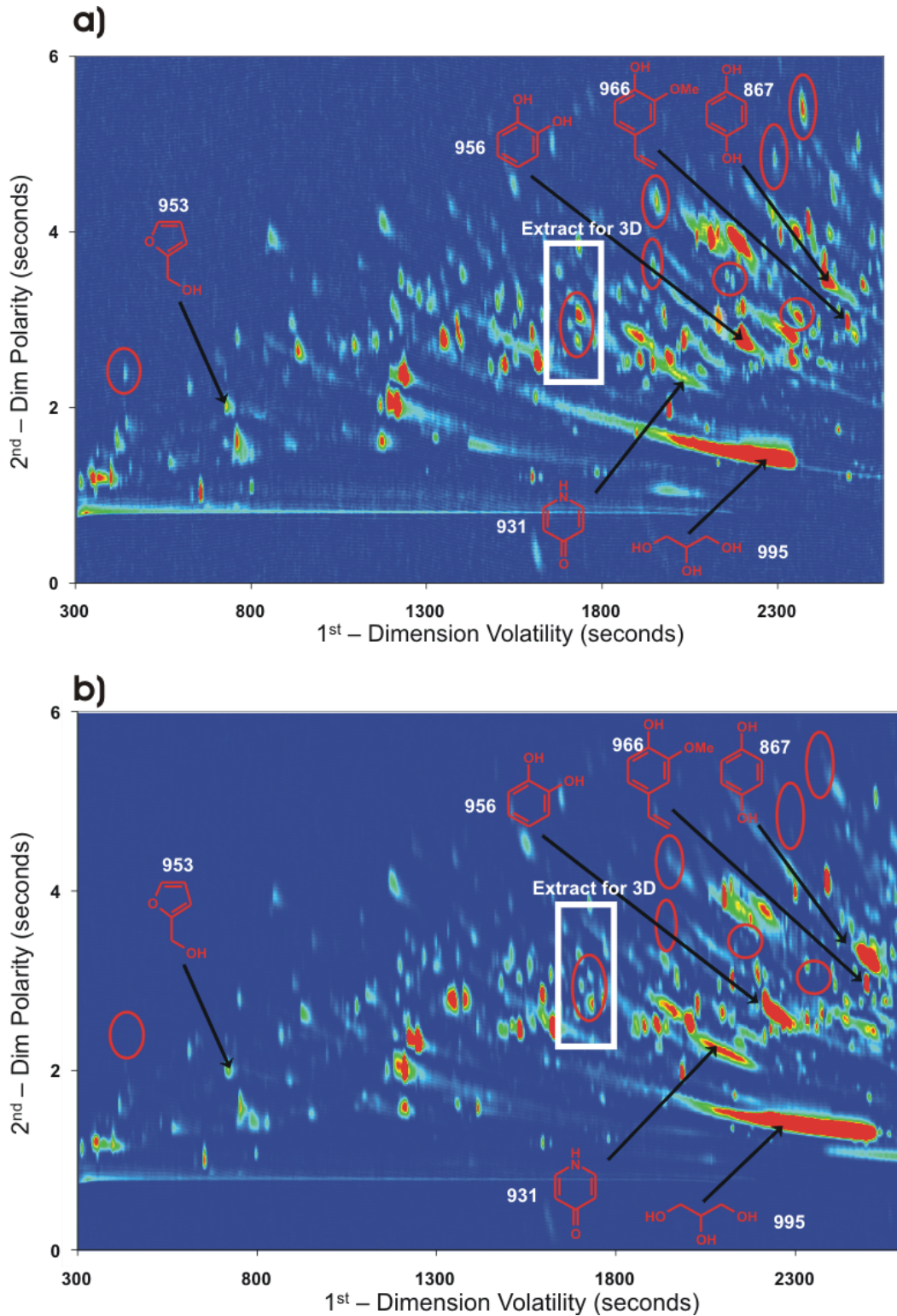
Figure 6.3: Comparison of the first section of the GCxGC chromatogram of the first (a) and fourth (b) puff of the particulate phase of a 2R4F research cigarette smoked under ISO conditions.

alcohol is indicated, also known as a key compound in tobacco leaf and smoke. Though the visual identification of differences is difficult, a small number can be observed, indicated by red circles. However, no clear assignment to substances can be done by automatical peak assignment. The comparison of the second section of the collected particulate phase of the first (a) and fourth (b) puff of a 2R4F research cigarette smoked under ISO conditions is presented in Fig. 6.4. Again, a selection of assigned compounds and the corresponding matching quality is added, including nicotine, methyl-indole, bipyridine, and some phenolic compounds, as well as visually observable differences, indicated by red circles. The numbers of such differences is significantly lower despite the fact that the section covers a larger portion of the first dimension retention time.

As the last part of the comparison of the first and fourth puff of cigarette mainstream smoke particulate matter extracts the third section of the chromatograms of the first (a) and fourth (b) puff of the particulate phase of a 2R4F research cigarette smoked under ISO conditions is shown in Fig. 6.5. No peaks can be observed at the higher retention times. As in the previous sections, some automatically assigned compounds are indicated, as well as the two visually observable differences. A number of plant components are visible on the far right of the spectra, including campesterol and β-sitosterol, well known natural tobacco leaf and smoke ingredients.

As illustrated in the previous figures a complete manual processing of the data is extremely time-consuming and therefore almost impossible. However, small differences can already be observed without further processing the data. As an example, a further investigation of a small section (indicated in Fig. 6.3) is presented here. In this case a 3D-plot of an enlarged part of the first section is presented in Fig. 6.6. On the upper half of the figure the total ion chromatogram (TIC) is presented. Significant differences between the first and the fourth puff in this region of the spectrum can be observed for maltol, 3-ethyl-2-hydroxy-2-cyclopenten-1-one, phenylethylalcohol, 3-hydroxypyridine monoacetate, 2,6-dimethyl-phenol, and 3-ethenyl-3-methylcyclopentanone. It is clear, that a change in chemical composition occurs from large quantities of 3-hydroxypyridine monoacetate towards larger amounts of 3-ethyl-2-hydroxy-2-cylopenten-1-one, 2,6-dimethylphenol, and 3-ethenyl-3-methylcyclopentanone. These changes can be additionally clarified by looking at the chromatograms of $m/z = 95$ (fragment of 3-hydroxy-pyridine) and $m/z = 126$ (maltol, 3-ethyl-2-hydroxy-2-cyclopenten-1-one), the latter appearing in much higher amounts in the fourth puff.

Fig. 6.7 exhibits the GCxGC analysis of the particulate phase of the fourth puff of a 2R4F research cigarette with the classification shown above the spectrum. The size of the bubbles represents the peak integral on a logarithmic scale, only those
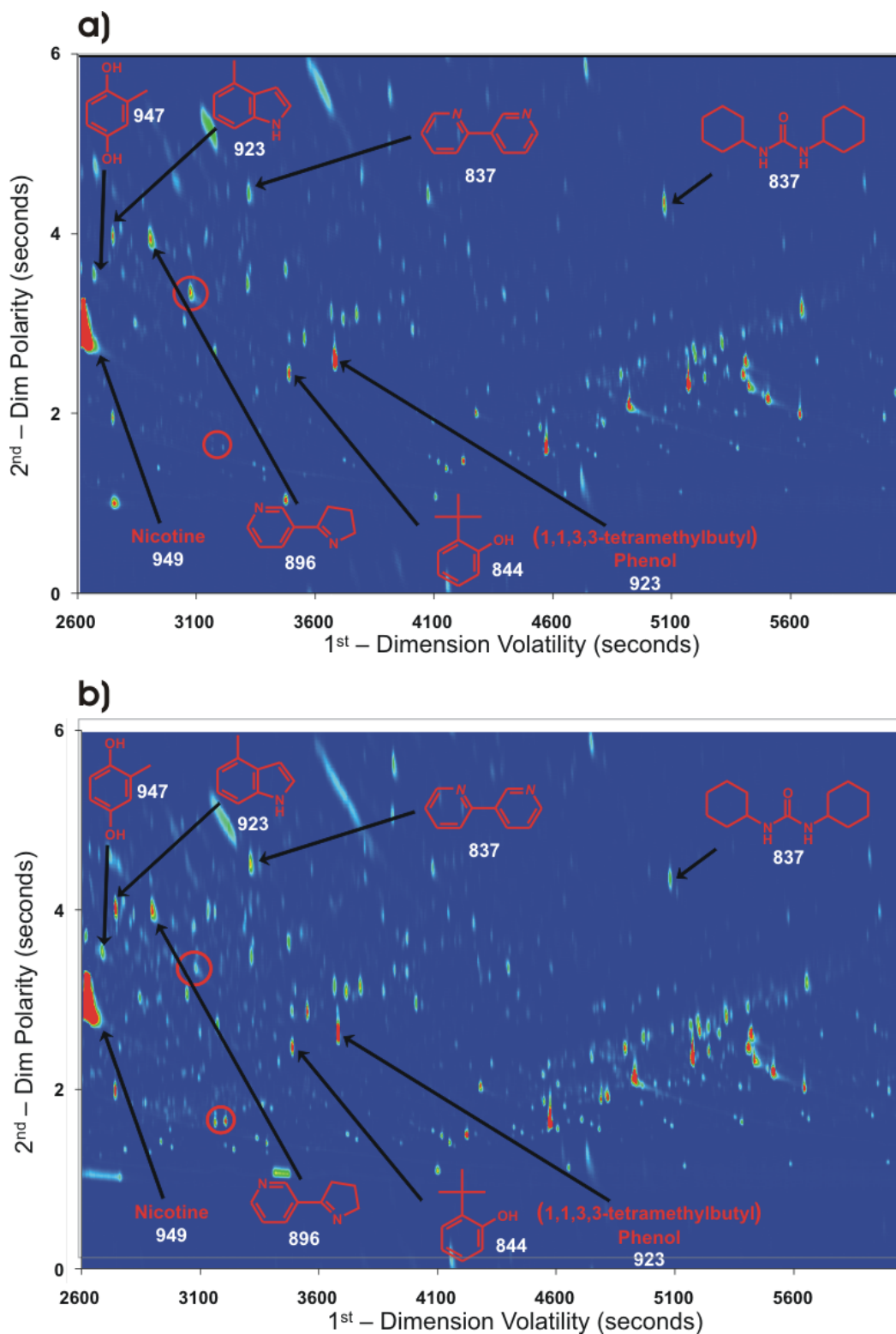
Figure 6.4: Comparison of the second section of the GCxGC chromatogram of the first (a) and fourth (b) puff of the particulate phase of a 2R4F research cigarette smoked under ISO conditions.
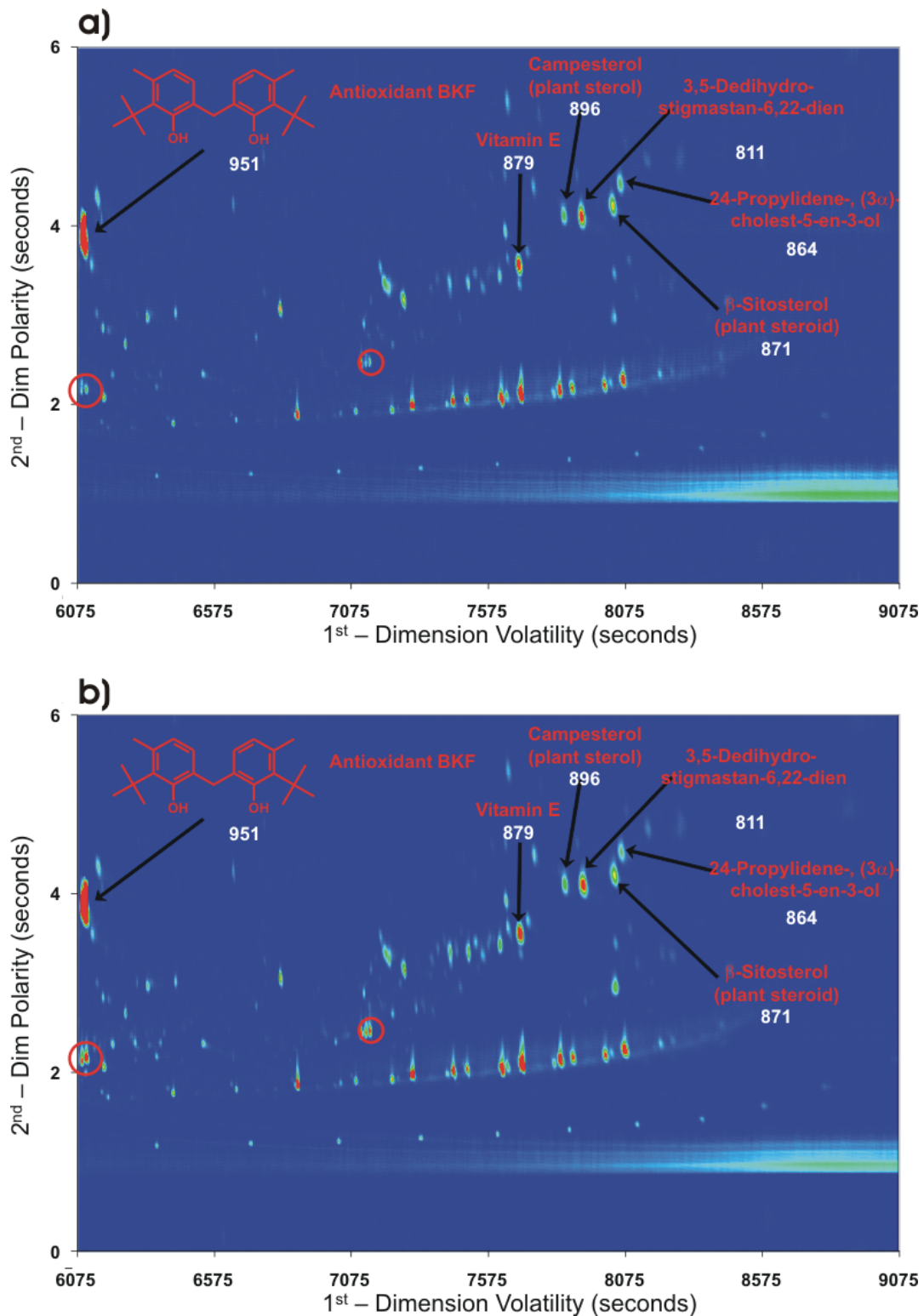
Figure 6.5: Comparison of the third section of the GCxGC chromatogram of the first (a) and fourth (b) puff of the particulate phase of a 2R4F research cigarette smoked under ISO conditions.
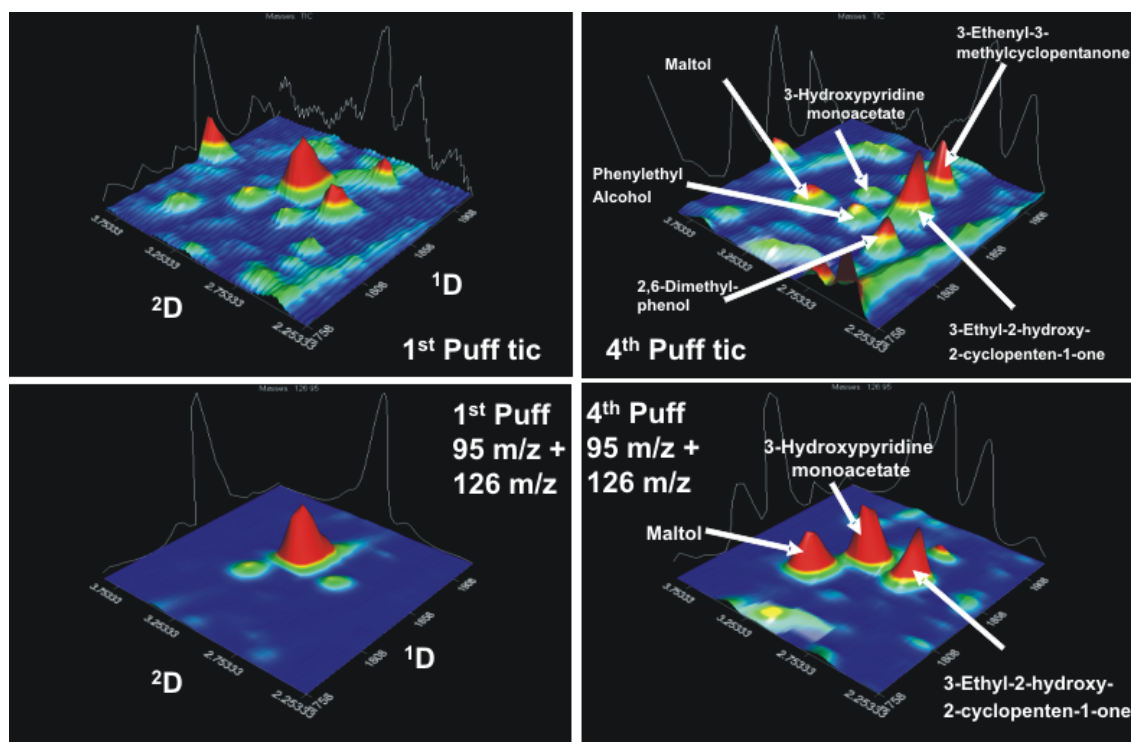
Figure 6.6: Comparison of a enlarged part of the first section of the GCxGC chromatogram of the first and fourth puff of the particulate phase of a 2R4F research cigarette smoked under ISO conditions.

substances are displayed, that are assigned to a single functional group. To achieve efficient classification of the different substance classes chromatographic information was used to limit the area where pattern analysis is applied. This is possible due to the multi-dimensionality of the technique and the fact, that substances can be found at distinct locations within the chromatogram. To clarify the areas of different compound classes the schematic overview of the applied retention time restrictions can be found in Fig. 6.8. As described earlier, the row of homologous alkanes (red), as well as alkenes and cycloalkanes (yellow), is clearly visible at low second dimension retention times. Furthermore, various acid derivatives, such as amides (purple) and esters (cyan), can be found, as well as the homologue row of n-alkane-2-ones. Additionally, three highly populated compound classes can be observed, namely alkyl substituted naphthalenes (blue) and PAH (dark blue), as well as terpenes and steroids (green). These groups and the PAH (black) in fact represent important substance classes of tobacco smoke condensate.

For a further analysis of tobacco smoke condensate the puff-resolved data combined into chemical classes is presented in Fig. 6.9, namely alkanes (a), alkenes and cycloalkanes (b), alkanoic acids (c), alkane-2-ones (d), PAH (e), alkyl substituted PAH
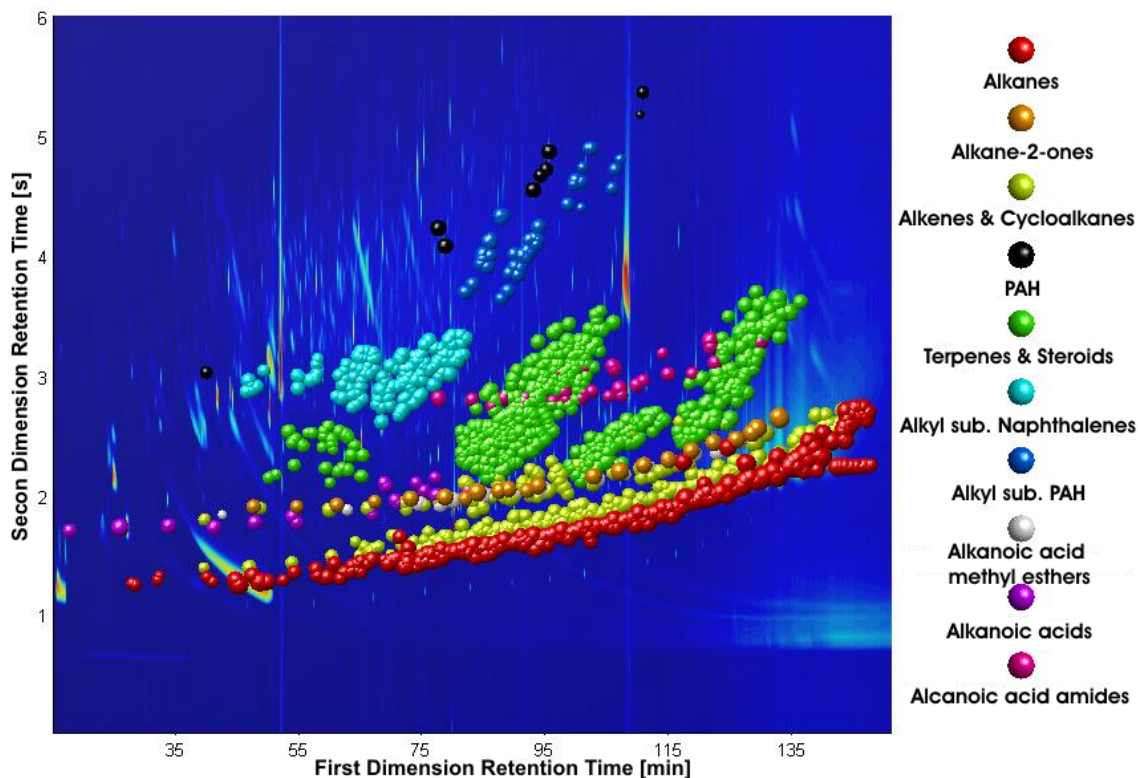
Figure 6.7: Classification of the GCxGC data of the particulate phase a fourth puff of a 2R4F research cigarette smoked under ISO conditions.

(f), alkylated naphthalenes (g), and terpenes & steroids (h). To enable a comparison of the chemical profile the chromatograms were normalised to their corresponding TIC. It can be seen in Fig. 6.9 b) that trends, similar to the first puff behaviour observed in the gas phase, are also visible for alkanes and alkenes/cycloalkanes. This fact can also be seen in the carboxylic acids (Fig. 6.9 c), which also now show clear puff-related behaviour. While the high content of unsaturated compounds in the first puff may be a result of different burning conditions after ignition the higher amounts of acids may be a result of desorption of various acids off the tobacco. The decrease in the content of alkanes during the different puffs (Fig. 6.9 b) may also be explained by the successive desorption of these compounds off the tobacco. While terpenes and steroids (Fig. 6.9 h) and alkane-2-ones (Fig. 6.9 d) show now distinctive puff behaviour the characterised aromatic substance classes do. In fact, PAH and the alkylated naphthalenes and PAH (Fig. 6.9 f) and g) increase steadily during the first puffs, probably resulting from more stable burning conditions.
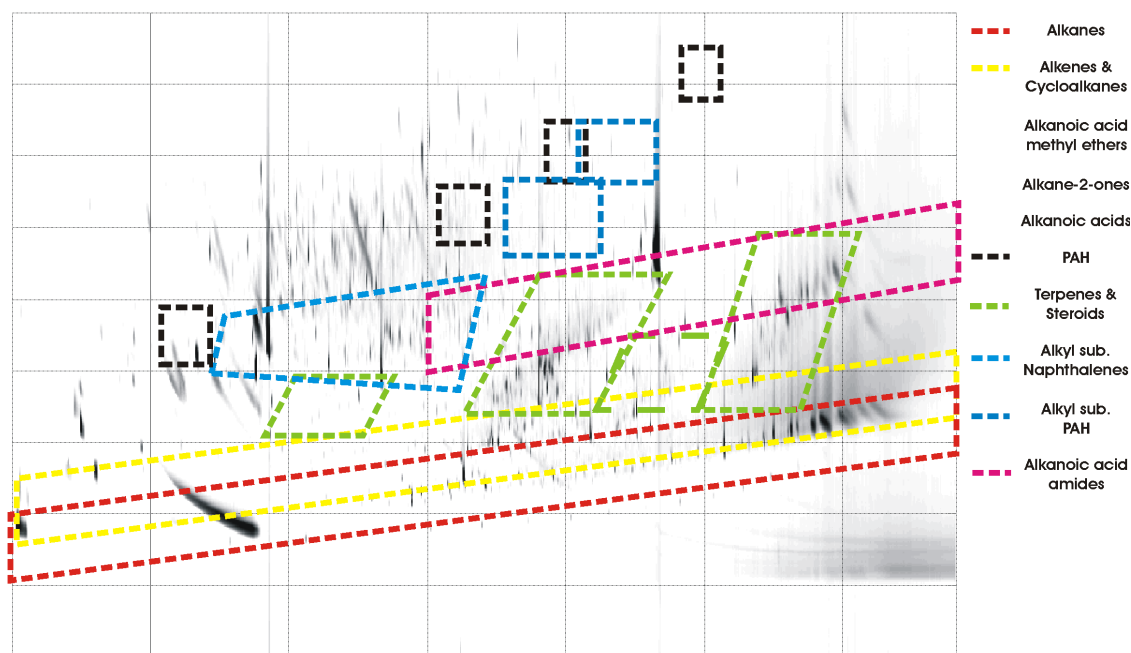
Figure 6.8: Areas where certain compound classes can be found in tobacco smoke.

6.5 Conclusion of the particulate phase analysis with comprehensive gas-chromatography

GCxGC-TOFMS is a relatively new high resolution technique which enables powerful investigation of highly complex mixtures, such as tobacco mainstream and sidestream smoke. A great variety of substances can be analysed simultaneously, which enables fingerprint characterisation of different samples. However, the large number of single identified peaks in these mixtures is challenging for a manual interpretation of every single peak. Recently, new concepts have been developed that classify the compounds by means of mass spectrometrical patterns into functional groups and generates sum parameters and it has been demonstrated that these can be used to classify complex matrices like tobacco smoke. However, it is still possible to examine individual compounds, which are not overlayed by several other substances in contrast to comparable one dimensional techniques. Nevertheless, no classification rules are available for substance classes, which are present in large amounts in tobacco smoke and tobacco leaf, in fact lactones, amines, and heterocyclic aromatic compounds are already known. This possibly results in overlaps and miss-classifications. However, especially for alkanes and alkenes/cycloalkanes the current selection rules are quite efficient, allowing the analysis this sum parameter on a puff-by-puff basis.
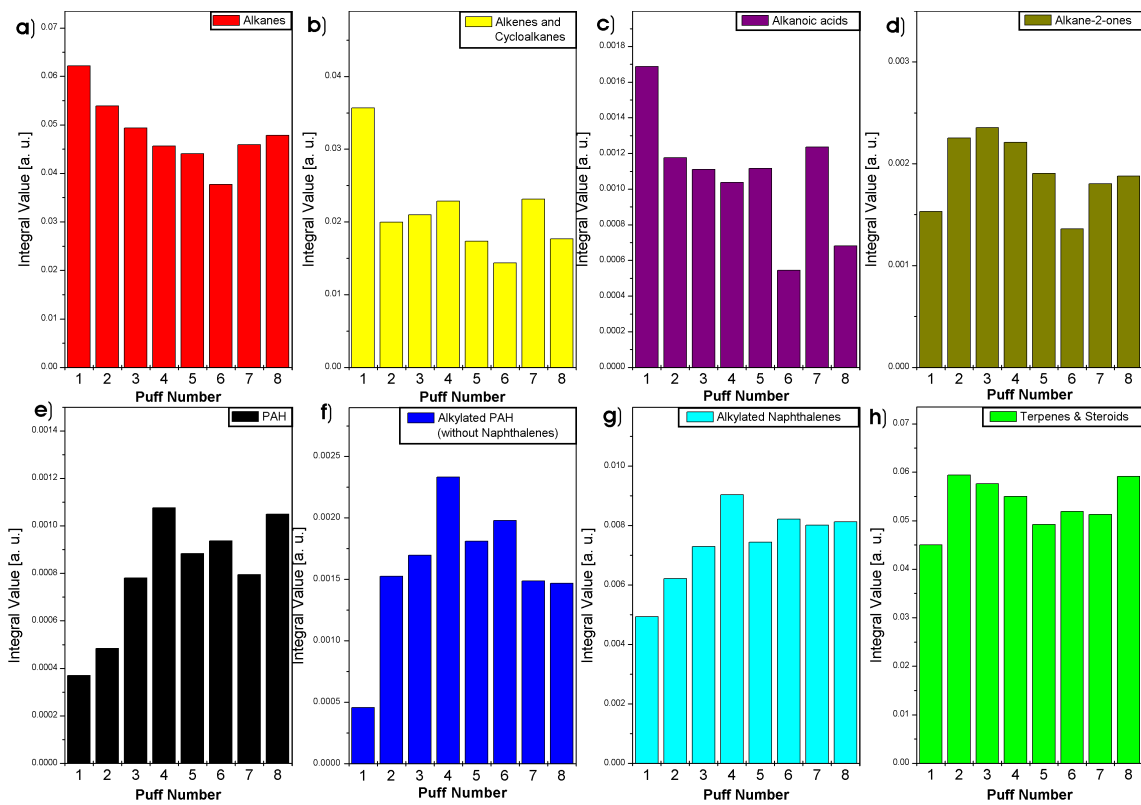
Figure 6.9: Puff profiles of substances combined into chemical classes: alkanes (a), alkenes and cycloalkanes (b), alkanoic acids (c), alkane-2-ones (d), PAH (e), alkyl substituted PAH (f), alkylated naphthalenes (g), and terpenes & steroids (h).

7 Conclusion and Outlook

This theses describes the application of novel mass spectrometrical techniques with soft photoionisation methods, in fact resonance enhanced multi photon ionisation (REMPI) and single photon ionisation (SPI) to tobacco smoke as well as new concepts for the analysis of the total particulate matter (TPM) of tobacco smoke by comprehensive gas chromatography mass spectrometry GCxGC-MS.

For an efficient use of mass spectrometry in the analytical application of complex chemical mixtures special consideration has to be taken to isobaric compounds. Therefore, methods based on conventional offline techniques still play an important role in the online analysis of complex mixtures. Additionally, several concepts for the distinction of isobaric compounds were provided, especially considering novel light sources, which can be adjusted to different wavelengths.

The use of SPI/REMPI-TOFMS for the analysis of thermodesorption (TD) and pyrolysis (py) off-gases of pure tobacco was shown, exhibiting the differences of various tobacco types and the chemical profile in the low temperature range up to 310 °C. In this case, three temperature steps were chosen, 190 °C, 250 °C and 310 °C, which have already proven to be crucial steps in the analysis of different tobacco types. It could be demonstrated that a very good distinction is achievable by applying advanced statistical methods, such as Fisher-values (FV) and principle component analysis (PCA). Though not utilising the high time resolution of the method, the analysis of relatively slow processes still offers the possibility of quality control in several fields of either tobacco or other consumable goods.

The use of online methods such as SPI/REMPI-TOFMS for tobacco smoke analysis could be demonstrated for mainstream and sidestream smoke, where a puff-by-puff analysis is possible for a broad range of health-related compounds. Usually the mainstream and sidestream yields of such compounds are determined by conventional off-line methods by smoking the cigarettes under standard ISO conditions. In general, SPI is very well suited for the analysis of several low volatile compounds, such as aldehydes, ketones, alkenes, and amines, as well as several other compound classes. On the other hand, REMPI is a highly selective technique, especially suitable for aromatic compounds. By selection of appropriate wavelengths and the use

of special inlet techniques, such as jet-cooling, several compound classes, e. g. phenols, polycyclic aromatic hydrocarbons (PAH), and amines are accessible. In a step towards the investigation of human smoking behaviour, different, more intense, machine smoking conditions were used, to examine the influence of filter ventilation hole blocking, puff duration and puff volume on the chemical composition of mainstream tobacco smoke on a puff-by-puff basis. Throughout the studies it was discovered that some puff parameters seem to have a similar influence on the whole spectrum of the analysed compounds, while others lead to different yields in certain compounds and compound-classes. Based on these results a concept for a forecast of certain compound yields with changing conditions was developed. However, this study can only represent a first step, as a much larger scale investigation has to be carried out, once the complicated prototype system evolves into a more friendly end-user, easy-to-use system, that has currently been developed.

During the investigation of sidestream smoke new details about the dynamics of sidestream smoke formation were revealed. A puff resolved quantification for selected compounds was done and compared to previous measurements. It could be shown that under standard smoking conditions there are significant differences between the chemical composition during the drawing of a puff, directly after, and in the relatively long period between two puffs. This holds especially for some low volatile oxygenated compounds as well as some unsaturated compounds and the majority of nitrogen compounds. Furthermore, it was shown, that the chemical differences in various tobacco types also have significant influence on the composition of sidestream smoke, as most of the chemical differences previously reported in the literature are also found there. Besides that, the chemical differences between sidestream smoke emissions directly after a mainstream puff and between two succeeding mainstream puffs were investigated. The composition of both could be related to the burning temperature inside the tobacco rod and to previous pyrolysis experiments. Hereby, the smoke emitted after a mainstream puff is drawn shows similarities to typical mainstream smoke composition. Furthermore, it could be demonstrated that the emissions have a distinguished puff behaviour which also is related to mainstream smoke in case of the post-puff emissions. As already shown, the use of different puff parameters has a vast influence on the chemical composition of mainstream smoke. Therefore, especially considering the role of sidestream smoke and environmental tobacco smoke (ETS) and its possible health effects on second-hand smokers, a further analysis of sidestream composition changes with different smoking behaviour will be of interest.

It could be demonstrated that the use of high resolution techniques, such as two dimensional comprehensive gas chromatography, enables the characterisation of complex matrices such as tobacco smoke. The investigation of TPM collected on a puff-

by-puff basis clearly shows that changes within the matrix, previously observed with online-methods in the analysis of vapour phase components, can also be observed in the particulate matter. This is especially valid for alkenes/cycloalkanes, which show a comparable first-puff behaviour. The use and development of further classification and selection rules, optimised for tobacco ingredients, may lead to an efficient characterisation of tobacco smoke or plant material by means of sum parameters.

7 Conclusion and Outlook

Appendices

A Sidestream/mainstream (SS/MS) yield ratios

Substance	MS yield	SS/MS
Small molecules		
Carbonyl sulphide	18–42 μg	0.03–0.1
HCN	160–500 μg	0.06–0.5
CO	10–23 mg	2.5–4.7
Hydrazine	20–40 μg	3
Methane	600–1000 μg	3.1–4.8
Acetylene	20–40 μg	0.8–2.5
Nitrogen oxides	100–600 μg	4–13
CO_2	20–50 mg	8–11
H_2O (gas phase)	3–14 mg	24–30
NH_3	50–130 μg	40–170
N_2 (generated)	< 10 μg	> 270
Neutral heteroatom organics		
Acetonitrile	160–210 μg	3–5
Benzonitrile	5–6 μg	7–10
Acetamide	70–100 μg	0.8–1.7
Methyl chloride	150–600 μg	1.7–3.3
Aldehydes, ketones, alcohols		
Acetaldehyde	0.5–1.2 mg	1.4
Propionaldehyde	175–250 μg	2.4–2.8
Acetone	100–250 μg	2–5
Acroleine	60–100 μg	8–15
2-Butanone	≈ 30 μg	2.9–4.3
2-Furaldehyde	15–43 μg	4.9–7.4
Furfuryl alcohol	18–65 μg	3.0–4.8
Cyclotene	3–5 μg	6–10
Pyranone	13–150 μg	0.1–1.2
Phytosterols		
β-Sitosterol	59 μg	0.5
Campesterol	43 μg	0.6

Table A.1 (continued on next page...)

Table A.1 – continued

Substance	MS yield	SS/MS
Cholesterol	22 μg	0.9
Phenols		
Phenol	60–140 μg	1.6–3.0
Cresols (*o*-, *m*-, *p*-)	11–37 μg	1.0–1.4
Catechol	100–360 μg	0.6–0.9
Hydrochinone	110–300 μg	0.7–1.0
Acids		
Formic acid	210–490 μg	1.4–1.6
Acetic acid	270–810 μg	1.9–3.9
3-Methylvaleric acid	20–60 μg	0.8–1.5
Lactic acid	60–170 μg	0.5–0.7
Benzoic acid	14–28 μg	0.7–1.0
Phenylacetic acid	11–38 μg	0.6–0.8
Succinic acid	70–140 μg	0.4–0.6
Gylcolic acid	40–130 μg	0.6–1.0
Amines, pyridines, alkaloids		
Methylamine	12–29 μg	4.2–6.4
n-Propylamine	1.6–3.4 μg	2.8–3.8
n-Butylamine	0.5–1.5 μg	2.2–4.0
Aniline	360 ng	30
Pyridine	16–46 μg	6.5–20
3-Ethenylpyridine	11–30 μg	6.5–20
Methylpyrazine	2-5 μg	3–4
Pyrrole	16–23 μg	9-14
Nicotine	0.8–2.3 mg	2.6–3.3
Myosmine	13–33 μg	4.0–7.5
Nicotyrine	4–40 μg	5–14
Anatabine	2–20 μg	0.1–0.5
2,3'-Bipyridyl	16–22 μg	2–3
Aza-arenes		
Quinoline	0.5–2.0 μg	8–11
Isoquinoline	1.6–2.0 μg	2.5–5
Benzo[*h*]quinoline	10 ng	10
Indole	16–38 μg	2.1–3.4
Hydrocarbons		
Isoprene	330–1100 μg	13–19
Benzene	36–68 μg	5–10
Toluene	100-200 μg	6–8
Limonene	15–50 μg	4–12

Table A.1 (continued on next page...)

Substance	MS yield	SS/MS
Neophytadiene	66–230 μg	1–2
Polynuclear aromatic hydrocarbons		
Naphthalene	2.6 μg	17
Pyrene	45–140 ng	2–11
Benzo[*a*]pyrene	9–40 ng	2–20
Anthracene	24 ng	30
Phenanthrene	77 ng	2–30
Fluoranthene	60–150 ng	11
Nitrosamines		
N-nitrosodimethylamine	10–40 ng	10–50
N-nitrosodiethylamine	nd–25 ng	3–35
N-nitrosopyrrolidine	6–30 ng	6–30
N-nitrosodiethanolamine	0–70 ng	1.2
N'-nitrosonornicotine	0.2–3 μg	0.5–3
NNK	0.1–1 μg	1–4
N'-nitrosoanatabine	0.3–5 μg	0.3–1
Inorganic constituents		
Cadmium	100 ng	4–7
Nickel	20–80 ng	0.2–30
Zinc	60 ng	0.2–7

Table A.1: Some typical sidestream/mainstream yield ratios for plain cigarettes [40]

A Sidestream/mainstream (SS/MS) yield ratios

B Mass assignment

m/z	compound	Smoke	Leaf	IP	aromatic	refs.
16	Methane	+	-	12.61 eV	-	[40, 157]
17	NH_3	+	+	10.070 eV	-	[8, 149]
26	Acetylene	+	-	11.4 eV	-	[8]
27	Hydrogencyanide	+	-	13.6 eV	-	[8, 86, 157]
30	NO	+	+	9.2642 eV	-	[86, 150]
31	Methylamine	+	+	8.9 eV	-	[8]
32	Methanol	+	+	10.84 eV	-	[8]
32	Hydrazine	+	-	8.1 eV	-	[8]
34	H_2S	+	-	10.457 eV	-	[8, 149]
40	Propyne	+	-	10.36 eV	-	[8]
41	Acetonitrile	+	-	12.2 eV	-	[8]
42	Propene	+	-	9.73 eV	-	[8, 86]
42	Ketene			9.617 eV	-	
43	Carbohydrate fragment: $C_3H_7^+$, $C_2H_3O^+$			n. a.	-	[86, 149, 225]
44	Acetaldehyde	+	+	10.229 eV	-	[4, 8, 158]
45	Ethylamine	+	+	9.5 eV	-	[8]
45	Dimethylamines	+	-	eV	-	[8]
46	Ethylalcohol	+	+	10.48 eV	-	[8]
46	Nitrogendioxide	+		9.586 eV	-	
46	Formic acid	+	+	11.05 eV	-	[8, 9]
48	Methylsulfide	+	-	9.439 eV	-	[8, 149]
50	Methylchloride	+	-	11.26 eV	-	[8]
52	1-Buten-3-yne	+	-	9.58 eV	-	[8]
54	1,3-Butadiene	+	-	9.072 eV	-	[8]
54	1-Butyne	+	-	10.18 eV	-	[8]
54	2-Butyne	+	-	9.58 eV	-	[8]
56	2-Propenal	+	+	10.11 eV	-	[4, 8, 146]
56	1-Butene	+	-	9.55 eV	-	[8, 86]

Table B.1 (continued on next page. . .)

163

m/z	compound	Smoke	Leaf	IP	aromatic	refs
56	2-Butene	+	-	9.13 eV	-	[8, 86]
56	2-Methylpropene	+	-	9.22 eV	-	[8]
57	carbohydrate fragment	+	-	eV		[8, 149]
57	2-Propen-1-amine	+	-	8.76–9.4 eV	-	[8]
58	Acetone	+	+	9.703 eV	-	[4, 8, 158]
58	Propanal	+	+	9.69 eV	-	[8]
59	Trimethylamine	+	+	7.85 eV	-	[8, 40]
59	Propylamine	+	-	8.5 eV	-	[8, 40]
59	Acetamide	+	-	9.69 eV	-	[8, 40]
59	Isopropylamine	+	-	8.6–8.86 eV	-	- [8, 40]
60	Propylalcohol	+	-	10.22 eV	-	[8]
60	Carbonyl sulphide	+	-	11.18 eV	-	[40]
60	Acetic acid	+	+	10.65 eV	-	[8, 9, 12, 151]
62	Ethylenglycol	+	-	10.16–10.55 eV	-	[8]
66	Cyclopentadiene	+	-	8.57 eV	-	[4, 8, 86]
67	Pyrrole	+	-	8.2 eV	+	[4,8,86,146,159]
68	Furan	+	-	8.88 eV	+	[4, 8, 86, 158]
68	Isoprene	+	-	8.86 eV	-	[4, 8, 86, 158]
68	1,3-Pentadiene	+	-	8.6 eV	-	[8, 158]
68	Cyclopentene	+	-	9.01 eV	-	[8]
69	Pyrroline	+	-	8.0–8.61 eV	-	[4, 8, 86, 149]
70	2-Butenal	+	-	9.72 eV	-	[8]
70	Methyl vinyl ketone			9.65 eV	-	[8]
70	Methylbutene	+	-	8.69 eV	-	[8]
70	1-Pentene	+	-	9.49 eV	-	[4, 8]
70	2-Pentene	+	-	9.01 eV	-	[8]
70	2-Methyl-2-propenal	+	-	9.92 eV	-	[8]
70	Butenone	+	-	9.65 eV	-	[158]
71	Pyrrolidine	+	+	8.41–8.82 eV	-	[8]
72	2-Methylpropanal	+	+	9.71 eV	-	[8]
72	2-Butanone	+	+	9.52 eV	-	[4, 8]
72	Butanal	+	+	9.82 eV	-	[8]
72	Tetrahydrofuran	+	-	9.4 eV	-	
73	Isobutylamine	+	+	8.5–8.7 eV	-	[8]
73	Butylamine	+	-	8.73 eV	-	[8]
74	Propionic acid	+	+	10.44 eV	-	[8, 9, 12, 40]
74	Butylalcohol	+	-	9.99 eV	-	[8, 40]

Table B.1 (continued on next page. . .)

m/z	compound	Smoke	Leaf	IP	aromatic	refs
	Table B.1 – continued					
74	Isobutylalcohol	+	-	10.02 eV	-	[8, 40]
74	Hydroxyaceton	-	+	10.0 eV	-	[12]
75	Glycine	+	+	8.8–9.3 eV	-	[8]
76	Glycolic acid	+	+	n. a.	-	[8, 40]
76	Propylenglycol	+	+	n. a.	-	[8, 40]
78	Benzene	+	-	9.24 eV	+	[4,8,86,158,159]
79	Pyridine	+	+	9.26 eV	+	[4,8,12,157,159]
80	Pyrazine	+	+	9.0–9.63 eV	+	[8, 9]
81	1-Methylpyrrole	+	-	7.99 eV	+	[8, 86, 149]
82	2-Methylfuran	+	-	8.38 eV	+	[4, 8, 158]
82	Methylcyclopentene	+	-	8.54–9.12 eV	-	[8]
82	Dimethylbutenes	+	-	9.44–9.62 eV	-	[8]
82	Hexene	+	-	9.44 eV	-	[8]
82	Cyclohexene	+	-	8.95 eV	-	[8]
82	2-Cyclopenten-1-one	+	-	8.47–9.35 eV	-	[146]
84	Nicotine fragment	+	-	n. a.	-	[4, 8, 86]
84	Cyclopentanone	+	-	9.26 eV	-	[8]
84	3-Methyl-3-buten-2-one	+	-	9.5 eV	-	[8]
84	Methylbutenal	+	-	9.58–9.72 eV	-	[8]
85	2-Methylpyrrolidine			n. a.	-	
85	Piperidine	+	+	8.03 eV	-	[8]
85	2-Pyrrolidone	+	-	9.2–9.53 eV	-	[149]
86	Methylbutanal	+	-	9.55–9.72 eV	-	[8]
86	3-Methyl-2-butanone			9.31 eV	-	[8]
86	Pentanones			9.31–9.38 eV	-	[8]
86	2,3-Butanedione			9.3–9.72 eV	-	[8]
86	Crotonic acid	-	+	9.9 eV	-	[8, 12]
87	Isoamylamine	+	+	n. a.	-	[8]
88	Butyric acid	+	+	10.17 eV	-	[8]
88	Pyruvic acid	+	+	9.3–9.42 eV	-	[8, 12]
88	2-Methyl-1-butanol	-	+	9.86 eV	-	[9]
88	3-Methyl-1-butanol	-	+	n. a.	-	[9]
88	Pentanol	-	+	10.0–10.42 eV	-	[9]
88	2-Methyl-propanic acid	-	+	10.24 eV	-	[12]
89	Alanines			8.88 eV	-	[8]
90	Lactic acid	+	+	n. a.	-	[8, 40]
92	Toluene	+	-	8.828 eV	+	[4, 8, 86, 149]

Table B.1 (continued on next page...)

m/z	compound	Smoke	Leaf	IP	aromatic	refs
92	Glycerol	+	+	n. a.	-	[8]
93	Aniline	+	-	7.720 eV	+	[4, 8, 151, 157]
93	Methylpyridines			9.0–9.55 eV	+	[8, 146, 159]
94	Phenol	+	+	8.49 eV	+	[4, 8, 9, 12, 146, 149, 151, 163]
94	2-Vinylfuran			n. a.	+	[4, 8, 163]
94	Methylpyrazine	+	+	n. a.	+	[9, 12, 146, 163]
95	Pyridinol	+	-	8.62–9.89 eV	+	[149]
95	Ethylpyrrol	+	-	7.97 eV	+	[86]
95	Dimethylpyrroles	+	-	7.54–7.69 eV	+	[86]
95	Formylpyrrole	-	+	8.93 eV	+	[9]
96	Dimethylfurans	+	-	7.8–8.25 eV	+	[4,8,86,146,151, 158]
96	Furfural	+	+	9.22 eV	+	[4, 8, 9, 12, 86, 146, 158]
97	Maleimide	-	+	n. a.	-	[12]
98	Furanmethanols	+	+	n. a.	+	[4, 9, 12, 146]
98	2-Methyl-2-pentenal			9.54 eV	-	[4]
98	5-Methyl-2(5H)-furanone	+	+	10.12 eV	-	[4, 12]
98	3-Methyl-2(5H)-furanone	+	+	9.62 eV	-	[4, 12]
99	Succinimide	-	+	10.01 eV	-	[12]
100	Tiglic acid	-	+	n. a.	-	[9]
100	3-Hexen-1-ol	-	+	n. a.	-	[12]
102	Valeric acid	+	+	10.53 eV	-	[8, 9, 12, 149]
102	Methylpentanoles	-	+		-	[8]
102	Methyl-butanoic acids	-	+	10.51 eV	-	[12]
102	Tetrahydro-2-furanmethanol	-	+	n. a.	-	[12]
102	Phenylacetylene	+	-	8.82 eV	+	[4]
103	Benzonitrile	+	-	9.73 eV	+	[4, 8, 146, 159]
103	α-Aminobutyric acid	+	+	8.7 eV	-	[8, 9]
103	γ-Aminobutyric acid	+	-	8.7 eV	-	[8, 9]
104	Styrene	+	-	8.464 eV	+	[4,8,86,159,163]
104	3-Pyridinecarbonitrile	+	+	10.1–10-4 eV	+	[8, 9, 159, 163]
105	Vinylpyridine	+	-	8.92 eV	+	[4,8,86,149,157, 163]
105	Serine	+	+	n. a.	-	[8, 163]
106	Xylenes	+	-	8.44–8.56 eV	+	[4, 8, 146]

Table B.1 (continued on next page. . .)

m/z	compound	Smoke	Leaf	IP	aromatic	refs
				Table B.1 – continued		
106	Ethylbenzene	+	+	8.77 eV	+	[8, 12, 146]
106	Benzaldehyde	+	-	9.5 eV	+	[8, 9, 12, 226]
106	Diethylenglycol			n. a.	-	[8]
107	Dimethylpyridines	+	+	8.8–9.25 eV	+	[8, 12]
107	Dimethylanilines	+	-	7.2–7.87 eV	+	[8]
107	Ethylanilines	+	-	7.6 eV	+	[8]
107	Formylpyridine	+	+	n. a.	+	[8, 9]
107	Ethylpyridine	+	-	n. a.	+	[149, 157]
108	Anisole			8.2 eV	+	[8, 163, 226]
108	Dimethylpyrazines	+	+	8.8 eV	+	[8, 9, 12, 163]
108	Methyl-phenols	+	+	8.29 eV	+	[4, 8, 9, 12, 146, 149, 163]
108	Benzylalcohol	+	+	8.26–9.53 eV	+	[8, 9, 12, 163]
109	Acetylpyrrole	-	+	8.72 eV	+	[9, 12]
109	2-Formyl-1-Methyl-Pyrrole	-	+	n. a.	+	[9]
109	Methoxypyridine	+	-	8.7–9.58 eV	+	[149]
110	Catechol	+	+	8.15–8.56 eV	+	[8, 149, 163]
110	Hydroquinone	+	-	7.94 eV	+	[8, 149, 163]
110	2-Acetylfuran	-	+	9.02–9.27 eV	+	[9, 12]
110	Methylfurfural	+	+	n. a.	+	[4, 8, 9, 149, 163]
110	2,4-Heptadienal	-	+	n. a.	-	[9, 12]
110	Acetylimidazole	-	+	9.38 eV	+	[9]
112	Acetylcylopentane			n. a.	-	[8, 40]
112	2-Hydroxy-3-methyl-2-cyclopenten-1-one	+	+	n. a.		[8, 12, 40, 149, 157]
112	Furoic acid	+	+	9.16–9.32 eV	+	[8, 12, 40]
112	1-Hexanol	-	+	9.89–10.35 eV	-	[9]
114	Hexenoic acid	-	+	n. a.	-	[9]
114	2-Heptanone	-	+	9.27 eV	-	[12]
114	4-Hydroxy-5,6-dihydro-2H-pyran-2-one	+	-	n. a.	-	[149]
113	N-Methylsuccinimide	-	+	10.71 eV	-	[12]
113	2-Methylsuccinimide	-	+	n. a.	-	[12]
115	Proline	+	+	8.3–9.36 eV	-	[8]
115	N-(3-Methylbutyl)-formamide	-	+	n. a.	-	[9]
116	Caproic acid	+	+	10.12 eV	-	[8, 9, 12]
116	3-Methylvaleric acid	+	+	n. a.	-	[8, 12]

Table B.1 (continued on next page. . .)

m/z	compound	Smoke	Leaf	IP	aromatic	refs
						Table B.1 – continued
116	Fumaric acid	-	+	10.7–10.9 eV	-	[8]
116	3-Oxopentanoic acid	-	+	n. a.	-	[12]
116	1-Heptanol	-	+	9.84–10.4	-	[12]
116	Methyl isovalerate	-	+	n. a.	-	[12]
116	Indene	+	-	8.14 eV	+	[4, 8, 86]
117	Indole	+	+	7.76 eV	+	[8, 9, 12, 86, 146, 149, 159]
117	Valine	+	+	8.71 eV	-	[8]
117	Betaine	-	+	n. a.	-	[8]
118	Indane	+	-	8.45-9.5 eV	+	[4, 40, 86]
118	Methylstyrenes	+	-	8.2–8.53 eV	+	[4, 8, 40, 86]
118	Benzofuran	+	-	8.36 eV	+	[4, 40]
118	Succinic acid	+	+	n. a.	-	[8, 40]
118	2-Methyl-Pentane-2,4-diol	-	+	n. a.	-	[9]
119	Homoserine	-	+	n. a.	-	[8]
119	3-(1-Propenyl)-pyridine	-	+	n. a.	+	[9, 12]
120	Methylethylbenzene	+	-	n. a.	+	[8, 146]
120	Trimethylbenzenes	+	-	8.0–8.42 eV	+	[4, 8, 146]
120	Phenylacetaldehyde	-	+	8.8–9.3 eV	+	[9]
120	o-Methylbenzaldehyde	-	+	n. a.	+	[9]
120	p-Vinylphenol	+	+	n. a.	+	[9, 12, 149]
120	Isopropenylpyrazine	-	+	n. a.	+	[9]
120	2-Vinyl-6-methyl-pyrazine	-	+	n. a.	+	[9]
120	α, β-Epoxy-styrene	-	+	9.04–9.23 eV	+	[9]
120	Acetophenone	-	+	9.28 eV	+	[9, 12]
121	2-Phenylethylamine	+	+	8.5–8.99 eV	+	[8]
121	Cysteine	-	+	n. a.	-	[8]
121	Acetylpyridine	+	+	8.9–9.35 eV	-	[9, 12, 86, 149]
121	Ethyl-Methyl-Pyridine	+	-	n. a.	+	[86, 149]
121	Dimethylaniline	+	-	7.33–7.78 eV	+	[151]
122	Benzoic acid	+	+	9.3–9.8 eV	+	[4, 8, 9, 12, 40, 163]
122	Ethylphenols	+	+	7.84 eV	+	[8, 12, 40, 146, 149, 163]
122	Hydroxybenzaldehydes			9.32 eV	+	[4, 8, 9, 40, 163]
122	Trimethylpyrazine	+	+	n. a.	+	[9, 12, 163]
122	Methyl-ethyl-pyrazines	+	+	n. a.	+	[9, 163]

Table B.1 (continued on next page...)

m/z	compound	Smoke	Leaf	IP	aromatic	refs
						Table B.1 – continued

m/z	compound	Smoke	Leaf	IP	aromatic	refs
122	α-Phenethylalcohol	-	+	n. a.	+	[9]
122	β-Phenethylalcohol	+	+	n. a.	+	[8, 9, 40, 163]
122	Acetylpyrazine	-	+	n. a.	+	[9]
123	Acetyl-methyl-pyrroles	-	+	n. a.	+	[9, 12]
124	Methyl-hydrochinone	+	-	n. a.	+	[4, 8]
124	Methyl-catecholes	+	-	n. a.	+	[4, 8]
124	Guaiacol	+	+	n. a.	+	[4, 8, 9, 12, 149, 151]
124	Dihydroxymethylbenzene	+	-	n. a.	+	[149]
124	2-Acetyl-5-methylfuran	-	+	n. a.	+	[9, 12]
125	Taurine	-	+	n. a.	-	[8]
125	Dimethylmaleimide	-	+	n. a.	-	[12]
126	Dimethylmaleic anhydride	-	+	n. a.	-	[9, 12]
126	Formyl-Methyl-Thiophenes	-	+	n. a.	+	[9]
126	Acetyl-Thiophenes	-	+	9.2 eV	+	[9]
126	Maltol	-	+	n. a.	-	[12]
126	5-Hydroxymethylfurfural	+	-	n. a.	+	[8, 86, 149]
128	Naphthalene	+	+	8.144 eV	+	[4,9,86,146,149]
128	2-Heptenoic acid	-	+	n. a.	-	[9]
128	5-Methylhex-2-enoic acid	-	+	n. a.	-	[9, 12]
128	6-Methylhept-5-en-2-ol	-	+	n. a.	-	[9]
128	1-Octen-3-ol	-	+	n. a.	-	[9]
129	Quinoline	+	+	8.62 eV	+	[4, 8, 9, 12, 159, 163]
129	Isoquinoline	+	-	8.53 eV	+	[4, 8, 159, 163]
129	Pipecolic acid	-	+	n. a.	-	[8]
129	Pyrrolidin-2-acetic acid	-	+	n. a.	-	[8]
129	N-(3-Methylbutyl)-acetamide	-	+	n. a.	-	[9]
130	Methylindenes	+	-	7.97–8.27 eV	+	[4]
130	Methylhexanoic acids	-	+	n. a.	-	[9, 12]
130	Octanoles	-	+	n. a.	-	[9, 12]
130	Heptanoic acid	+	+	n. a.	-	[8, 9, 12]
130	Ethyl isovalerate	-	+	n. a.	-	[12]
131	3-Methyl-1H-indole	+	-	7.514 eV	+	[8, 146, 149, 163]
131	Hydroxyproline	-	+	9.1 eV	-	[8]
131	Isoleucine	-	+	8.66–9.5 eV	-	[8]
131	Norleucine	-	+	8.52–9.09 eV	-	[8]

Table B.1 (continued on next page. . .)

		Smoke	Leaf		aromatic	
m/z	compound			IP		refs
132	Methylbenzofuran	+	-	n. a.	+	[8, 163]
132	1-Indanone	+	-	9.13 eV	+	[8, 163]
132	Ornithine	+	+	n. a.	-	[8, 163]
132	Asparagine	-	+	n. a.	-	[8]
132	Cinnamaldehyde	-	+	n. a.	+	[9, 12]
133	Aspartic acid	+	+	n. a.	-	[8]
134	p-Isopropyltoluene	+	-	8.29 eV	+	[8]
134	Maleic acid	-	+	n. a.	-	[8]
135	Trimethylaniline	+	-	7.15–7.24 eV	+	[8]
135	3-Propionylpyridine	-	+	n. a.	+	[9]
135	5-Isoproyl-2-methyl-pyridine	-	+	n. a.	+	[9]
135	Benzothiazole	-	+	8.65–8.85 eV	+	[9]
135	2,3-Dimethyl-5-ethylpyridine	-	+	n. a.	+	[12]
136	Limonene	+	-	8.3 eV	-	[4, 8, 40, 86, 146, 163]
136	p-Methoxybenzaldehyde	+	+	8.43–8.87 eV	+	[8, 40, 163, 226]
136	2-Ethyl-5-methylphenol	+	+	n. a.	+	[8, 12, 40, 146, 163]
136	Dimethyl-ethyl-pyrazine	+	+	n. a.	+	[9, 163]
136	Tetramethylpyrazine	+	+	8.6 eV	+	[12, 163]
136	Phenylacetic acid	+	+	8.26 eV	+	[8, 12, 40, 163]
136	1-(p-Tolyl)-ethanol	-	+	n. a.	+	[9]
136	2-Acetyl-methyl-pyrazines	-	+	n. a.	+	[9]
136	Trimethylphenols	+	+	8.0 eV	+	[8, 12]
136	m-Toluic acid	-	+	9.2–9.4 eV	+	[12]
136	Myrcene	-	+	n. a.	-	[12]
136	α-Terpinene	-	+	n. a.	-	[12]
137	p-Tyramine	-	+	8.41 eV	+	[8]
138	5-Acetyl-2-furaldehyd	-	+	n. a.	+	[9]
138	Salicyclic Acid	-	+	n. a.	+	[12]
138	Isophorone	-	+	9.07 eV	-	[12]
139	Ethyl-methylmaleimides	-	+	n. a.	-	[9, 12]
139	2-Propyl-maleimide	-	+	n. a.	-	[12]
139	2-Ethylidene-3-methyl-succinimide	-	+	n. a.	-	[12]
140	Ethylmethylmaleic anhydride	-	+	n. a.	-	[9]
142	Methylnaphthalenes	+	-	n. a.	+	[4,8,86,149,227]

Table B.1 (continued on next page. . .)

m/z	compound	Smoke	Leaf	IP	aromatic	refs
						Table B.1 – continued

m/z	compound	Smoke	Leaf	IP	aromatic	refs
142	2-Octenoic acid	-	+	n. a.	-	[12]
142	5-Hydroxymaltol	-	+	n. a.	-	[12]
143	Methylquinolines	+	+	n. a.	+	[9, 163]
144	5-Quinolineamine	+	-	n. a.	+	[40]
144	Pyranone	+	-	n. a.	-	[40, 146, 149]
144	Dimethylmaleic/fumaric acid	-	+	n. a.	-	[9]
144	Octanoic acid	+	+	n. a.	-	[8, 9, 12]
144	Phenylfuran	-	+	n. a.	+	[9]
144	Ethyl caproate	-	+	n. a.	-	[12]
145	2-(4-Pyridyl)furan	+	-	n. a.	+	[8]
145	2,3-Dimethyl-1H-indole	+	-	n. a.	+	[8]
145	3-Ethylindole	+	-	n. a.	+	[8]
146	Myosmine	+	+	n. a.	+	[8, 12, 146, 149]
146	Glutamine	+	+	n. a.	-	[8]
146	Lysine	-	+	8.6–9.5 eV	-	[8]
146	2,3-Octanediol	-	+	n. a.	-	[9]
146	α-Phenylcrotonaldehyde	-	+	n. a.	-	[9]
147	Glutamic acid	+	+	n. a.	-	[8]
148	p-Isopropylbenzaldehyde	-	+	n. a.	+	[9]
148	Cinnamic acid	-	+	9.0 eV	+	[12]
148	Phthalic anhydride	-	+	10.1–10.25 eV	+	[12]
149	Methionine	-	+	8.3–9.0 eV	-	[8]
150	Vinylguaiacol	+	+	n. a.	+	[9, 12, 12, 149]
150	Thymol	+	-	n. a.	+	[8]
150	Triethylenglycol	+	+	n. a.	-	[8]
150	p-Allylcatechol	-	+	n. a.	+	[8]
150	Guanine	-	+	7.85–8.25 eV	-	[8]
150	o-Acetyl-p-Cresol	-	+	n. a.	+	[9]
150	Carvone	-	+	n. a.	-	[12]
152	Vanillin	+	+	n. a.	+	[8, 12, 226]
152	β-Cyclocitral	-	+	n. a.	-	[9, 12]
152	Methylsalicylate	-	+	7.65 eV	+	[9, 12]
152	o-Anisic acid	-	+	n. a.	+	[12]
152	Camphor	-	+	8.76 eV	-	[12]
152	3-Methoxy-2-hydroxybenzaldehyde	+	-	n. a.	+	[149]
152	4-Ethyl-2-methoxyphenol	+	-	n. a.	+	[149]

Table B.1 (continued on next page. . .)

m/z	compound	Smoke	Leaf	IP	aromatic	refs
152	Acenaphthylene	+	-	8.12 eV	+	[157]
154	1-Linalool	-	+	n. a.	-	[8, 9, 9, 12]
154	α-Terpineol	-	+	n. a.	-	[9, 12]
154	Geraniol	-	+	n. a.	-	[9, 12]
154	2,6-Nonadienoic acid	-	+	n. a.	-	[12]
154	1,8-Cineol	-	+	n. a.	-	[12]
154	Dimethoxyphenol	+	-	n. a.	+	[4, 8]
155	Phenylpyridine	+	+	n. a.	+	[9, 149, 163]
155	Histidine	-	+	n. a.	-	[8]
156	2,3'-Bipyridine	+	+	n. a.	+	[4,8,12,149,151, 163]
156	Dimethylnaphthalenes	+	-	7.89–8.2 eV	+	[8, 163]
156	Menthol	+	+	n. a.	-	[8, 12, 163]
156	Decanal	-	+	n. a.	-	[9, 12]
157	Dimethylchinolines	+	-	n. a.	+	[163]
158	Nicotyrine	+	+	n. a.	+	[8, 9, 146]
158	Ethylmethyl-maleic/-fumaric acid	-	+	n. a.	-	[9]
158	Nonanoic acid	+	+	n. a.	-	[8, 9, 12]
158	1,3,3-Trimethylcyclo-hexan-1,2-diol	-	+	n. a.	-	[9]
159	Leucine	+	+	8.51 eV	-	[8]
160	2-Methyl-5-(furyl-2')-pyrazine	+	-	n. a.	+	[163]
161	Aminoadipic acid	-	+	n. a	-	[8]
162	Nicotine	+	+	n. a	+	[4,8,12,146,149, 151]
162	Anabasine	+	+	n. a	+	[8, 146]
162	5-Isopropenyl-2-methyl-anisole	-	+	n. a.	+	[9]
164	p-Allylguaiacol	+	+	n. a.	+	[8]
164	Ethyl-phenylacetate	-	+	n. a.	+	[12]
165	Phenylalanine	+	+	n. a	+	[8]
165	1-(3-Methylbutyl)-2-formyl-pyrrole	-	+	n. a.	+	[9]
168	Vanillic acid	+	+	n. a	+	[8, 12]
168	Trimethoxybenzenes	-	+	7.5–8.2 eV	+	[8]
168	4,8-Dimethyl-nona-3,7-dien-1-ol	-	+	n. a.	-	[9]

Table B.1 – continued

Table B.1 (continued on next page. . .)

m/z	compound	Smoke	Leaf	IP	aromatic	refs
Table B.1 – continued
168	Geranic acid	-	+	n. a.	-	[12]
169	Cysteic acid	-	+	n. a	+	[8]
170	Linalool oxide	-	+	n. a	-	[9, 12]
172	3,5-Dimethyl-1-phenylpyrazole	+	-	n. a	+	[228]
172	Decanoic acid	+	+	n. a.	-	[8, 12]
172	Oxononanoic acid	-	+	n. a.	-	[12]
172	1,2-Dihydro-2,5,8-trimethyl-naphthalene	-	+	n. a.	+	[12]
172	Ethyl carpylate	-	+	n. a.	-	[12]
172	Methyl pelargonate	-	+	n. a.	-	[12]
174	Ionene	+	-	n. a	+	[8]
174	Arginine	-	+	n. a	-	[8]
175	Citrulline	-	+	n. a	-	[8]
178	Anthracene	+	-	7.439 eV	+	[8, 157]
178	Phenanthrene	+	-	7.891 eV	+	[8]
178	Esculetin	+	+	n. a	+	[8]
178	2,6,6-Trimethyl-4-oxo-cyclohex-2-enylidene-acetaldehyd	-	+	n. a.	-	[9]
180	Caffeic acid	+	-	n. a.	+	[8]
180	Inositol	-	+	n. a.	-	[8]
181	Methioninesulfone	-	+	n. a.	-	[8]
181	Tyrosine	-	+	8.0–8.5 eV	+	[8]
186	Undecanoic acid	-	+	n. a.	-	[12]
186	Ethyl pelargonate	-	+	n. a.	-	[12]
188	Azelaic acid	-	+	n. a.	-	[8]
190	Damascenone	-	+	n. a.	-	[12]
192	Scopoletin	+	+	n. a.	+	[8, 11, 12]
192	Citric acid	-	+	n. a.	-	[8]
192	Citrylideneaceton	-	+	n. a.	-	[12]
192	β-Damascone	-	+	n. a.	-	[12]
192	α-/β-Ionone	-	+	n. a.	-	[12]
194	Ferulic acid	+	+	n. a.	+	[8]
194	Nerylacetone	-	+	n. a.	-	[12]
194	Geranylacetone	-	+	n. a.	-	[12]
196	Solanol	-	+	n. a.	-	[9, 12]
196	Terpinyl acetate	-	+	n. a.	-	[12]
198	Tridecanal	-	+	n. a.	-	[9]

Table B.1 (continued on next page. . .)

m/z	compound	Smoke	Leaf	IP	aromatic	refs
	Table B.1 – continued					
198	Tetrahydrogeranylaceton	-	+	n. a.	-	[12]
200	6,10-Dimethyl-undecan-2-ol	-	+	n. a.	-	[9]
200	Ethyl-Caprate	-	+	n. a.	-	[12]
202	Fluoranthene	+	-	7.9 eV	+	[8, 157]
202	Pyrene	+	-	7.426 eV	+	[8, 157]
202	Tryptophane	-	+	8.43 eV	+	[8]
208	9,10-Anthraquinone	-	+	9.25 eV	+	[8]
208	3,4-Dimethoxy-cinnamic acid	-	+	n. a.	+	[12]
208	4-Oxo-α-Ionol	-	+	n. a.	-	[12]
208	4-Hydroxydamascone	-	+	n. a.	-	[12]
214	Methyl-Laurate	-	+	n. a.	-	[12]
216	11-H-Benzo[a]fluorene	+	-	n. a.	+	[157]
216	11-H-Benzo[b]fluorene	+	-	n. a.	+	[157]
226	Pentadecanal	-	+	n. a.	-	[9]
226	Benzo[ghi]fluoranthene	+	-	n. a.	+	[157]
228	Myristic acid	+	+	n. a.	-	[8, 12]
228	Ethyl-Laurate	-	+	n. a.	-	[12]
230	Methyl-11-H-Benzo[a]fluorene	+	-	n. a.	+	[157]
240	Cystine	-	+	n. a.	-	[8]
242	Pentadecanoic acid	-	+	n. a.	-	[8]
242	12-Methyl-tetradecanoic acid	-	+	n. a.	-	[12]
242	Methyl-chrysenes	+	-	7.4 eV	+	[157]
252	Benz[a]pyrene	+	-	7.12 eV	+	[8, 157]
252	Benzo[k]fluoranthene	+	-	n. a.	+	[157]
252	Perylene	+	-	6.960 eV	+	[157]
256	Palmitic acid	+	+	n. a.	-	[8, 12, 149]
256	Ethyl myristate	-	+	n. a.	-	[12]
256	1-Heptadecanol	+	+	n. a.	-	[8]
256	Dimethyl-chrysenes	+	-	n. a.	+	[157]
262	Farnesylacetone	-	+	n. a.	-	[12]
268	Homocystine	-	+	n. a.	-	[8]
262	Phytone	-	+	n. a.	-	[12]
270	1-Octadecanol	+	+	n. a.	-	[8]
270	Heptadecanoic acid	-	+	n. a.	-	[12]
270	Methyl palmitate	-	+	n. a.	-	[12]
276	Benzo[ghi]perylene	+	-	7.17 eV	+	[157]
276	Anthanthrene	+	-	6.84–7.11 eV	+	[157]

Table B.1 (continued on next page. . .)

m/z	compound	Smoke	Leaf	IP	aromatic	refs
	Table B.1 – continued					
278	Neophytadiene	+	+	n. a.	-	[8,9,12,146,151]
278	Linolenic acid	+	+	n. a.	-	[8, 12]
280	Linoleic acid	+	+	n. a.	-	[8, 12]
282	Oleic acid	+	+	n. a.	-	[8, 12]
284	1-Nonadecanol	+	+	n. a.	-	[8]
284	Octadecanoic acid	-	+	n. a.	-	[12]
284	Ethyl palmitate	-	+	n. a.	-	[12]
284	Methyl heptadecanoat	-	+	n. a.	-	[12]
284	Methyl-15-methylhexadeca-noate	-	+	n. a.	-	[12]
294	Methyl linoleate	-	+	n. a.	-	[12]
296	Phytoles	-	+	n. a.	-	[12]
298	1-Eicosanol	+	+	n. a.	-	[8, 12]
298	Nonadecanoic Acid	-	+	n. a.	-	[12]
298	Methyl isostearate	-	+	n. a.	-	[12]
298	Methyl stearate	-	+	n. a.	-	[12]
310	Ethyl oleate	-	+	n. a.	-	[12]
312	1-Heneicosanol	+	+	n. a.	-	[8]
312	Eicosanoic acic	-	+	n. a.	-	[12]
312	Ethyl stearate	-	+	n. a.	-	[12]
326	1-Docosanol	+	+	n. a.	-	[8, 12]
340	1-Tricoscanol	+	+	n. a	-	[8]
354	1-Tetracosanol	+	-	n. a	-	[8]
386	Cholesterol	+	+	n. a	-	[8, 40]
400	Campesterol	+	+	n. a	-	[8, 40]
414	β-Sitosterol	+	+	n. a.	-	[8, 40]

Table B.1: Assignment of the observed masses to the corresponding compounds

B Mass assignment

Bibliography

[1] G. K. Palmer and R. C. Pearce. *Tobacco - Production, Chemistry, and Technology*, chapter 5B Light Air-cured Tobacco, pages 143–153. Blackwell Science, Oxford, 1999.

[2] G. H. Bokelman and W. S. Ryan, Jr. Analyses of Bright and Burley Tobacco Laminae and Stems. *Beiträge zur Tabakforschung International*, 13(1):29–36, 1985.

[3] G. F. Peedin. *Tobacco - Production, Chemistry, and Technology*, chapter 5A Flue-cured Tobacco, pages 104–142. Blackwell Science, Oxford, 1999.

[4] W. S. Schlotzhauer and O. T. Chortyk. Recent Advances in Studies of the Pyrosynthesis of Cigarette Smoke Constituents. *Journal of Analytical and Applied Pyrolysis*, 12(3–4):193–222, 1987.

[5] S. N. Gilchrist. *Tobacco - Production, Chemistry, and Technology*, chapter 5C Oriental Tobacco, pages 154–163. Blackwell Science, Oxford, 1999.

[6] T. Adam. *Investigation of Tobacco Pyrolysis Gases and Puff-by-puff Resolved Cigarette Smoke by Single Photon Ionisation (SPI) — Time-of-flight Mass Spectrometry (TOFMS)*. PhD dissertation, Technische Universität München, Fakultät Wissenschaftszentrum Weihenstephan, 2006.

[7] W. R. Harlan and J. M. Moseley. *Kirk-Othmer Encyclopedia of Chemical Technology*, volume 14, chapter Tobacco, pages 242–261. John Wiley & Sons, New York, 1955.

[8] R. L. Stedman. Chemical Composition of Tobacco and Tobacco Smoke. *Chemical Revisions*, 68(2):153–207, 1968.

[9] E. Demole and D. Berthet. A Chemical Study of *Burley* Tobacco Flavour (*Nicotiana tabacum L.*). I. Volatile to medium-volatile constituents (b.p. $\leq 84°/0.001$ Torr). *Helvetica Chimica Acta*, 55(6):1866–1882, 1972.

[10] E. Demole and D. Berthet. A Chemical Study of *Burley Tobacco* Flavour (*Nicotiana tabacum L.*). II. Medium-Volatile, free Acidic Constituents (b. p. ≈ 84–$114°/0.001$ Torr)). *Helvetica Chimica Acta*, 55(6):1898–1901, 1972.

Bibliography

[11] D. L. Roberts and W. A. Rohde. Isolation and Identification of Flavor Components of Burley Tobacco. *Tobacco Science*, 16:107–112, 1972.

[12] R. A. Lloyd, C. W. Miller, D. L. Roberts, and J. A. Giles. Flure-Cured Tobacco Flavor. I. Essence and Essential Oil Components. *Tobacco Science*, 20:43–51, 1976.

[13] W. A. Court and J. G. Hendel. Determination of Nonvolatile Organic and Fatty Acids in Flue-Cured Tobacco by Gas-Liquid Chromatography. *Journal of Chromatographic Science*, 16:314–317, 1978.

[14] B. Kimland, A. J. Aasen, and C. R. Enzell. Tobacco Chemistry 12. Neutral Volatile Constituents of Greek Tobacco. *Acta Chemica Scandinavica*, 26:1281–1284, 1972.

[15] B. Kimland, A. J. Aasen, and C. R. Enzell. Tobacco Chemistry 10. Volatile Neutral Constituents of Greek Tobacco. *Acta Chemica Scandinavica*, 26(6):2177–2184, 1972.

[16] B. Kimland, R. A. Appleton, A. J. Aasen, J. Roeraade, and C. R. Enzell. Neutral Oxygen-Containing Volatile Constituents of Greek Tobacco. *Phytochemistry*, 11(1):309–316, 1972.

[17] B. Kimland, A. J. Aasen, S.-O. Almqvist, P. Arpino, and C. R. Enzell. Volatile Acids of Sun-Cured Greek *Nicotiana tabacum*. *Phytochemistry*, 12(4):835–847, 1973.

[18] J. N. Schumacher and L. Vestal. Isolation and Identification of Smoke Components of Turkish Tobacco. *Tobacco Science*, 18:43–48, 1974.

[19] T. Chuman and M. Noguchi. Acidic Aroma Constituents of Turkish Tobacco. *Agricultural and Biological Chemistry*, 41(6):1021–1030, 1977.

[20] W. J. Irvine and M. J. Saxby. The Constituents of Certain Tobacco Types—I. Steam Volatile Phenols of Latakia. *Phytochemistry*, 7(2):277–281, 1968.

[21] W. J. Irvine and M. J. Saxby. Further Volatile Phenols of Latakia Tobacco Leaf. *Phytochemistry*, 8(10):2067–2070, 1969.

[22] A. I. Kosak. The Composition of Tobacco Smoke. *Experientia*, 10(2):69–71, 1954.

[23] M. F. Dube and C. R. Green. Methods of Collection of Smoke for Analytical Purposes. *Recent Advances in Tobacco Science*, 8:42–102, 1982.

[24] C. R. Green and A. Rodgman. The Tobacco Chemists' Research Conference: a Half Century Forum for Advances in Analytical Methology of Tobacco and Its Products. *Recent Advances in Tobacco Science*, 22:131–304, 1996.

[25] V. Norman. An Overview of the Vapour Phase, Semivolatile and Nonvolatile Components of Cigarette Smoke. *Recent Advances in Tobacco Science*, 3:28–58, 1977.

[26] G. Neurath, H. Ehmke, and H. Schneemann. Über den Wassergehalt von Haupt- und Nebenstromrauch. *Beiträge zur Tabakforschung International*, 3(5):351–357, 1966.

[27] W. R. Johnson, R. W. Hale, J. W. Nedlock, H. J. Grubbs, and D. H. Powell. The Distribution of Products between Mainstream and Sidestream Smoke. *Tobacco Science*, 17:141–144, 1973.

[28] C. L. Browne, C. H. Keith, and R. E. Allen. The Effect of Filter Ventilation on the Yield and Composition of Mainstream and Sidestream Smokes. *Beiträge zur Tabakforschung International*, 10(2):81–90, 1980.

[29] R. R. Baker. Product Formation Mechanisms Inside a Burning Cigarette. *Progress in Energy and Combustion Science*, 7(2):135–153, 1981.

[30] H. Klus and H. Kuhn. Verteilung verschiedener Tabakrauchbestandteile auf Haupt- und Nebenstromrauch (Eine Übersicht). *Beiträge zur Tabakforschung International*, 11(5):229–265, 1982.

[31] V. Norman, A. M. Ihrig, T. M. Larson, and B. L. Moss. The Effect of Some Nitrogenous Blend Components on NO/NO_x and HCN Levels in Mainstream and Sidestream Smoke. *Beiträge zur Tabakforschung International*, 12(2):55–62, 1983.

[32] H. Sakuma, M. Kusama, S. Munakata, T. Ohsumi, and S. Sugawara. The Distribution of Cigarette Smoke Components between Mainstream and Sidestream Smoke: I. Acidic Components. *Beiträge zur Tabakforschung International*, 12(2):63–71, 1983.

[33] H. Sakuma, M. Kusama, K. Yamaguchi, T. Matsuki, and S. Sugawara. The Distribution of Cigarette Smoke Components between Mainstream and Sidestream Smoke: II. Bases. *Beiträge zur Tabakforschung International*, 12(4):199–209, 1984.

[34] H. Sakuma, M. Kusama, K. Yamaguchi, and S. Sugawara. The Distribution of Cigarette Smoke Components between Mainstream and Sidestream Smoke: III. Middle and Higher Boiling Components. *Beiträge zur Tabakforschung International*, 12(5):251–258, 1984.

[35] M. R. Guerin. *Passive Smoking*, volume 9 of *Environmental Carcinogens, Methods of Analysis and Exposure Measurement*, chapter 2 Formation and Physico-Chemical Nature of Sidestream Smoke, pages 11–23. IARC Publication No. 81, Lyon, France, 1987.

Bibliography

[36] D. J. Eatough, L. D. Hansen, and E. A. Lewis. *Environmental Tobacco Smoke: Proceedings of the International Symposium at McGill University, 1989*, chapter The Chemical Characterization of Environmental Tobacco Smoke, pages 3–39. Lexington Books, Massachusetts, 1990.

[37] H. Klus. Distribution of Mainstream and Sidestream Cigarette Smoke Components. *Recent Advances in Tobacco Science*, 16:189–232, 1990.

[38] M. R. Guerin. *Organic Chemistry of the Atmosphere*, chapter Environmental Tobacco Smoke, pages 79–119. CRC Press, Baco Raton, Ann Arbor, Boston, London, 1991.

[39] M. R. Guerin, R. A. Jenkins, and B. A. Tomkins. *The Chemistry of Environmental Tobacco Smoke: Composition and Measurement.* Indoor Air Research Series. Lewis Publishers, Chelsea, Michigan, 1992.

[40] R. R. Baker. *Tobacco - Production, Chemistry, and Technology*, chapter 12 Smoke Chemistry, pages 398–439. Blackwell Science, Oxford, 1999.

[41] M. J. Reasor. The Composition and Dynamics of Environmental Tobacco Smoke. *Journal of Environmental Health*, 50(1):20–24, 1987.

[42] R. R. Baker and C. J. Proctor. The Origins and Properties of Environmental Tobacco Smoke. *Environment International*, 16(3):231–245, 1990.

[43] D. Kotzias, O. Geiss, P. Leva, A. Bellinanti, A. Arvanitidis, and S. Kephalopoulos. Impact of Various Air Exchange Rates on the Levels of Environmental Tobacco Smoke (ETS) Components. *Fresenius Environmental Bulletin*, 13(12b):1536–1549, 2004.

[44] C. R. Green, F. W. J. Conrad, K. A. Bridle, and M. F. Borgerding. A Liquid Chromatography Procedure for Analysis of Nicotine on Cellulose Acetate Filters. *Beiträge zur Tabakforschung International*, 13(1):11–16, 1985.

[45] G. Jeanty, J. Massé, P. Berçot, and F. Coq. Quantitative Analysis of Cigarette Smoke Condensate Monophenoles by Reverse-Phase High-Performance Liquid Chromatography. *Beiträge zur Tabakforschung International*, 12(5):245–250, 1984.

[46] G. Zurek, A. Büldt, and U. Karst. Determination of Acetaldehyde in Tobacco Smoke Using N-methyl-4-hydrazino-7-nitrobenzofurazan and Liquid Chromatography / Mass Spectrometry. *Fresenius Journal of Analytical Chemistry*, 366(4):396–399, 2000.

[47] M. B. Clarke, D. Z. Bezabeh, and C. T. Howard. Determination of Carbohydrates in Tobacco Products by Liquid Chromatography-Mass Spectrometry/Mass Spectrometry: A Comparison with Ion Chromatography and Appli-

cation to Product Discrimination. *Journal of Agricultural and Food Chemistry*, 54(6):1975–1981, 2006.

[48] R. F. Arrendale, R. F. Severson, and M. E. Snook. Quantitative Determination of Naphtalenes in Tobacco Smoke by Gas Chromatography. *Beiträge zur Tabakforschung International*, 10(2):100–105, 1980.

[49] F. Omori, N. Higashi, M. Chida, Y. Sone, and S. Suhara. Internal Standard-based Analytical Method for Tobacco Smoke Vapor Phase Components. *Beiträge zur Tabakforschung International*, 18(4):131–146, 1999.

[50] J.-Z. Dong and S. C. Moldoveanu. Gas Chromatrography - Mass Spectrometry of Carbonyl Compounds in Cigarette Mainstream Smoke after Derivatization with 2,4- dinitrophenylhydrazine. *Journal of Chromatography A*, 1027(1–2):25–35, 2004.

[51] G. Holzer, J. Oró, and W. Bertsch. Gas Chromatographic - Mass Spectrometric Evaluation of Exhaled Tobacco Smoke. *Journal of Chromatography*, 126:771–785, 1976.

[52] G. Gmeiner, G. Stehlik, and H. Tausch. Determination of Seventeen Polycyclic Aromatic Hydrocarbons in Tobacco Smoke Condensate. *Journal of Chromatography A*, 767(1–2):163–169, 1997.

[53] S. B. Stanfill and D. L. Ashley. Quantitation of Flavor-Related Alkenylbenzenes in Tobacco Smoke Particulate by Selected Ion Monitoring Gas Chromatography - Mass Spectrometry. *Journal of Agricultural and Food Chemistry*, 48(4):1298–1306, 2000.

[54] E. J. Nanni, M. E. Lovette, R. D. Hicks, K. W. Fowler, and M. F. Borgerding. Separation and Quantitation of Phenolic Compounds in Mainstream Cigarette Smoke by Capillary Gas Chromatography with Mass Spectrometry in the Selected-Ion Mode. *Journal of Chromatography*, 505(2):365–374, 1990.

[55] D. G. Hatzinikolaou, V. Lagesson, A. J. Stavridou, A. E. Pouli, L. Lagesson-Andrasko, and J. C. Stavrides. Analysis of the Gas-Phase of Cigarette Smoke by Gas Chromatography Coupled with UV-Diode Array Detection. *Analytical Chemistry*, 78(13):4509–4516, 2006.

[56] H. Sakuma, Kusama, N. Shimojima, and S. Sugawara. Gas Chromatographic Analysis of the p-Nitrophenylhydrazones of Low Boiling Carbonyl Compounds in Cigarette Smoke. *Tobacco Science*, 22:158–160, 1978.

[57] J. R. Holtzclaw, S. L. Rose, J. R. Wyatt, D. P. Rounbehler, and D. H. Fine. Simultaneous Determination of Hydrazine, Methylhydrazine, and 1,1-Dimethylhydrazine in Air by Derivatization/Gas Chromatography. *Analytical Chemistry*, 56(14):2952–2956, 1984.

Bibliography

[58] A. Caballo-Lopéz and M. D. L. de Castro. Continous Ultrasound-Assisted Extraction Coupled to Flow Injection-Pervaporation, Derivatization, and Spectrophotometric Detection for the Determination of Ammonia in Cigarettes. *Analytical Chemistry*, 78(7):2297–2301, 2006.

[59] X. Lu, J. Cai, H. Kong, M. Wu, R. Hua, M Zhao, J. Liu, and G. Xu. Analysis of Cigarette Smoke Condensates by Comprehensive Two-Dimensional Gas Chromatography/Time-of-Flight Mass Spectrometry. I Acidic Fraction. *Analytical Chemistry*, 75(17):4441, 2003.

[60] U. Boesl, H. J. Neusser, and E. W. Schlag. Two-Photon Ionization of Polyatomic Molecules in a Mass Spectrometer. *Zeitschrift für Naturforschung*, 33 a:1546–1548, 1978.

[61] U. Boesl, H. J. Neusser, and E. W. Schlag. Multi-Photon Ionization in the Mass Spectrometry of Polyatomic Molecules: Cross Sections. *Chemical Physics*, 55:193–204, 1981.

[62] J. W. Hager and S. C. Wallace. Two-Laser Photoionization Supersonic Jet Mass Spectrometry of Aromatic Molecules. *Analytical Chemistry*, 60(1):5–10, 1988.

[63] D. M. Lubman, editor. *Lasers and Mass Spectrometry.* Oxford University Press, New York, 1990.

[64] V. S. Letokhov. *Laser Photoionization Spectroscopy.* Academic Press, Orlando, 1987.

[65] K. Hafner, R. Zimmermann, E. R. Rohwer, Dorfnerm R., and A. Kettrup. A Capillary-Based Supersonic Jet Inlet System for Resonance-Enhanced Laser Ionization Mass Spectrometry: Principle and First On-line Process Analytical Applications. *Analytical Chemistry*, 73(17):4171–4180, 2001.

[66] H. S. Katzenstein and S. S. Friedland. New Time-of-Flight Mass Spectrometer. *Review of Scientific Instruments*, 26(4):324–327, 1955.

[67] W. C. Wiley and I. H. McLaren. Time-of-Flight Mass Spectrometer with Improved Resolution. *Reviews of Scientific Instruments*, 26(12):1150–1157, 1955.

[68] U. Boesl, R. Weinkauf, and E. W. Schlag. Reflectron Time-of-Flight Mass Spectrometry and Laser Excitation for the Analysis of Neutrals, Ionized Molecules and Secondary Fragments. *International Journal of Mass Spectrometry and Ion Processes*, 112(2–3):121–166, 1992.

[69] B. A. Mamyrin, V. I. Karataev, D. V. Shmikk, and V. A. Zagulin. The Mass-reflectron, a New Nonmagnetic Time-of-Flight Mass Spectrometer with High Resolution. *Journal of Experimental and Theoretical Physics*, 37:45–48, 1973.

[70] F. Mühlberger. *Entwicklung von Online-Analyseverfahren auf der Basis von Einphotonenionisations- Massenspektrometrie.* PhD dissertation, Technische Universität München, Fakultät Wissenschaftszentrum Weihenstephan, 2003.

[71] F. Mühlberger, K. Hafner, S. Kaesdorf, T. Ferge, and R. Zimmermann. Comprehensive On-Line Characterization of Complex Gas Mixtures by Quasi-Simultaneous Resonance-Enhanced Multiphoton Ionization, Vacuum-UV Single-Photon Ionization, and Electron Impact Ionization in a Time-of-Flight Mass Spectrometer: Setup and Instrument Characterization. *Analytical Chemistry*, 76(22):6753–6764, 2004.

[72] B. A. Williams and T. A. Cool. Resonance Ionization Detection Limits for Hazardous Emissions. In *24th Symposium (International) on Combustion*, pages 1587–1596, Pittsburgh, 1992. The Combustion Institute.

[73] K. Hafner. *Untersuchungen zur Bildung brennstoffabhängiger Stickoxide bei der Abfallverbrennung mittels on-line analytischer Messmethoden.* PhD dissertation, Technische Universität München, Fakultät Wissenschaftszentrum Weihenstephan, 2004.

[74] K. Tonokura, T. Nakamura, and M. Koshi. Detection of Chlorobenzene Derivates Using Vacuum Ultraviolet Ionization Time-of-Flight Mass Spectrometry. *Analytical Sciences*, 19:1109–1113, 2003.

[75] H. Oser, R. Thanner, H.-H. Grotheer, U. Richters, R. Walter, and A. Merz. *Jet-REMPI for Process Control in Incineration*, volume 3108 of *SPIE Proceeding Series*, pages 21–29. Tacke, M. and Stricker, W., 1997.

[76] H. Oser, R. Thanner, and H.-H. Grotheer. Jet-REMPI for the Detection of Trace Gas Compounds in Complex Gas Mixtures, a Tool for Kinetic Research and Incinerator Process Control. *Combustion Science and Technology*, 116-117:567–582, 1996.

[77] S. Mitschke, T. Adam, T. Streibel, R. R. Baker, and R. Zimmermann. Application of Time-of-Flight Mass Spectrometry with Laser-Based Photoionization Methods for Time-Resolved On-Line Analysis of Mainstream Cigarette Smoke. *Analytical Chemistry*, 77(8):2288–2296, 2005.

[78] D. Hoffmann and I. Hoffmann. *Monograph 13: Risks associated with smoking cigarettes with low tar machine-measured yields of tar and nicotine*, chapter 5 Risks associated with smoking cigarettes with low tar machine-measured yields of tar and nicotine, pages 159–185. Rockville, Maryland, U. S., 2001.

[79] A. Norman. *Tobacco - Production, Chemistry, and Technology*, chapter 11B Cigarette design and materials, pages 353–387. Blackwell Science, Oxford, 1999.

Bibliography

[80] A. Rodgman. Some Studies of the Effects of Additives on Cigarette Main-stream Smoke Properties. II. Casing Materials and Humectants. *Beiträge zur Tabakforschung International*, 20(4):279–299, 2002.

[81] C. Liu. Glycerol Transfer in Cigarette Mainstream Smoke. *Beiträge zur Tabakforschung International*, 21(2):111–116, 2004.

[82] P. X. Chen and S. C. Moldoveanu. Mainstream Smoke Chemical Analyses for 2R4F Kentucky Reference Cigarette. *Beiträge zur Tabakforschung International*, 20(7):448–458, 2003.

[83] T. Adam, S. Mitschke, T. Streibel, R. R. Baker, and R. Zimmermann. Puff-by-Puff Resolved Characterisation of Cigarette Mainstream Smoke by Single Photon Ionisation (SPI) - Time of Flight Mass Spectrometry (TOFMS): Comparison of the 2R4F Research Cigarette and Pure Burley, Virginia, Oriental and Maryland Tobacco Cigarettes. *Analytica Chimica Acta*, 572(2):219–229, 2006.

[84] D. A. Shaw, D. M. P. Holland, M. A. MacDonald, M. A. Hayes, L. G. Shpinkova, E. E. Rennie, C. A. F. Johnson, J. E. Parker, and W. von Niessen. An Experimental and Theoretical Study of the Spectroscopic and Thermodynamic Properties of Toluene. *Chemical Physics*, 230(1):97–116, 1998.

[85] S. Mitschke, W. Welthagen, and R. Zimmermann. Comprehensive Gas Chromatography-Time-of-Flight Mass Spectrometry Using Soft and Selective Photoionization Techniques. *Analytical Chemistry*, 78(18):6364–6375, 2006.

[86] E.-J. Shin, M. R. Hajaligol, and F. Rasouli. Characterizing Biomatrix Materials Using Pyrolysis Molecular Beam Mass Spectrometer and Pattern Recognition. *Journal of Analytical and Applied Pyrolysis*, 68–69:213–229, 2003.

[87] C. Huang, L. Wei, J. Wang, Y. Li, L. Sheng, Y. Zhang, and F. Qi. Lean Premixed Gasoline/Oxygen Flame Studied with Tunable Synchrotron Vacuum UV Photoionization. *Energy and Fuels*, 20(4):1505–1513, 2006.

[88] G. Reichardt, J. Bahrdt, J.-S. Schmidt, W. Gudat, A. Ehresmann, R. Müller-Albrecht, H. H. Molter, Schmoranzer, M. Martins, N. Schwentner, and S. Sasaki. A 10 m-Normal Incidence Monochromator at the Quasi-Periodic Undulator U125-2 at BESSY II . *Nuclear Instruments and Methods in Physics Research A*, 467–468(1):462–465, 2001.

[89] J. Bahrdt, W. Frentrup, A. Gaupp, M. Scheer, W. Gudat, G. Ingold, and S. Sasaki. A Quasi-Periodic Hybrid Undulator at BESSY II. *Nuclear Instruments and Methods in Physics Research A*, 467–468(1):130–133, 2001.

[90] F. Mühlberger, T. Streibel, J. Wieser, A. Ulrich, and R. Zimmermann. Single Photon Ionization Time-of-Flight Mass Spectrometry with a Pulsed Electron

Beam Pupmed Excimer VUV Lamp for On-Line Gas Analysis: Setup and First Results on Cigarette Smoke and Human Breath. *Analytical Chemistry*, 77(22):7408–7414, 2005.

[91] R. Zimmermann, U. Boesl, C. Weickhardt, D. Lenoir, K.-W. Schramm, A. Kettrup, and E. W. Schlag. Isomer-Selective Ionization of Chlorinated Aromatics with Lasers for Analytical Time-of-Flight Mass Spectrometry: First Results for Polychlorinated Dibenzo-p-dioxins (PCDD), Biphenyls (IFBCB) and Benzenes (PCBz). *Chemosphere*, 29(9–11):1877–1888, 1994.

[92] R. A. Fisher. The Use of Multiple Measurements in Taxonomic Problems. *Annals of Eugenics*, 7:179–188, 1936.

[93] A. L. Marini, F. Magrí, F. Balestrieri, F. Fabretti, and D. Marini. Supervised Pattern Recognition Applied to the Discrimination of the Floral Origin of Six Types of Italian Honey Samples. *Analytica Chimica Acta*, 515(1):117–125, 2004.

[94] H. Yoshida, R. Leardi, K. Funatsu, and K. Varmuza. Feature Selection by Genetic Algorithms for Mass Spectral Classifiers. *Analytica Chimica Acta*, 446(1–2):483–492, 2001.

[95] W. J. Egan, R. C. Galipo, B. K. Kochanowski, S. L. Morgan, E. G. Bartick, M. L. Miller, D. C. Ward, and R. F. Mothershead, II. Forensic Discrimination of Photocopy and Printer Toners. III: Multivariate Statistics Applied to Scanning Electron Microscopy and Pyrolysis Gas Chromatography/Mass Spectrometry. *Analytical and Bioanalytical Chemistry* , 376(8):1286–1297, 2003.

[96] A. D. Shaw, A. diCamillo, G. Vlahov, A. Jones, G. Bianchi, J. Rowland, and D. B. Kell. Discrimination of the Variety and Region of Origin of Extra Virgin Olive Oils Using ^{13}C NMR and Multivariate Calibration with Variable Reduction. *Analytica Chimica Acta*, 348(1–3):357–374, 1997.

[97] R. O. Douda and P. E. Hart. *Pattern Classification and Scene Analysis*, page 482. John Wiley & Sons, New York, 1973.

[98] S. Krishnan, K. Samudravijaya, and P. V. S. Rao. Feature Selection for Pattern Classification with Gaussian Mixture Models: A New Objective Criterion. *Pattern Recognition Letters*, 17(8):803–809, 1996.

[99] P. Malkavaara, R. Alén, and E. Kolehmainen. Chemometrics: An Important Tool for the Modern Chemist, an Example from Wood-Processing Chemistry. *Journal of Chemical Information and Computer Science*, 40(2):438–441, 2000.

[100] M. A. Sharaf, D. L. Illman, and B. R. Kowalski. *Chemometrics*, chapter Chemical Analysis, pages 1–295. John Wiley & Sons, New York, 1986.

Bibliography

[101] D. L. Massart and L. Kaufman. *Interpretation of Analytical Chemical Data by the Use of Cluster Analysis*, volume 65 of *Chemical Analysis - A Series of Monographs on Analytical Chemistry and its Applications*, pages 1–231. John Wiley & Sons, New York, 1983.

[102] D. L. Massart, B. G. M. Vandeginste, S. N. Deming, Y. Michotte, and L. Kaufman. *Chemometrics: A Textbook*, volume 2 of *Data Handling in Science and Technology*. Elsevier Science Publishers B. V., Amsterdam, 1988.

[103] J. W. Einax, H. W. Zwanziger, and S. Geiß. *Chemometrics in Environmental Analysis*. VCH Verlagsgesellschaft mbH, Weinheim, 1997.

[104] S. Wold and M. Sjöström. Chemometrics, Present and Future Success. *Chemometrics and Intelligent Laboratory Systems*, 44(1):3–14, 1998.

[105] C. Fischbacher. *Analytiker-Taschenbuch*, volume 19, chapter Chemometrische Datenanalyse. Springer, Berlin, 1998.

[106] B. Lavine and J. J. Workman, Jr. Chemometrics. *Analytical Chemistry*, 76(12):3365–3372, 2004.

[107] I. T. Jolliffe. *Principle Component Analysis*. Springer Series in Statistics. Springer, New York, 1986.

[108] S. Wold, K. Esbensen, and P. Geladi. Principal Component Analysis. *Chemometrics and Intelligent Laboratory Systems*, 2(1–3):37–52, 1987.

[109] R. G. Brereton. Introduction to Multivariate Calibration in Analytical Chemistry. *Analyst*, 125(11):2125–2154, 2000.

[110] R. Dorfner, T. Ferge, C. Yeretzian, A. Kettrup, and R. Zimmermann. Laser Mass Spectrometry as On-line Sensor for Industrial Process Analysis: Process Control of Coffee Roasting. *Analytical Chemistry*, 76(5):1368–1402, 2004.

[111] I. Duarte, A. Barros, P. S. Belton, R. Righelato, M. Spraul, E. Humpfer, and A. M. Gil. High-resolution Nuclear Magnetic Resonance Spectroscopy and Multivariate Analysis for the Characterization of Beer. *Journal of Agricultural and Food Chemistry*, 50(9):2475–2481, 2002.

[112] M. J. Martín, F. Pablos, and A. G. González. Application of Pattern Recognition to the Discrimination of Roasted Coffees. *Analytica Chimica Acta*, 320(2–3):191–197, 1996.

[113] M. J. Martín, F. Pablos, and A. G. González. Discrimination between Arabica and Robusta Green Coffee Varieties According to their Chemical Composition. *Talanta*, 46(6):1259–1264, 1998.

[114] R. Briandet, E. K. Kemsley, and R. H. Wilson. Discrimination of *Arabica* and *Robusta* in Instant Coffee by Fourier Transform Infrared Spectroscopy and

Chemometrics. *Journal of Agricultural and Food Chemistry*, 44(1):170–174, 1996.

[115] L. Maeztu, C. Sanz, S. Andueza, M. P. de Peña, J. Bello, and C. Cid. Characterization of Espresso Coffee Aroma by Static Headspace GC-MS and Sensory Flavor Profile. *Journal of Agricultural and Food Chemistry*, 49(11):5437–5444, 2001.

[116] S. J. Haswell and A. D. Walmsley. Multivariate Data Visualisation Methods Based on Multi-Elemental Analysis of Wines and Coffees Using Total Reflection X-Ray Fluorescence Analysis. *Journal of Analytical Atomic Spectrometry*, 13(2):131–134, 1998.

[117] K. Héberger, E. Csomós, and L. Simon-Sarkadi. Principal Component and Linear Discriminant Analyses of Free Amino Acids and Biogenic Amines in Hungarian Wines. *Journal of Agricultural and Food Chemistry*, 51(27):8055–8060, 2003.

[118] C. P. Bicchi, A. E. Binello, M. M. Legovich, G. M. Pellegrino, and A. C. Vanni. Characterization of Roasted Coffee by S-HSGC and HPLC-UV and Principal Component Analysis. *Journal of Agricultural and Food Chemistry*, 41(12):2324–2328, 1993.

[119] K. Wada, H. Sasaki, M. Shimoda, and Y. Osajima. Objective Evaluation of Various Trade Varieties of Coffee by Coupling of Analytical Data and Multivariate Analyses. *Agricultural and Biological Chemistry*, 51(7):1753–1760, 1987.

[120] R. M. Alonso-Salces, S. Guyot, C. Herrero, L. A. Berrueta, J. F. Drilleau, B. Gallo, and F. Vicente. Chemometric Characterisation of Basque and French Ciders According to their Polyphenolic Profiles. *Analytical and Bioanalytical Chemistry*, 379(3):464–475, 2004.

[121] K. L. Goodner and R. L. Russell. Using an Ion-Trap MS Sensor to Differentiate and Identify Individual Components in Grapefruit Juice Headspace Volatiles. *Journal of Agricultural and Food Chemistry*, 41(1):250–253, 2001.

[122] E. Guchu, M. C. Díaz-Maroto, M. S. Pérez-Coello, M. A. Gonzáles-Viñas, and M. D. Cabezudo Ibáñez. Volatile Composition and Sensory Characteristics of Chardonnay Wines Treated with American and Hungarian Oak Chips. *Food Chemistry*, 99(2):350–359, 2006.

[123] H.-R. Schulten. Pyrolysis-Field Ionization Mass Spectrometry — A New Method for Direct, Rapid Characterization of Tobacco. *Beiträge zur Tabakforschung International*, 13(5):219–227, 1986.

Bibliography

[124] N. Simmleit and H.-R. Schulten. Differentiation of Commercial Tobacco Blends by Pyrolysis Field Ionization Mass Spectrometry and Pattern Recognition. *Fresenius Journal of Analytical Chemistry*, 324(1):9–12, 1986.

[125] L.-K. Ng, M. Hupé, M. Vanier, and D. Moccia. Characterization of Cigar Tobaccos by Gas Chromatographic/Mass Spectrometric Analysis of Nonvolatile Organic Acids: Application to the Authentication of Cuban Cigars. *Journal of Agricultural and Food Chemistry*, 49(3):1132–1138, 2001.

[126] M. Cocchi, G. Foca, M. Lucisano, A. Marchetti, M. A. Pagani, Tassi L., and A. Ulrici. Classification of Cereal Flours by Chemometric Analysis of MIR Spectra. *Journal of Agricultural and Food Chemistry*, 52(5):1062–1067, 2004.

[127] C. Armanino and M. R. Festa. Characterization of Wheat by four Analytical Parameters. A Chemometric Study. *Analytica Chimica Acta*, 331(1–2):43–51, 1996.

[128] C. Cordella, I. Moussa, A.-C. Martel, N. Sbirrazzuoli, and L. Lizzani-Cuvelier. Recent Developments in Food Characterization and Adulteration Detection: Technique-Oriented Perspectives. *Journal of Agricultural and Food Chemistry*, 50(3):1751–1764, 2002.

[129] R. Bucci, A. D. Magrí, A. L. Magrí, D. Marini, and F. Marini. Chemical Authentication of Extra Virgin Olive Oil Varieties by Supervised Chemometric Procedures. *Journal of Agricultural and Food Chemistry*, 50(3):413–418, 2002.

[130] M. A. E. Schmidt, B. S. Radovic, M. Lipp, G. Harzer, and E. Anklam. Characterisation of Milk Samples with Various Whey Protein Contents by Pyrolysis—Mass Spectrometry (Py—MS). *Food Chemistry*, 65(1):123–128, 1999.

[131] E. Anklam, M. Lipp, B. Radovic, E. Chiavarob, and G. Pallab. Characterisation of Italian Vinegar by Pyrolysis—Mass Spectrometry and a Sensor Device ("Electronic Nose"). *Food Chemistry*, 61(1–2):243–248, 1998.

[132] A. Martinez and A. Kak. PCA versus LDA. *IEEE Transactions on Pattern Analysis and Machine Intelligence*, 23(2):228–233, 2001.

[133] H. L. Meuzelaar, W. Windig, A. M. Harper, S. M. Huff, W. H. McClennen, and J. M. Richards. Pyrolysis Mass Spectrometry of Complex Organic Materials. *Science*, 226(4672):268–274, 1984.

[134] M. Blazsó. Recent Trends in Analytical and Applied Pyrolysis of Polymers. *Journal of Analytical and Applied Pyrolysis*, 39(1):1–25, 1997.

[135] T. P. Wampler. Introduction to Pyrolysis-Capillary Gas Chromatography. *Journal of Chromatography A*, 842(1–2):207–220, 1999.

[136] T. P. Wampler. Practical Applications of Analytical Pyrolysis. *Journal of Analytical and Applied Pyrolysis*, 71(1):1–12, 2004.

[137] K. G. H. Raemakers and J. C. J. Bart. Applications of Simultaneous Thermogravimetry-Mass Spectrometry in Polymer Analysis. *Thermochimica Acta*, 295(1–2):1–58, 1997.

[138] T. Ozawa, T. Arii, and A. Kishi. Thermogravimetry and Evolved Gas Analysis of Polyimide. *Thermochimica Acta*, 352–353:177–180, 1997.

[139] M. Herrera, G. Matuscheka, and A. Kettrup. Main Products and Kinetics of the Thermal Degradation of Polyamides. *Chemosphere*, 42(5–7):601–607, 2001.

[140] R. M. A. Heeren, C. G. de Koster, and J. J. Boon. Direct Temperature Resolved HRMS of Fire-Retarded Polymers by In-Source PyMS on an External Ion Source Fourier Transform Ion Cyclotron Resonance Mass Spectrometer. *Analytical Chemistry*, 67(21):3965–3970, 1995.

[141] D. O. Hummel, S. Göttgens, U. Neuhoff, and H.-J. Düssel. Linear-Temperature Programmed Pyrolysis of Thermoresistant Polymers-Mass and FT-IR Spectrometries Part 3. Poly(1,4-phenylene terephthalamide) and Aromatic Polyimides. *Journal of Analytical and Applied Pyrolysis*, 33:195–212, 1995.

[142] M. Lipp, B. S. Radovic, and E. Anklam. Characterisation of Vinegar by Pyrolysis—Mass Spectrometry. *Food Control*, 9(6):349–355, 1998.

[143] G. L. Alonso, M. R. Salinas, F. J. Esteban-Infantes, and M. A. Sánchez-Fernández. Determination of Safranal from Saffron (*Crocus sativus* L.) by Thermal Desorption—Gas Chromatography. *Journal of Agricultural and Food Chemistry*, 44(1):185–188, 1996.

[144] J.-F. Cavalli, X. Fernandez, L. Lizanni-Cuvelier, and A.-M. Loiseau. Comparison of Static Headspace, Headspace Solid Phase Microextraction, Headspace Sorptive Extraction, and Direct Thermal Desorption Techniques on Chemical Composition of French Olive Oils. *Journal of Agricultural and Food Chemistry*, 51(26):7709–7716, 2003.

[145] K. D. Brunnemann and D. Hoffmann. Pyrolytic Origins of Major Gas Phase Constituents of Cigarette Smoke. *Recent Advances in Tobacco Science*, 8:103–140, 1982.

[146] R. R. Baker. A Review of Pyrolysis Studies to Unravel Reaction Steps in Burning Tobacco. *Journal of Analytical and Applied Pyrolysis*, 11:555–573, 1987.

[147] H. R. Burton and G. Childs, Jr. Thermal Decomposition of Tobaccos. *Beiträge zur Tabakforschung International*, 9(1):45–52, 1977.

[148] I. Schmeltz, A. Wenger, D. Hoffmann, and T.C. Tso. Chemical Studies on

Bibliography

Tobacco Smoke. 63. On the Fate of Nicotine during Pyrolysis and in a Burning Cigarette. *Journal of Agricultural and Food Chemistry*, 27(3):602–608, 1979.

[149] M. A. Scheijen, B. Brandt-de Boer, J. J. Boon, W. Hass, and V. Heemann. Evaluation of a Tobacco Fractioning Procedure using Pyrolysis Mass Spectrometry Combined with Multivariate Analysis. *Beiträge zur Tabakforschung International*, 14(5):261–282, 1989.

[150] H. Im, F. Rasouli, and M. Hajaligol. Formation of Nitric Oxide during Tobacco Oxidation. *Journal of Agricultural and Food Chemistry*, 51(25):7366–7372, 2003.

[151] J. M. Halket and H.-R. Schulten. Rapid Characterization of Tobacco by Combined Direct Pyrolysis-Field Ionization Mass Spectrometry and Pyrolysis-Gas Chromatography-Mass Spectrometry. *Journal of Analytical and Applied Pyrolysis*, 8:547–560, 1985.

[152] R. R. Baker, S. Coburn, and C. Liu. The Pyrolytic Formation of Formaldehyde from Sugars and Tobacco. *Journal of Analytical and Applied Pyrolysis*, 77(1):12–21, 2006.

[153] R. R. Baker and L. J. Bishop. The Pyrolysis of Tobacco Ingredients. *Journal of Analytical and Applied Pyrolysis*, 71(1):223–311, 2004.

[154] R. R. Baker, S. Coburn, C. Liu, and J. Tetteh. Pyrolysis of Saccharide Tobacco Ingredients: a TGA-FTIR Investigation. *Journal of Analytical and Applied Pyrolysis*, 74(1–2):171–180, 2005.

[155] R. A. Fenner. Thermoanalytical Characterization of Tobacco Constituents. *Recent Advances in Tobacco Science*, 14:82–113, 1988.

[156] R. A. Fenner. Application of Fourier Transform lnfrared Evolved Gas Analysis (FT-IR-EGA) to the Study of Tobacco Curing. *Beiträge zur Tabakforschung International*, 14(2):85–91, 1988.

[157] E. L. Wynder and D. Hoffmann. *Tobacco and Tobacco Smoke; Studies in Experimental Carcinogenesis*, pages 94–105. Academic Press, New York and London, 1967.

[158] J. I. Seeman, M. Dixon, and H.-J. Haussmann. Acetaldehyde in Mainstream Tobacco Smoke: Formation and Occurrence in Smoke and Bioavailability in the Smoker. *Chemical Research in Toxicology*, 15(11):1331–1350, 2002.

[159] I. Schmeltz, W. S. Schlotzahauer, and E. B. Higman. Characteristic Products from Pyrolysis of Nitrogenous Organic Substances. *Beiträge zur Tabakforschung International*, 6(3):134–138, 1972.

[160] W. A. Court, J. G. Hendel, and R. Pocs. Influence of Transplanting and Harvesting Date on the Agronomic and Chemical Characteristics of Flue-Cured Tobacco. *Tobacco Science*, 37:59–64, 1993.

[161] T. Streibel, J. Weh, S. Mitschke, and R. Zimmermann. Thermal Desorption/Pyrolysis Coupled with Photoionization Time-of-Flight Mass Spectrometry for the Analysis of Molecular Organic Compounds and Oligomeric and Polymeric Fractions in Urban Particulate Matter. *Analytical Chemistry*, 78(15):5354–5361, 2006.

[162] T. Adam, T. Ferge, T. Streibel, S. Mitschke, R. R. Baker, and R. Zimmermann. Discrimination of Three Tobacco Types (Burley, Virginia and Oriental) by Pyrolysis Single-Photon Ionisation-Time-of-Flight Mass Spectrometry and Advanced Statistical Methods. *Analytical and Bioanalytical Chemistry*, 381(2):487–499, 2005.

[163] G. Neurath and M. Dünger. Isolierung schwach basischer Heteroaromaten aus dem Tabakrauch. *Beiträge zur Tabakforschung International*, 5(1):1–4, 1969.

[164] B. Pfyl, R. Kölliker, B. Dwilling, and M. Obermiller. The Determination of Nicotine in Tobacco Smoke. II. *European Food Research and Technology*, 66(5):501–510, 1933.

[165] J. A. Bradford, W. R. Harlan, and H. R. Hanmer. Nature of Cigaret Smoke: Technic of Experimental Smoking. *Industrial and Engineering Chemistry*, 28(7):836–839, 1936.

[166] H. C. Pillsbury, C. C. Bright, K. J. O'Connor, and F. W. Irish. Tar and Nicotine in Cigarette Smoke. *Journal of the Association of Official Analytical Chemists*, 52(3):458–462, 1969.

[167] W. B. Wartman, Jr., E. C. Cogbill, and E. S. Harlow. Determination of Particulate Matter in Concentrated Aerosols. Application to Analysis of Cigarette Smoke. *Analytical Chemistry*, 31(10):1705–1709, 1959.

[168] C. L. Ogg. Determination of Particulate Matter and Alkaloids (as Nicotine) in Cigarette Smoke. *Journal of the Association of Official Agricultural Chemists*, 47(2):356–362, 1964.

[169] CORESTA Recommended Method No. 10. Machine Smoking of Cigarettes, Determination of Crude and Dry Smoke Condensate. *CORESTA Information Bulletin No. 1*, pages 24–33, 1969.

[170] International Organisation for Standardisation. *Routine Analytical Cigarette Smoking Machine. Specification for the Machine and Auxiliary Equipment; ISO 3308, First Edition.* 1977.

Bibliography

[171] R. R. Baker. The Development and Significance of Standards for Smoking-Machine Methodology. *Beiträge zur Tabakforschung International*, 20(1):23–41, 2002.

[172] P. I. Adams. Measurements on puffs taken by human smokers; paper presented at 20th tobacco chemists' research conference. In *Programme Booklet and Abstracts*, volume 31, Winston Salem, NC. U.S.A., 1982.

[173] G. Scherer. Smoking Behaviour and Compensation: A Review of the Literature. *Psychopharmacology*, 145(1):1–20, 1999.

[174] F. V. Djordjevic, S. D. Stellman, and E. Zang. Doses of Nicotine and Lung Carcinogens Delivered to Cigarette Smokers. *Journal of the National Cancer Institute*, 92(2):106–111, 2000.

[175] T. Adam, S. Mitschke, T. Streibel, R. R. Baker, and R. Zimmermann. Quantitative Puff-by-Puff-Resolved Characterization of Selected Toxic Compounds in Cigarette Mainstream Smoke. *Chemical Research in Toxicology*, 19(4):511–520, 2006.

[176] D. R. Meckley, J. R. Hayes, K.R. Van Kampen, P. H. Ayres, A. T. Mosberg, and J. E. Swauger. Comparative Study of Smoke Condensates from 1R4F Cigarettes that Burn Tobacco versus ECLIPSE Cigarettes that Primarily Heat Tobacco in the SENCAR Mouse Dermal Tumor Promotion Assay. *Food and Chemical Toxicology*, 42(5):851–863, 2004.

[177] B. R. Bombick, H. Murli, J. T. Avalos, D. W. Bombick, W. T. Morgan, K. P. Putnam, and D. J. Doolittle. Chemical and Biological Studies of a New Cigarette that Primarily Heats Tobacco. Part 2. *In Vitro* Toxicology of Mainstream Smoke Condensate. *Food and Chemical Toxicology*, 36(3):183–190, 1997.

[178] D. W. Bombick, P. H. Ayres, K. Putnam, B. R. Bombick, and D. J. Doolittle. Chemical and Biological Studies of a New Cigarette that Primarily Heats Tobacco. Part 3. *In Vitro* Toxicity of Whole Smoke. *Food and Chemical Toxicology*, 36(3):191–197, 1997.

[179] J. D. deBethizy, M. F. Borgerding, D. J. Doolittle, J. H. Robinson, K. T. McManus, C. A. Rahn, A. D. Riley, G. T. Burger, J. R. Hayes, J. H. Reynolds, and A. W. Hayes. Chemical and Biological Studies of a Cigarette that Heats Rather than Burns Tobacco. *Journal of Clinical Pharmacology*, 30(8):755–763, 1990.

[180] J. W. D. Foy, B. R. Bombick, D. W. Bombick, D. J. Doolittle, A. T. Mosberg, and J. E. Swauger. A Comparison of *In Vitro* Toxicities of Cigarette Smoke Condensate from Eclipse Cigarettes and four Commercially Available Ultra Low-"Tar" Cigarettes. *Food and Chemical Toxicology*, 42(2):237–243, 2004.

192

[181] A. P. Wehner, R. A. Renne, B. J. Greenspan, H. S. DeFord, H. A. Ragan, R. B. Westerberg, C. W. Wright, R. L. Buschborn, G. T. Burger, A. W. Hayes, C. R. E. Coggins, and A. T. Mosberg. Comparative Subchronic Inhalation Bioassay in Hamsters of a Cigarette that only Heats Tobacco. *Inhalation Toxicology*, 2:255–284, 1990.

[182] D. L. Bowman, C. J. Smith, B. R. Bombick, J. T. Avalos, R. A. Davis, W. T. Morgan, and D. J. Doolittle. Relationship between FTC "Tar" and Urine Mutagenicity in Smokers of Tobacco-Burning or Eclipse Cigarettes. *Mutation Research*, 521(1–2):137–149, 2002.

[183] Eclipse Expert Panel. A Safer Cigarette? A Comparative Study. A Consensus Report. *Inhalation Toxicology*, 12(12 (Supplement 5)):1–48, 2000.

[184] D. J. Doolittle, C. K. Lee, J. L. Ivett, J. C. Mirsalis, E. Riccio, C. J. Rudd, G. T. Burger, and A. W. Hayes. Genetic Toxicology Studies Comparing the Activity of Sidestream Smoke from Cigarettes which Burn or only Heat Tobacco. *Mutation Research*, 240(2):59–72, 1990.

[185] W. A. Pryor, D. F. Church, M. D. Evans, W. Y. Rice, Jr., and J. R. Hayes. A Comparison of the Free Radical Chemistry of Tobacco-Burning Cigarettes and Cigarettes that only Heat Tobacco. *Free Radical Biology and Medicine*, 8(3):275–279, 1990.

[186] M. F. Borgerding, J. A. Bodnar, H. L. Chung, P. P. Mangan, C. C. Morrison, C. H. Risner, D. F. Rogers, J. C.and Simmons, M. S. Uhrig, F. N. Wendelboe, D. E. Wingate, and L. S. Winkler. Chemical and Biological Studies of a New Cigarette that Primarily Heats Tobacco. Part 1. Chemical Composition of Mainstream Smoke. *Food and Chemical Toxicology*, 36(3):169–182, 1997.

[187] C. H. Risner. The Determination of Benzo[*a*]Pyrene and Benz[*a*]Anthracene in Mainstream and Sidestream Smoke of the Kentucky Reference Cigarette 1R4F and a Cigarette Which Heats but Does Not Burn Tobacco: A Comparison. *Beiträge zur Tabakforschung International*, 15(1):11–17, 1991.

[188] N. L. Benowitz, J. Peyton, III., J. Slade, and L. Yu. Nicotine Content of the Eclipse Nicotine Delivery Device. *American Journal of Public Health*, 87(11):1865–1866, 1997.

[189] J. F. Pankow, K. C. Barsanti, and D. H. Peyton. Fraction of Free-Base Nicotine in Fresh Smoke Particulate Matter from the Eclipse "Cigarette" by ^{1}H NMR Spectroscopy. *Chemical Research in Toxicology*, 16(1):23–27, 2003.

[190] E. M. Lee, J. L. Malson, E. T. Moolchan, and W. B. Pickworth. Quantitative Comparisons between a Nicotine Delivery Device (Eclipse) and Conventional Cigarette Smoking. *Nicotine and Tobacco Research*, 6(1):95–102, 2004.

Bibliography

[191] K. G. Darrall. Smoking Machine Parameters and Cigarette Smoke Yields. *The Science of the Total Environment*, 74:263–278, 1988.

[192] K. A. Wagner, R. Higby, and K. Stutt. Puff-by-puff Analysis of Selected Mainstream Smoke Constituents in the Kentucky Reference 2R4F Cigarette. *Beiträge zur Tabakforschung International*, 21(5):273–279, 2005.

[193] M. E. Counts, F. S. Hsu, S. W. Laffoon, R. W. Dwyer, and R. H. Cox. Mainstream Smoke Constituent Yields and Predicting Relations from a Worldwide Market Sample of Cigarette Brands: ISO Smoking Conditions. *Regulatory Toxicology and Pharmacology*, 39(2):111–134, 2004.

[194] M. E. Counts, M. J. Morton, S. W. Laffoon, R. H. Cox, and P. J. Lipowicz. Smoke Composition and Predicting Relations for International Commercial Cigarettes Smoked with Three Machine-Smoking Conditions. *Regulatory Toxicology and Pharmacology*, 41(3):185–227, 2005.

[195] UK Department of Health, Smoking Policy Unit. *Cigarette Yields using Intense Smoking Protocols. Part 1 - NFDPM, Nicotine and Carbon Monoxide. LGC Report FN40/M08/00*, April 2000.

[196] UK Department of Health, Smoking Policy Unit. *Cigarette Yields using Intense Smoking Protocols. Part 2 - Polycyclic Aromatic Hydrocarbons. LGC Report FN40/M14/00*, July 2000.

[197] UK Department of Health, Smoking Policy Unit. *Cigarette Yields using Intense Smoking Protocols. Part 3 - Nitric Oxide: LGC Report FN40/M32/00*, December 2000.

[198] K. D. Brunnemann and D. Hoffmann. The pH of Tobacco Smoke. *Food and Cosmetics Toxicology*, 12(1):115–124, 1974.

[199] M. R. Guerin, C. E. Higgins, and R. A. Jenkins. Measuring Environmental Emissions for Tobacco Combustion: Sidestream Smoke Literature Review. *Atmospheric Environment*, 21(2):291–297, 1987.

[200] D. D. McRae. The Pysical and Chemical Nature of Tobacco Smoke. *Recent Advances in Tobacco Science*, 16:233–323, 1990.

[201] T. Okada and K. Matsunuma. Determination of Particle-Size Distribution and Concentration of Cigarette Smoke by a Light Scattern Method. *Journal of Colloid and Interface Science*, 48(3):461–469, 1974.

[202] D. Yoshida. Determination of Nicotine in the Sidestream of Cigarette Smoke. *Japan Tobacco Monopoly. Central Research Institute. Scientific Papers*, 118:203–206, 1976.

[203] O. T. Chortyk and W. S. Schlotzhauer. Modification of an Automatic Cigarette Smoking Machine for Sidestream Smoke Collection. *Tobacco Science*, 30:122–126, 1986.

[204] G. Neurath and H. Ehmke. Apparatur zur Untersuchung des Nebenstromrauches. *Beiträge zur Tabakforschung International*, 2(4):117–121, 1964.

[205] T. H. Houseman. Studies of Cigarette Smoke Transfer Using Radioisotopically Labelled Tobacco Constituents: Part II: The Transference of Radioisotopically Labelled Nicotine to Cigarette Smoke. *Beiträge zur Tabakforschung International*, 7(3):142–147, 1973.

[206] J. D. Green, J. Chalmer, and P. J. Kinnard. The Transfer of Tobacco Additives to Cigarette Smoke: Examination of the Possible Contribution of Pyrolysis Products to Mainstream Smoke Composition. *Beiträge zur Tabakforschung International*, 14(5):283–288, 1989.

[207] C. J. Proctor, C. Martin, J. L. Beven, and H. F. Dymond. Evaluation of an Apparatus Designed for the Collection of Sidestream Tobacco Smoke. *Analyst*, 113:1509–1513, 1988.

[208] K. D. Brunnemann, M. R. Kagan, J. E. Cox, and D. Hoffmann. Determination of Benzene, Toluene and 1,3-Butadiene in Cigarette Smoke by GC-MSD. *Experimental Pathology*, 37(1–4):108–113, 1989.

[209] K. D. Brunnemann, M. R. Kagan, J. E. Cox, and D. Hoffmann. Analysis of 1,3-Butadiene and other Selected Gas-Phase Components in Cigarette Mainstream and Sidestream Smoke by Gas Chromatography-Mass Selective Detection. *Carcinogenesis*, 11(10):1863–1868, 1990.

[210] D. R. Hardy and M. E. Hobbs. The Use of ^{15}N and ^{15}N and ^{16}O in added Nitrates for the Study of some Generated Constituents of Normal Cigarette Smoke. In *Proceedings of the 173rd American Chemical Society (Agricultural and Food Chemistry Group) Symposium on recent Advances in the Chemical Composition of Tobacco and Tobacco Smoke*, pages 489–510, New Orleans, Louisiana, 1977.

[211] R. R. Baker. Temperature Variation within a Cigarette Combustion Coal during the Smoking Cycle. *High Temperature Science*, 7(3):236–247, 1975.

[212] R. Dittmann, H.-J. Feld, B.-H. Müller, and W. Schneider. Time Resolved Emission of Sidestream Smoke Particles. *Beiträge zur Tabakforschung International*, 15(2):53–57, 1992.

[213] K Grob. *On-line coupled LC—GC*. Hüthig Buch Verlag, Heidelberg, 1991.

[214] J. C. Giddings. Two-Dimensional Separations: Concept and Promise. *Analytical Chemistry*, 56(12):A1258–A1270, 1984.

Bibliography

[215] J. B. Phillips and J. Beens. Comprehensive Two-Dimensional Gas Chromatography: A Hyphenated Method with Strong Coupling Between the Two Dimensions. *Journal of Chromatography A*, 856(1–2):331–347, 1999.

[216] R. E. Murphy, M. R. Schure, and J. P. Foley. Effect of Sampling Rate on Resolution in Comprehensive Two-Dimensional Liquid Chromatography. *Analytical Chemistry*, 70(8):1585–1594, 1998.

[217] P. J. Marriott and R. Shellie. Principles and Applications of Comprehensive Two-Dimensional Gas Chromatography. *Trends in Analytical Chemistry*, 21(9–10):573–583, 2002.

[218] J. C. Giddings. Sample Dimensionality: A Predictor of Order-Disorder in Component Peak Distribution in Multidimensional Separation. *Journal of Chromatography A*, 703(1–2):3–15, 1995.

[219] J. Beens, R. Tijssen, and J. Blomberg. Prediction of Comprehensive Two-Dimensional Gas Chromatographic Separations: A Theoretical and Practical Exercise. *Journal of Chromatography A*, 822(2):233–251, 1998.

[220] J.-M. D. Dimandja, S. B. Stanfill, J. Grainger, and D. G. Patterson, Jr. Application of Comprehensive Two-Dimensional Gas Chromatography (GCxGC) to the Qualitative Analysis of Essential Oils. *Journal of High Resolution Chromatography*, 23(3):208–214, 2000.

[221] W. Welthagen, J. Schnelle-Kreis, and R. Zimmermann. Search Criteria and Rules for Comprehensive Two-Dimensional Gas Chromatography-Time-of-Flight Mass Spectrometry Analysis of Airborne Particulate Matter. *Journal of Chromatography A*, 1019(1–2):233–249, 2003.

[222] H.-G. Janssen, S. de Koning, and U. A. Th. Brinkman. On-line LC-GC and Comprehensive Two-Dimensional LCxGC-ToF MS for the Analysis of Complex Samples. *Analytical and Bioanalytical Chemistry*, 378(8):1944–1947, 2004.

[223] A. Venter and E. R. Rohwer. Comprehensive Two-Dmensional Supercritical Fluid and Gas Chromatography with Independent Fast Programmed Heating of the Gas Chromatographic Column. *Analytical Chemistry*, 76(13):3699–3706, 2004.

[224] L. Vogt, T. Gröger, and R. Zimmermann. Automated Compound Classification for Aerosol Sample Separations Using Comprehensive Two-Dimensional Gas Chromatography. *Analytical Chemistry*, accepted.

[225] R. R. Baker and K. D. Kilburn. The Distribution of Gases within the Combustion Coal of a Cigarette. *Beiträge zur Tabakforschung International*, 7(2):79–87, 1973.

[226] S. Stotesbury, H. Digard, L. Willoughby, and A. Couch. The Pyrolysis of Tobacco Additives as a Means of Predicting their Behaviour in a Burning Cigarette. *Beiträge zur Tabakforschung International*, 18(4):147–163, 1999.

[227] R. F. Severson, W. S. Schlotzhauer, R. F. Arrendale, M. E. Snook, and H. C. Higman. Correlation of Polynuclear Aromatic Hydrocarbon Formation between Pyrolysis and Smoking. *Beiträge zur Tabakforschung International*, 9(1):23–37, 1977.

[228] Q. Zha and S. C. Moldoveanu. The Influence of Cigarette Moisture to the Chemistry of Particulate Phase Smoke of a Common Commercial Cigarette. *Beiträge zur Tabakforschung International*, 21(3):184–191, 2004.

Bibliography

Abbreviations

1R4F, 2R4F	Research cigarette codes
AVG	Average
Bp	Boiling point
CORESTA	Centre de Coopération pour les Recherches Scientifiques Relatives au Tabac
DIN	Deutsche Industrie Norm
EC	Elemental carbon content
EI	Electron impact
ETS	Environmental Tobacco Smoke
EU	European Union
Fig.	Figure
FTC	Federal Trade Commission
FV	Fischer-Value, Fisher-Ratio
GC	Gas chromatography
GCxGC	Comprehensive gas chromatography
GmbH	Gesellschaft mit begrenzter Haftung
i.d.	Inner diameter
IARC	International Agency for Research on Cancer
IE	Ionisation energy
Inc.	Incorporation
IP	Ionisation potential
IR	Infrared spectroscopy
ISO	International Organisation for Standards
KTRDC	Kentucky Tobacco Research & Development Center
MCP	Multi Channel Plate
MS	Mass spectrometry
MSS	Mainstream smoke
m/z	mass-to-charge ratio
NFDPM	Nicotine free dry particulate matter
OC	Organic carbon content
PAH	Polycyclic aromatic hydrocarbon
PC	Principal component

PCA	Principal component analysis
PhD	Doctorate thesis
PI	Photoionisation
ppb	Parts per billion
ppm	Parts per million
Py	Pyrolysis
REMPI	Resonance enhanced multiphoton ionisation
S/N	Signal to noise ratio
SPI	Single Photon Ionisation
SSS	Sidestream smoke
TBME	tert.-Butyl-methyl-ether
TC	Total Carbon Content
THG	Third harmonic generator
TIC	Total ion chromatogram
TOF	Time-Of-Flight
TPM	Total Particulate Matter
TSNA	Tobacco-specific nitroamine
UK	United Kingdom
USA	United States of America
UV	ultraviolet
VUV	Vacuum ultraviolet
WHO	World Health Organisation

List of Figures

List of Tables

Acknowledgment

Freunden, meinen Bandkollegen und Kommilitonen, ohne die ich die oft nervenzerreißende Zeit des Studiums vermutlich nicht überstanden hätte.

Ganz herzlich bedanken möchte ich mich bei Mary und Hans, ohne deren familiäre Gastfreundlichkeit diese Arbeit vermutlich nicht zustande gekommen wäre.

List of publications

[1] T. Adam, T. Ferge, S. Mitschke, T. Streibel, R. R. Baker, and R. Zimmermann. Discrimination of Three Tobacco Types (Burley, Virginia and Oriental) by Pyrolysis Singlephoton Ionisation-Time-of-Flight Mass Spectrometry and Advanced Statistical Methods. *Analytical and Bioanalytical Chemistry*, 381(2):487–499,2005.

[2] S. Mitschke, T. Adam, T. Streibel, R. R. Baker, and R. Zimmermann. Application of Time-of-Flight Mass Spectrometry with Laser-Based Photoionization Methods for Time-Resolved On-Line Analysis of Mainstream Cigarette Smoke. *Analytical Chemistry*, 77(8):2288–2296, 2005.

[3] T. Adam, T. Streibel, S. Mitschke, F. Mühlberger, R. R. Baker, and R. Zimmermann. Application of Time-of-Flight Mass Spectrometry with Laser-Based Photoionization Methods for Analytical Pyrolysis of PVC and Tobacco. *Journal of Analytical and Applied Pyrolysis*, 74(1-2):454–464, 2005.

[4] T. Adam, S. Mitschke, T. Streibel, R. R. Baker, and R. Zimmermann. Quantitative Puff-by-Puff Resolved Characterisation of Selected Toxic Compounds in Cigarette Mainstream Smoke. *Chemical Research in Toxicology*, 19(4):511–520, 2006.

[5] T. Adam, S. Mitschke, T. Streibel, R. R. Baker, and R. Zimmermann. Puff-by-Puff Resolved Characterisation of Cigarette Mainstream Smoke by Single Photon Ionisation (SPI) - Time of Flight Mass Spectrometry (TOFMS): Comparison of the 2R4F Research Cigarette and Pure Burley, Virginia, Oriental and Maryland Tobacco Cigarettes. *Analytica Chimica Acta*, 572(2):219–229, 2006.

[6] S. Mitschke, W. Welthagen and R. Zimmermann. Comprehensive Gas Chromatography-Time-of-Flight Mass Spectrometry Using Soft and Selective Photoionization Techniques. *Analytical Chemistry*, 78(18):6364–6375, 2006.

[7] T. Streibel, J. Weh, S. Mitschke, and R. Zimmermann. Thermal Desorption/Pyrolysis Coupled with Photoionization Time-of-Flight Mass Spectrometry for the Analysis of Molecular Organic Compounds and Oligomeric and Polymeric Fractions in Urban Particulate Matter. *Analytical Chemistry*, 78(15):5354–5361, 2006.

[8] T. Streibel, S. Mitschke, J. Weh, and R. Zimmermann. Thermal Desorption/Pyrolysis Coupled with Photo Ionisation Time-of-Flight Mass Spectrometry for the Analysis and Discrimination of Pure Tobacco Samples. Accepted for publication *Journal of Analytical and Applied Pyrolysis.*

212

Curriculum vitae

Persönliche Daten

Name: Stefan Manfred Mitschke

geboren: 28.06.1978 in München

Schulausbildung

09/84–07/88   Grundschule in Germering b. München

09/88–07/97   Gymnasium in Germering b. München

Studium

11/97–05/99   Grundstudium der Chemie an der Technischen Universität München

05/99–07/02   Hauptstudium der Chemie an der Technischen Universität München

08/02–02/03   Diplomarbeit am Lehrstuhl für Organische Chemie 2 der Technischen Universität München (Titel: "Synthese photoreaktiver Neuraminsäurederivate")

seit 05/03   Doktorarbeit im Institut für Ökologische Chemie des GSF Forschungszentrums für Umwelt und Gesundheit, Neuherberg